

Sequence-Defined Oligo(*ortho*-Arylene) Foldamers Derived From the Benzannulation of *ortho*(Arylene Ethynylene)s

Dan Lehnherr,^[a] Chen Chen,^[b] Zahra Pedramrazi,^[b] Catherine R. DeBlase,^[a] Joaquin M. Alzola,^[a] Ivan Keresztes,^[c]
Emil B. Lobkovsky,^[d] Michael F. Crommie^{[b]*} and William R. Dichtel^{[a,e]*}

^[a]*Department of Chemistry and Chemical Biology, Cornell University, Ithaca, New York 14853-1301, United States*

^[b]*Department of Physics, University of California at Berkeley, Berkeley, California 94720, United States*

^[c]*Nuclear Magnetic Resonance Laboratory, Cornell University, Ithaca, New York 14853-1301, United States*

^[d]*X-ray Crystallography Laboratory, Cornell University, Ithaca, New York 14853-1301, United States*

^[e]*Department of Chemistry, Northwestern University, Evanston, Illinois 60208, United States*

crommie@berkeley.edu

wdichtel@cornell.edu

Table of Contents for the Supporting Information

1. Procedures, Materials and Instrumentation.....	S-3
2. Synthetic Procedures and Spectral Characterization	
2.1 Benzaldehydes.....	S-5
2.2 <i>ortho</i> -Phenylethynylenes.....	S-5
2.3 Hydrocarbon <i>ortho</i> -Arylenes.....	S-15
2.4 Fluorinated <i>ortho</i> -Arylenes.....	S-26
2.5 Chlorinated <i>ortho</i> -Arylenes.....	S-41
2.6 <i>ortho</i> -Arylenes from Diynes.....	S-53
3. Thermoanalytical Characterization.....	S-63
4. UV-vis Absorption and Emission Spectroscopy.....	S-64
5. Electrochemistry.....	S-66
6. X-ray Crystallographic Structures of Foldamers H-Ar-[n] , F-Ar-[n] , and Cl-Ar-[n]	S-73
7. DFT Computational Study	
7.1 DFT Computed Conformations of Foldamers X-Ar-3	S-76
7.2 DFT Analysis of Rotational Barrier for Interconverting AAAA and AAAB in X-Ar-3	S-82
7.3 DFT Computed Conformations AAA...A and AAA...AB of Foldamers X-Ar-4 , F-Ar-5 , F-Ar-6	S-84
7.4 DFT Computed Structures and Properties of Graphene Nanoribbons X-GNR-[n]	S-88
8. Determination of Thermodynamic Parameters for the Interconversion of Conformers AAAA and AAAB of X-Ar-3	
8.1 Determination of the Equilibrium Constants and van 't Hoff Analysis.....	S-94
8.2 Determination of the Rate and Activation Parameters for Unfolding Process.....	S-96
9. 2-D NMR Data and Solution-Structure Assignment of X-Ar-3 , X-Ar-4 , F-Ar-5 , and F-Ar-6	
9.1 NMR Assignment of Conformers AAAA and AAAB of X-Ar-3	S-99
9.2 NMR Assignment of Conformers AAAA of X-Ar-4	S-104
9.3 NMR Assignment of Folded Conformer (AAA...A) of F-Ar-5 and F-Ar-6	S-107
9.4 nOe Correlations Illustrated on DFT Computed 3-D Structures for X-Ar-3	S-109
9.4.1 ROSEY NMR Spectra of X-Ar-3 Relevant to Conformational Assignment.....	S-113
9.5 nOe Correlations Illustrated on DFT Computed 3-D Structures for X-Ar-4	S-119
9.6 nOe Correlations Illustrated on DFT Computed 3-D Structures for F-Ar-5 and F-Ar-6	S-121
9.7 1-D and 2-D NMR Spectra of X-Ar-3	S-123
9.8 1-D and 2-D NMR Spectra of X-Ar-4	S-154
9.9 1-D and 2-D NMR Spectra of F-Ar-5 and F-Ar-6	S-186

1. Procedures, Materials and Instrumentation

General experimental procedures. All reactions were performed in standard, dry glassware fitted with a rubber septa under an inert atmosphere of nitrogen unless otherwise described. Stainless steel syringes or cannulae were used to transfer air- and moisture-sensitive liquids. Reported concentrations refer to solution volumes at room temperature. Heating of reaction mixtures was carried out with the aid of a silicon oil bath (ChemGlass High temperature silicon oil part number CG-1100-31) using a temperature controlled stirring/heating plate. Evaporation and concentration *in vacuo* was done at using variable vacuum controlled pumps (ca. 400–40 mmHg). Column chromatography was done using standard flash chromatography technique using SiliaFlash® P60 silica gel (40–63 micron, 230–400 mesh) from Silicycle and pressurized (ca. 30–50 psi) using compressed air. Thin layer chromatography (TLC) was used for reaction monitoring and product detection using pre-coated glass plates covered with 0.20 mm silica gel with fluorescent indicator UV 254 nm; visualization by UV light or KMnO₄ stain.

Materials. Reagents were purchased in reagent grade from commercial suppliers and used without further purification, unless otherwise described. Diphenylacetylene (**1**) was commercially available, oligo(*o*-phenylene ethynylene)s **2–6** were previously reported in the literature.¹ Benzaldehydes **S1**, **S2** and **S3** were synthesized according to reported procedures.² Anhydrous solvents (toluene, THF, Et₂O, DMF) were obtained from a solvent purification system (JC Myer System).

Instrumentation. Proton nuclear magnetic resonance (¹H NMR) spectra and carbon nuclear magnetic resonance (¹³C NMR) spectra were recorded at 25 °C (unless stated otherwise) on Varian-Mercury-300 (300 MHz), Varian-Mercury-400 (400 MHz), Varian Unity/Inova 500 (500 MHz), or Varian Unity/Inova 600 (600 MHz) spectrometers at the Nuclear Magnetic Resonance Facility of the Department of Chemistry and Chemical Biology, Cornell University. All 800 MHz NMR data presented were acquired on a Bruker Avance 800 MHz NMR equipped with a cryoprobe at the State University of New York, College of Environmental Science and Forestry in Syracuse, NY. Chemical shifts for protons are reported in parts per million downfield from tetramethylsilane and are referenced to residual protium in the NMR solvent according to values reported in the literature.³ Chemical shifts for carbon are reported in parts per million downfield from tetramethylsilane and are referenced to the carbon resonances of the solvent. The solvent peak was referenced to 7.26 ppm for ¹H and 77.0 ppm for ¹³C for CDCl₃. Data are represented as follows: chemical shift, integration, multiplicity (br = broad, s = singlet, d = doublet, t = triplet, q = quartet, m = multiplet), coupling constants in Hertz (Hz). In the case of compounds containing one or more fluorine atom(s), it should be noted that ¹³C NMR experiments were obtained in which only the ¹H nuclei was decoupled, (i.e., ¹³C {¹H}).

Infrared spectra were recorded using a Nicolet iS10 FT-IR spectrometer equipped with a diamond ATR. Data are represented as follows: frequency of absorption (cm⁻¹), intensity of absorption (s = strong, m = medium, w = weak, vw = very weak, br = broad).

High-resolution mass spectrometry was measured using a ThermoFisher Scientific Exactive DART-MS, sample introduction was carried out by coating the outer walls of a capillary melting point tube with the sample solution (typically in CDCl₃ or CH₂Cl₂) and exposing such tubes to the sample inlet port.

UV-vis absorption spectra were acquired using a Varian Cary 5000 Scan Spectrometer; λ_{max} in nm (ϵ in L•mol⁻¹•cm⁻¹). Emission spectra were recorded using Horiba Jobin Yvon Nanolog-3 Fluorometer. All absorption and emission spectra were recorded at rt in the presence of air.

Differential scanning calorimetry (DSC) measurements were measured on a TA Q1000 DSC instrument. Thermogravimetric analyses (TGA) were carried out on a TA Q500 TGA instrument. All thermal analyses were carried out under a flow of nitrogen with a heating rate of 10 °C/min. Thermal decomposition temperature as

(1) (a) Grubbs, R. H.; Kratz, D. *Chem. Ber.* **1993**, *126*, 149–157. (b) Schriener, P. R.; Prall, M.; Lutz, V. *Angew. Chem. Int. Ed.* 2003, *42*, 5757–5760. (c) Spence, J. D.; Lackie, M. L.; Clayton, N. A.; Toscano, S. A.; Farmer, M. A.; Popova, E.; Olmstead, M. M. *Tet. Lett.* **2014**, *55*, 1569–1572.

(2) Lehnher, D.; Alzola, J. M.; Lobkovsky, E. B.; Dichtel, W. R. *Chem. Eur. J.* **2015**, *21*, 18122–18127.

(3) Gottlieb, H. E.; Kotlyar, V.; Nudelman, A. *J. Org. Chem.* **1997**, *62*, 7512–7515.

measured by TGA (as sample weight loss) are reported as T_d in which the temperature listed corresponds to the intersection of the tangent lines of the baseline and the edge of the peak corresponding to the first significant weight loss, typically >5%. Melting points from DSC analysis are reported as the peak maxima, except in cases when the sample decomposed, in which case the onset temperature of the decomposition exothermic peak is reported, as well as the exothermic maxima corresponding to the decomposition.

Electrochemistry experiments were performed on a Princeton Applied Research Versastat 3. All samples were analyzed in MeCN with recrystallized tetrabutylammonium perchlorate (TBAP) as the supporting electrolyte (0.1 M). All solutions were deoxygenated with N_2 before each experiment and a blanket of N_2 was used over the solution during the experiment. A three-electrode cell was used, using a glassy carbon working electrode and a platinum wire counter electrode. Silver/silver ion (Ag in 0.1 M $AgClO_4$, 0.1 M TBAP solution in MeCN) was used as a reference electrode. The potential values (E) were calculated using the following equation (except where otherwise noted): $E = (E_{pc} + E_{pa})/2$, where E_{pc} and E_{pa} correspond to the cathodic and anodic peak potentials, respectively.

X-ray crystallographic data was collected and refined at the Cornell University X-ray Laboratory in the Department of Chemistry and Chemical Biology. The structural refinement details for the X-ray crystallographic data is described in the individual cif files. X-ray crystallographic data for **H-Ar-2** (CCDC 1483959), **H-Ar-3** (CCDC 1483961), **H-Ar-4** (CCDC 1483960), **F-Ar-1** (CCDC 1483962), **F-Ar-2** (CCDC 1483963), **F-Ar-3** (CCDC 1483964), **F-Ar-6** (CCDC 1483965), **Cl-Ar-1** (CCDC 1483966), and **Cl-Ar-2** (CCDC 1483967) have been deposited at the Cambridge Crystallographic Data Centre (CCDC), 12 Union Road, Cambridge CB21EZ, UK; fax: (+44)122-333-6033. These data can be obtained free of charge from The Cambridge Crystallographic Data Centre via the Internet at www.ccdc.cam.ac.uk/data_request/cif using the CCDC numbers given above.

STM imaging. A polished Au(111) single crystal was used as the substrate for STM experiment. Standard Ar^+ sputtering/annealing cycles were applied to obtain an atomically clean Au(111) surface (note: Ar^+ = argon cation in this context). A home built Knudsen cell was used to sublime **H-Ar-3** at 181 °C. STM measurements were performed using a home-built low-temperature STM operating at 7 K in UHV. A Pt-Ir tip was used for topographic measurements at constant current mode. All STM images were processed using the WSxM software.

Abbreviations. atm = atmosphere, DART = direct analysis in real time, 1,2-DCE = 1,2-dichloroethane, EtOAc = ethyl acetate, HR = high-resolution, IR = infrared, LC = liquid chromatography, LR = low-resolution, MALDI = matrix-assisted laser desorption/ionization, MeOH = methanol, MS = mass spectrometry, NMR = nuclear magnetic resonance, rt = room temperature, THF = tetrahydrofuran.

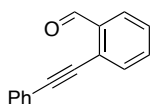
Computational Method and Graphical Representation. Calculations were performed using the Gaussian 09 program.⁴ Default geometric and SCF convergence criteria were used. Stationary points were characterized by the presence of all positive eigenvalues of the Hessian for minima or a single negative eigenvalue of the Hessian for transition states. All DFT methods were used as their default implementations in Gaussian 09. All electronic energies reported are uncorrected energies with regards to zero point energy (ZPE) corrections. All molecular structures were rendered in CYLView.⁵ All CYLView generated images have the following color-coding for labeling elements: C = silver, H = white, Cl = dark green, F = light green.

(4) Gaussian 09, Revision D.01, M. J. Frisch, G. W. Trucks, H. B. Schlegel, G. E. Scuseria, M. A. Robb, J. R. Cheeseman, G. Scalmani, V. Barone, B. Mennucci, G. A. Petersson, H. Nakatsuji, M. Caricato, X. Li, H. P. Hratchian, A. F. Izmaylov, J. Bloino, G. Zheng, J. L. Sonnenberg, M. Hada, M. Ehara, K. Toyota, R. Fukuda, J. Hasegawa, M. Ishida, T. Nakajima, Y. Honda, O. Kitao, H. Nakai, T. Vreven, J. A. Montgomery, Jr., J. E. Peralta, F. Ogliaro, M. Bearpark, J. J. Heyd, E. Brothers, K. N. Kudin, V. N. Staroverov, T. Keith, R. Kobayashi, J. Normand, K. Raghavachari, A. Rendell, J. C. Burant, S. S. Iyengar, J. Tomasi, M. Cossi, N. Rega, J. M. Millam, M. Klene, J. E. Knox, J. B. Cross, V. Bakken, C. Adamo, J. Jaramillo, R. Gomperts, R. E. Stratmann, O. Yazyev, A. J. Austin, R. Cammi, C. Pomelli, J. W. Ochterski, R. L. Martin, K. Morokuma, V. G. Zakrzewski, G. A. Voth, P. Salvador, J. J. Dannenberg, S. Dapprich, A. D. Daniels, O. Farkas, J. B. Foresman, J. V. Ortiz, J. Cioslowski, and D. J. Fox, Gaussian, Inc., Wallingford CT, 2013.

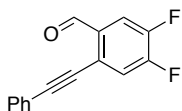
(5) CYLview, 1.0b; Legault, C. Y., Université de Sherbrooke, 2009 (<http://www.cylview.org>).

2. Synthetic Procedures and Spectral Characterization

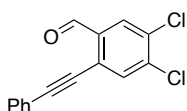
2.1 Benzaldehydes



S1: Synthesized following a literature procedure;⁶ spectral data was consistent with previously reported data.

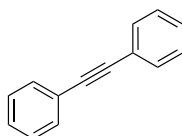


S2: Synthesized following a literature procedure;⁶ spectral data was consistent with previously reported data.

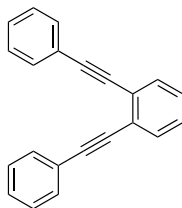


S3: Synthesized following a literature procedure;⁶ spectral data was consistent with previously reported data.

2.2 *ortho*-Phenylethynylenes



1: The compound is commercially available and was used directly without further purification.



2: To a flask containing Pd(PPh₃)₄ (0.525 g, 0.455 mmol) and CuI (0.139 g, 0.727 mmol) under an atmosphere of nitrogen was added via cannula a solution of phenylacetylene (2.40 mL, 2.23 g, 21.8 mmol) and 1,2-diiodobenzene (1.19 mL, 3.00 g, 9.09 mmol) in THF (45 mL) and diisopropylamine (20 mL, 14 g, 142 mmol) which had been deoxygenated by sparging with N₂ for 10 min. The mixture was stirred for 4 h at rt before being diluted with CH₂Cl₂. The organic phase was washed with H₂O, 5% aq. NH₄Cl (2×), and dried over anhyd. Na₂SO₄, filtered through a short pad of silica gel (using 1:1 CH₂Cl₂/hexanes as eluent), and the solvent was removed *in vacuo*. Column chromatography (silica gel, gradient 0% to 15% CH₂Cl₂ in hexanes) afforded **2** (2.37 g, 94%) as a yellow liquid. *R*_f = 0.7 (10 % CH₂Cl₂ in hexanes). IR (CDCl₃ cast film): 3057 (w), 2214 (w), 1597 (w), 1494 (m), 1471 (w), 1441 (m), 1090 (w), 1068 (w), 913 (w), 750 (s), 686 (m) cm⁻¹. ¹H NMR (400 MHz, CDCl₃): δ 7.65–7.58 (m, 6H), 7.41–7.31 (m, 8H). ¹³C NMR (100 MHz, CDCl₃): δ 131.7, 131.6, 128.4, 128.3, 128.0, 125.8, 123.2, 93.6, 88.3. DART HRMS *m/z* calcd. for C₂₂H₁₅ ([M + H]⁺), 279.1168, found 279.1160.

(6) Lehnher, D.; Alzola, J. M.; Lobkovsky, E. B.; Dichtel, W. R. *Chem. Eur. J.* **2015**, *21*, 18122–18127.

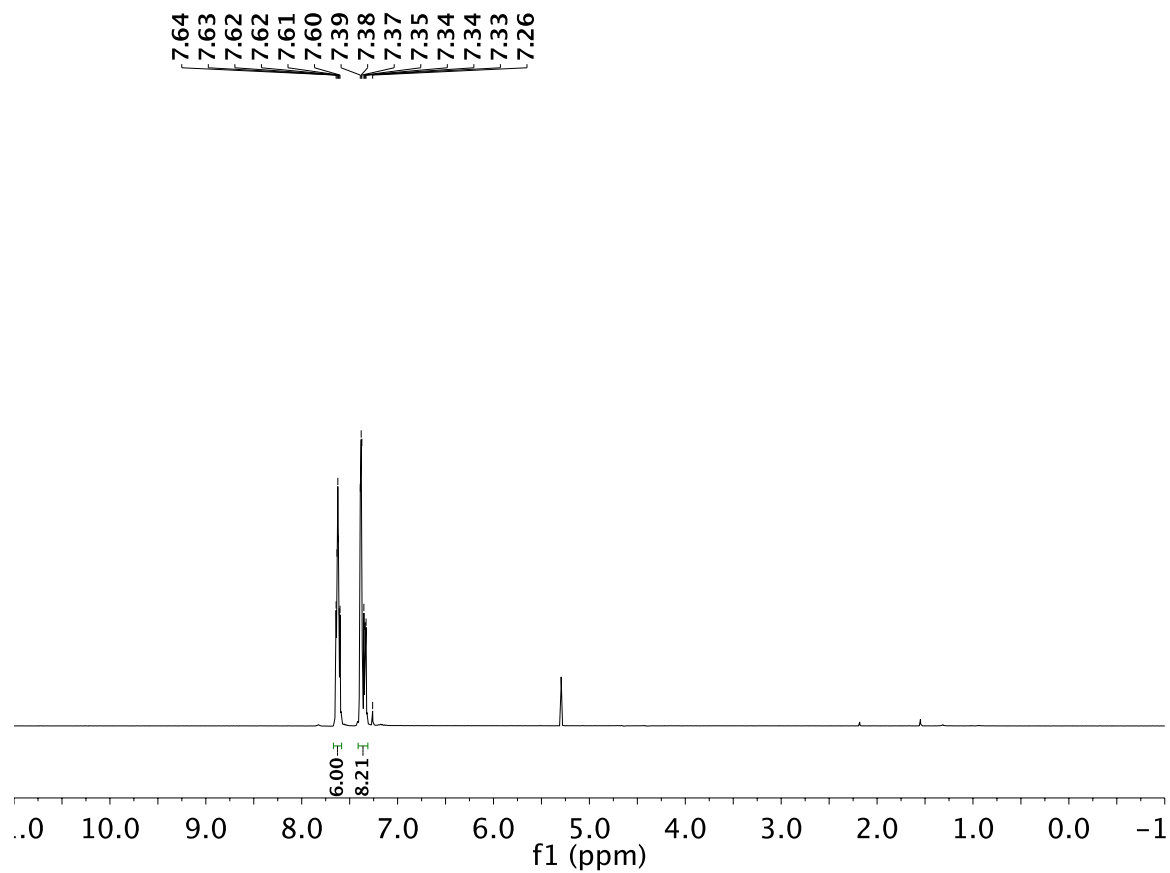


Figure S1. ^1H NMR (400 MHz) spectrum of **2** in CDCl_3 .

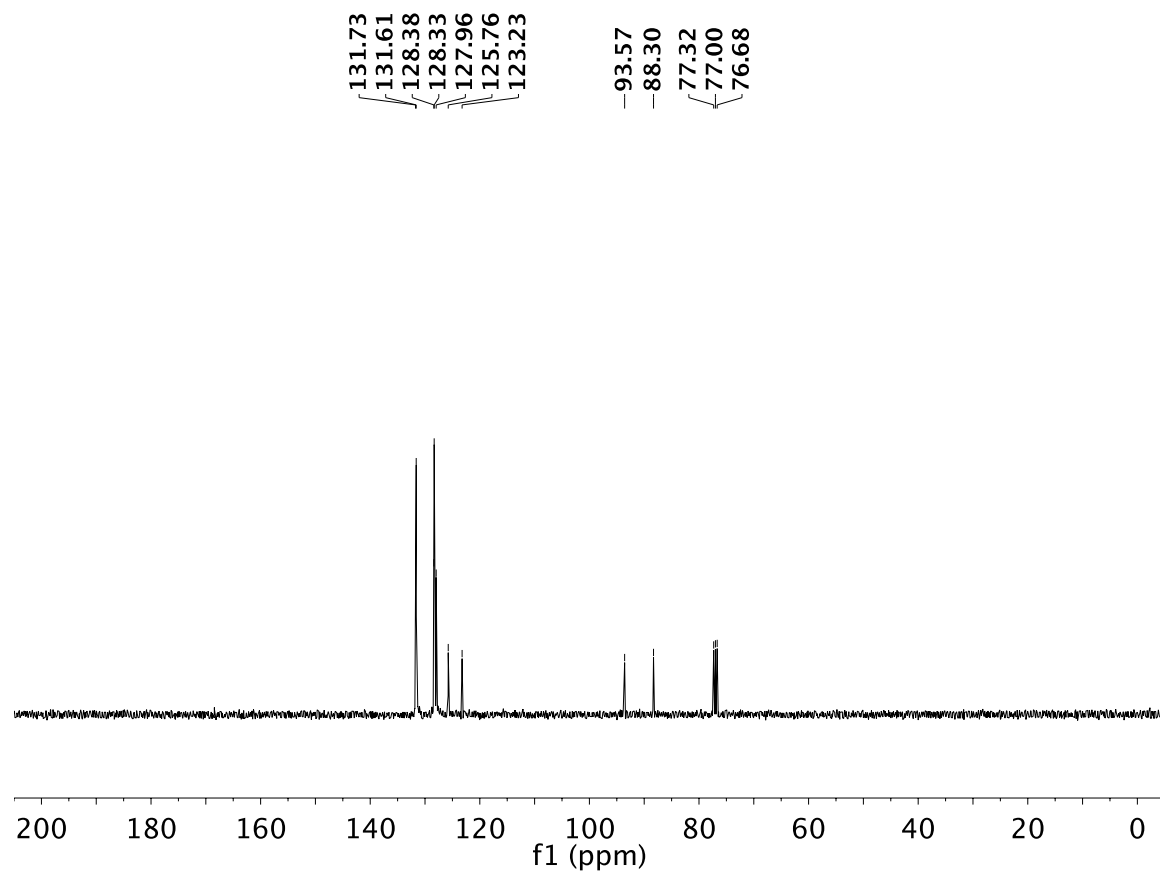
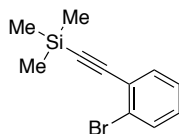
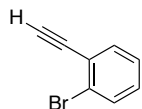


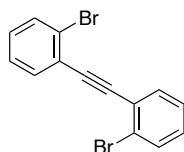
Figure S2. ^{13}C NMR (100 MHz) spectrum of **2** in CDCl_3 .



S4: This compound has been previously reported in the literature.



S5: To a solution of **S4** (3.00 g, 11.8 mmol) in MeOH (60 mL) was added K_2CO_3 (2.13 g, 15.4 mmol) and H_2O (1 mL). The reaction was stirred at rt for 1.5 h prior to being diluted with hexanes. The organic phase was washed with H_2O (2×) and the combined aqueous phase was extracted one additional time with hexanes. The combined organic phase was dried over anhyd. Na_2SO_4 , filtered through a short pad of silica gel (using 20% CH_2Cl_2 in hexanes as eluent), and the solvent was removed *in vacuo* to afford **S5** (1.99 g, 93%) as a clear colorless liquid. 1H NMR was consistent with the reported literature spectra and the compound was used immediately without further characterization.



S6: To a flask containing $Pd(PPh_3)_4$ (0.476 g, 0.412 mmol) and CuI (0.118 g, 0.618 mmol) under an atmosphere of nitrogen was added via cannula a solution of **S5** (1.99 g, 11.0 mmol) and 1,2-diiodobenzene (3.11 g, 11.0 mmol) in THF (42 mL) and diisopropylamine (15.4 mL, 11.1 g, 110 mmol) which had been deoxygenated by sparging with N_2 for 10 min. The mixture was stirred for 2 h at rt before being diluted with CH_2Cl_2 . The organic phase was washed with H_2O , 5% aq. NH_4Cl (2×), and dried over anhyd. Na_2SO_4 , filtered through a short pad of silica gel (using CH_2Cl_2 as eluent), and the solvent was removed *in vacuo*. Column chromatography (silica gel, gradient 5% to 10% CH_2Cl_2 in hexanes) followed by recrystallization as describe below afforded **S6** (2.69 g, 78%) as a white solid. The recrystallization was achieved by dissolving the sample in minimal amount of CH_2Cl_2 followed by the dropwise addition of this solution to a flask containing MeOH accompanied with stirring. The mixture was then cooled to $-78\text{ }^\circ C$ and filtered and washed with minimal cold MeOH. $R_f = 0.8$ (10 % CH_2Cl_2 in hexanes). IR ($CDCl_3$ cast film): 3059 (w), 1591 (w), 1557 (w), 1479 (m), 1458 (m), 1433 (m), 1049 (m), 1040 (m), 1027 (m), 945 (w), 749 (s), 723 (w), 710 (w), 661 (w) cm^{-1} . 1H NMR (400 MHz, $CDCl_3$): δ 7.61 (ddd, $J = 7.6, 3.2, 1.3$ Hz, 4H), 7.30 (td, $J = 7.6, 1.2$ Hz, 2H), 7.19 (td, $J = 7.9, 1.7$ Hz, 2H). ^{13}C NMR (100 MHz, $CDCl_3$): δ 133.6, 132.5, 129.7, 127.0, 125.5, 125.1, 92.2. DART HRMS m/z calcd. for $C_{14}H_9Br_2$ ($[M + H]^+$), 334.9066, found 334.9051.

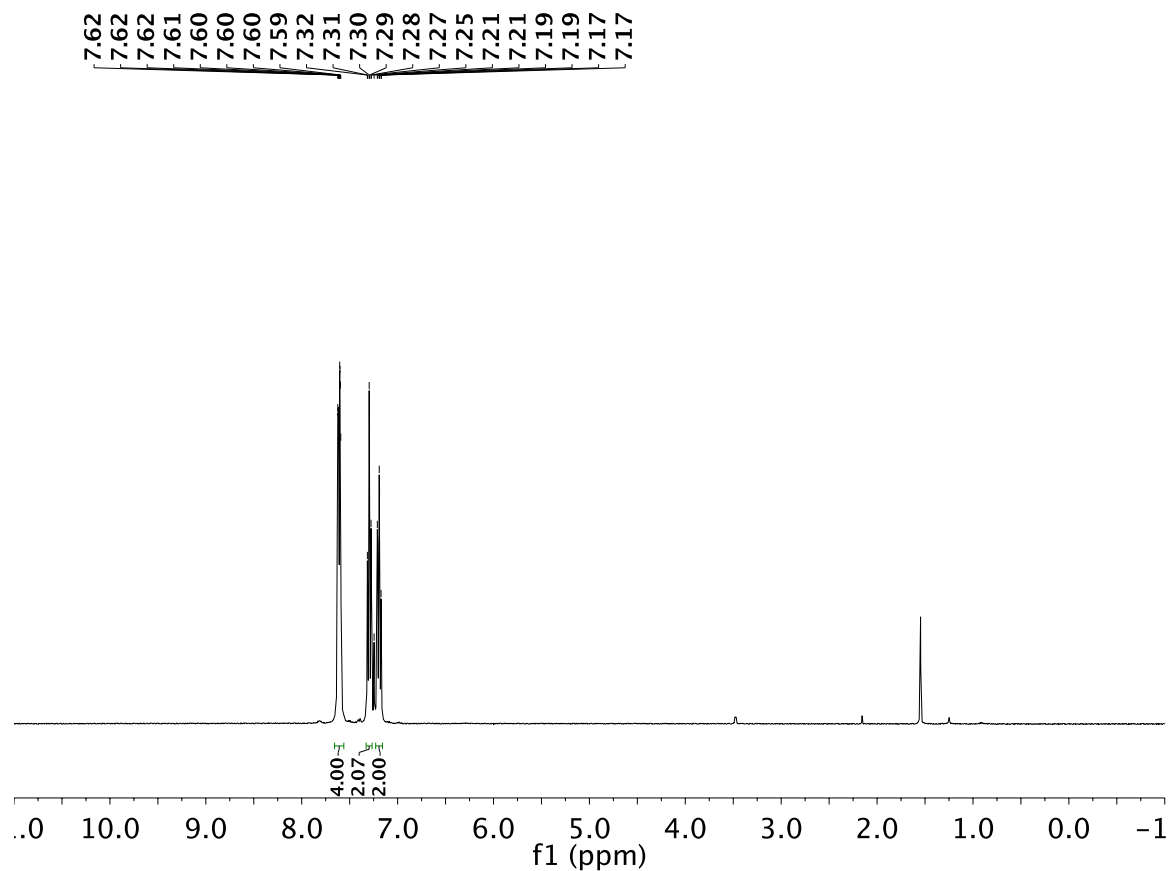


Figure S3. ^1H NMR (400 MHz) spectrum of **S6** in CDCl_3 .

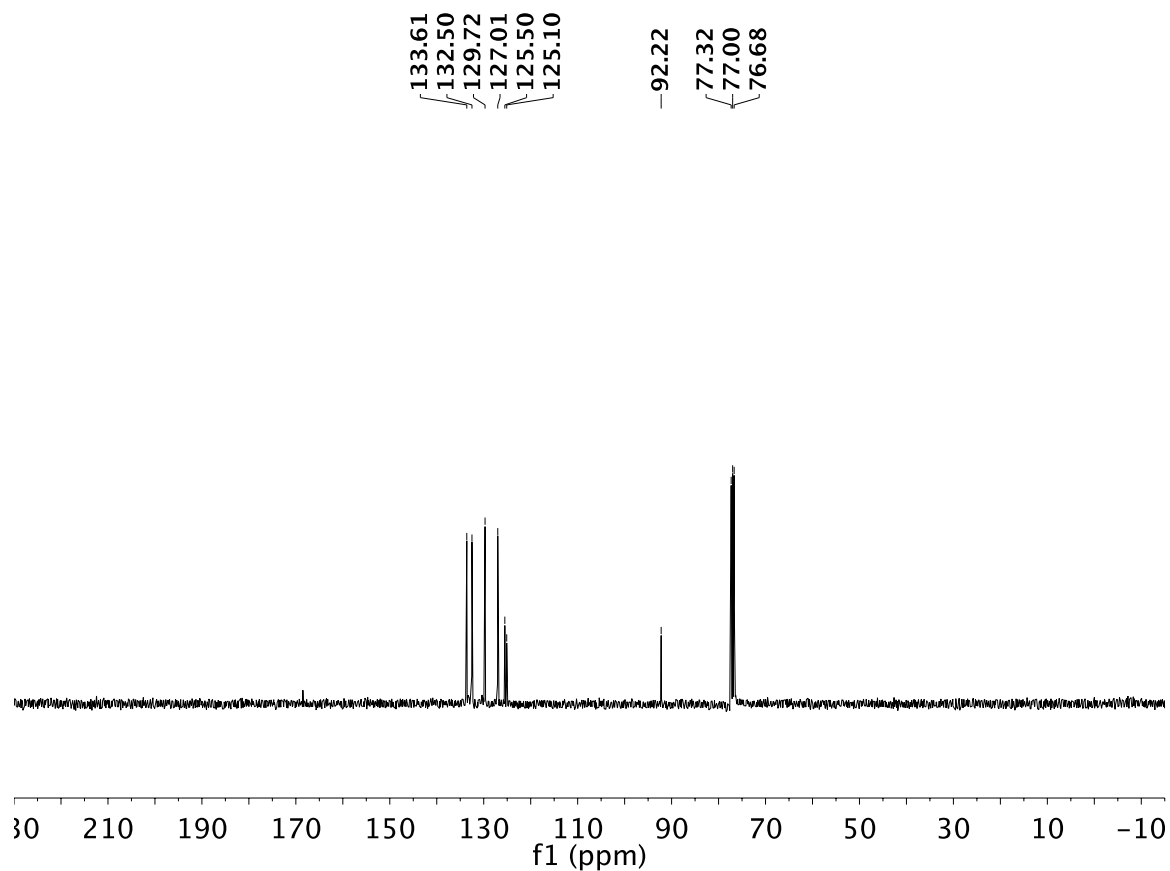
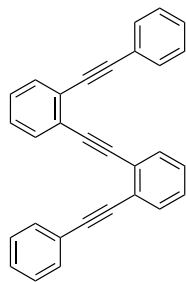


Figure S4. ^{13}C NMR (100 MHz) spectrum of **S6** in CDCl_3 .



3: To a flask containing $\text{Pd}(\text{PhCN})_2\text{Cl}_2$ (0.086 g, 0.223 mmol), $t\text{-Bu}_3\text{PHBF}_4$ (0.129 g, 0.446 mmol) and CuI (0.043 g, 0.223 mmol) under an atmosphere of nitrogen was added anhydrous, deoxygenated dioxane (6 mL) followed by deoxygenated diisopropylamine (6.3 mL, 4.5 g, 45 mmol) accompanied by stirring at rt. To this mixture was added a solution of phenylacetylene (1.2 mL, 1.1 g, 11 mmol) and 1,2-bis(2-bromophenyl)ethyne (**S6**, 1.50 g, 4.46 mmol) in anhydrous, deoxygenated dioxane (20 mL). Deoxygenated mixtures were obtained by sparging with N_2 . The combined mixture was stirred for 16 h at rt before being diluted with CH_2Cl_2 . The organic phase was washed with H_2O (2 \times), 5% aq. NH_4Cl , and dried over anhyd. Na_2SO_4 , filtered through a short pad of silica gel (using 1:1 CH_2Cl_2 /hexanes as eluent), and the solvent was removed *in vacuo*. Column chromatography (silica gel, 15% CH_2Cl_2 in hexanes) followed by recrystallization from EtOH provided **3** (1.29 g, 76%) as a light beige solid. R_f = 0.3 (15 % CH_2Cl_2 in hexanes). IR (CDCl_3 cast film): 3059 (w), 2216 (w), 1598 (w), 1495 (m), 1444 (w), 753 (s), 689 (m) cm^{-1} . ^1H NMR (600 MHz, CDCl_3): δ 7.65–7.58 (m, 4H), 7.57–7.53 (m, 4H), 7.36–7.27 (m, 10H). ^{13}C NMR (150 MHz, CDCl_3): δ 132.0, 131.8, 131.7, 128.3, 128.2, 128.1, 127.9, 125.80, 125.76, 123.2, 93.7, 92.3, 88.2. DART HRMS m/z calcd. for $\text{C}_{30}\text{H}_{19}$ ($[\text{M} + \text{H}]^+$), 379.1481, found 379.1467.

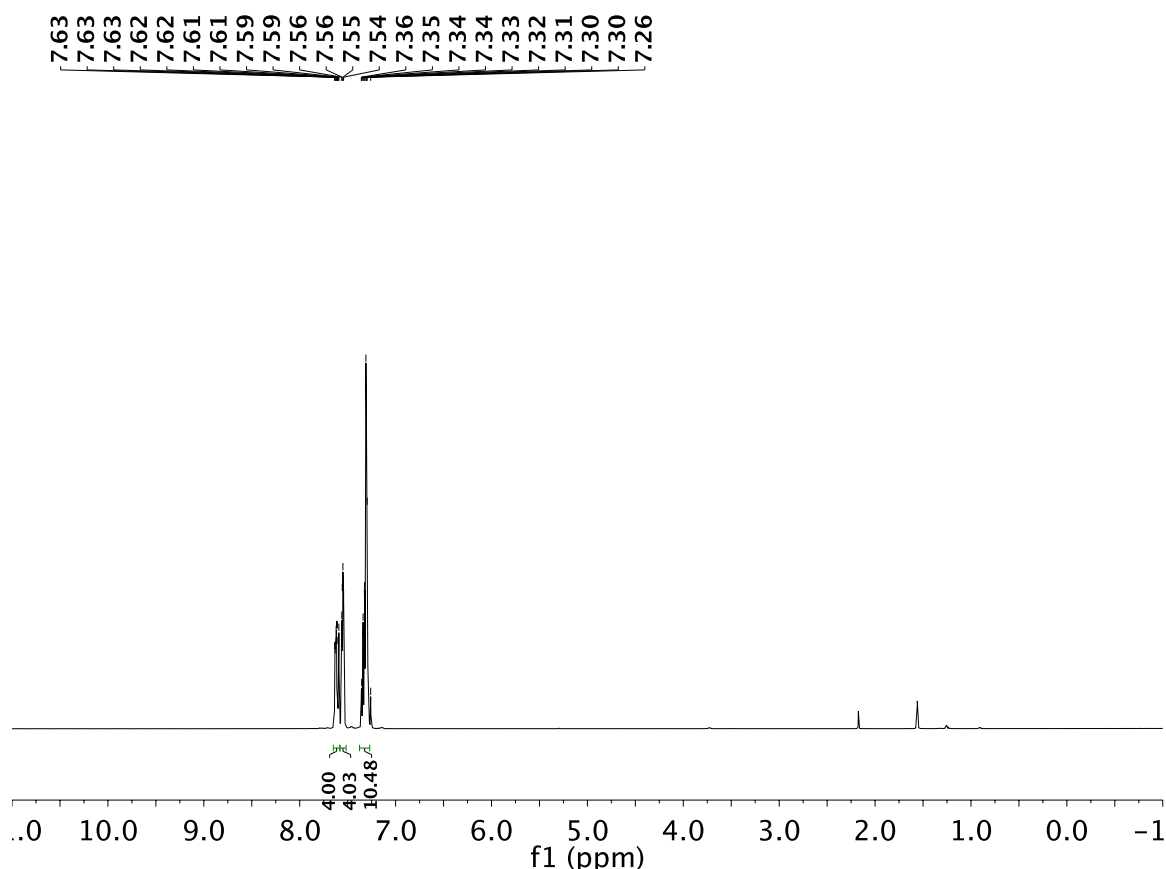


Figure S5. ^1H NMR (500 MHz) spectrum of **3** in CDCl_3 .

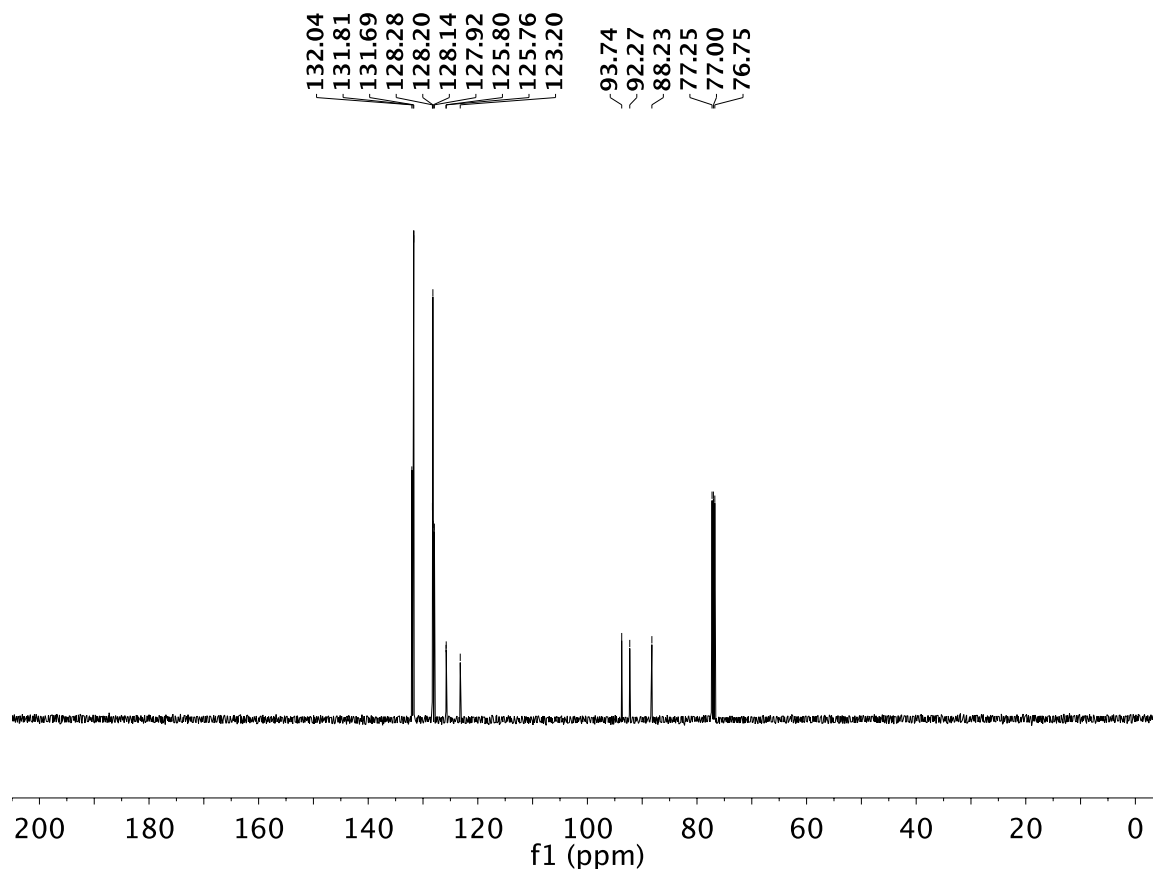
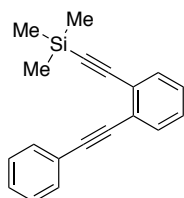


Figure S6. ^{13}C NMR (125 MHz) spectrum of **3** in CDCl_3 .



S7: The synthesis of this compound was previously reported in the literature. IR (CDCl_3 cast film): 3059 (vw), 2981 (w), 2970 (w), 2961 (w), 2897 (w), 2158 (w), 1598 (w), 1493 (m), 1472 (w), 1443 (m), 1249 (m), 1210 (w), 1160 (vw), 1094 (w), 1069 (w), 1036 (w), 1027 (w), 869 (m), 838 (s), 752 (s), 689 (m), 643 (m) cm^{-1} . ^1H NMR (500 MHz, CDCl_3): δ 7.66–7.63 (m, 2H), 7.60–7.56 (m, 2H), 7.44–7.38 (m, 3H), 7.36–7.28 (m, 2H), 0.35 (s, 9H). ^{13}C NMR (125 MHz, CDCl_3): δ 132.2, 131.6, 128.35, 128.24, 128.17, 127.8, 126.0, 125.5, 123.2, 103.5, 98.5, 93.4, 88.2, 0.0. DART HRMS m/z calcd. for $\text{C}_{19}\text{H}_{19}\text{Si}$ ($[\text{M} + \text{H}]^+$), 275.1215, found 275.1250.

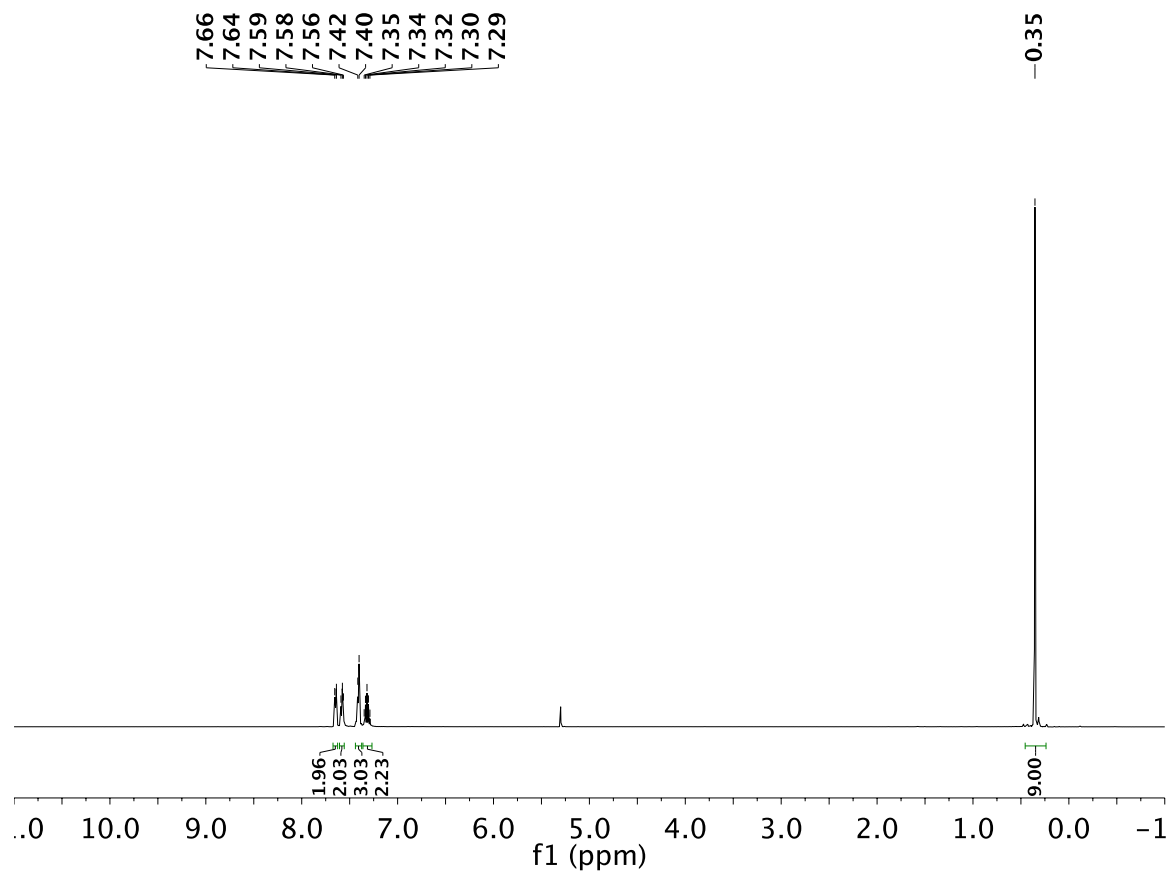


Figure S7. ^1H NMR (500 MHz) spectrum of **S7** in CDCl_3 .

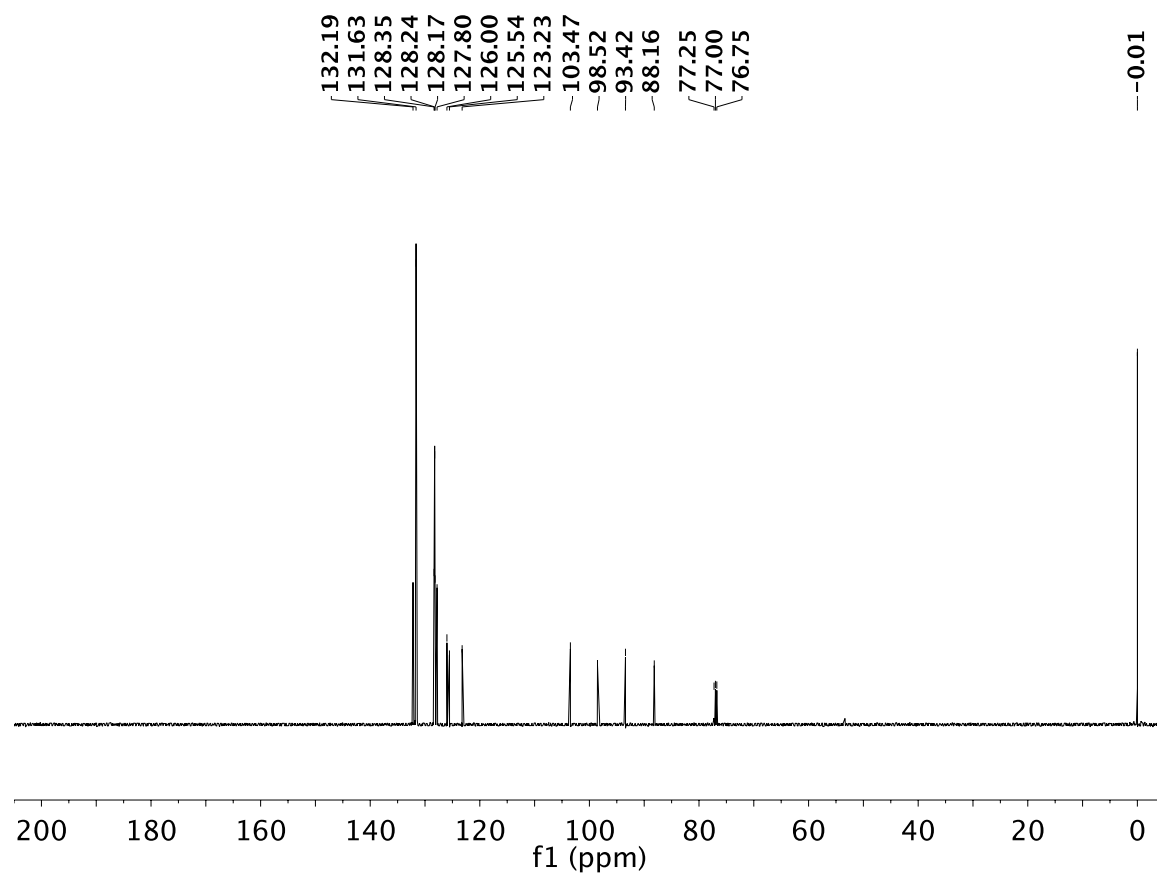
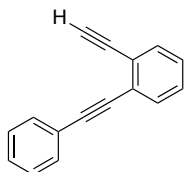
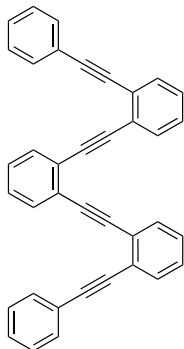


Figure S8. ^{13}C NMR (125 MHz) spectrum of **S7** in CDCl_3 .



S8: To a solution of **S7** (2.62 g, 9.55 mmol) in MeOH (50 mL) was added K_2CO_3 (1.72 g, 12.3 mmol) and H_2O (1 mL). The reaction was stirred at rt for 1.5 h prior to being diluted with hexanes. The organic phase was washed with H_2O (2 \times) and dried over anhyd. Na_2SO_4 , filtered through a short pad of silica gel (using 20% CH_2Cl_2 in hexanes as eluent), and the solvent was removed *in vacuo* to afford **S8** as a pale yellow liquid. ^1H NMR was consistent with the reported literature spectra and the compound was used immediately without further characterization.



4: To a flask containing $\text{Pd}(\text{PPh}_3)_4$ (0.130 g, 0.113 mmol) and CuI (0.021 g, 0.113 mmol) under an atmosphere of nitrogen was added via cannula a solution of **S8** (0.760 g, 3.76 mmol) and 1,2-diiodobenzene (0.250 mL, 0.620 g, 1.88 mmol) in toluene (12.5 mL) and diisopropylamine (4.0 mL, 2.9 g, 28 mmol) which had been deoxygenated by sparging with N_2 for 10 min. The mixture was stirred for 16 h at rt before being diluted with CH_2Cl_2 . The organic phase was washed with H_2O , 5% aq. NH_4Cl (2 \times), and dried over anhyd. Na_2SO_4 , filtered through a short pad of silica gel (using CH_2Cl_2 as eluent), and the solvent was removed *in vacuo*. Column chromatography (silica gel, hexanes) afforded a light beige solid which was purified by crystallization via dissolving the solid in a mixture of CH_3Cl (ca. 1 mL), CH_2Cl_2 (ca. 1 mL), and MeOH (ca. 30 mL) by heating the mixture to 40 $^\circ\text{C}$ accompanied by stirring. Once fully dissolved, the mixture was cooled to -78 $^\circ\text{C}$ and the solid was collected by filtration and washed with cold MeOH to afford **4** (0.798 g, 89%) as a white solid. $R_f = 0.6$ (30 % CH_2Cl_2 in hexanes). IR (CDCl_3 cast film): 3059 (w), 2216 (w), 1597 (w), 1495 (m), 1477 (m), 1442 (m), 1316 (w), 907 (w), 750 (s), 732 (s), 688 (s) cm^{-1} . ^1H NMR (500 MHz, CDCl_3): δ 7.74–7.69 (m, 2H), 7.68–7.58 (m, 8H), 7.39–7.26 (m, 12H). ^{13}C NMR (125 MHz, CDCl_3): δ 132.14, 132.05, 131.62, 131.60, 128.24, 128.17, 128.1, 128.0, 127.8, 125.71, 125.67, 125.6, 123.2, 93.6, 92.5, 92.2, 88.3. DART HRMS m/z calcd. for $\text{C}_{38}\text{H}_{23}$ ($[\text{M} + \text{H}]^+$), 479.1794, found 479.1779.

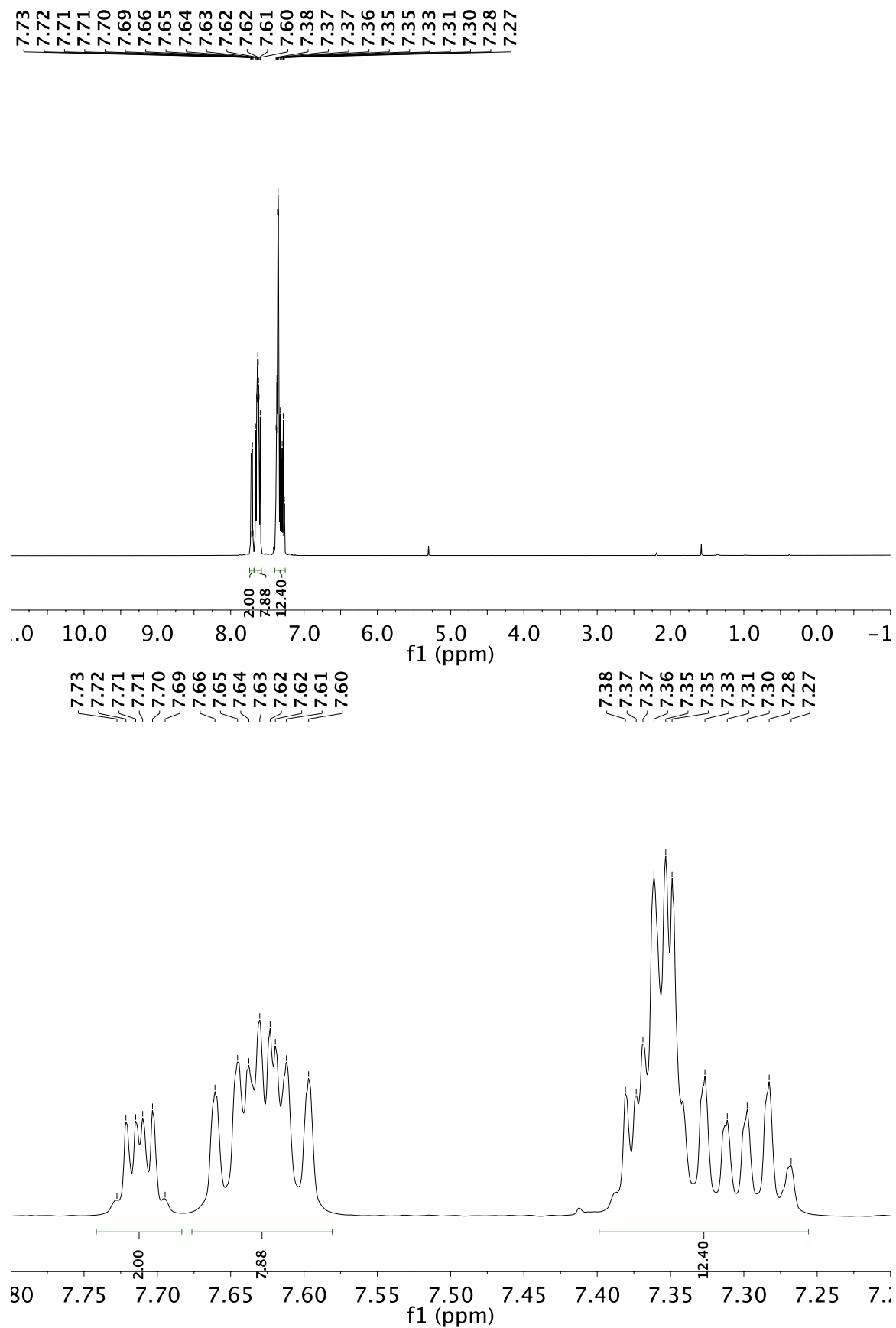


Figure S9. ^1H NMR (500 MHz) spectrum of **4** in CDCl_3 : (top) full view, (bottom) 7.80 to 7.20 ppm region.

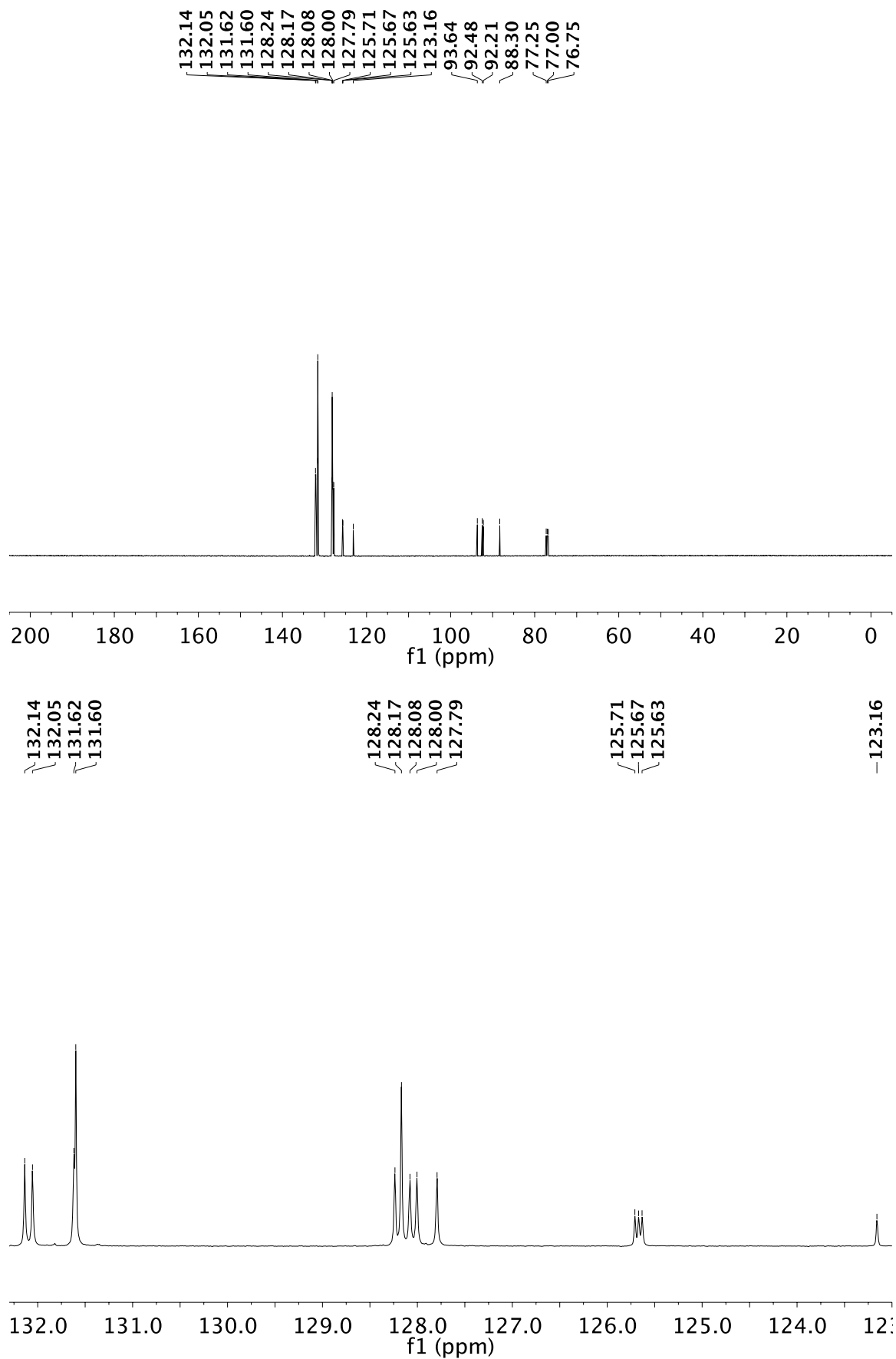
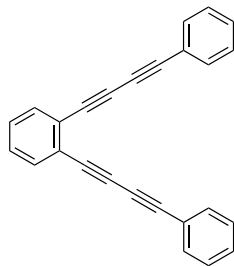
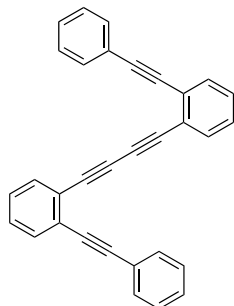


Figure S10. ^{13}C NMR (125 MHz) spectrum of **4** in CDCl_3 : (top) full view, (bottom) 132.3 to 122.0 ppm region.

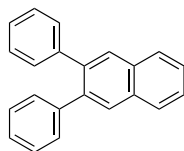


5: The synthesis of compound **5** has been previously reported.⁷



6: The synthesis of compound **6** has been previously reported.⁸

2.3 Hydrocarbon *ortho*-Arylenes



H-Ar-1: A solution of 1,2-diphenylacetylene (**1**, 0.300 g, 1.68 mmol) and benzaldehyde **S1** (0.625 g, 3.03 mmol) in 1,2-dichloroethane (24 mL), which had been deoxygenated by sparging with N₂ for 5 min, was transferred via cannula into a round bottom flask equipped with a water-cooled condenser containing Cu(OTf)₂ (0.061 g, 0.17 mmol) under a nitrogen atmosphere. TFA (0.64 mL, 0.96 g, 0.84 mmol) was immediately added. The mixture was heated in an oil bath to 100 °C for 1.5 h. The mixture was cooled to rt and diluted with CH₂Cl₂, poured into satd. aq. NaHCO₃ (150 mL), and extracted twice with CH₂Cl₂ (150 mL, 75 mL). The combined organic phase was washed with satd. aq. NH₄Cl, dried (Na₂SO₄), filtered, and the solvent was removed *in vacuo*. Column chromatography (silica gel, hexanes to 30% CH₂Cl₂ in hexanes) afforded **H-Ar-1** (0.454 g, 96%) as a white solid. *R*_f = 0.6 (30 % CH₂Cl₂ in hexanes). IR (CDCl₃ cast film): 3055 (w), 1601 (w), 1490 (m), 1449 (w), 1440 (w), 1074 (w), 1022 (w), 907 (m), 891 (m), 798 (w), 765 (s), 747 (m), 731 (m), 699 (s) cm⁻¹. ¹H NMR (300 MHz, CDCl₃): δ 8.03–7.98 (m, 2H), 7.98–7.89 (m, 2H), 7.6–7.52 (m, 2H), 7.39–7.28 (m, 10H). ¹³C NMR (75 MHz, CDCl₃): δ 141.4, 139.0, 132.7, 130.0, 129.4, 127.8, 127.6, 126.5, 126.2. DART HRMS *m/z* calcd. for C₂₂H₁₆ (M⁺), 280.1247, found 280.1237.

(7) Schriener, P. R.; Prall, M.; Lutz, V. *Angew. Chem. Int. Ed.* **2003**, 42, 5757–5760.

(8) Spence, J. D.; Lackie, M. L.; Clayton, N. A.; Toscano, S. A.; Farmer, M. A.; Popova, E.; Olmstead, M. M. *Tet. Lett.* **2014**, 55, 1569–1572.

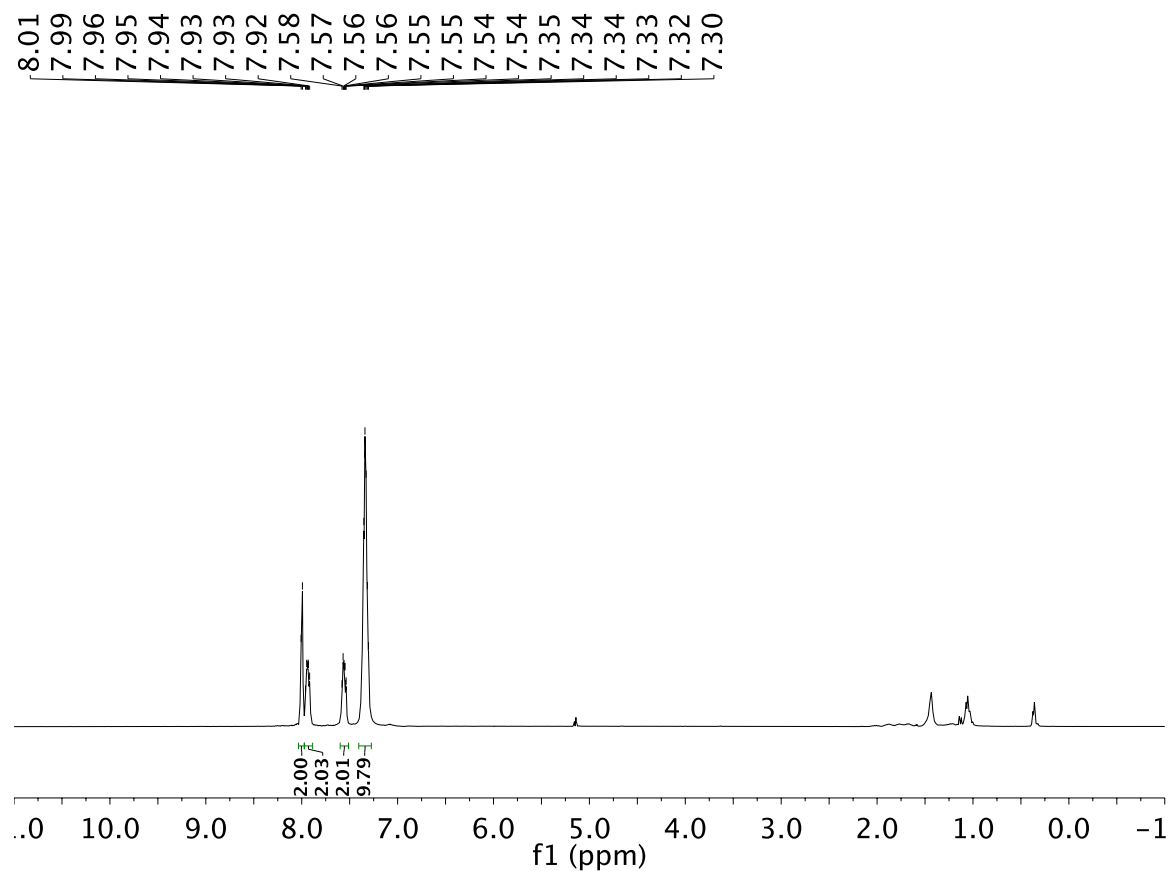


Figure S11. ^1H NMR (300 MHz) spectrum of **H-Ar-1** in CDCl_3 .

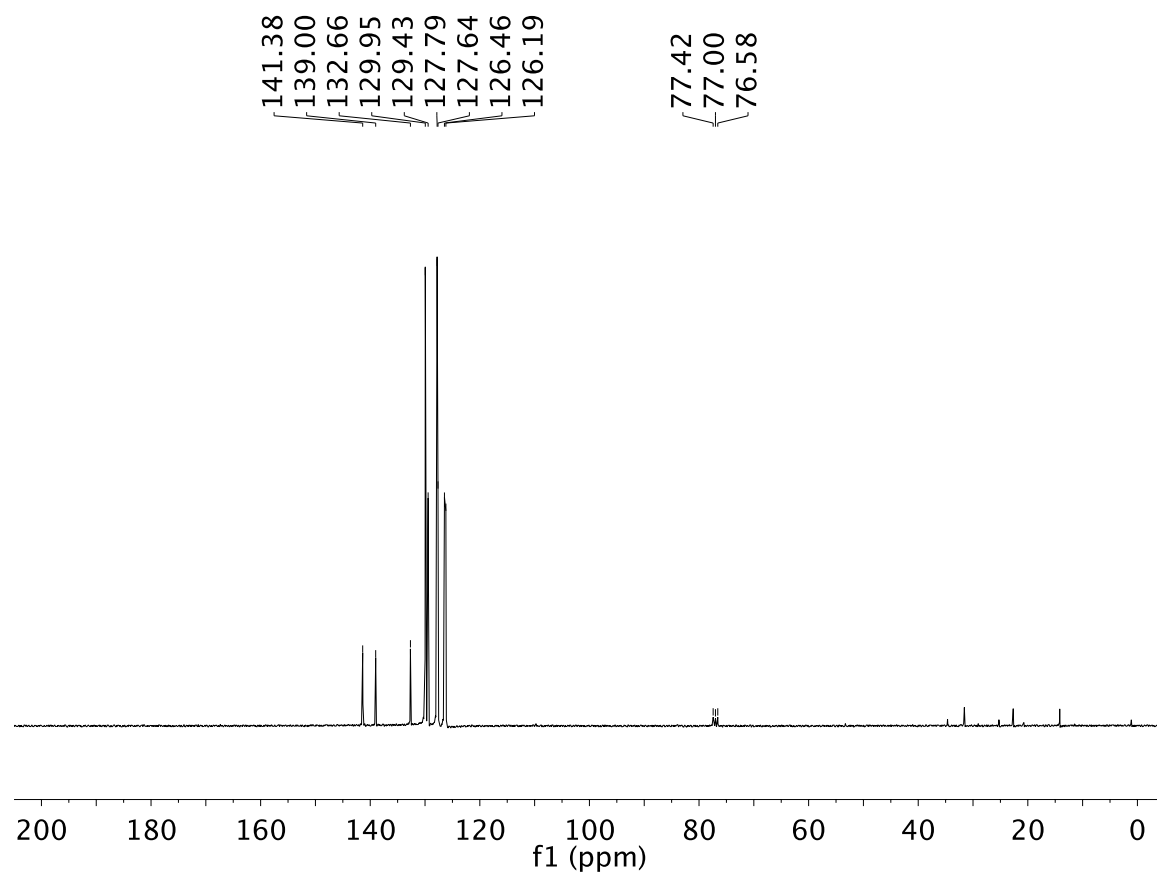
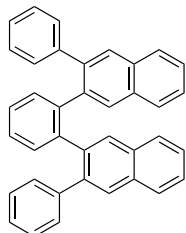


Figure S12. ^{13}C NMR (75 MHz) spectrum of **H-Ar-1** in CDCl_3 .



H-Ar-2: A solution of 1,2-bis(phenylethynyl)benzene (**o-PE-2**, 0.250 g, 0.898 mmol) and benzaldehyde **S1** (0.741 g, 3.59 mmol) in 1,2-dichloroethane (15 mL), which had been deoxygenated by sparging with N₂ for 5 min, was transferred via cannula into a round bottom flask equipped with a water-cooled condenser containing Cu(OTf)₂ (0.064 g, 0.180 mmol) under a nitrogen atmosphere. TFA (0.55 mL, 0.82 g, 7.2 mmol) was immediately added. The mixture was heated in an oil bath to 100 °C for 1 h. The mixture was cooled to rt and diluted with CH₂Cl₂, poured into satd. aq. NaHCO₃ (150 mL), and extracted twice with CH₂Cl₂ (150 mL, 75 mL). The combined organic phase was washed with satd. aq. NH₄Cl, dried (Na₂SO₄), filtered, and the solvent was removed *in vacuo*. Column chromatography (silica gel, hexanes to 20% CH₂Cl₂ in hexanes) afforded **H-Ar-2** (0.328 g, 76%) as a white solid. *R*_f = 0.6 (20% CH₂Cl₂ in hexanes). IR (CDCl₃ cast film): 3055 (w), 1599 (w), 1489 (m), 1445 (w), 1431 (w), 1023 (w), 895 (m), 763 (s), 748 (m), 733 (m), 714 (m), 700 (s) cm⁻¹. ¹H NMR (500 MHz, CDCl₃): δ 7.71–7.65 (m, 2H), 7.51–7.33 (m, 12H), 7.15 (t, *J* = 7.3 Hz, 2H), 6.91 (t, *J* = 7.5 Hz, 4H), 6.50–6.44 (m, 6H). ¹³C NMR (125 MHz, CDCl₃): δ 141.2, 141.0, 138.8, 138.1, 132.5, 132.3, 131.7, 130.8, 129.1, 128.3, 127.8, 127.5, 127.4, 127.3, 125.9, 125.7, 125.3. DART HRMS *m/z* calcd. for C₃₈H₂₇ ([M + H]⁺), 483.2107, found 483.2091. Crystals suitable for X-ray crystallographic analysis were obtained from solutions of **H-Ar-2** in 1,2-dichloroethane that were allowed to slowly cool from 100 °C to rt, for X-ray data of **H-Ar-2**, see: CCDC-1483959.

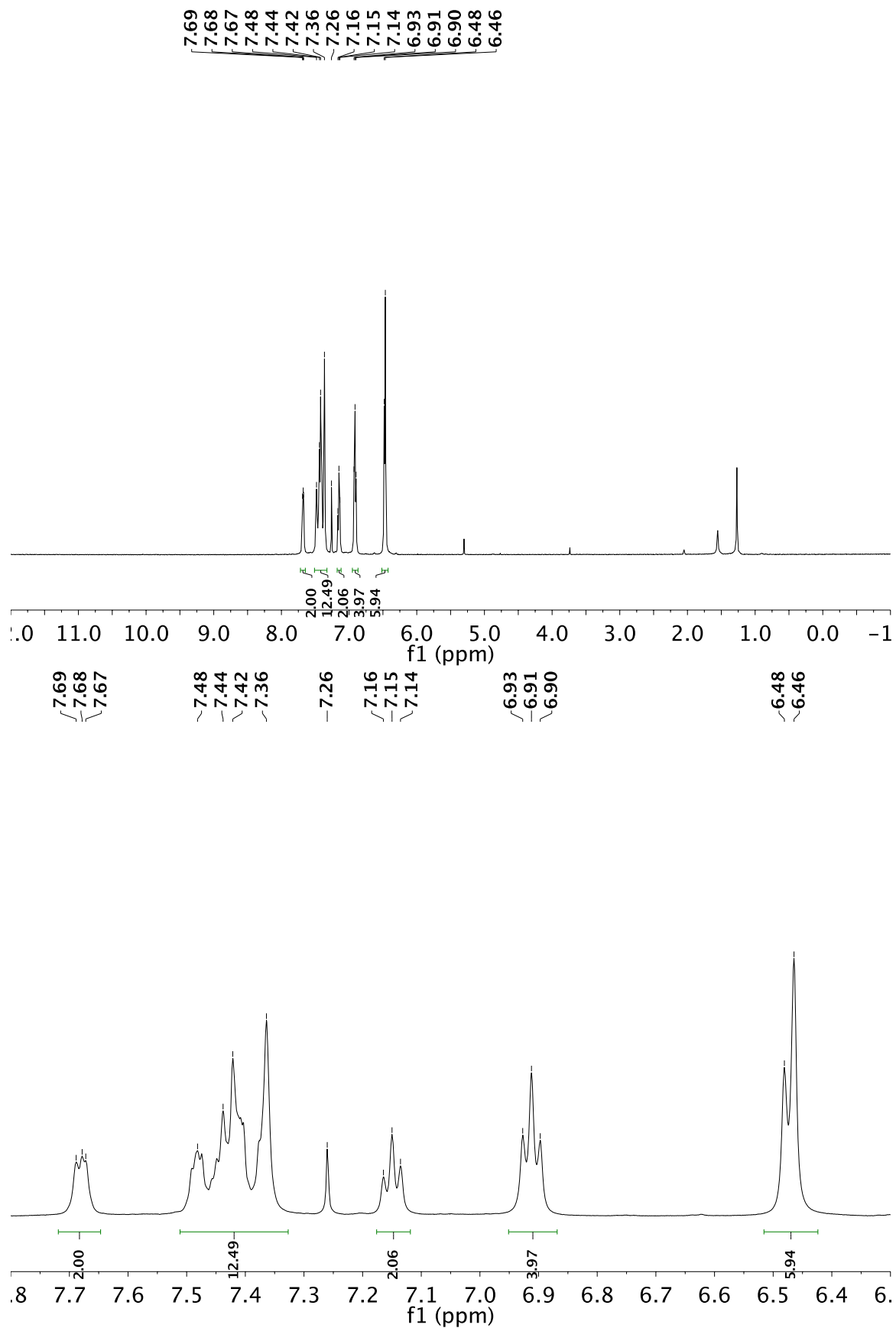


Figure S13. ^1H NMR (500 MHz) spectrum of **H-Ar-2** in CDCl_3 : (top) full view, (bottom) 7.80 to 6.30 ppm region.

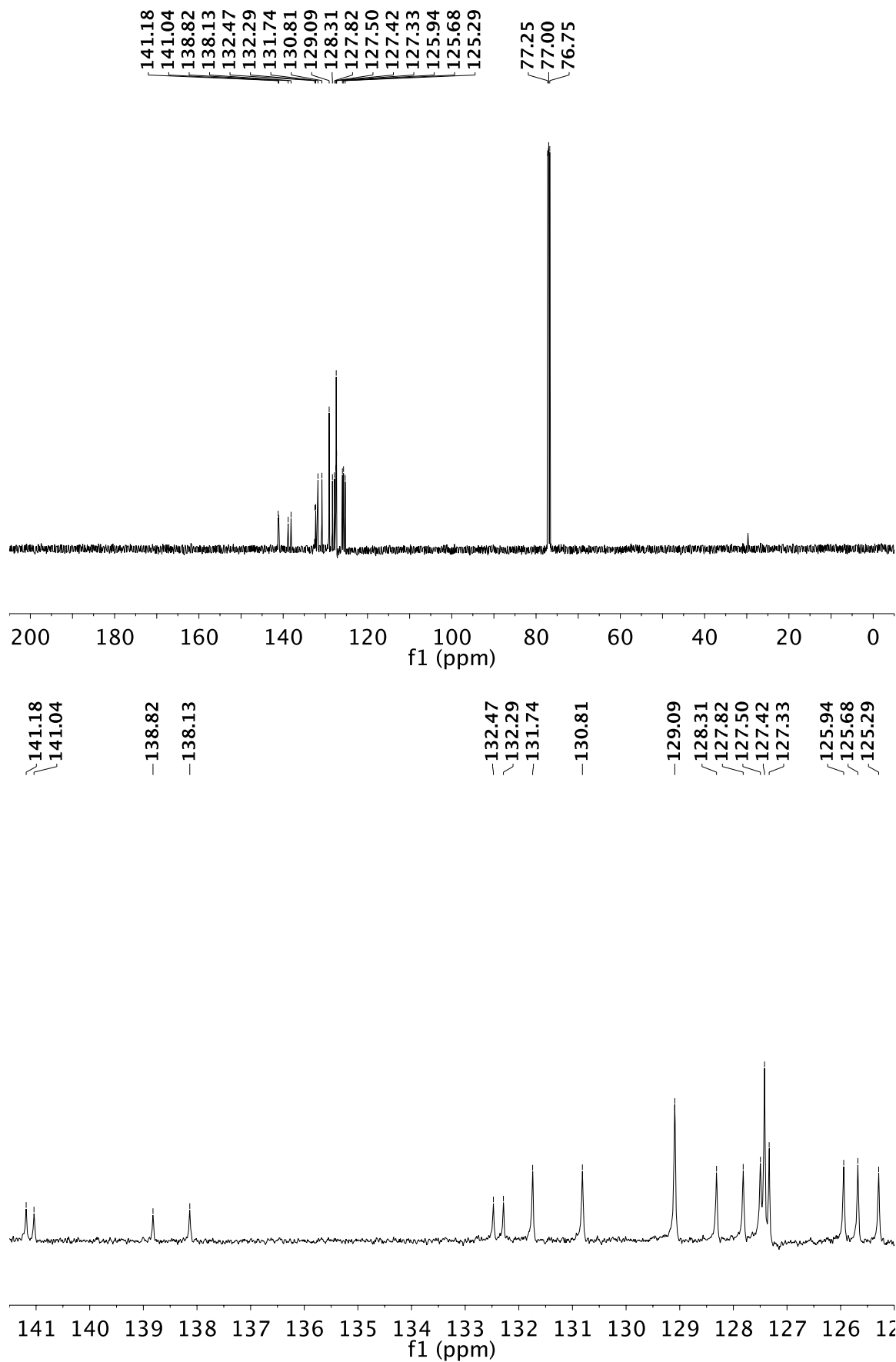
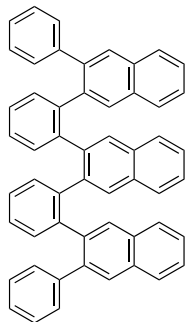


Figure S14. ^{13}C NMR (125 MHz) spectrum of **H-Ar-2** in CDCl_3 : (top) full view, (bottom) 141.5 to 125.0 ppm region.



H-Ar-3: A solution of **3** (0.600 g, 1.59 mmol) and benzaldehyde **S1** (1.96 g, 9.51 mmol) in 1,2-dichloroethane (21 mL), which had been deoxygenated by sparging with N₂ for 5 min, was transferred via cannula into a round bottom flask equipped with a water-cooled condenser containing Cu(OTf)₂ (0.172 g, 0.476 mmol) under a nitrogen atmosphere. TFA (1.5 mL, 2.2 g, 19.0 mmol) was immediately added. The mixture was heated in an oil bath to 100 °C for 1.5 h. The mixture was cooled to rt and diluted with CH₂Cl₂, poured into satd. aq. NaHCO₃ (150 mL), and extracted twice with CH₂Cl₂ (150 mL, 75 mL). The combined organic phase was washed with satd. aq. NH₄Cl, dried (Na₂SO₄), filtered, and the solvent was removed *in vacuo*. Column chromatography (silica gel, 20% to 40% CH₂Cl₂ in hexanes) afforded **H-Ar-3** (0.574 g, 53%) as a white solid. *R*_f = 0.8 (30% CH₂Cl₂ in hexanes). IR (CDCl₃ cast film): 3052 (w), 1593 (w), 1490 (m), 1446 (w), 1428 (w), 1025 (w), 908 (m), 889 (m), 761 (s), 744 (s), 733 (s), 697 (s) cm⁻¹. ¹H NMR (500 MHz, CDCl₃): δ 7.70 (d, *J* = 7.8 Hz, 2H), 7.60 (d, *J* = 8.0 Hz, 2H), 7.51–7.42 (m, 4H), 7.33–7.27 (m, 6H), 7.25–7.21 (m, 2H), 7.18 (t, *J* = 7.3 Hz, 2H), 6.97 (s, 2H), 6.90 (t, *J* = 7.2 Hz, 2H), 6.57 (t, *J* = 7.5 Hz, 4H), 6.21 (t, *J* = 7.3 Hz, 2H), 6.14 (d, *J* = 7.4 Hz, 4H), 6.01 (s, 2H), 5.69 (d, *J* = 7.5 Hz, 2H). ¹³C NMR (125 MHz, CDCl₃): δ 141.17, 141.08, 139.3, 139.1, 138.7, 138.6, 133.0, 132.5, 132.3, 131.9, 131.5, 130.7, 130.3, 128.5, 128.2, 128.0, 127.38, 127.34, 127.2, 126.6, 125.54, 125.50, 125.3, 124.5. DART HRMS *m/z* calcd. for C₅₄H₃₇ (M + H)⁺, 685.2890, found 685.2863. Crystals suitable for X-ray crystallographic analysis were obtained from solutions of **H-Ar-3** in CHCl₃ that were layered with hexanes and allowed to slowly evaporate at rt, for X-ray data of **H-Ar-3**, see: CCDC-1483961.

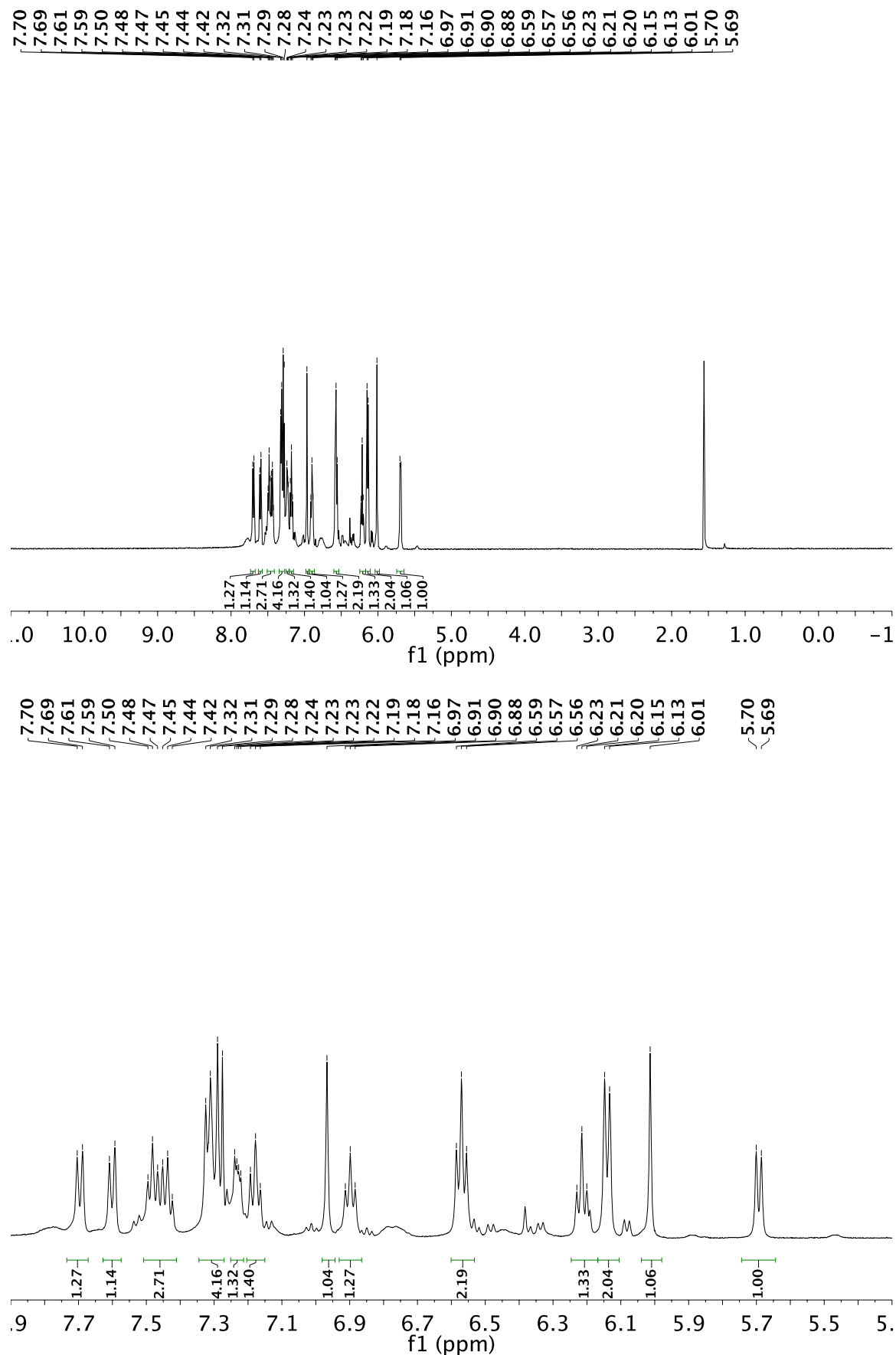


Figure S15. ^1H NMR (500 MHz) spectrum of **H-Ar-3** in CDCl_3 : (top) full view, (bottom) 7.90 to 5.30 ppm region.

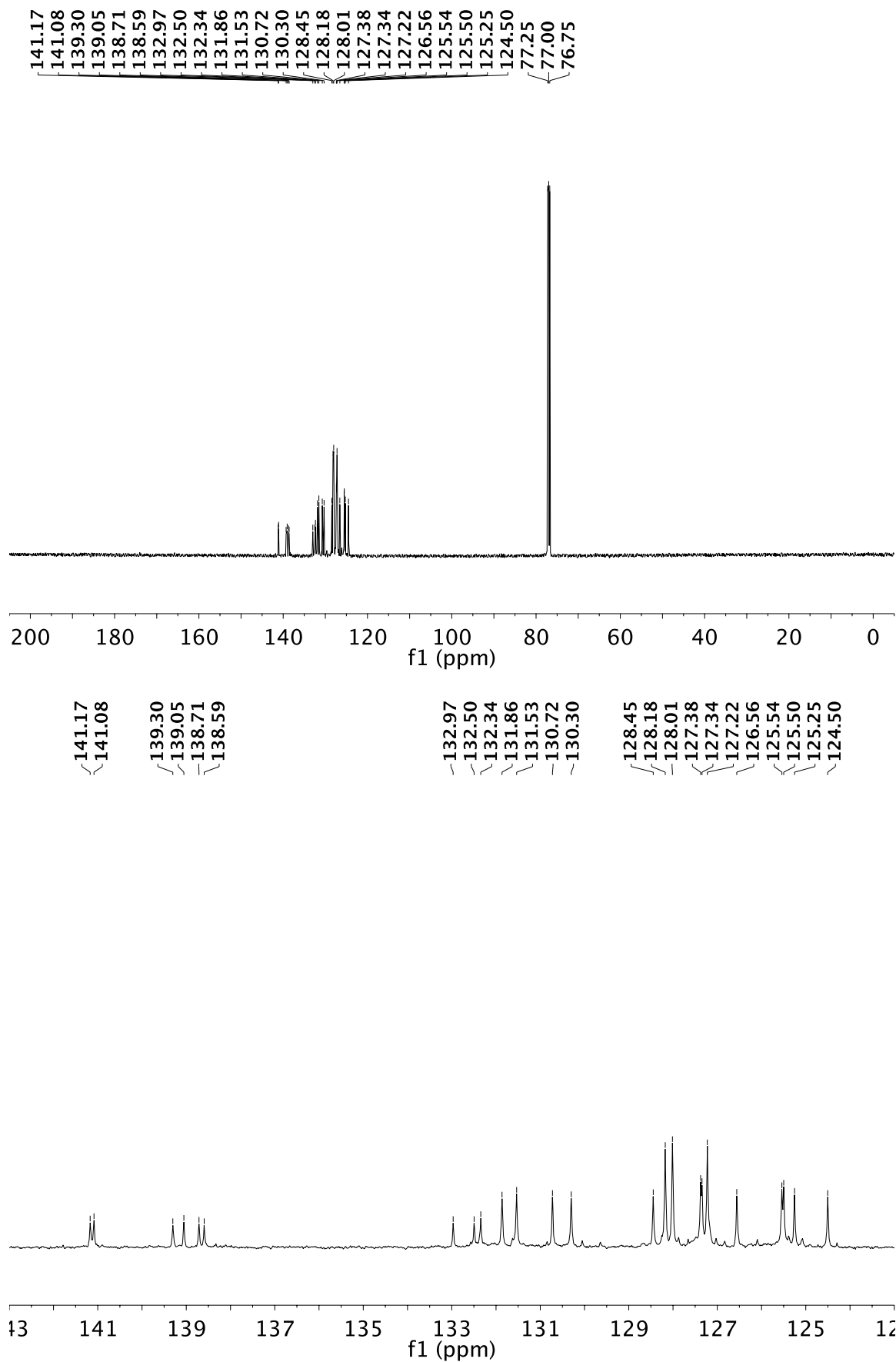
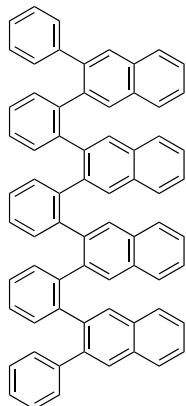


Figure S16. ^{13}C NMR (125 MHz) spectrum of **H-Ar-3** in CDCl_3 : (top) full view, (bottom) 143.0 to 123.0 ppm region.



H-Ar-4: A solution of **4** (0.400 g, 0.836 mmol) and benzaldehyde **S1** (1.72 g, 8.36 mmol) in 1,2-dichloroethane (16 mL), which had been deoxygenated by sparging with N₂ for 5 min, was transferred via cannula into a round bottom flask equipped with a water-cooled condenser containing Cu(OTf)₂ (0.181 g, 0.501 mmol) under a nitrogen atmosphere. TFA (1.92 mL, 2.86 g, 25.1 mmol) was immediately added. The mixture was heated in an oil bath to 100 °C for 1.5 h. The mixture was cooled to rt and diluted with CH₂Cl₂, poured into satd. aq. NaHCO₃ (150 mL), and extracted twice with CH₂Cl₂ (150 mL, 75 mL). The combined organic phase was washed with satd. aq. NH₄Cl, dried (Na₂SO₄), filtered, and the solvent was removed *in vacuo*. Column chromatography (silica gel, 20% to 50% CH₂Cl₂ in hexanes) afforded **H-Ar-4** (0.232 g, 31%) as a white solid. *R*_f = 0.4 (40% CH₂Cl₂ in hexanes). IR (CDCl₃ cast film): 3051 (m), 1594 (w), 1490 (m), 1427 (w), 1024 (w), 909 (m), 888 (m), 760 (s), 744 (s), 733 (s), 697 (m) cm⁻¹. ¹H NMR (600 MHz, CDCl₃): δ 7.64 (d, *J* = 8.1 Hz, 2H), 7.41–7.35 (m, 10H), 7.33 (t, *J* = 7.1 Hz, 2H), 7.23 (s, 1H), 7.22 (s, 1H), 7.21 (s, 2H), 7.09 (d, *J* = 7.4 Hz, 2H), 6.90 (t, *J* = 7.4 Hz, 2H), 6.87 (t, *J* = 7.3 Hz, 2H), 6.63 (s, 2H), 6.54 (t, *J* = 7.4 Hz, 4H), 6.49 (s, 2H), 6.07 (d, *J* = 7.5 Hz, 4H), 5.95 (s, 2H), 5.87 (dd, *J* = 5.4, 3.3 Hz, 2H), 5.78 (t, *J* = 7.4 Hz, 2H), 5.69 (dd, *J* = 5.3, 3.4 Hz, 2H), 5.54 (d, *J* = 7.6 Hz, 2H). ¹³C NMR (150 MHz, CDCl₃): δ 141.04, 140.99, 139.5, 139.3, 138.8, 138.6, 138.4, 138.3, 132.9, 132.8, 132.4, 132.3, 131.6, 131.2, 131.1, 130.4, 130.3, 129.8, 128.5, 128.2, 128.1, 128.0, 127.8, 127.3, 127.2, 127.1, 126.6, 126.2, 125.4, 125.3, 125.0, 124.6, 124.3. DART HRMS *m/z* calcd. for C₇₀H₄₇ ([M + H]⁺), 887.3672, found 887.3630. Crystals suitable for X-ray crystallographic analysis were obtained from solutions of **H-Ar-4** in CHCl₃ that were layered with CH₂Cl₂ (to afford ca. 1:1 v/v CH₂Cl₂/CHCl₃) followed by additional layering with hexanes and allowed to slowly evaporate at rt, for X-ray data of **H-Ar-4**, see: CCDC-1483960.

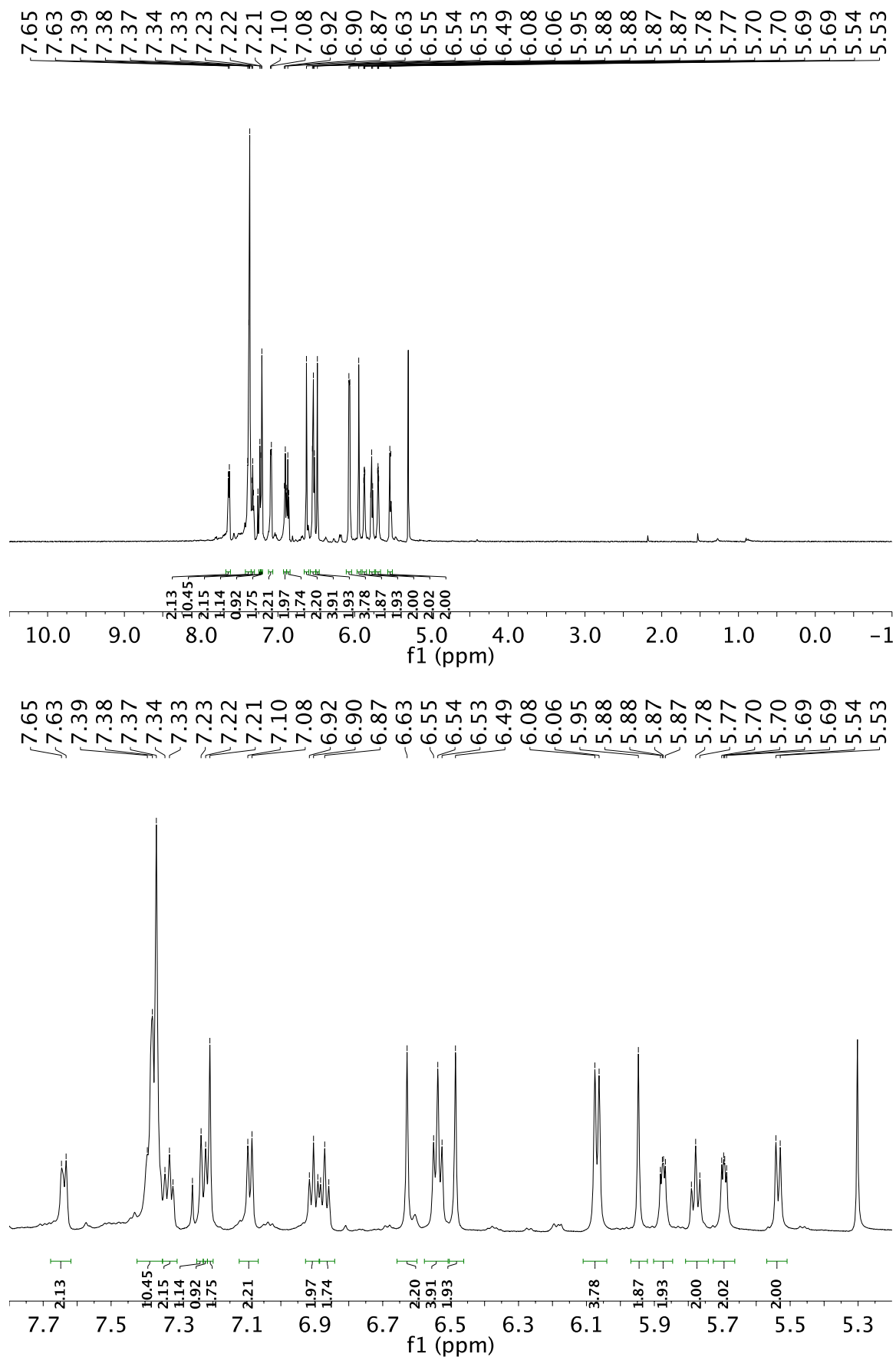


Figure S17. ^1H NMR (600 MHz) spectrum of **H-Ar-4** in CDCl_3 : (top) full view, (bottom) 7.80 to 5.20 ppm region (singlet at 5.3 ppm is CH_2Cl_2).

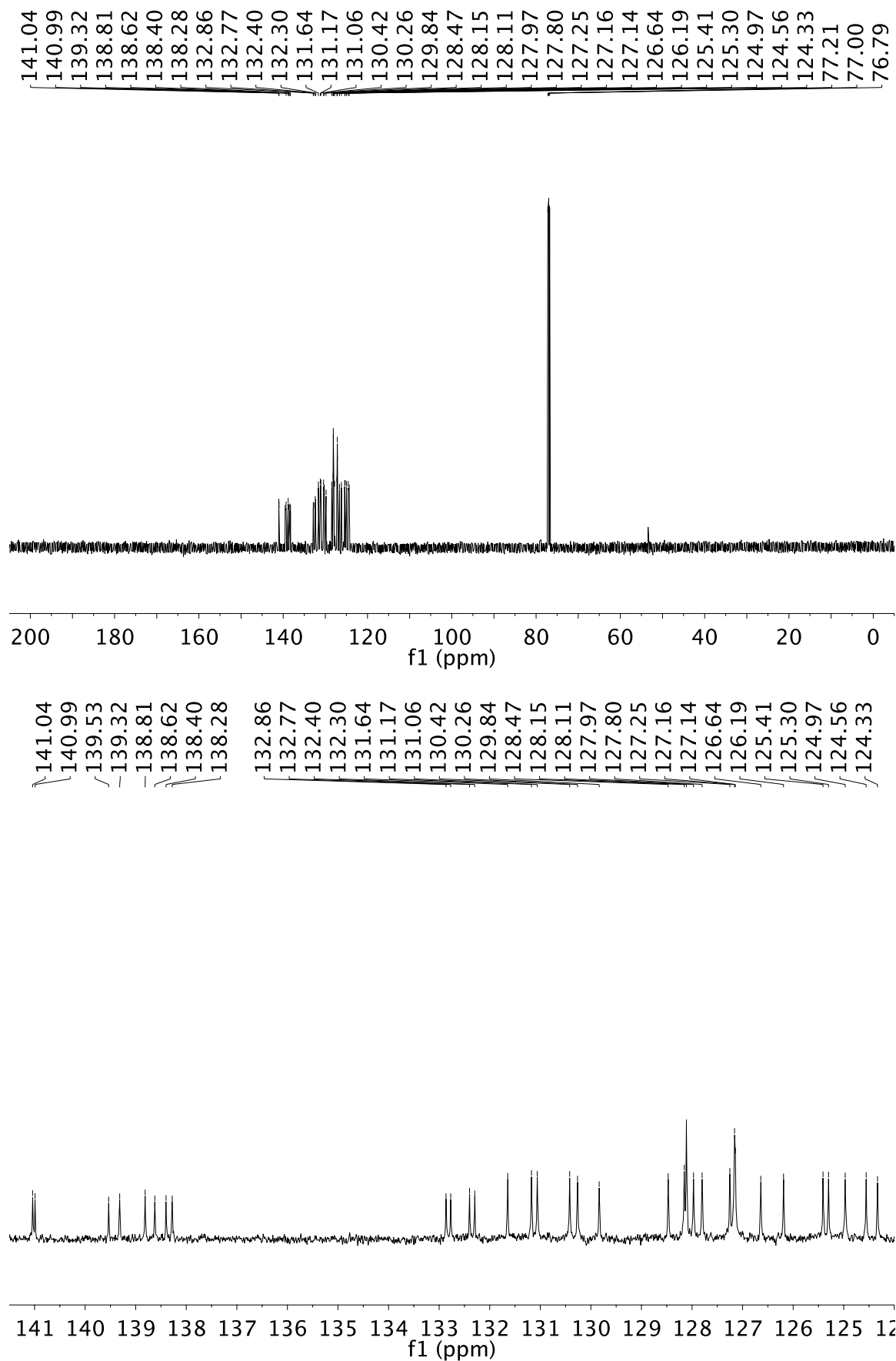
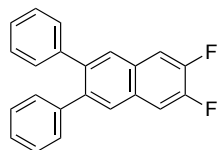


Figure S18. ^{13}C NMR (150 MHz) spectrum of **H-Ar-4** in CDCl_3 : (top) full view, (bottom) 141.5 to 124.0 ppm region.

2.4 Fluorinated ortho-Arylenes



F-Ar-1: A solution of 1,2-diphenylacetylene (**1**, 0.200 g, 1.12 mmol) and benzaldehyde **S2** (0.544 g, 2.24 mmol) in 1,2-dichloroethane (11 mL), which had been deoxygenated by sparging with N₂ for 5 min, was transferred via cannula into a round bottom flask equipped with a water-cooled condenser containing Cu(OTf)₂ (0.041 g, 0.11 mmol) under a nitrogen atmosphere. TFA (0.34 mL, 0.51 g, 4.5 mmol) was immediately added. The mixture was heated in an oil bath to 100 °C for 2 h. The mixture was cooled to rt and diluted with CH₂Cl₂, poured into satd. aq. NaHCO₃ (150 mL), and extracted twice with CH₂Cl₂ (150 mL, 75 mL). The combined organic phase was washed with satd. aq. NH₄Cl, dried (Na₂SO₄), filtered, and the solvent was removed *in vacuo*. Column chromatography (silica gel, hexanes to 20% CH₂Cl₂ in hexanes) afforded **F-Ar-1** (0.351 g, 99%) as a white solid. *R*_f = 0.6 (20% CH₂Cl₂ in hexanes). IR (CDCl₃ cast film): 3059 (vw), 3029 (vw), 1601 (w), 1506 (m), 1499 (m), 1448 (w), 1441 (w), 1399 (w), 1362 (w), 1284 (w), 1243 (m), 1202 (w), 1132 (w), 1074 (w), 1022 (w), 902 (m), 860 (m), 780 (w), 756 (m), 700 (s), 671 (w) cm⁻¹. ¹H NMR (500 MHz, CDCl₃): δ 7.83 (s, 2H), 7.62 (t, *J* = 9.4 Hz, 2H), 7.31–7.25 (m, 3H), 7.25–7.20 (m, 2H). ¹³C NMR (125 MHz, CDCl₃): δ 150.3 (dd, *J* = 252.4, 17.6 Hz), 140.8, 139.6, 129.9, 129.4 (t, *J* = 4.5 Hz), 128.6, 127.9, 126.8, 113.4 (dd, *J* = 12.7, 5.2 Hz). ¹⁹F NMR (470 MHz, CDCl₃): δ –136.57 (t, *J* = 9.4 Hz, 2F). DART HRMS *m/z* calcd. for C₂₂H₁₄F₂ (M⁺), 316.1058, found 316.1047. Crystals suitable for X-ray crystallographic analysis were obtained from solutions of **F-Ar-1** in CH₂Cl₂ that were layered with hexanes and allowed to slowly evaporate at rt, for X-ray data of **F-Ar-1**, see: CCDC-1483962.

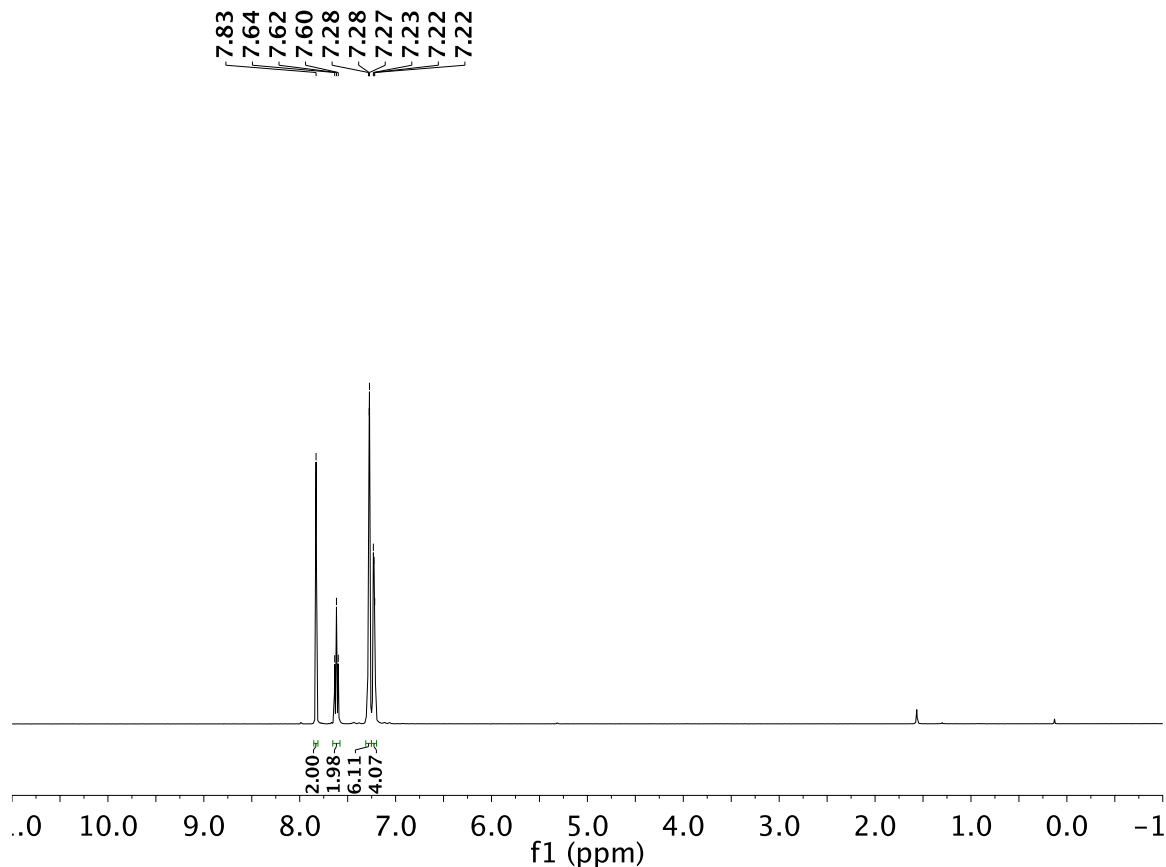


Figure S19. ¹H NMR (500 MHz) spectrum of **F-Ar-1** in CDCl₃.

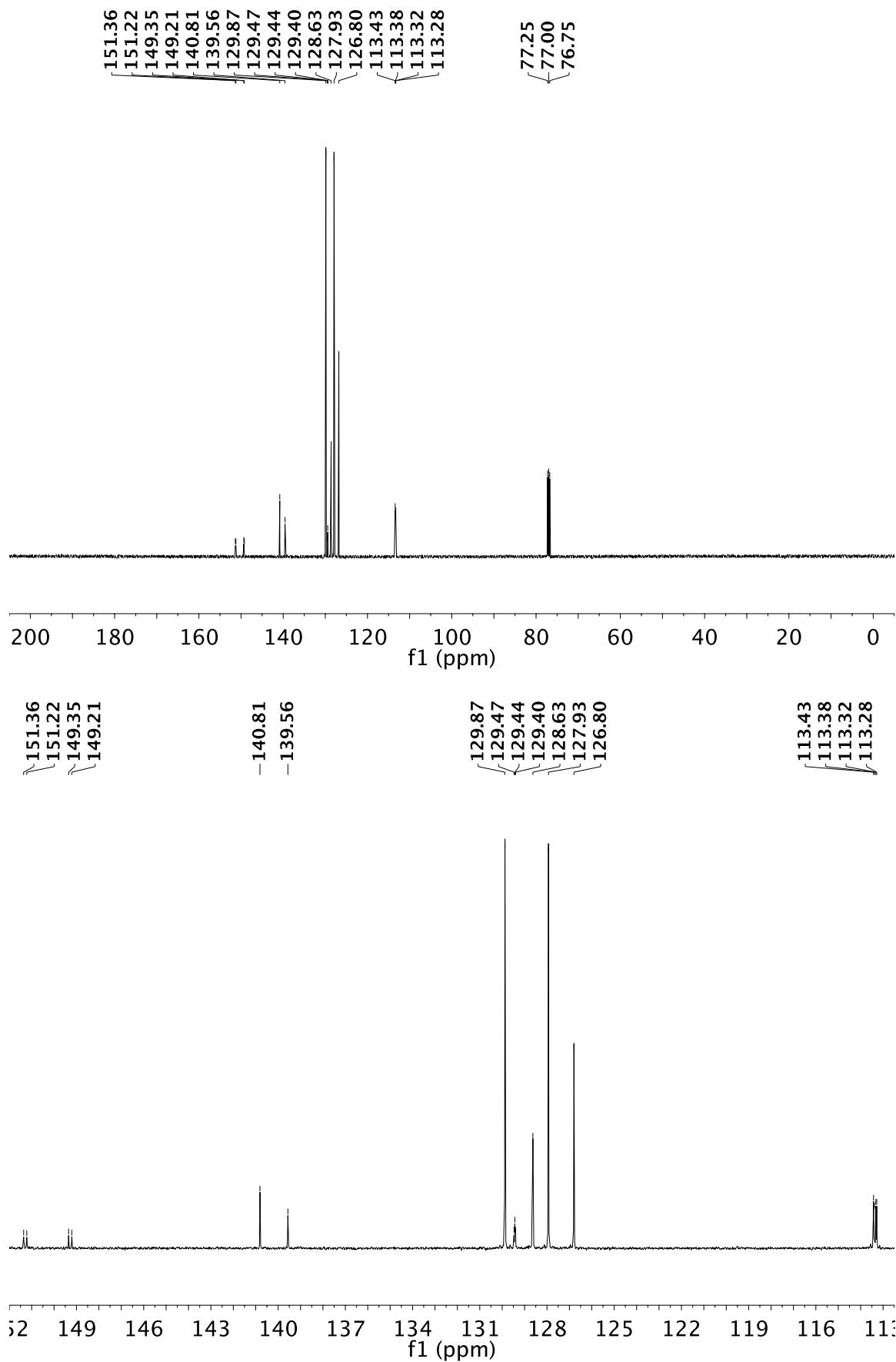


Figure S20. ^{13}C NMR (125 MHz) spectrum of **F-Ar-1** in CDCl_3 : (top) full view, (bottom) 152.0 to 112.5 ppm region.

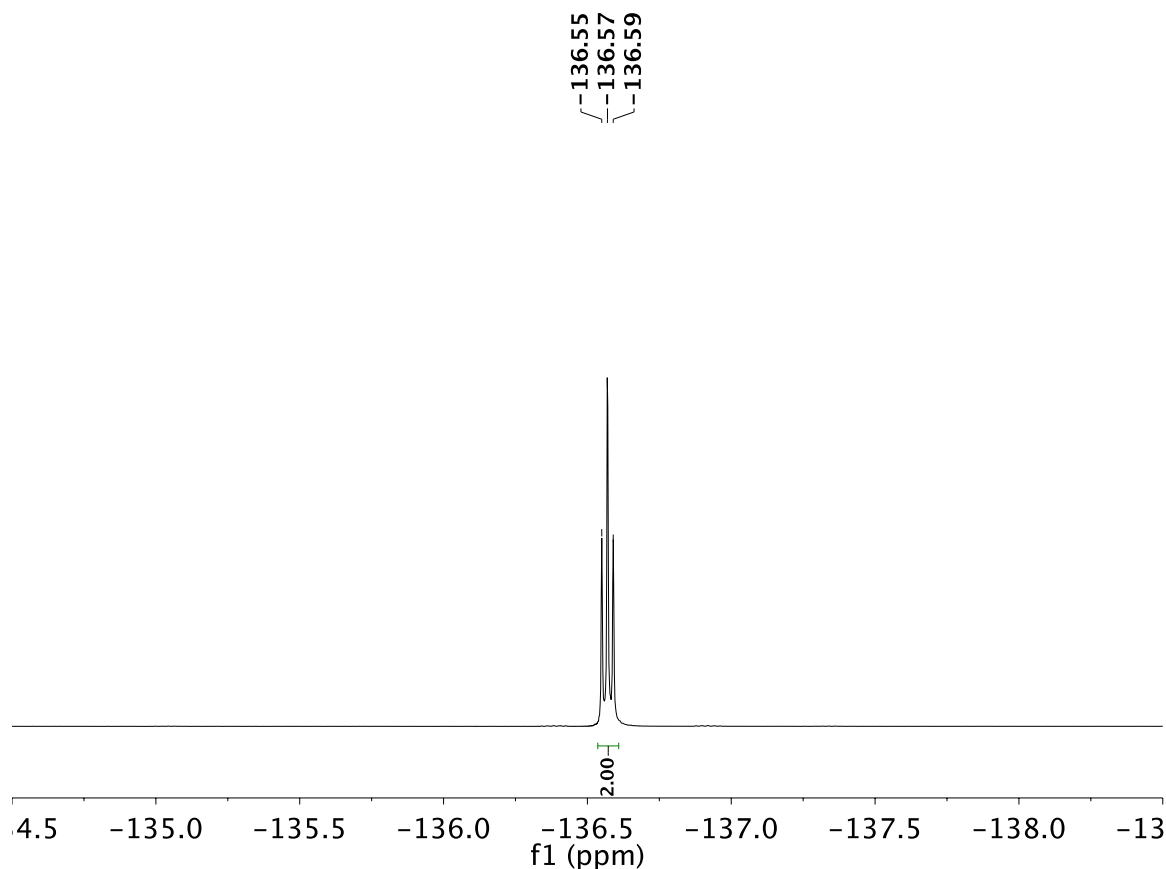
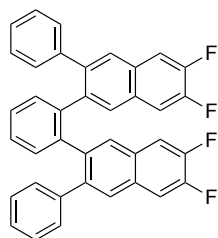


Figure S21. ^{19}F NMR (470 MHz) spectrum of **F-Ar-1** in CDCl_3 .



F-Ar-2: A solution of 1,2-bis(phenylethynyl)benzene (**2**, 0.265 g, 0.952 mmol) and benzaldehyde **S2** (0.922 g, 3.81 mmol) in 1,2-dichloroethane (19 mL), which had been deoxygenated by sparging with N_2 for 5 min, was transferred via cannula into a round bottom flask equipped with a water-cooled condenser containing $\text{Cu}(\text{OTf})_2$ (0.069 g, 0.190 mmol) under a nitrogen atmosphere. TFA (0.58 mL, 0.87 g, 7.6 mmol) was immediately added. The mixture was heated in an oil bath to 100 $^\circ\text{C}$ for 2 h. The mixture was cooled to rt and diluted with CH_2Cl_2 , poured into satd. aq. NaHCO_3 (150 mL), and extracted twice with CH_2Cl_2 (150 mL, 75 mL). The combined organic phase was washed with satd. aq. NH_4Cl , dried (Na_2SO_4), filtered, and the solvent was removed *in vacuo*. Column chromatography (silica gel, 15% to 40% CH_2Cl_2 in hexanes) afforded **F-Ar-2** (0.426 g, 81%) as a white solid. R_f = 0.5 (30% CH_2Cl_2 in hexanes). IR (CDCl_3 cast film): 3059 (vw), 3029 (vw), 1600 (vw), 1511 (s), 1505 (s), 1472 (w), 1445 (w), 1400 (m), 1359 (m), 1242 (s), 1199 (m), 1133 (m), 1076 (w), 1023 (w), 961 (w), 904 (s), 863 (m), 788 (w), 761 (m), 752 (m), 733 (m), 703 (m), 698 (m), 677 (w) cm^{-1} . ^1H NMR (500 MHz, CDCl_3): δ 7.50 (dd, J = 5.4, 3.5 Hz, 2H), 7.40 (dd, J = 10.7, 8.0 Hz, 2H), 7.33 (dd, J = 5.3, 3.5 Hz, 2H), 7.28 (s, 2H), 7.20–7.11 (m, 4H), 6.93 (t, J = 7.6 Hz, 2H). ^{13}C NMR (125 MHz, CDCl_3):⁹ δ 150.82, 150.77, 150.73, 150.71, 150.67, 150.65, 150.61, 150.52, 150.48, 149.18, 149.15, 149.13, 149.10, 149.07, 149.05, 149.01, 148.97, 148.93, 148.88, 148.84, 140.57, 140.52, 140.49, 140.44, 140.36, 140.34, 140.32, 140.30, 138.99, 138.37, 138.35, 138.33, 132.21, 132.17, 132.14, 131.17, 131.14, 131.10, 130.71, 130.28, 129.54, 129.50, 129.47, 129.43, 129.30, 129.27, 129.22, 129.18, 129.13, 129.08, 129.05, 129.01, 128.46, 128.41, 128.23, 128.09, 128.04, 127.91, 127.86, 127.80, 127.58, 127.53, 127.40, 127.35, 127.03, 126.98,

⁹ A complete line list is provided since the combination of C–F coupling and multiple conformations rendered interpretation of the spectra challenging.

126.87, 126.82, 126.78, 126.58, 126.52, 126.48, 125.83, 125.79, 125.74, 114.28, 114.27, 114.17, 114.16, 113.56, 113.53, 113.45, 113.42, 113.22, 113.20, 113.11, 113.09, 112.49, 112.46, 112.38, 112.35. ^{19}F NMR (470 MHz, CDCl_3): δ -137.19 (ddd, $J = 19.3, 10.6, 8.3$ Hz), -137.69 (ddd, $J = 19.6, 10.7, 8.1$ Hz). DART HRMS m/z calcd. for $\text{C}_{38}\text{H}_{22}\text{F}_4$ (M^+), 554.1652, found 554.1700. Crystals suitable for X-ray crystallographic analysis were obtained from solutions of **F-Ar-2** in CHCl_3 that were allowed to slowly evaporate at rt, for X-ray data of **F-Ar-2**, see: CCDC-1483963.

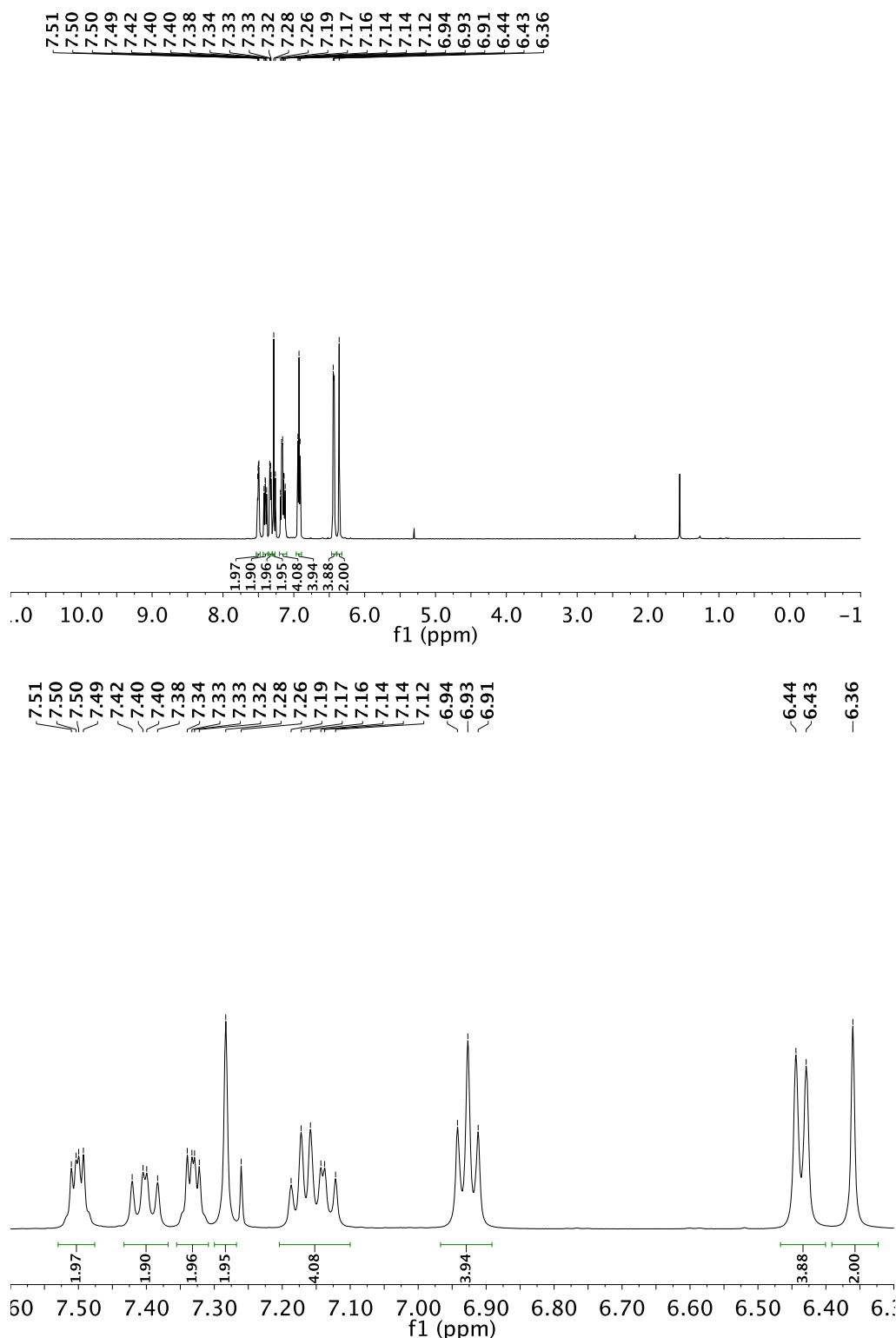


Figure S22. ^1H NMR (500 MHz) spectrum of **F-Ar-2** in CDCl_3 : (top) full view, (bottom) 7.60 to 6.30 ppm region.

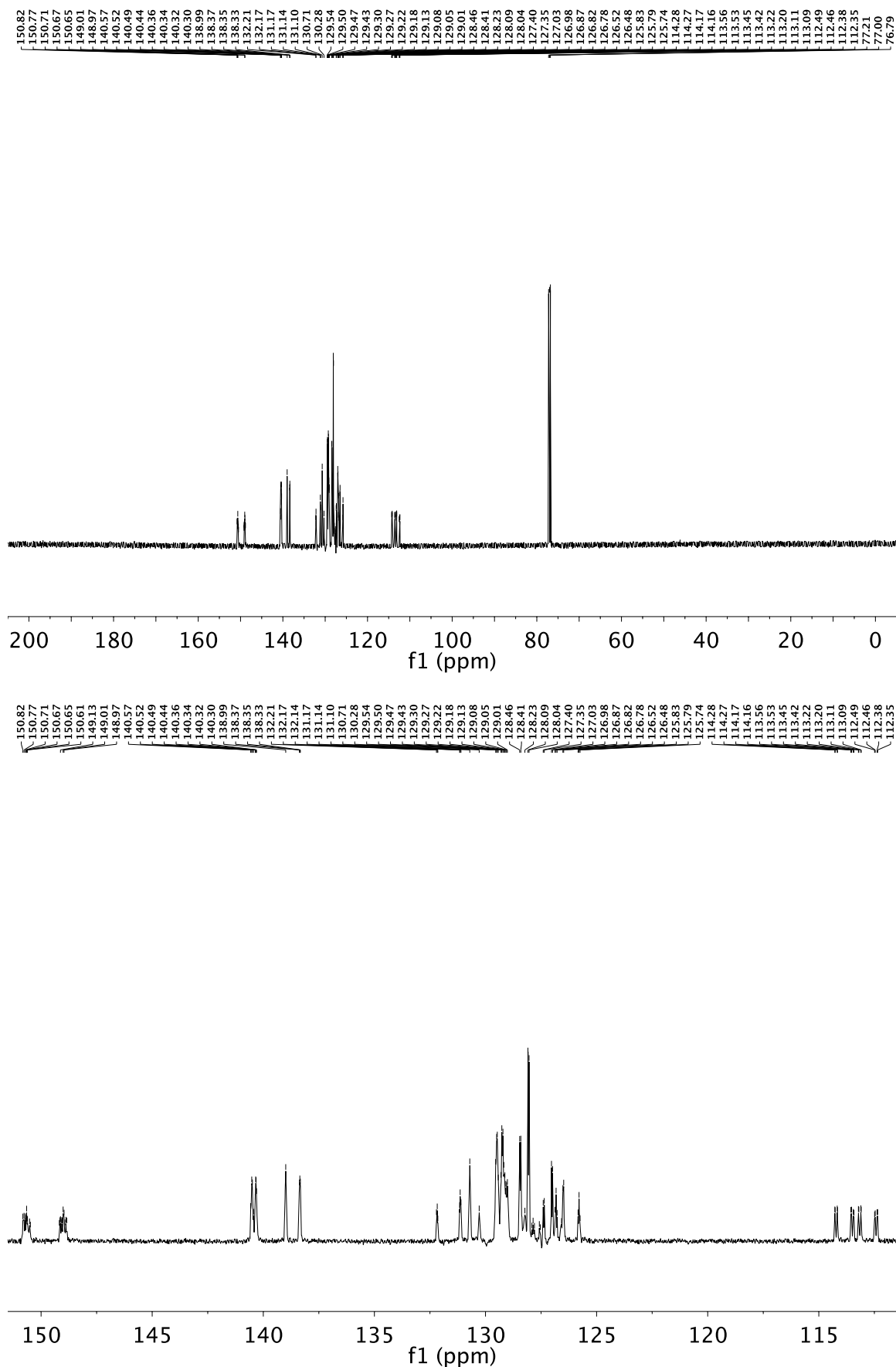


Figure S23. ^{13}C NMR (125 MHz) spectrum of **F-Ar-2** in CDCl_3 : (top) full view, (bottom) 151.5 to 111.5 ppm region.

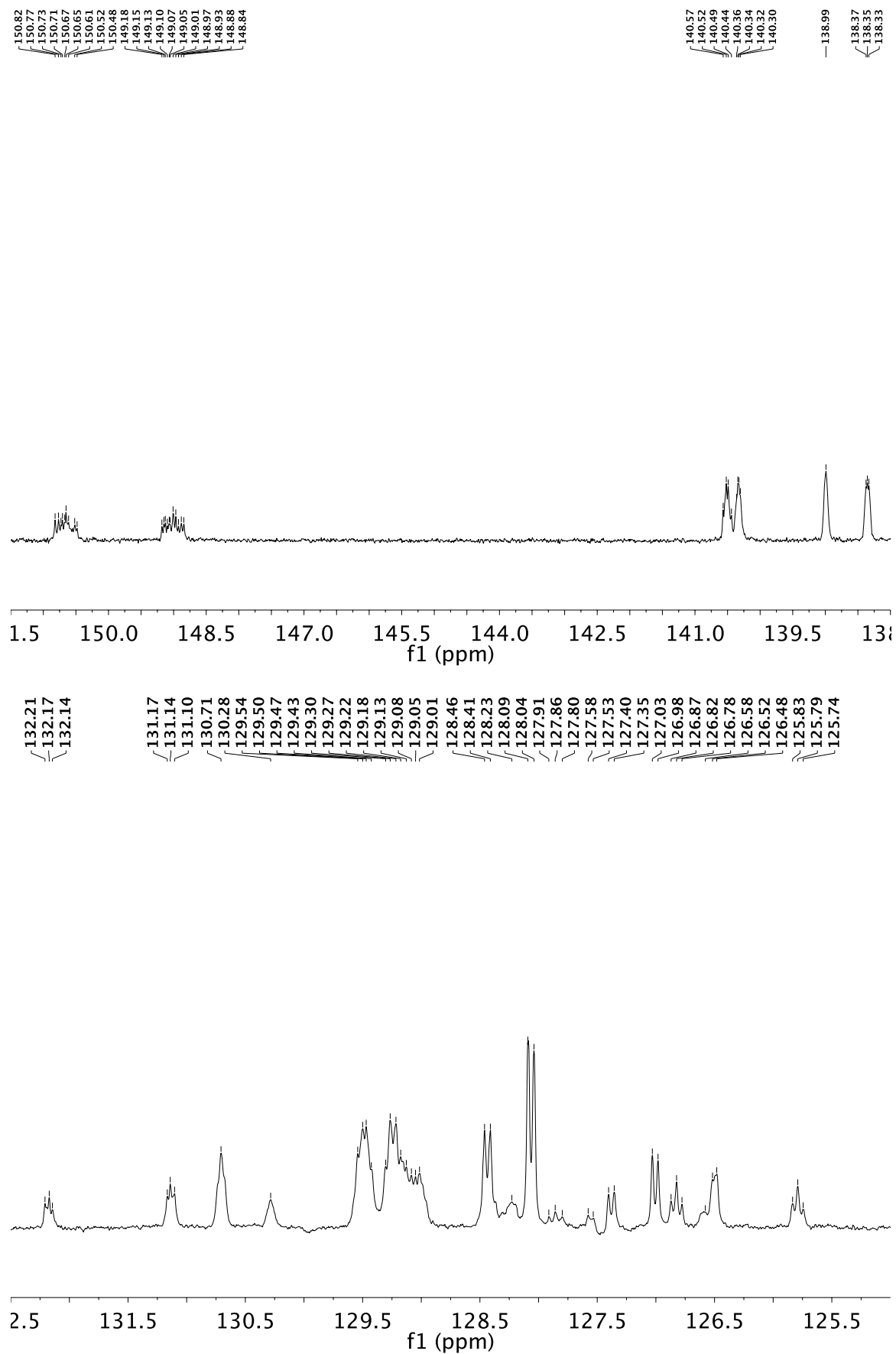


Figure S24. ^{13}C NMR (125 MHz) spectrum of **F-Ar-2** in CDCl_3 : (top) 151.5 to 138.0 ppm, (bottom) 132.5 to 125.0 ppm region.

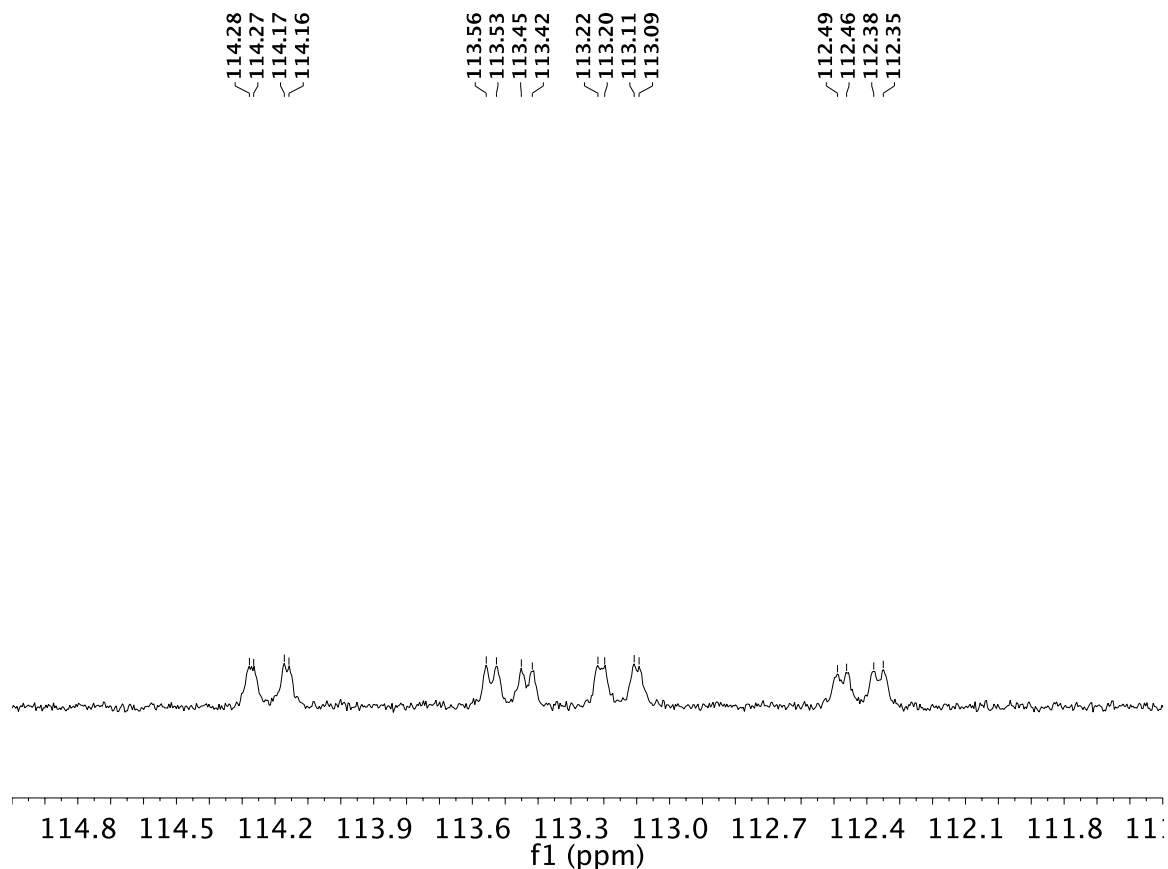


Figure S25. ¹³C NMR (125 MHz) spectrum of **F-Ar-2** in CDCl₃: 115.0 to 111.5 ppm region.

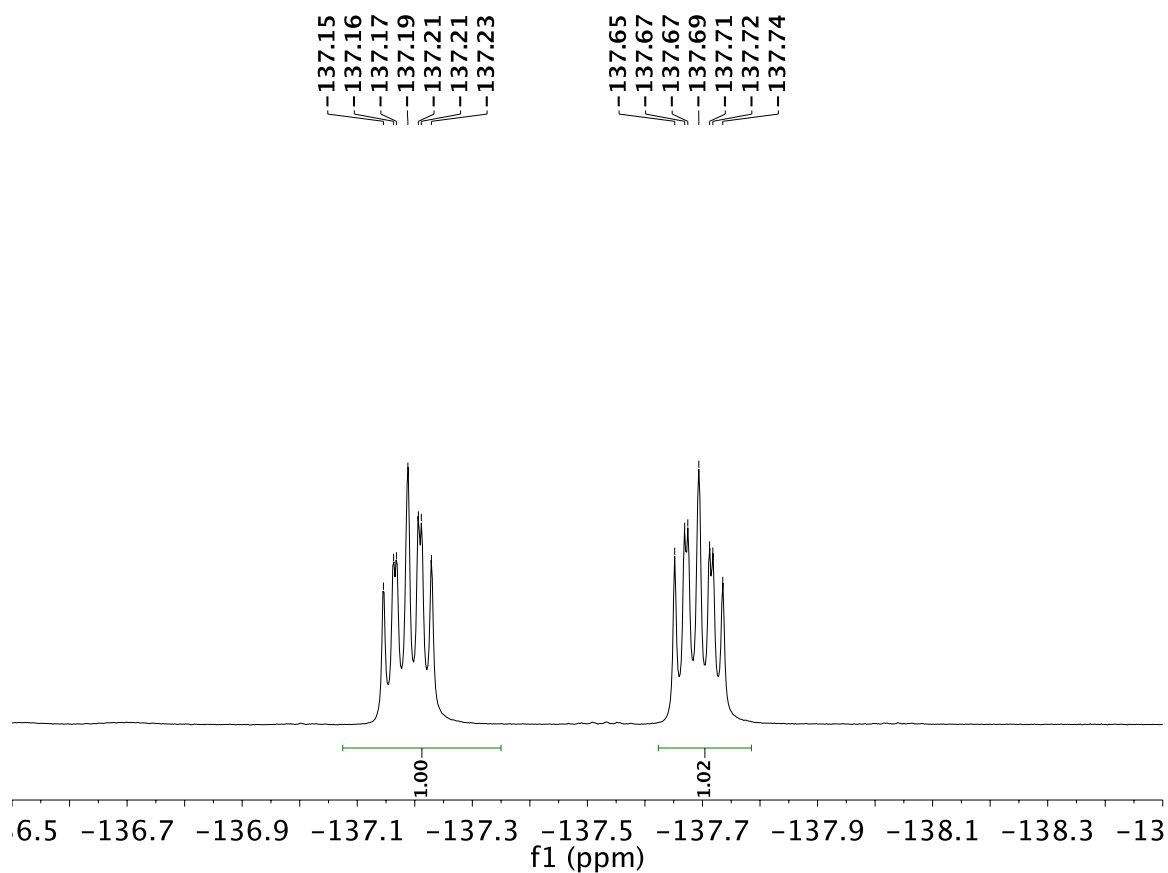
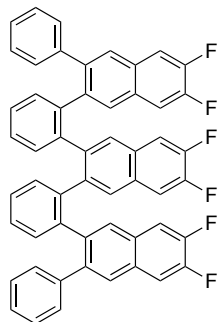


Figure S26. ¹⁹F NMR (470 MHz) spectrum of **F-Ar-2** in CDCl₃.



F-Ar-3: To a round bottom flask was added **3** (0.290 g, 0.766 mmol) and benzaldehyde **S2** (1.11 g, 4.60 mmol), followed by 1,2-dichloroethane (9.6 mL). The resulting suspension was deoxygenated by sparging with N₂ for 2 min prior to adding Cu(OTf)₂ (0.083 g, 0.230 mmol), followed by immediately equipping the round bottom flask with a water-cooled condenser, resuming sparging with N₂ for 1 min and followed by adding TFA (0.70 mL, 1.0 g, 9.2 mmol) to this mixture. The mixture was heated in an oil bath to 100 °C for 2 h. The mixture was cooled to rt and diluted with CH₂Cl₂, poured into satd. aq. NaHCO₃ (150 mL), and extracted twice with CH₂Cl₂ (150 mL, 75 mL). The combined organic phase was washed with satd. aq. NH₄Cl, dried (Na₂SO₄), filtered, and the solvent was removed *in vacuo*. Column chromatography (silica gel, 20% to 40% CH₂Cl₂ in hexanes) afforded **F-Ar-3** (0.287 g, 47%) as a white solid. *R*_f = 0.5 (40% CH₂Cl₂ in hexanes). IR (CDCl₃ cast film): 3056 (vw), 3026 (vw), 1601 (vw), 1510 (s), 1506 (s), 1477 (w), 1401 (m), 1356 (m), 1276 (w), 1241 (s), 1199 (m), 1154 (w), 1133 (m), 1075 (vw), 1025 (w), 962 (w), 903 (s), 861 (m), 762 (m), 751 (m), 734 (m), 700 (m), 679 (w) cm⁻¹. ¹H NMR (500 MHz, CDCl₃): δ 7.41 (dd, *J* = 10.3, 8.1 Hz, 2H), 7.32 – 7.25 (m, 4H), 7.24–7.18 (m, 4H), 6.98 – 6.90 (m, 4H), 6.85 (s, 2H), 6.60 (t, *J* = 7.5 Hz, 4H), 6.30 (t, *J* = 7.4 Hz, 2H), 6.09 (d, *J* = 7.6 Hz, 4H), 5.94 (s, 2H), 5.68 (d, *J* = 7.5 Hz, 2H). ¹³C NMR¹⁰ (125 MHz, CDCl₃): δ 150.95, 150.89, 150.84, 150.77, 150.45, 150.30, 148.98, 148.91, 148.87, 148.79, 148.45, 148.31, 140.58, 140.40, 139.19, 139.17, 138.86, 138.84, 138.82, 138.69, 131.70, 131.58, 129.87, 129.86, 129.83, 129.82, 129.73, 129.65, 129.20, 129.14, 129.01, 128.98, 128.94, 128.01, 127.54, 127.39, 127.36, 127.35, 127.03, 125.92, 113.83, 113.70, 113.33, 113.29, 113.23, 113.19, 113.07, 112.94. ¹⁹F NMR (470 MHz, CDCl₃): δ –137.10 – –137.24 (m, 2F), –137.52 – –137.66 (m, 2F), 138.36 (t, *J* = 9.5 Hz, 2F). DART HRMS *m/z* calcd. for C₅₄H₃₀F₆ (M⁺), 792.2246, found 792.2211. Crystals suitable for X-ray crystallographic analysis were obtained from solutions of **F-Ar-3** in CH₂Cl₂ that were layered with pentane and allowed to slowly evaporate at rt, for X-ray data of **F-Ar-3**, see: CCDC-1483964.

(10) The complete line list of signals for the proton decoupled ¹³C NMR is provided without interpretation of the coupling to ¹⁹F due to the complex nature of the spectrum.

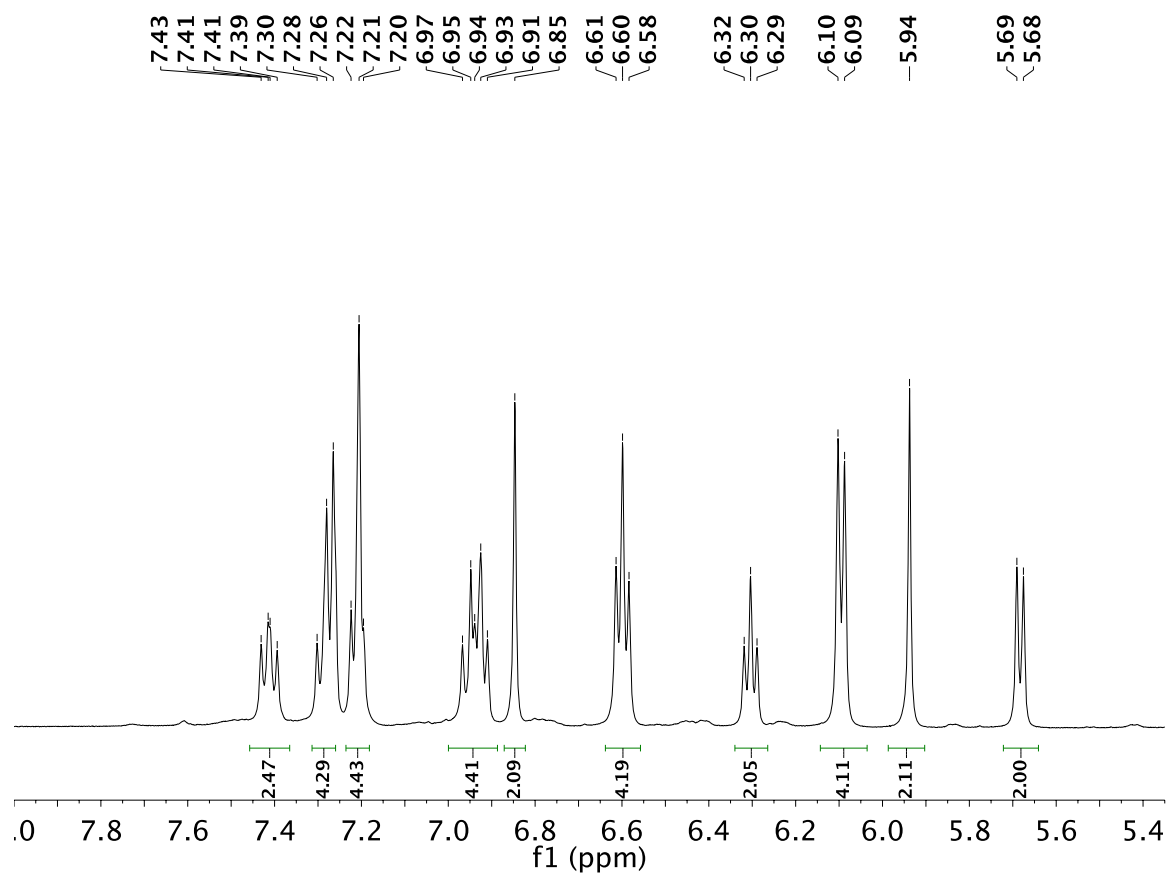
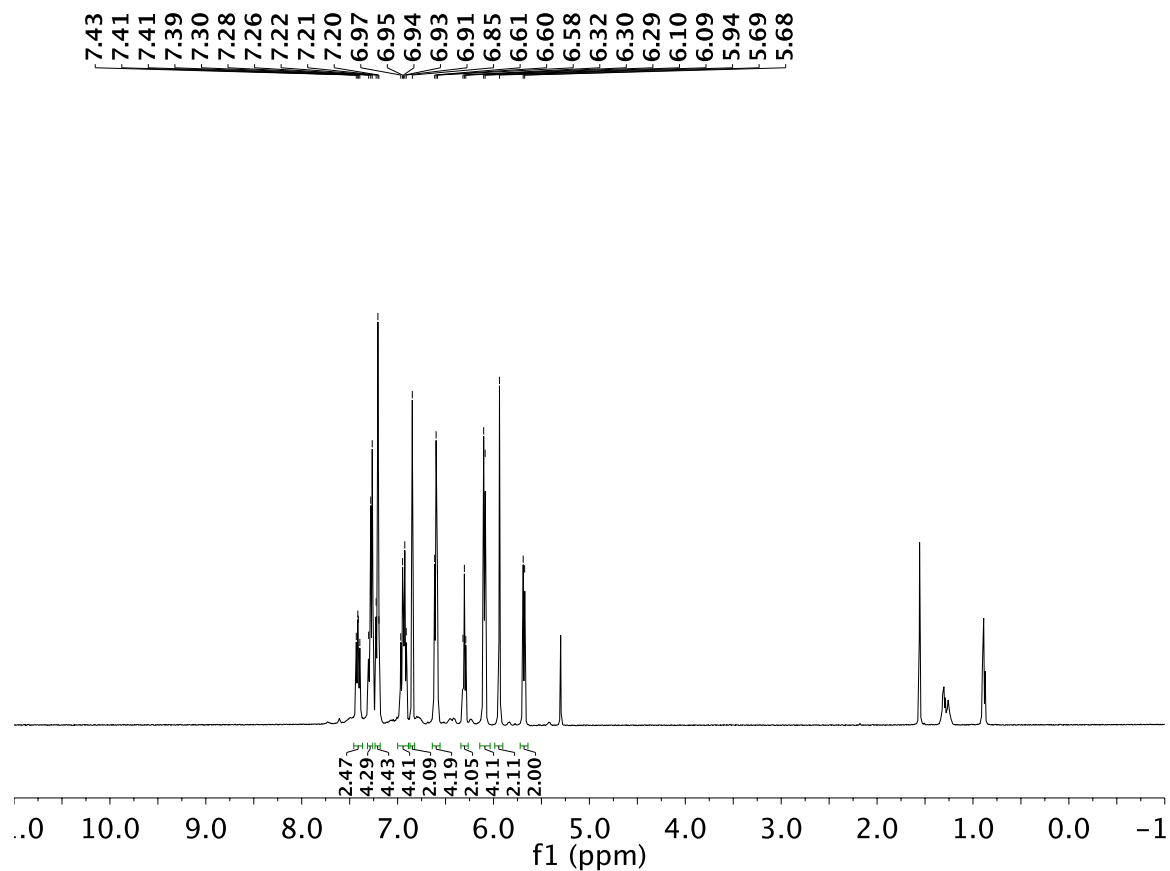


Figure S27. ^1H NMR (500 MHz) spectrum of **F-Ar-3** in CDCl_3 : (top) full view (signal at 5.30 ppm is CH_2Cl_2), (bottom) 8.00 to 5.35 ppm region.

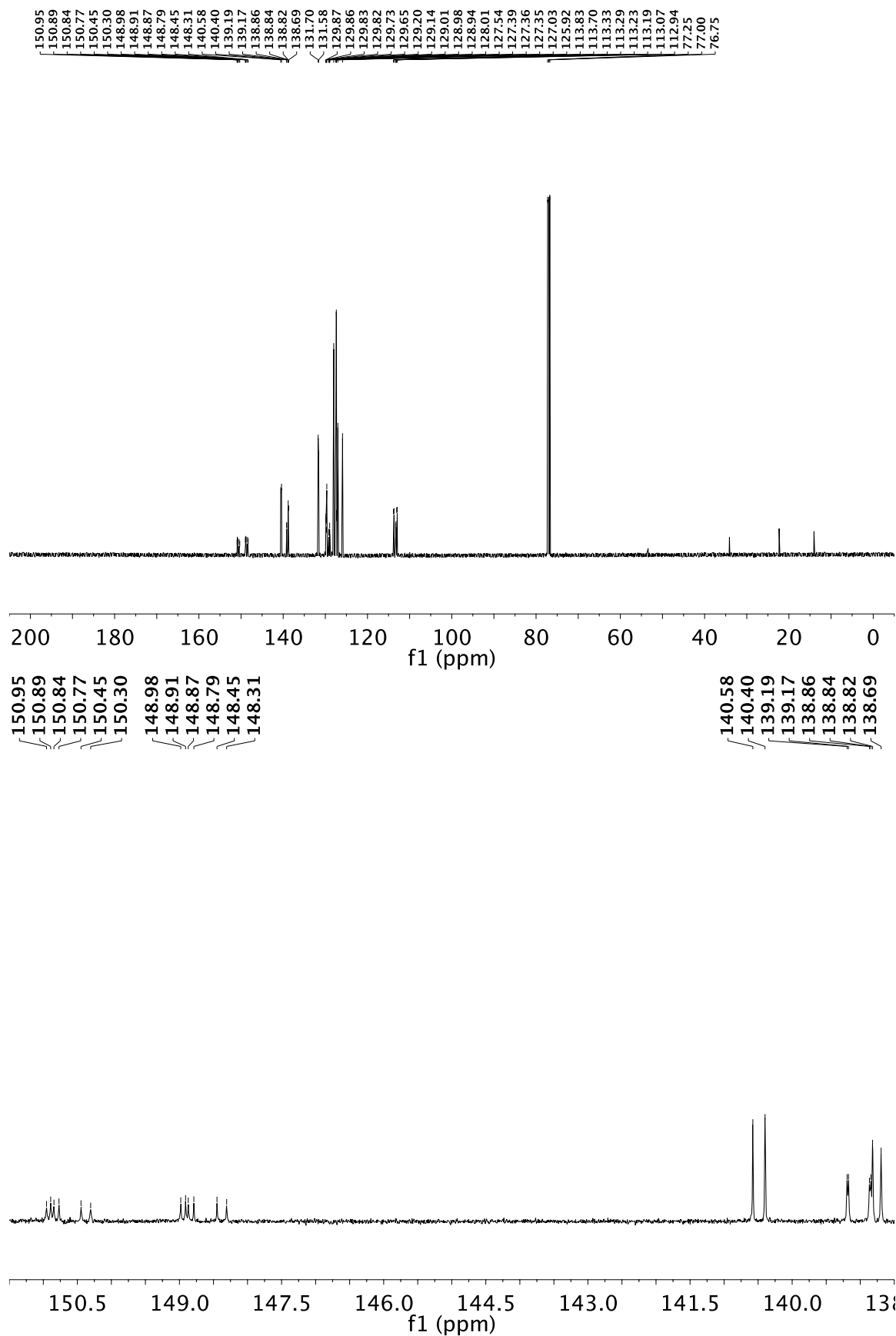


Figure S28. ^{13}C NMR (125 MHz) spectrum of **F-Ar-3** in CDCl_3 : (top) full view, (bottom) 151.5 to 138.5 ppm region.

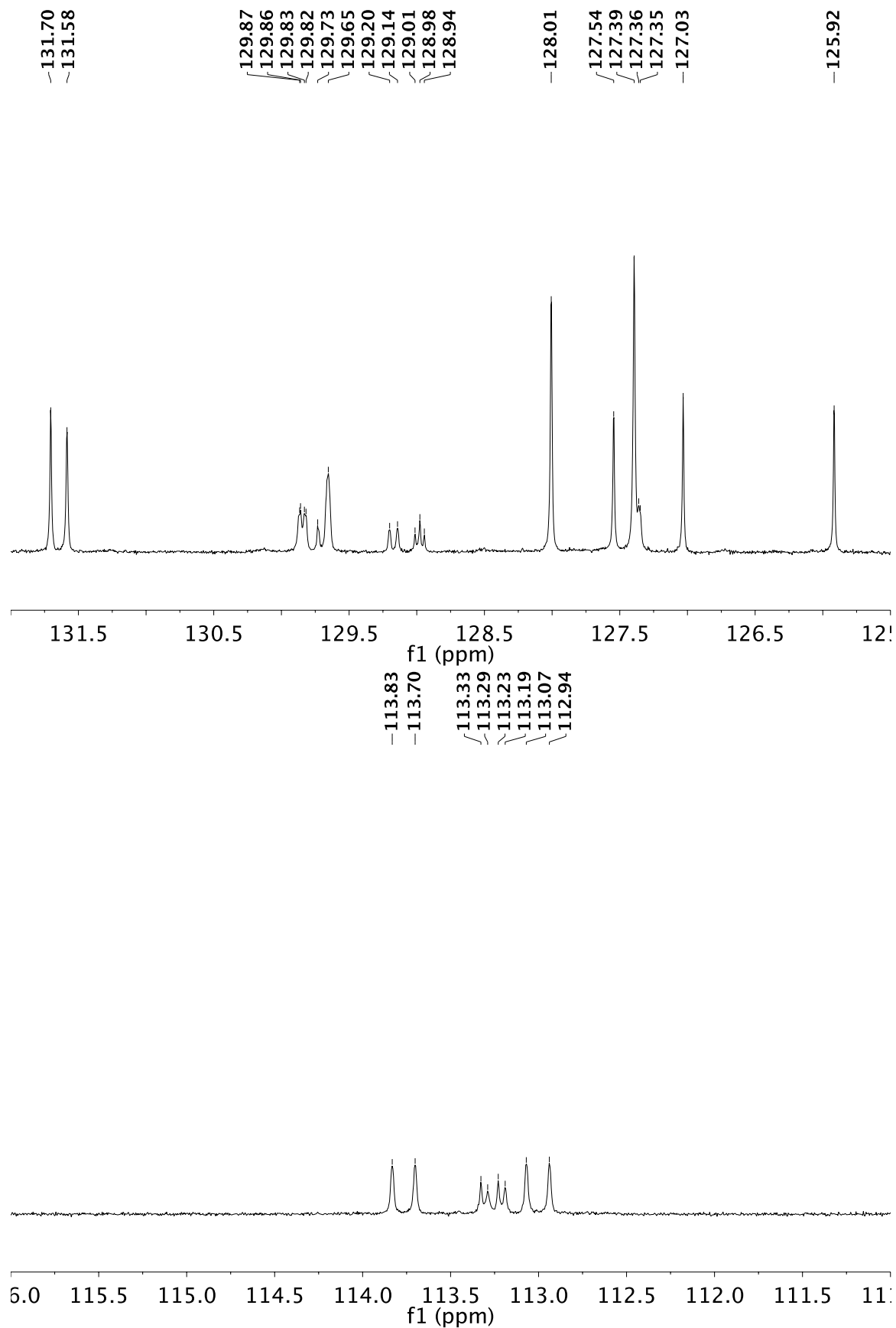


Figure S28 (continued). ^{13}C NMR (125 MHz) spectrum of **F-Ar-3** in CDCl_3 : (top) 132.0 to 125.5 ppm, (bottom) 116.0 to 111.0 ppm region.

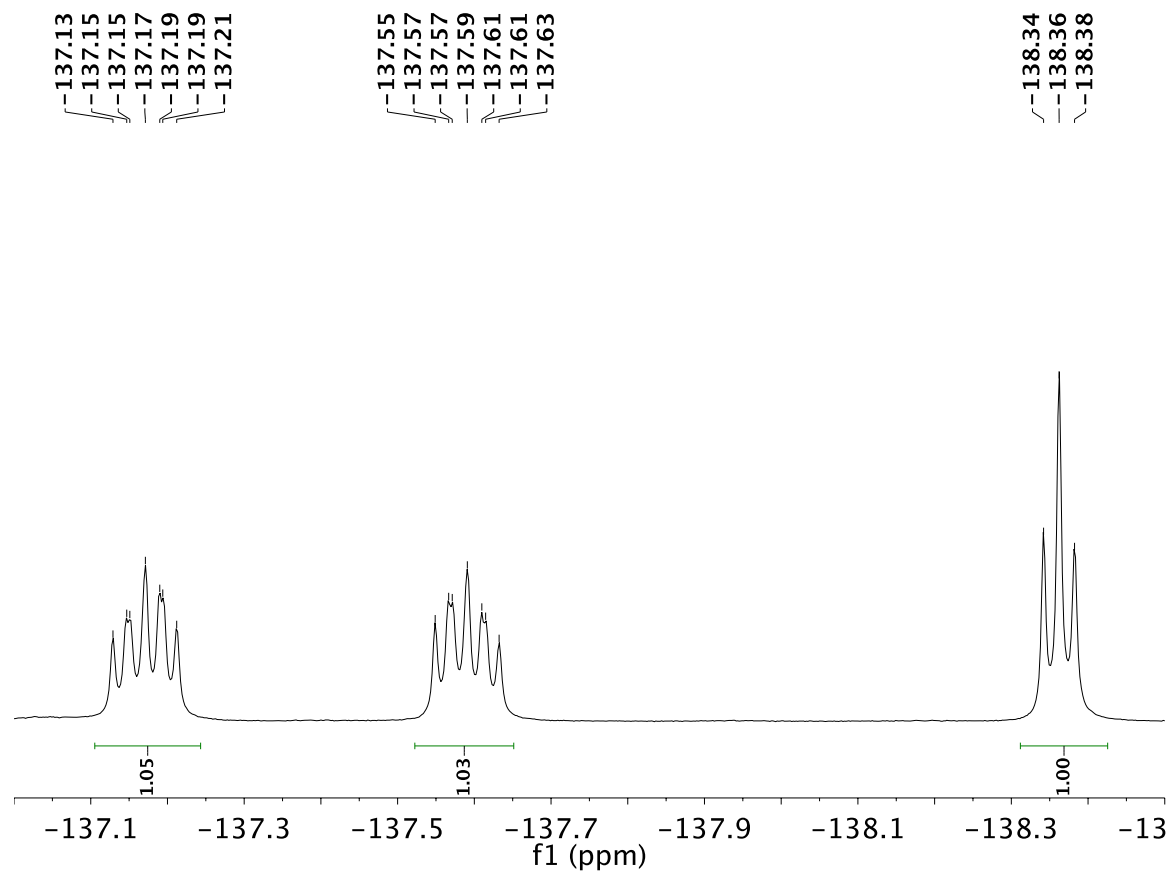
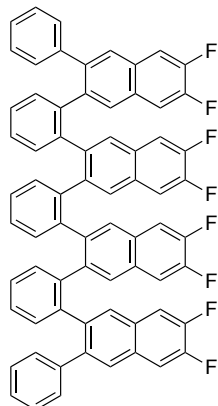


Figure S29. ^{19}F NMR (470 MHz) spectrum of **F-Ar-3** in CDCl_3 .



F-Ar-4: A solution of **4** (0.390 g, 0.815 mmol) and benzaldehyde **S2** (1.97 g, 8.15 mmol) in 1,2-dichloroethane (16 mL), which had been deoxygenated by sparging with N₂ for 5 min, was transferred via cannula into a round bottom flask equipped with a water-cooled condenser containing Cu(OTf)₂ (0.300 g, 0.829 mmol) under a nitrogen atmosphere. TFA (0.94 mL, 1.4 g, 12 mmol) was immediately added. The mixture was heated in an oil bath to 100 °C for 12 h. The mixture was cooled to rt and diluted with CH₂Cl₂, poured into satd. aq. NaHCO₃ (150 mL), and extracted twice with CH₂Cl₂ (150 mL, 75 mL). The combined organic phase was washed with satd. aq. NH₄Cl, dried (Na₂SO₄), filtered, and the solvent was removed *in vacuo*. Column chromatography (silica gel, 20% to 30% CH₂Cl₂ in hexanes) afforded **F-Ar-4** (0.269 g, 32%) as an off white solid. *R*_f = 0.5 (40% CH₂Cl₂ in hexanes). IR (CDCl₃ cast film): 3059 (vw), 1503 (m), 1401 (w), 1349 (w), 1241 (m), 1133 (w), 903 (s), 863 (w), 761 (m), 732 (s), 700 (m) cm⁻¹. ¹H NMR (500 MHz, CDCl₃): δ 7.37 (t, *J* = 8.9 Hz, 2H), 7.17–7.04 (m, 8H), 7.01–6.94 (m, 4H), 6.91 (t, *J* = 7.1 Hz, 2H), 6.58 (t, *J* = 7.2 Hz, 4H), 6.52 (s, 2H), 6.40 (s, 2H), 6.07–5.98 (m, 6H), 5.94 (t, *J* = 7.2 Hz, 2H), 5.89 (s, 2H), 5.73–5.67 (br s, 2H), 5.55 (d, *J* = 7.4 Hz, 2H). ¹³C NMR¹¹ (125 MHz, CDCl₃): δ 150.93, 150.78, 150.71, 150.65, 150.59, 150.44, 150.36, 150.28, 148.92, 148.78, 148.72, 148.58, 148.56, 148.42, 148.33, 140.38, 140.36, 139.51, 139.50, 138.99, 138.85, 138.84, 138.52, 138.37, 138.36, 138.27, 131.62, 131.41, 130.91, 129.92, 129.89, 129.53, 129.51, 129.47, 129.45, 129.40, 129.36, 129.05, 129.03, 127.96, 127.36, 127.31, 127.27, 127.24, 126.81, 126.73, 125.87, 113.78, 113.65, 113.46, 113.33, 113.26, 113.14, 113.96, 112.83. ¹⁹F NMR (470 MHz, CDCl₃): δ -137.17 (dt, *J* = 18.9, 9.4 Hz, 1F), -137.41 (dt, *J* = 19.3, 9.4 Hz, 1F), -138.11 (dt, *J* = 19.0, 9.5 Hz, 1F), -138.36 (dt, *J* = 19.3, 9.6 Hz). DART HRMS *m/z* calcd. for C₇₀H₃₈F₈ (M⁺), 1030.2840, found 1030.2795.

(11) The complete line list of signals for the proton decoupled ¹³C NMR is provided without interpretation of the coupling to ¹⁹F due to the complex nature of the spectrum.

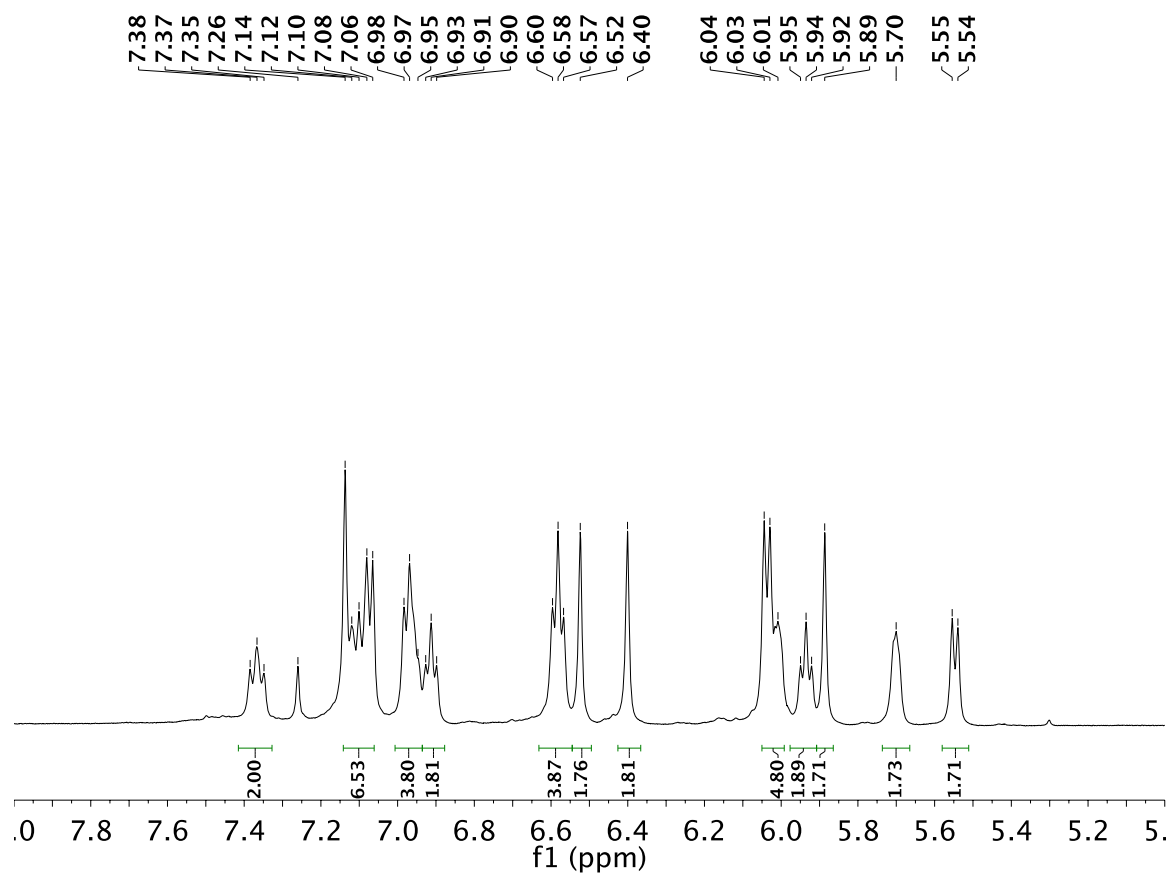
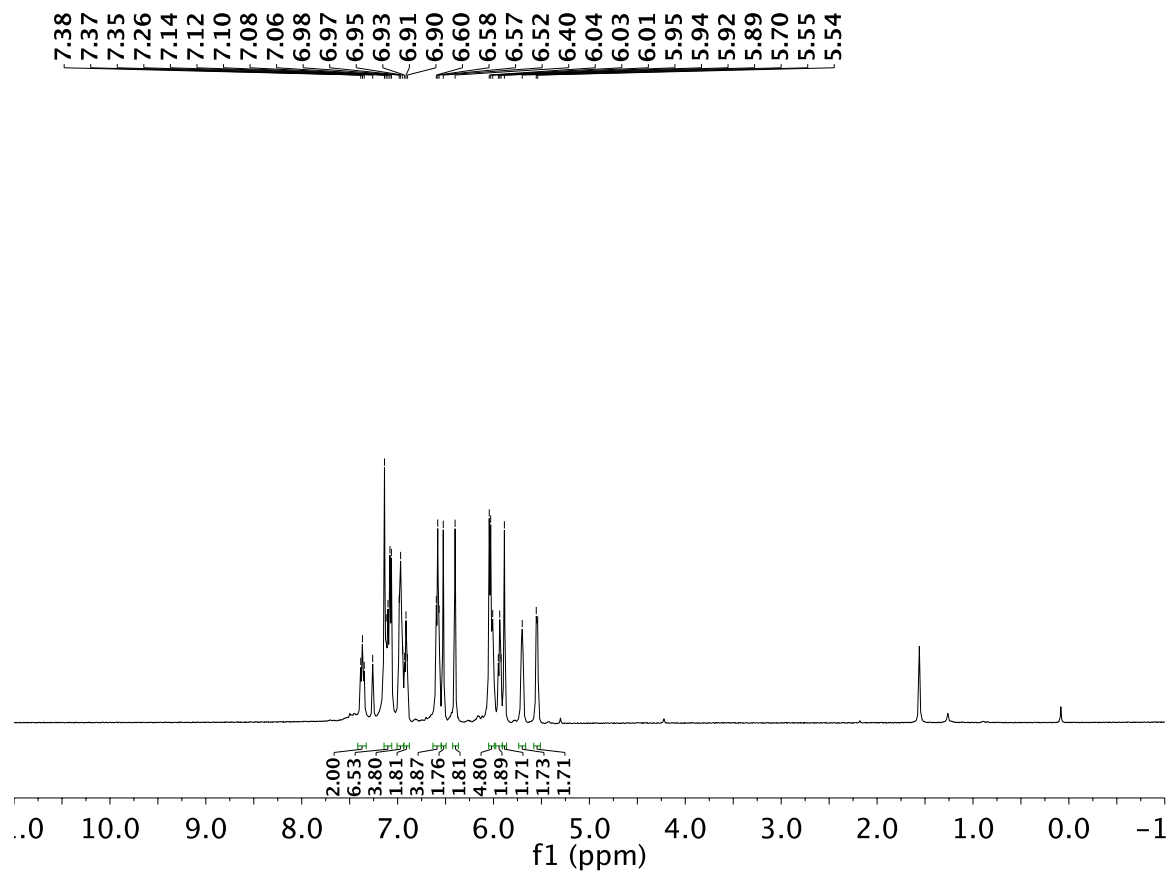


Figure S30. ^1H NMR (500 MHz) spectrum of **F-Ar-4** in CDCl_3 : (top) full view, (bottom) 8.00 to 5.00 ppm region.

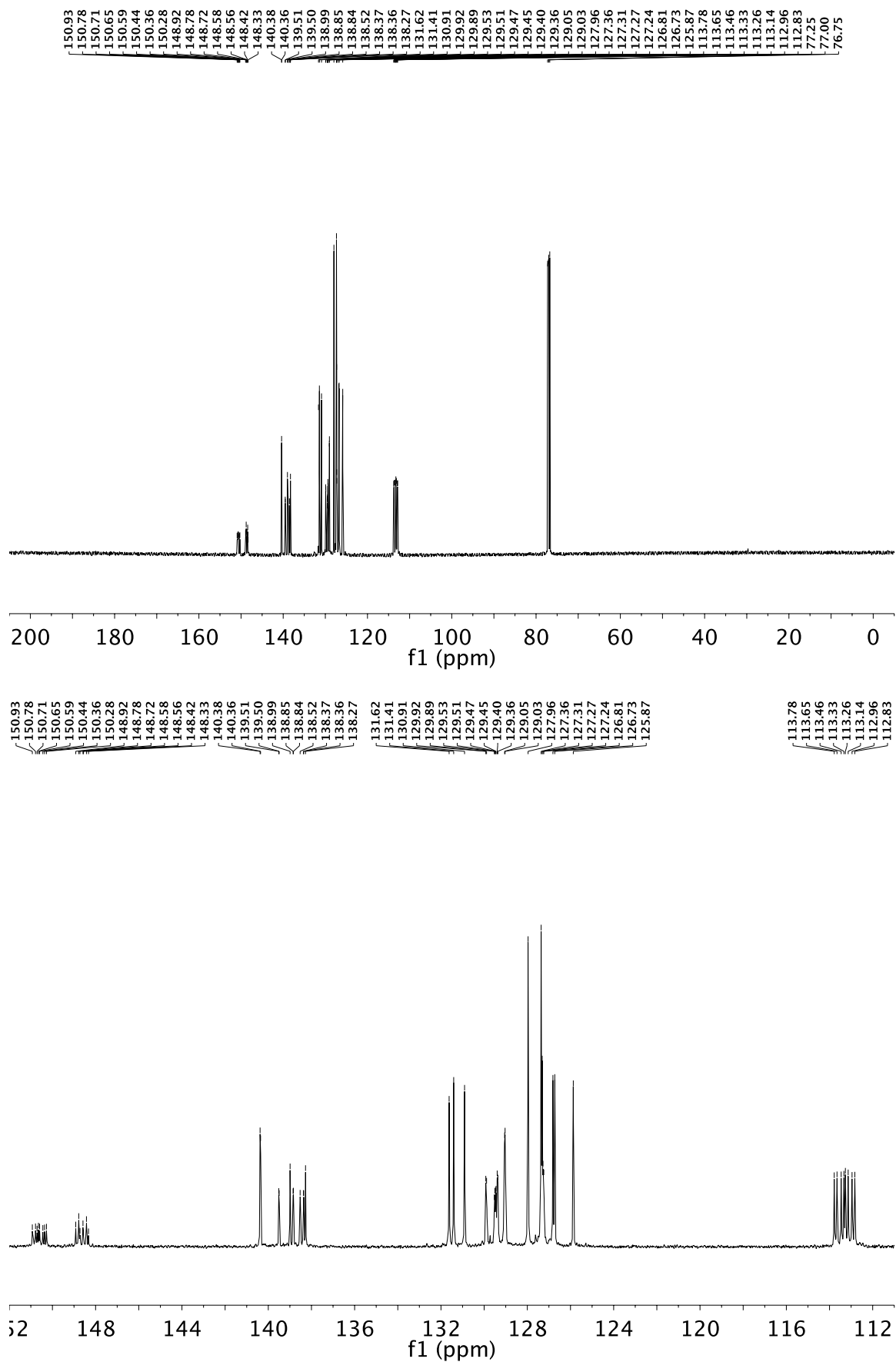


Figure S31. ^{13}C NMR (125 MHz) spectrum of **F-Ar-4** in CDCl_3 : (top) full view, (bottom) 152.0 to 111.0 ppm region.

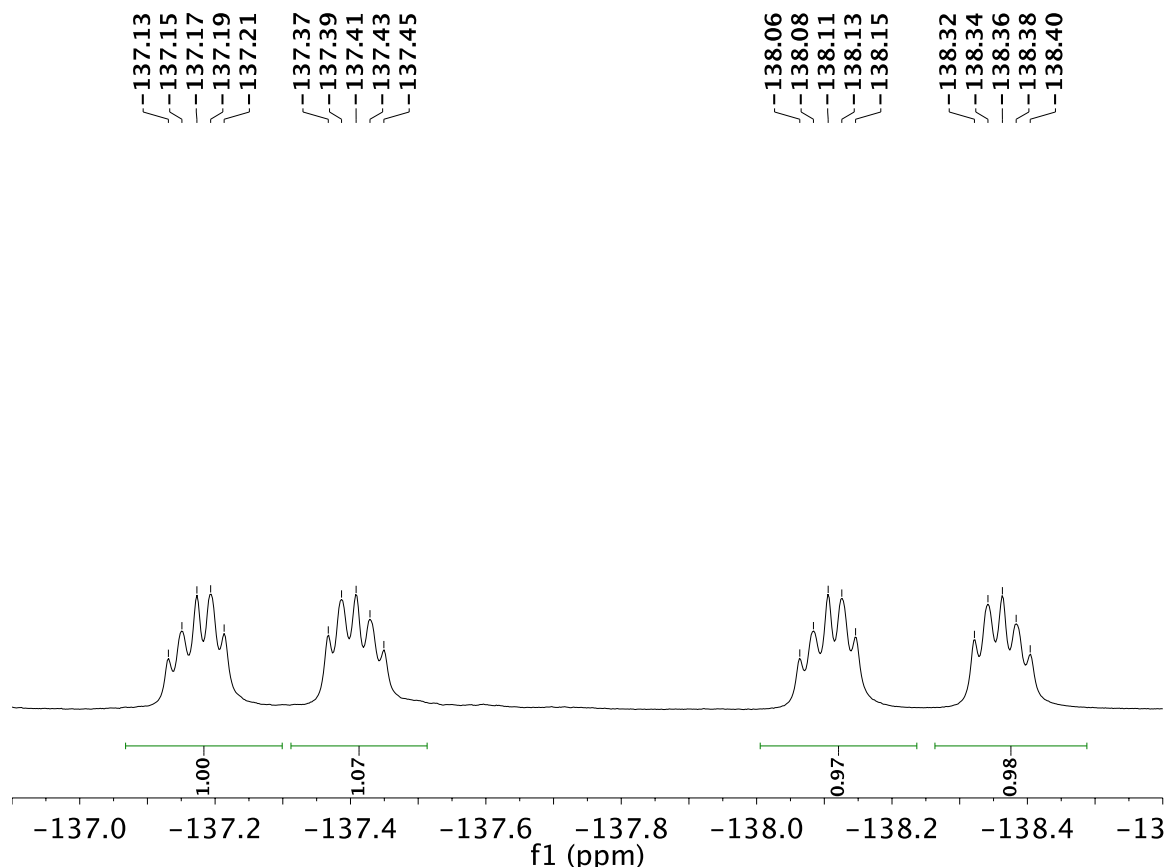
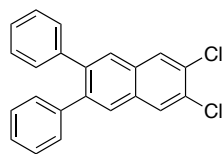


Figure S32. ^{19}F NMR (470 MHz) spectrum of **F-Ar-4** in CDCl_3 .

2.5 Chlorinated *ortho*-Arylenes



Cl-Ar-1: A solution of **1** (0.181 g, 1.02 mmol) and benzaldehyde **S3** (0.377 g, 1.37 mmol) in 1,2-dichloroethane (18 mL), which had been deoxygenated by sparging with N_2 for 5 min, was transferred via cannula into a round bottom flask equipped with a water-cooled condenser containing $\text{Cu}(\text{OTf})_2$ (0.024 g, 0.065 mmol) under a nitrogen atmosphere. Additional 1,2-dichloroethane (0.5 mL) was used to complete the solution transfer. TFA (0.25 mL, 0.37 g, 3.3 mmol) was immediately added. The mixture was heated in an oil bath to 100 °C for 2 h. The mixture was cooled to rt, NaHCO_3 (ca. 2 g) was added, and the mixture was filtered through a short pad of silica gel using 1:1 hexanes/ CH_2Cl_2 . The solvent from the filtrate was removed *in vacuo*. Column chromatography (silica gel, gradient 0% to 10% CH_2Cl_2 in hexanes) afforded **Cl-Ar-1** (0.353 g, 99%) as a white solid. R_f = 0.7 (10% CH_2Cl_2 in hexanes). IR (CDCl_3 cast film): 3021 (w), 1599 (w), 1584 (w), 1463 (w), 1442 (w), 1347 (w), 1260 (w), 1209 (w), 1179 (w), 1153 (w), 1120 (m), 1074 (w), 1020 (m), 981 (w), 944 (m), 903 (s), 891 (m), 856 (w), 825 (w), 774 (m), 765 (m), 751 (m), 728 (s), 699 (s), 659 (m), 636 (m) cm^{-1} . ^1H NMR (400 MHz, CDCl_3): δ 7.93 (s, 2H), 7.75 (s, 2H), 7.33–7.28 (s, 6H), 7.26–7.20 (m, 4H). ^{13}C NMR (100 MHz, CDCl_3): δ 140.6, 140.3, 131.4, 130.3, 129.8, 128.4, 128.2, 127.9, 126.9. DART HRMS m/z calcd. for $\text{C}_{22}\text{H}_{14}^{35}\text{Cl}_2$ (M^+), 348.0467, found 348.0462. Crystals suitable for X-ray crystallographic analysis were obtained from solutions of **Cl-Ar-1** in CHCl_3 that were layered with pentane and allowed to slowly evaporate at rt, for X-ray data of **Cl-Ar-1**, see: CCDC-1483966.

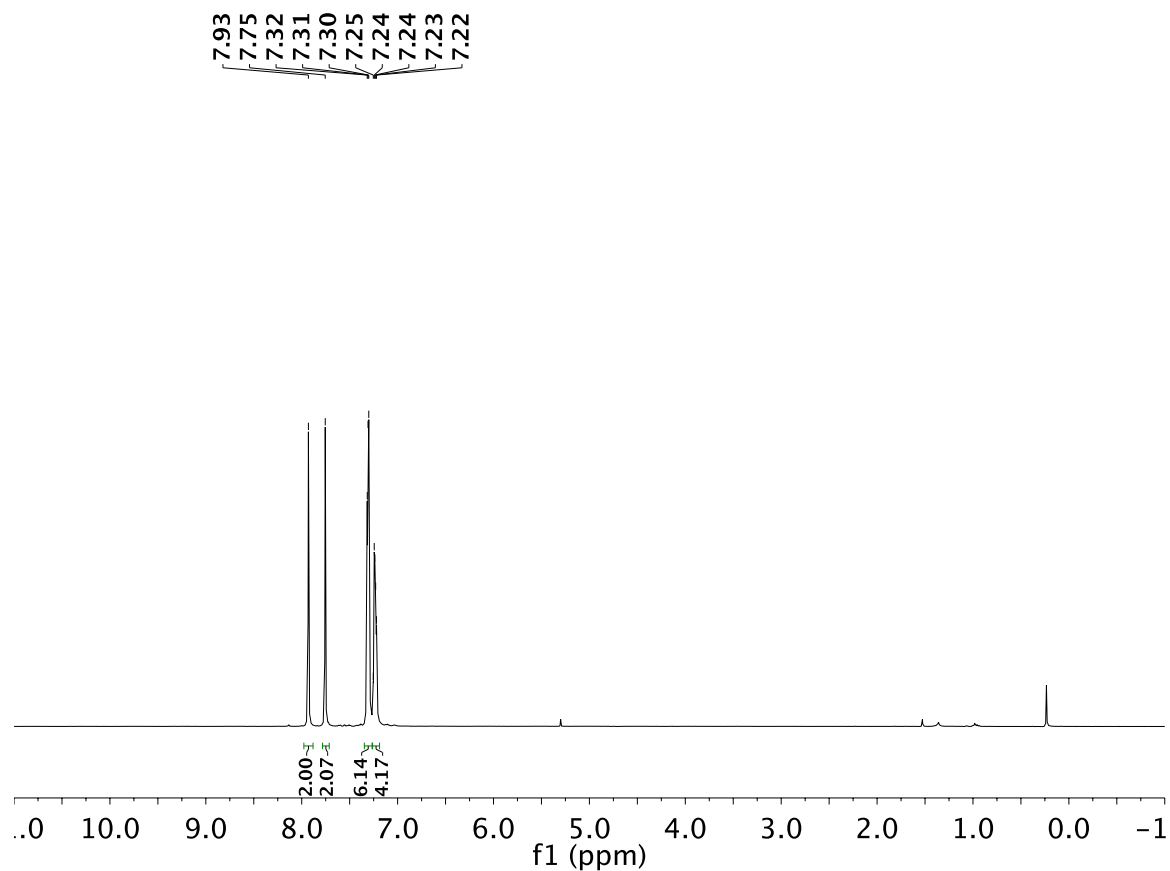


Figure S33. ^1H NMR (400 MHz) spectrum of **Cl-Ar-1** in CDCl_3 .

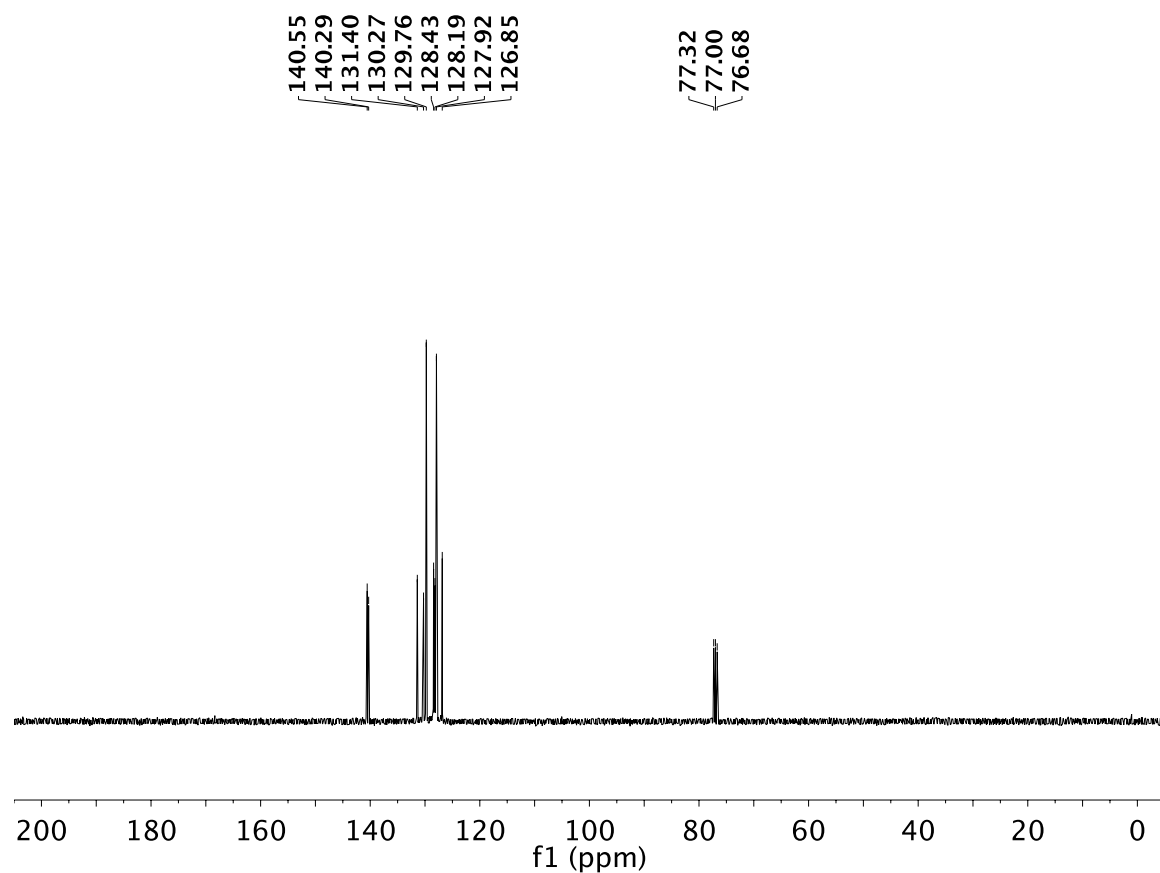
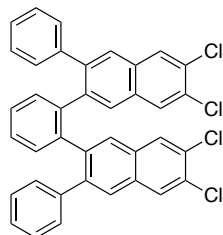


Figure S34. ^{13}C NMR (100 MHz) spectrum of **Cl-Ar-1** in CDCl_3 .



Cl-Ar-2: A solution of **2** (0.150 g, 0.539 mmol) and benzaldehyde **S2** (0.385 g, 1.40 mmol) in 1,2-dichloroethane (13 mL), which had been deoxygenated by sparging with N₂ for 5 min, was transferred via cannula into a round bottom flask equipped with a water-cooled condenser containing Cu(OTf)₂ (0.029 g, 0.081 mmol) under a nitrogen atmosphere. Additional 1,2-dichloroethane (0.5 mL) was used to complete the solution transfer. TFA (0.25 mL, 0.37 g, 3.3 mmol) was immediately added. The mixture was heated in an oil bath to 100 °C for 2 h. The mixture was cooled to rt, NaHCO₃ (ca. 2 g) was added, and the mixture was filtered through a short pad of silica gel using CH₂Cl₂. The solvent from the filtrate was removed *in vacuo*. Column chromatography (silica gel, gradient 0% to 10% CH₂Cl₂ in hexanes) afforded **Cl-Ar-2** (0.233 g, 78%) as a white solid. *R*_f = 0.5 (10% CH₂Cl₂ in hexanes). IR (CDCl₃ cast film): 3056 (w), 2889 (m), 1476 (m), 1443 (s), 1382 (m), 1344 (m), 1252 (m), 1178 (m), 1120 (s), 1076 (m), 1023 (w), 979 (m), 942 (m), 907 (s), 765 (m), 754 (m), 733 (m), 698 (s) cm⁻¹. ¹H NMR (500 MHz, CDCl₃): δ 7.77 (s, 2H), 7.58–7.52 (m, 4H), 7.34 (dd, 5.5, 3.5 Hz, 2H), 7.27–7.22 (m, 4H), 6.97 (t, *J* = 7.7 Hz, 4H), 6.46 (d, *J* = 7.3 Hz, 4H), 6.37 (s, 2H). ¹³C NMR (125 MHz, CDCl₃): δ 140.2, 140.1, 139.8, 139.1, 131.5, 131.2, 131.1, 129.8, 129.7, 129.5, 128.9, 128.8, 128.2, 128.0, 127.5, 126.6, 126.5. DART HRMS *m/z* calcd. for C₃₈H₂₃³⁵Cl₄ ([M + H]⁺), 619.0548, found 619.0531. Crystals suitable for X-ray crystallographic analysis were obtained from solutions of **Cl-Ar-2** in CHCl₃ that were layered with pentane and allowed to slowly evaporate at rt, for X-ray data of **Cl-Ar-2**, see: CCDC-1483967.

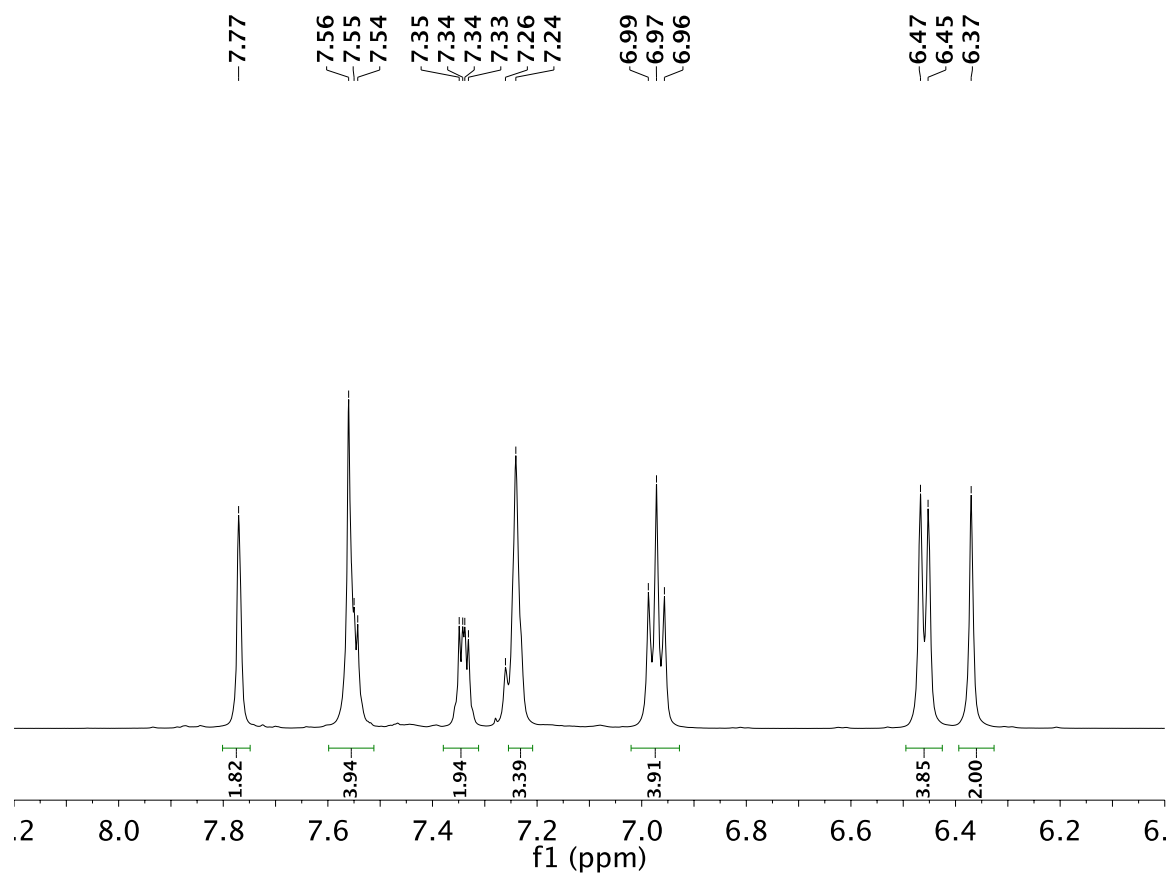
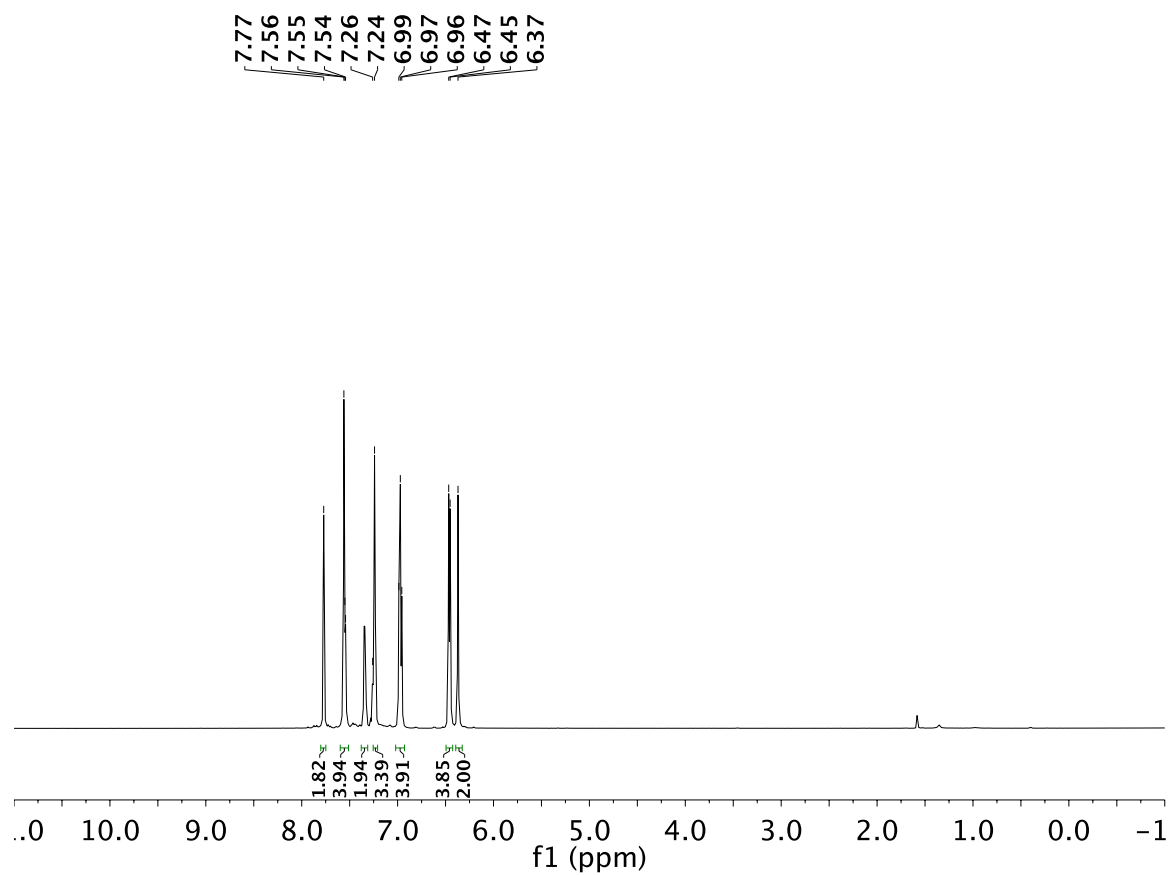


Figure S35. ^1H NMR (500 MHz) spectrum of **Cl-Ar-2** in CDCl_3 : (top) full view, (bottom) 8.20 to 6.00 ppm region.

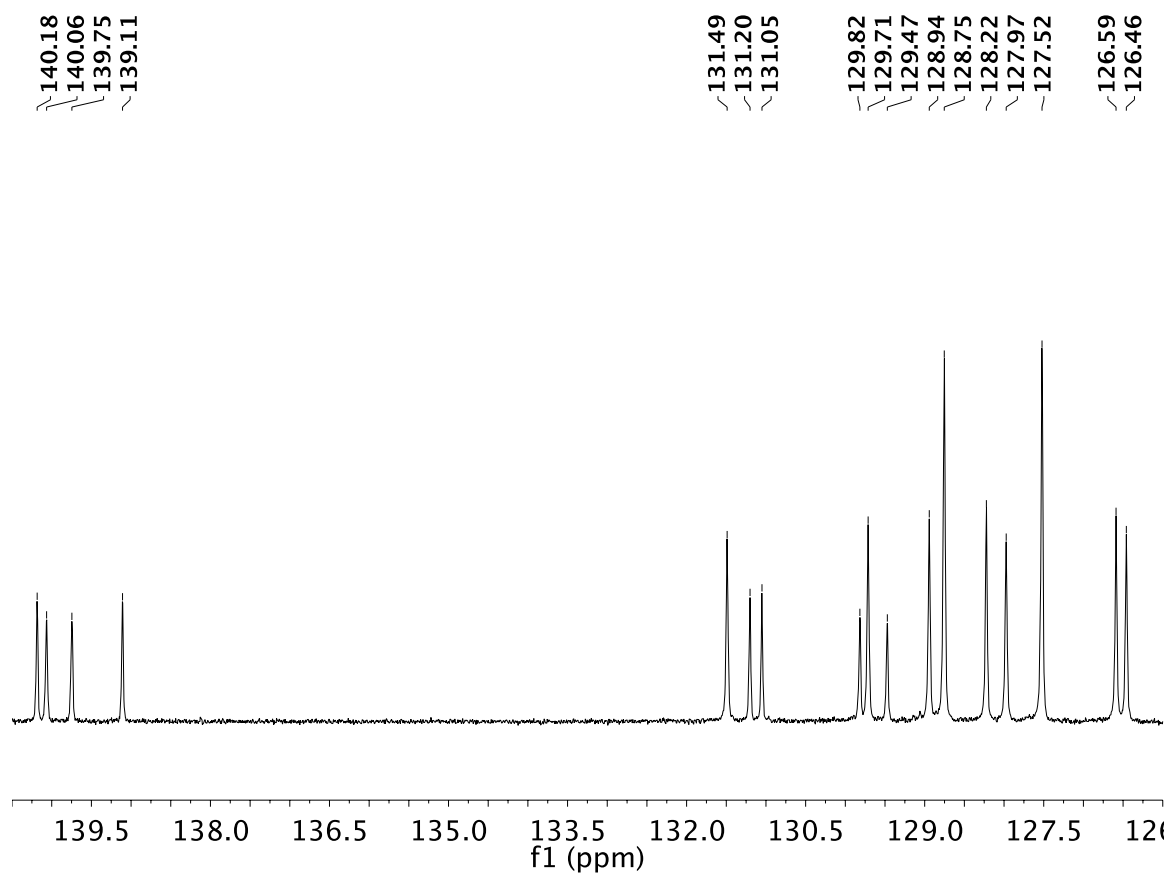
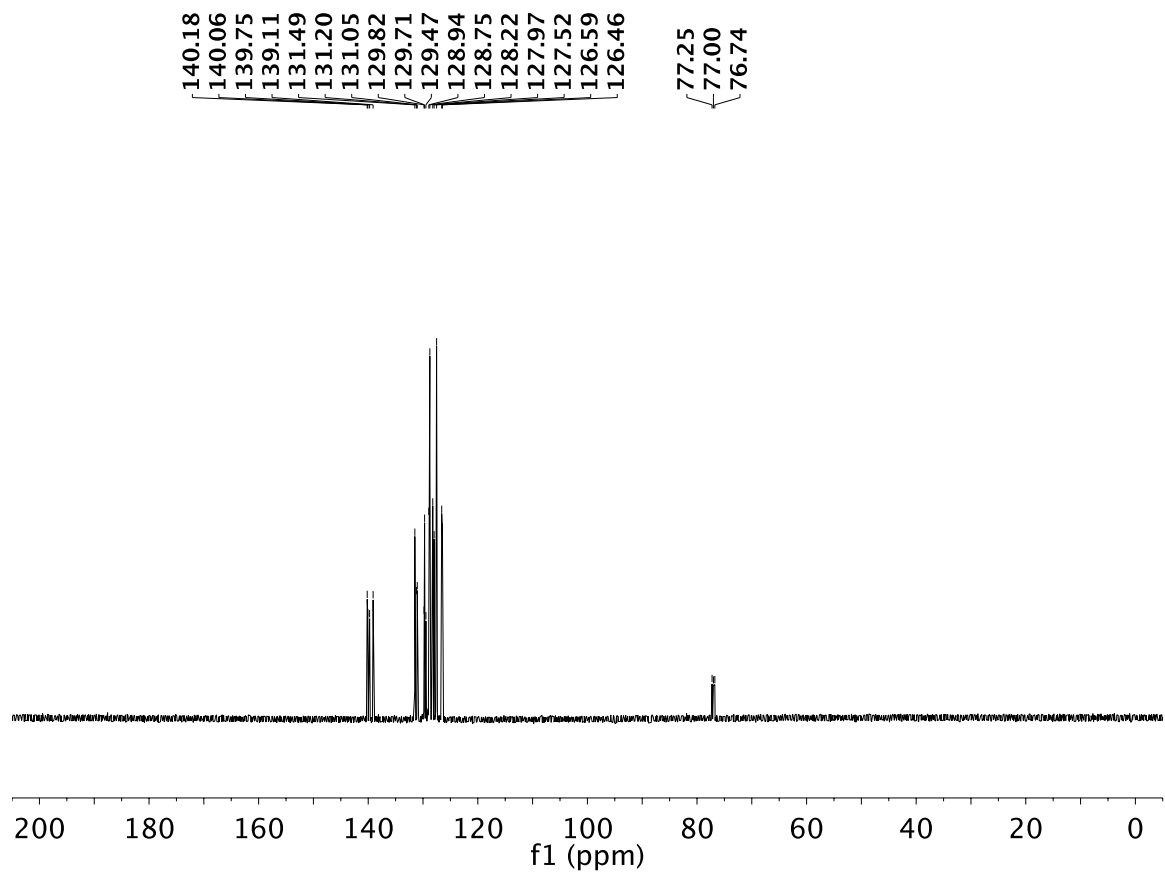
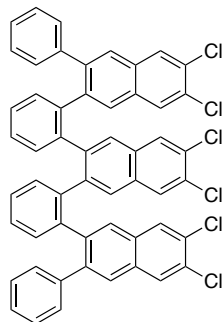


Figure S36. ^{13}C NMR (125 MHz) spectrum of **Cl-Ar-2** in CDCl_3 : (top) full view, (bottom) 140.5 to 126.0 ppm region.



Cl-Ar-3: To a round bottom flask was added **3** (0.250 g, 0.661 mmol) and benzaldehyde **S3** (0.818 g, 2.97 mmol), followed by 1,2-dichloroethane (9.4 mL). The resulting suspension was deoxygenated by sparging with N₂ for 2 min prior to adding Cu(OTf)₂ (0.072 g, 0.198 mmol), followed by immediately equipping the round bottom flask with a water-cooled condenser, resuming sparging with N₂ for 1 min and followed by adding TFA (0.46 mL, 0.68 g, 5.9 mmol) to this mixture. The mixture was heated in an oil bath to 100 °C for 2 h. The mixture was cooled to rt, NaHCO₃ (ca. 2 g) was added, and the mixture was filtered through a short pad of silica gel using CH₂Cl₂. The solvent from the filtrate was removed *in vacuo*. Column chromatography (silica gel, gradient 10% to 20% CH₂Cl₂ in hexanes) followed by trituration using CH₂Cl₂/pentane afforded **Cl-Ar-3** (0.209 g, 35%) as an off white solid. *R*_f = 0.8 (20% CH₂Cl₂ in hexanes). IR (CDCl₃ cast film): 3046 (vw), 1477 (w), 1442 (m), 1178 (w), 1117 (m), 906 (s), 765 (m), 752 (m), 733 (m), 704 (m), 697 (m) cm⁻¹. ¹H NMR (800 MHz, CDCl₃): δ 7.80 (s, 2H), 7.66 (s, 2H), 7.33 (s, 2H), 7.28–7.27 (m, 2H), 7.22 (dt, *J* = 7.4, 1.1 Hz, 2H), 7.18 (s, 2H), 6.95 (t, *J* = 7.3 Hz, 2H), 6.81 (s, 2H), 6.59 (t, *J* = 7.1 Hz, 4H), 6.28 (dt, *J* = 7.4, 1.2 Hz, 2H), 6.07 (d, *J* = 7.4 Hz, 4H), 5.90 (s, 2H), 5.66 (dd, *J* = 7.5, 0.8 Hz, 2H). ¹³C NMR (125 MHz, CDCl₃): δ 140.4, 140.2, 140.1, 139.8, 139.6, 138.7, 131.9, 131.7, 131.6, 131.4, 131.2, 129.9, 129.7, 129.6, 129.4, 129.2, 129.0, 128.8, 128.4, 128.0, 127.8, 127.5, 127.3, 127.1, 126.2. DART HRMS *m/z* calcd. for C₅₄H₃₁³⁵Cl₆ ([M + H]⁺), 889.0551, found 889.0507.

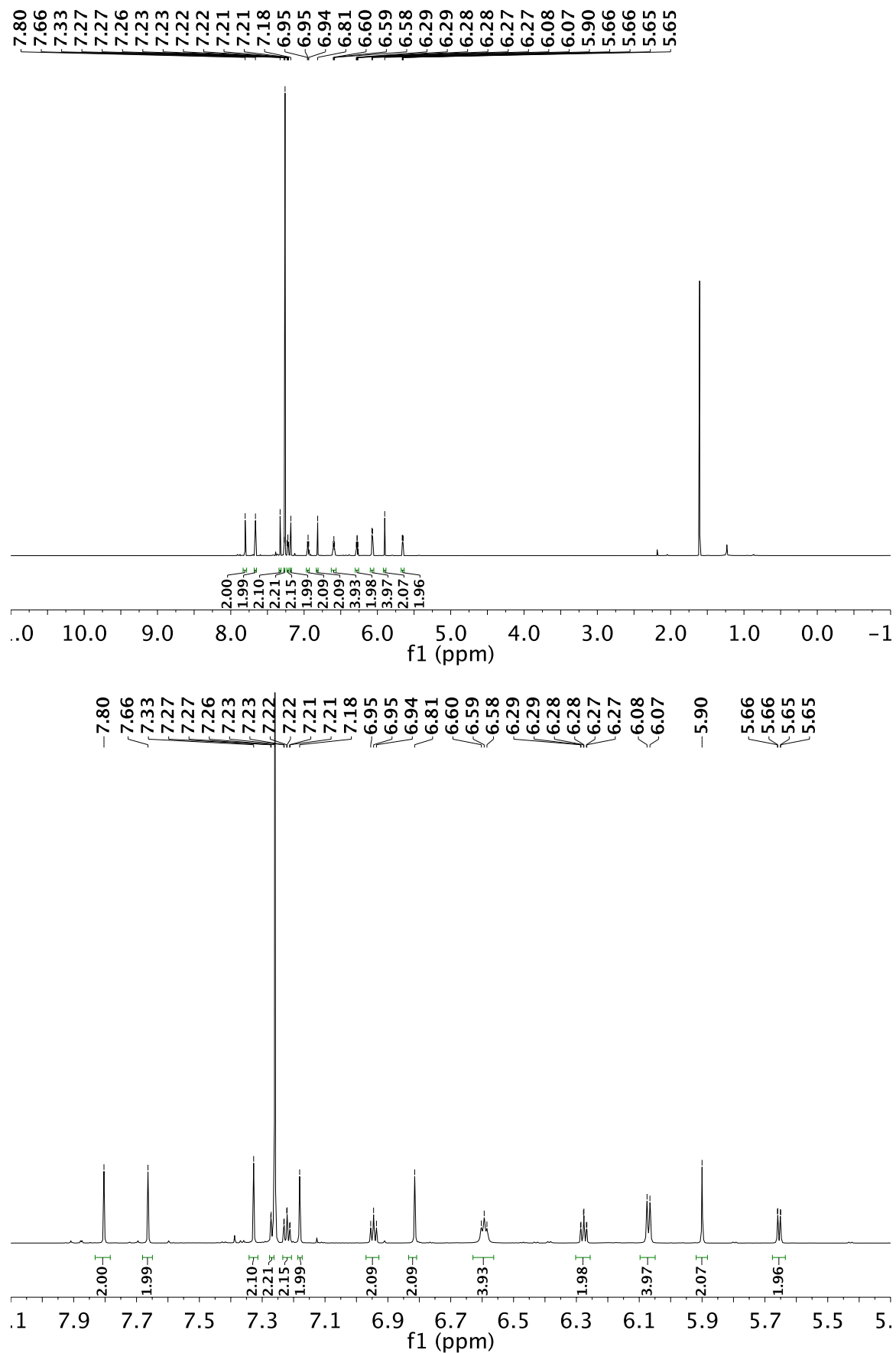


Figure S37. ^1H NMR (800 MHz) spectrum of **Cl-Ar-3** in CDCl_3 : (top) full view, (bottom) 8.10 to 5.30 ppm region.

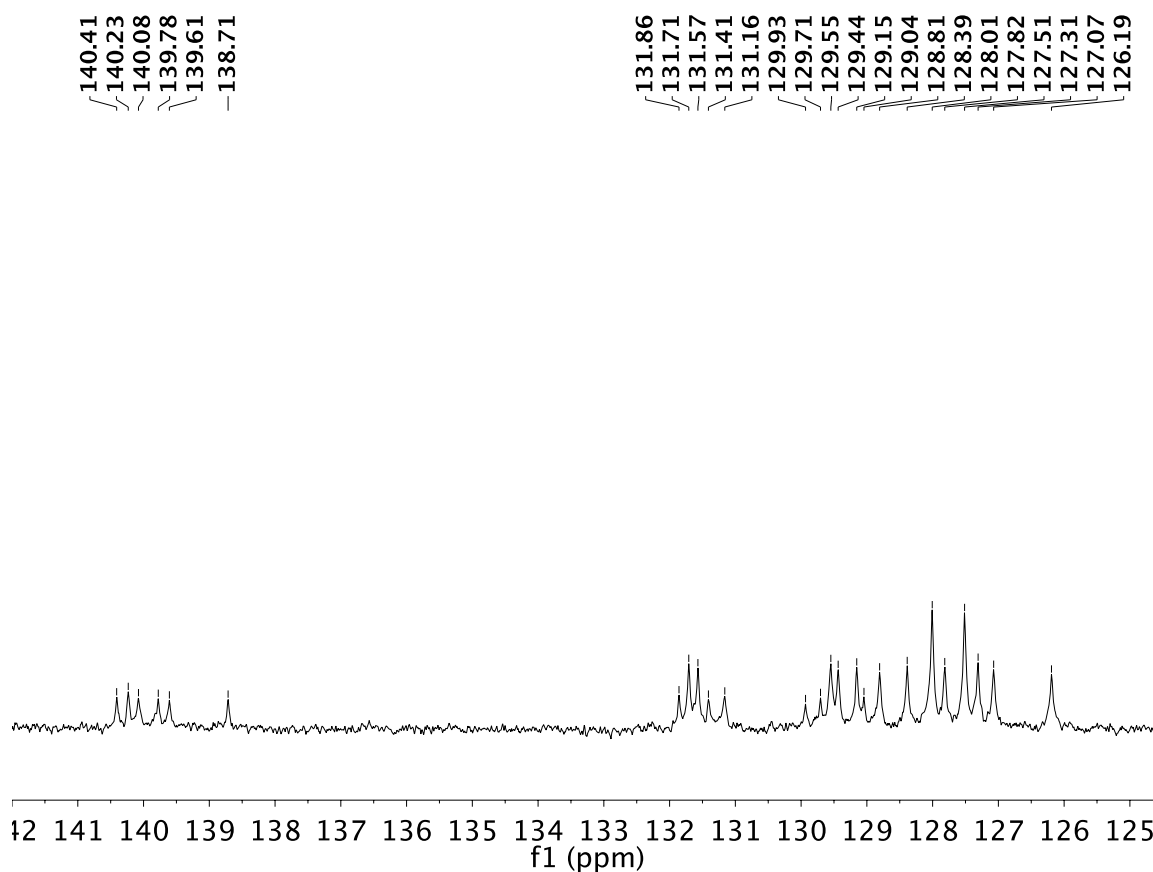
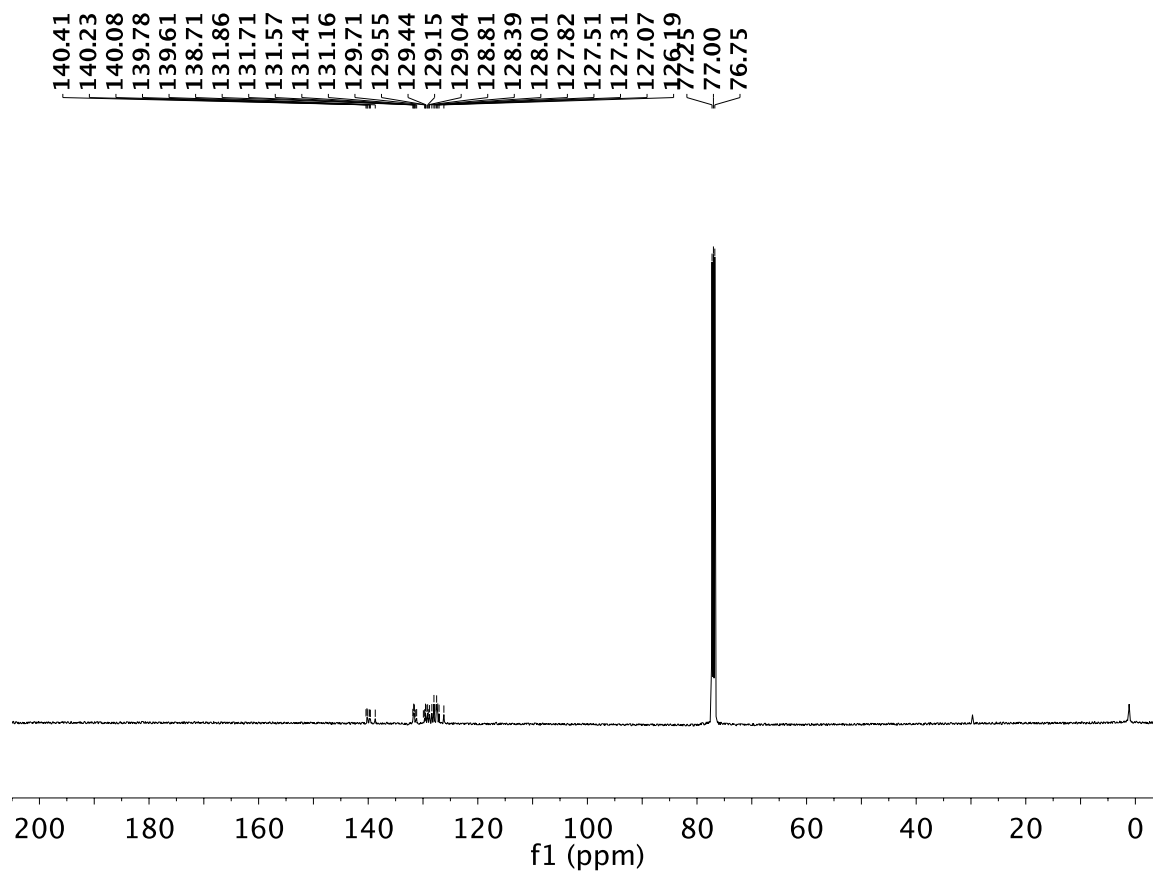
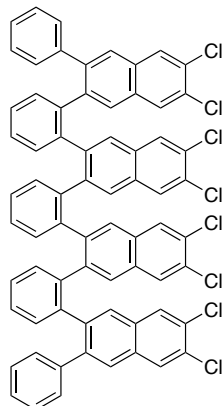


Figure S38. ^{13}C NMR (125 MHz) spectrum of **Cl-Ar-3** in CDCl_3 : (top) full view, (bottom) 142.0 to 124.5 ppm region.



Cl-Ar-4: To a round bottom flask was added **4** (0.250 g, 0.522 mmol) and benzaldehyde **S3** (0.862 g, 3.13 mmol), followed by 1,2-dichloroethane (13.1 mL). The resulting suspension was deoxygenated by sparging with N₂ for 2 min prior to adding Cu(OTf)₂ (0.076 g, 0.209 mmol), followed by immediately equipping the round bottom flask with a water-cooled condenser, resuming sparging with N₂ for 1 min and followed by adding TFA (0.48 mL, 0.72 g, 6.3 mmol) to this mixture. The mixture was heated in an oil bath to 100 °C for 2 h. The mixture was cooled to rt, NaHCO₃ (ca. 2 g) was added, and the mixture was filtered through a short pad of silica gel using CH₂Cl₂. The solvent from the filtrate was removed *in vacuo*. Column chromatography (silica gel, 20% CH₂Cl₂ in hexanes) followed by trituration using CH₂Cl₂/pentane afforded **Cl-Ar-4** (0.167 g, 28%) as an off white solid. *R*_f = 0.4 (20% CH₂Cl₂ in hexanes). IR (CDCl₃ cast film): 3055 (w), 1580 (w), 1480 (m), 1441 (m), 1342 (w), 1178 (m), 1118 (m), 1025 (w), 980 (w), 942 (w), 906 (s), 764 (m), 753 (m), 733 (m), 699 (m) cm⁻¹. ¹H NMR (500 MHz, CDCl₃): δ 7.74(s, 2H), 7.52 (s, 2H), 7.47 (s, 2H), 7.35 (s, 2H), 7.10 (s, 2H), 7.05 (d, *J* = 7.0 Hz, 2H), 6.97 (t, *J* = 7.3 Hz, 2H), 6.94 (t, *J* = 7.3 Hz, 2H), 6.59 (t, *J* = 7.8 Hz, 4H), 6.48 (s, 2H), 6.38 (s, 2H), 6.06 (dd, *J* = 5.6, 3.3 Hz, 2H), 6.02 (d, *J* = 7.4 Hz, 4H), 5.92 (dt, *J* = 7.5, 0.6 Hz, 2H), 5.85 (s, 2H), 5.70 (dd, *J* = 5.6, 3.4 Hz, 2H), 5.53 (d, *J* = 7.4 Hz, 2H). ¹³C NMR (125 MHz, CDCl₃): δ 140.4, 140.2, 140.1, 139.7, 139.4, 139.2, 138.9, 138.1, 131.63, 131.61, 131.58, 131.4, 131.2, 130.8, 129.8, 129.6, 129.2, 128.99, 128.97, 128.93, 128.82, 128.75, 128.3, 127.9, 127.6, 127.5, 127.1, 127.0, 126.1. DART HRMS *m/z* calcd. for C₇₀H₃₉³⁵Cl₈ ([M + H]⁺), 1159.0555, found 1159.0508.

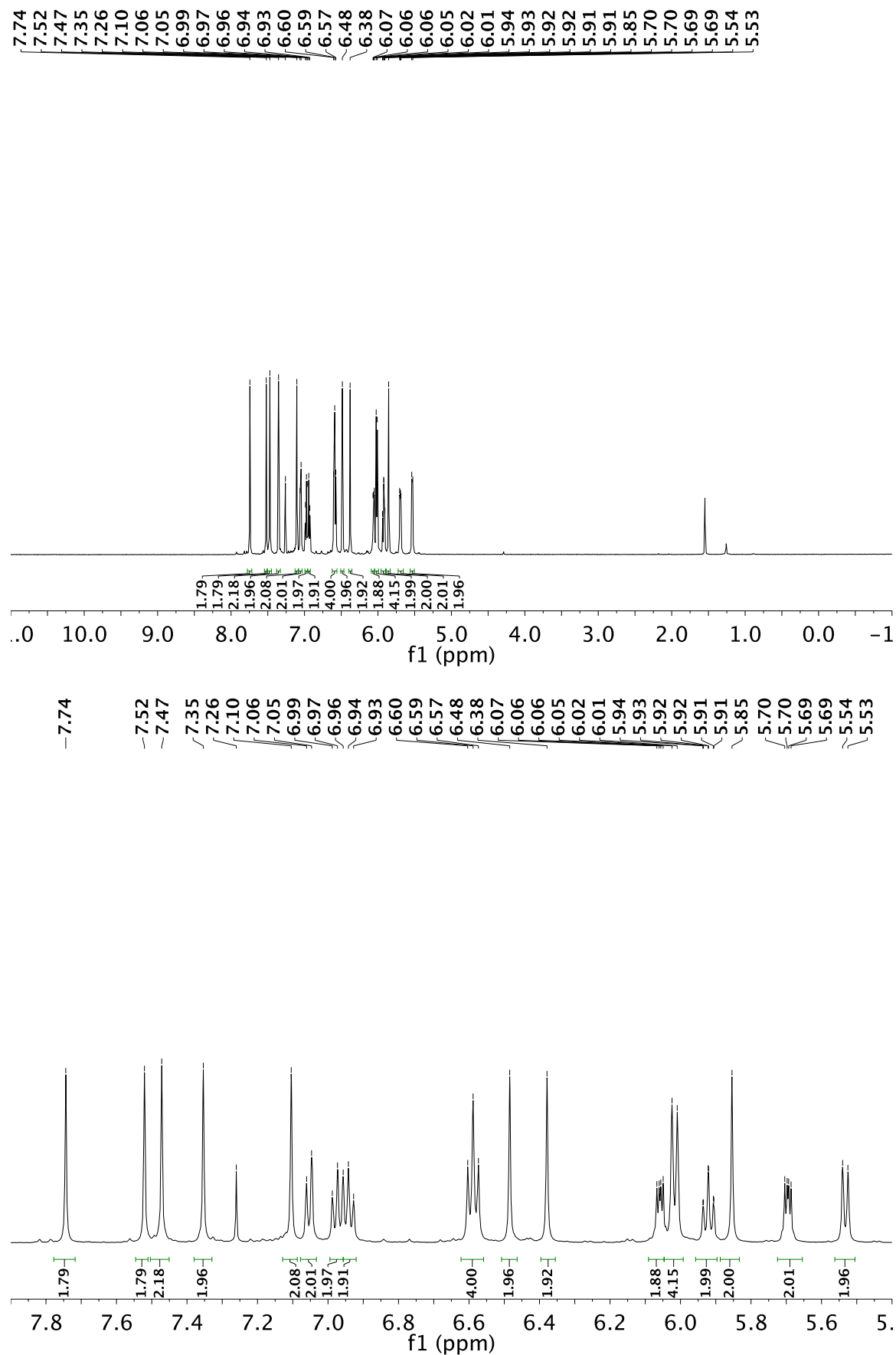


Figure S39. ¹H NMR (500 MHz) spectrum of Cl-Ar-4 in CDCl₃: (top) full view, (bottom) 7.90 to 5.40 ppm region.

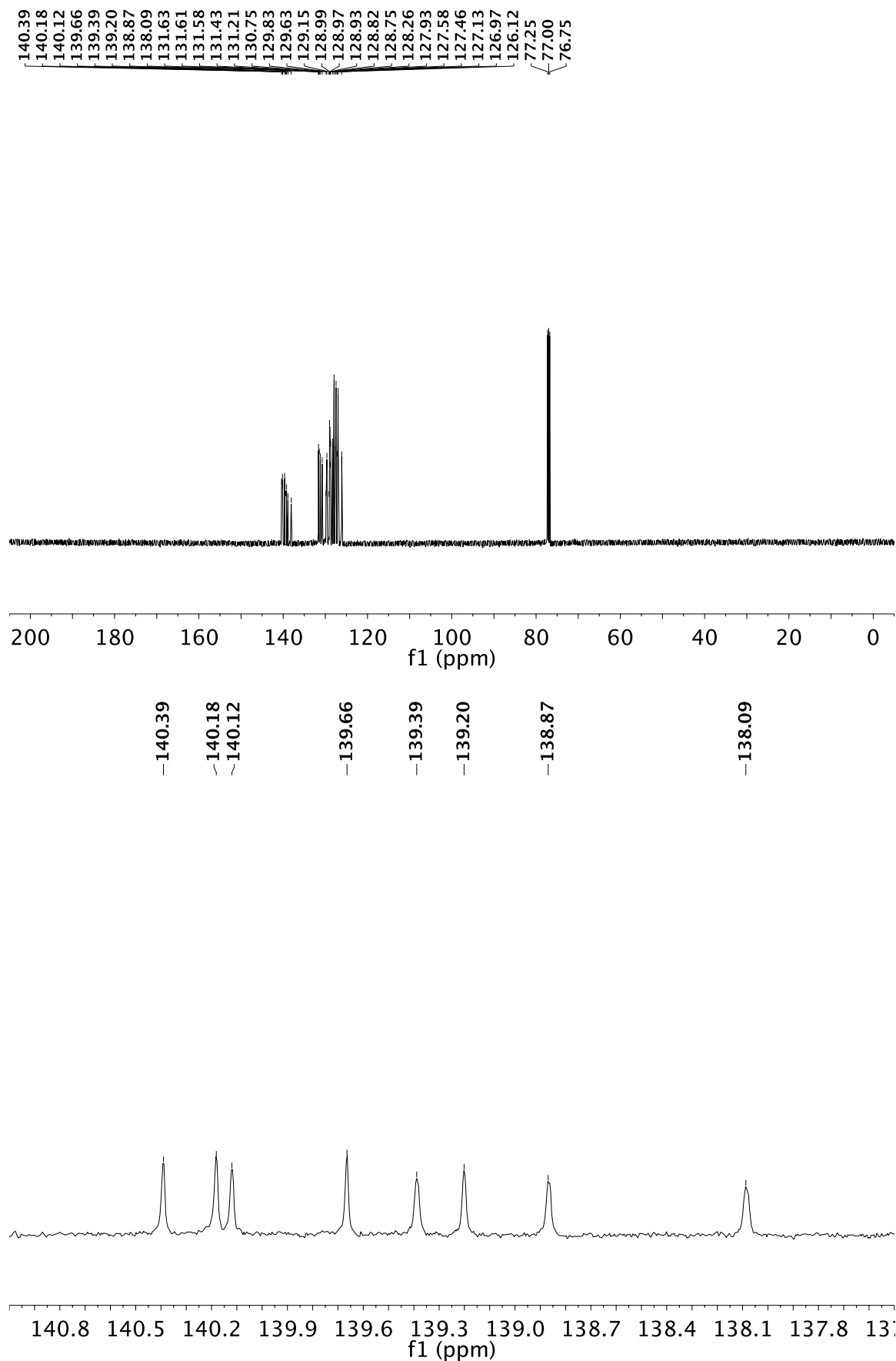


Figure S40. ^{13}C NMR (125 MHz) spectrum of **Cl-Ar-4** in CDCl_3 : (top) full view, (bottom) 141.0 to 137.5 ppm region.

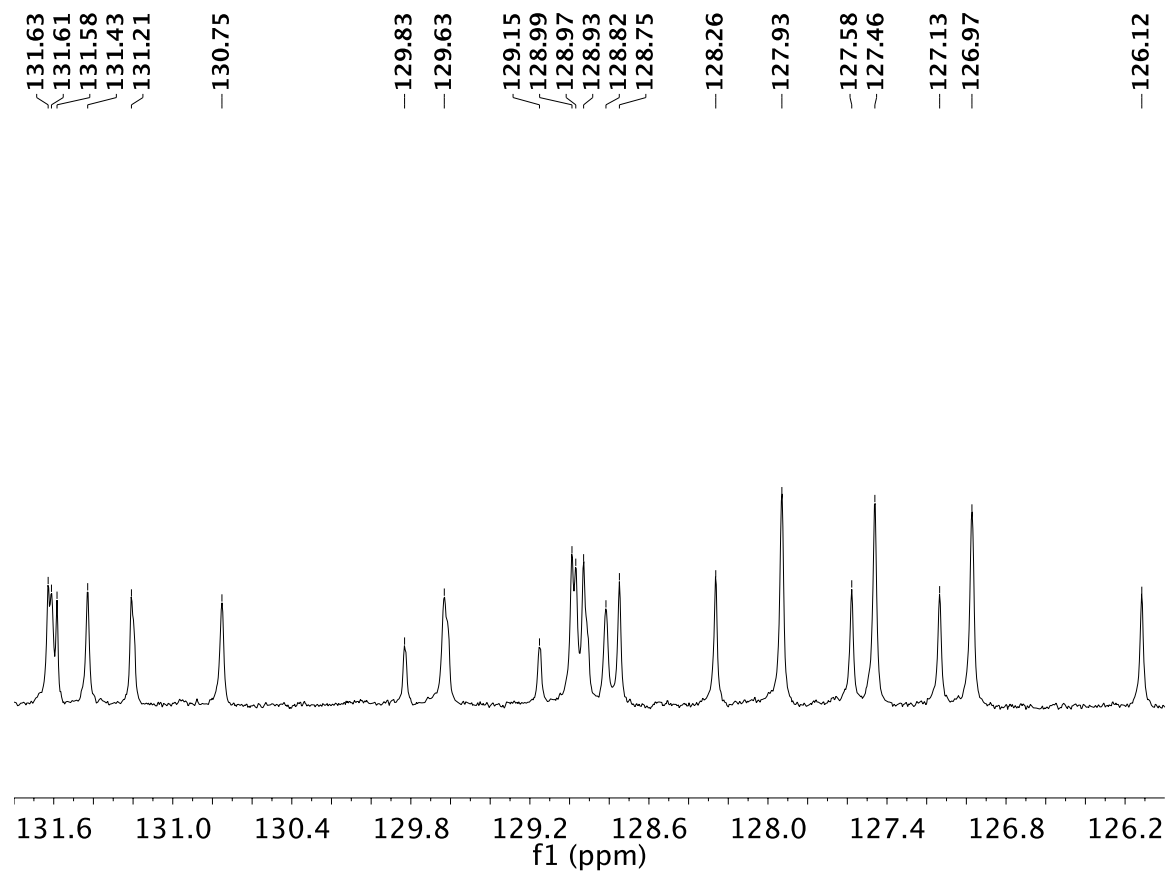
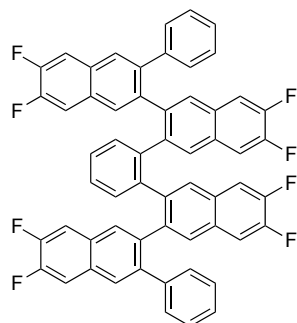


Figure S41. ^{13}C NMR (125 MHz) spectrum of **Cl-Ar-4** in CDCl_3 : 131.8 to 126.0 ppm region.

2.6. *ortho*-Arylenes from Diynes



F-Ar-5: A solution of **5** (0.200 g, 0.613 mmol) and benzaldehyde **S2** (1.04 g, 4.29 mmol) in 1,2-dichloroethane (31 mL), which had been deoxygenated by sparging with N₂ for 5 min, was transferred via cannula into a round bottom flask equipped with a water-cooled condenser containing Cu(OTf)₂ (0.089 g, 0.245 mmol) under a nitrogen atmosphere. TFA (1.88 mL, 2.80 g, 24.5 mmol) was immediately added. The mixture was heated in an oil bath to 100 °C for 2 h. The mixture was cooled to rt, NaHCO₃ (ca. 6 g) was added, and the mixture was filtered through a short pad of silica gel using 1:1 hexanes/CH₂Cl₂. The solvent from the filtrate was removed *in vacuo*. The residue was suspended in CH₂Cl₂ (ca. 15 mL) accompanied with stirring for 5 h. The mixture was filtered and the solid wash washed with CH₂Cl₂ (3 x ca. 2 mL) to afford **F-Ar-5** (0.157 g, 35%) as a white solid. *R*_f = 0.5 (35% CH₂Cl₂ in hexanes). IR (neat solid): 3056 (vw), 1602 (w), 1511 (s), 1471 (m), 1445 (w), 1396 (w), 1356 (m), 1272 (m), 1241 (s), 1154 (w), 1125 (m), 941 (w), 914 (m), 901 (s), 852 (s), 776 (m), 759 (m), 745 (s), 712 (m), 696 (s) cm⁻¹. ¹H NMR (600 MHz, CDCl₃): δ 7.63 (s, 2H), 7.54 (dd, *J* = 9.5, 8.2 Hz, 2H), 7.43 (t, *J* = 9.9, 8.1 Hz, 2H), 7.32 (s, 2H), 6.98 (t, *J* = 7.40 Hz, 2H), 6.80 (t, *J* = 7.40 Hz, 2H), 6.71 (s, 2H), 6.64 (dd, *J* = 5.4, 3.5 Hz, 2H), 6.43 (dd, *J* = 9.7, 8.0 Hz, 2H), 6.36 (dd, *J* = 10.3, 8.6 Hz, 2H), 6.27 (d, *J* = 7.2 Hz, 4H), 6.18 (s, 2H), 5.70 (dd, *J* = 5.3, 3.5 Hz, 2H). ¹³C NMR¹² (125 MHz, CDCl₃): δ 151.35, 151.34, 151.25, 151.21, 150.97, 150.84, 150.80, 150.68, 149.38, 149.33, 149.28, 149.21, 148.97, 148.85, 148.81, 148.68, 140.51, 140.12, 138.75, 138.57, 138.47, 131.66, 129.81, 129.75, 129.39, 129.29, 129.25, 129.11, 129.08, 128.87, 128.81, 128.70, 128.65, 128.02, 127.76, 127.57, 127.54, 127.22, 126.01, 112.56, 112.44, 112.31, 112.24, 112.10. ¹⁹F NMR (470 MHz, CDCl₃): δ -136.76 – -136.95 (m, 4F), -137.21 – -137.34 (m, 2F), -137.42 – -137.54 (m, 2F). DART HRMS *m/z* calcd. for C₅₈H₃₀F₈ (M⁺), 878.2214, found 878.2225.

(12) The complete line list of signals for the proton decoupled ¹³C NMR is provided without interpretation of the coupling to ¹⁹F due to the complex nature of the spectrum.

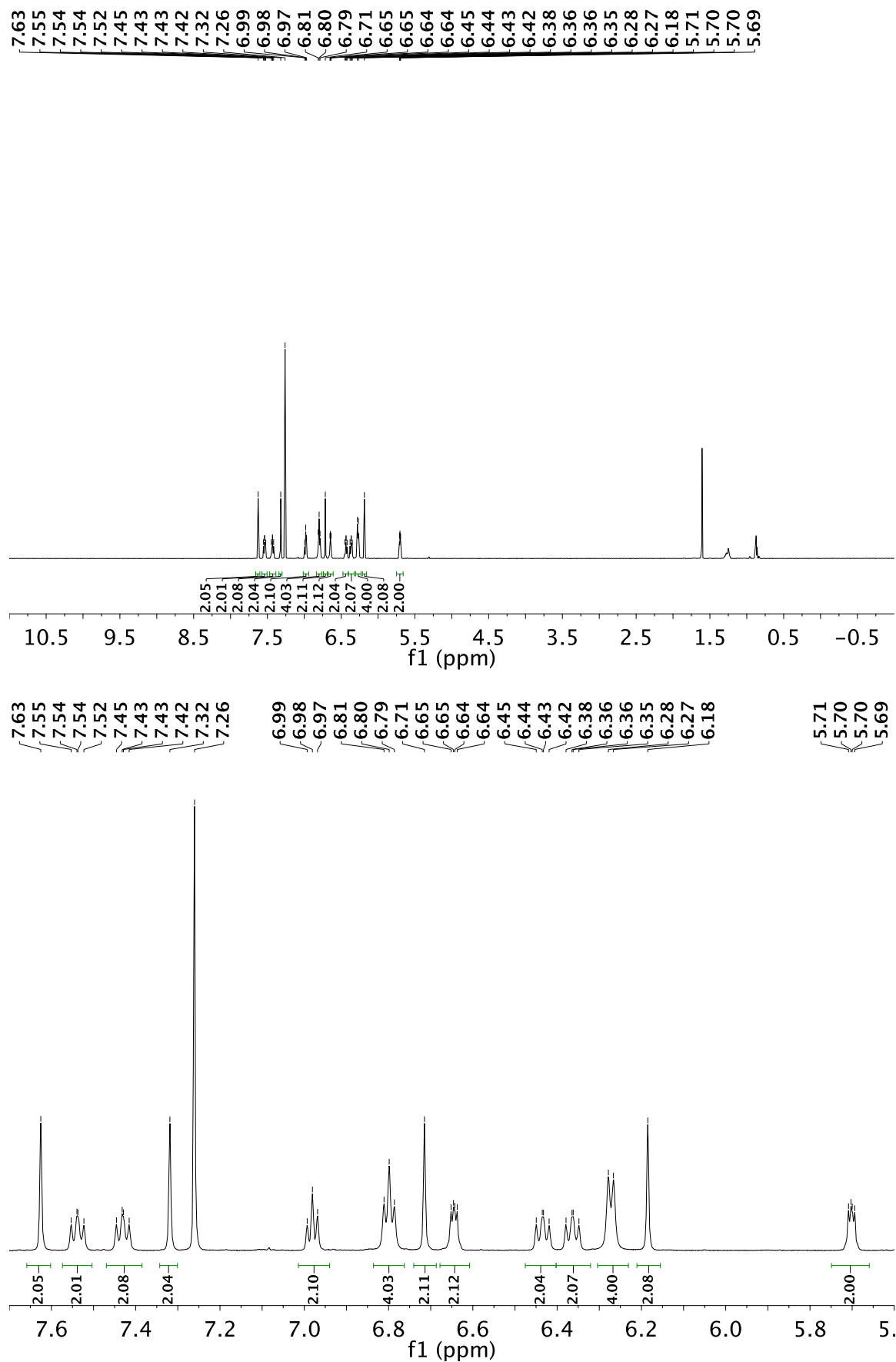


Figure S42. ^1H NMR (600 MHz) spectrum of **F-Ar-5** in CDCl_3 : (top) full view, (bottom) 7.70 to 5.60 ppm region.

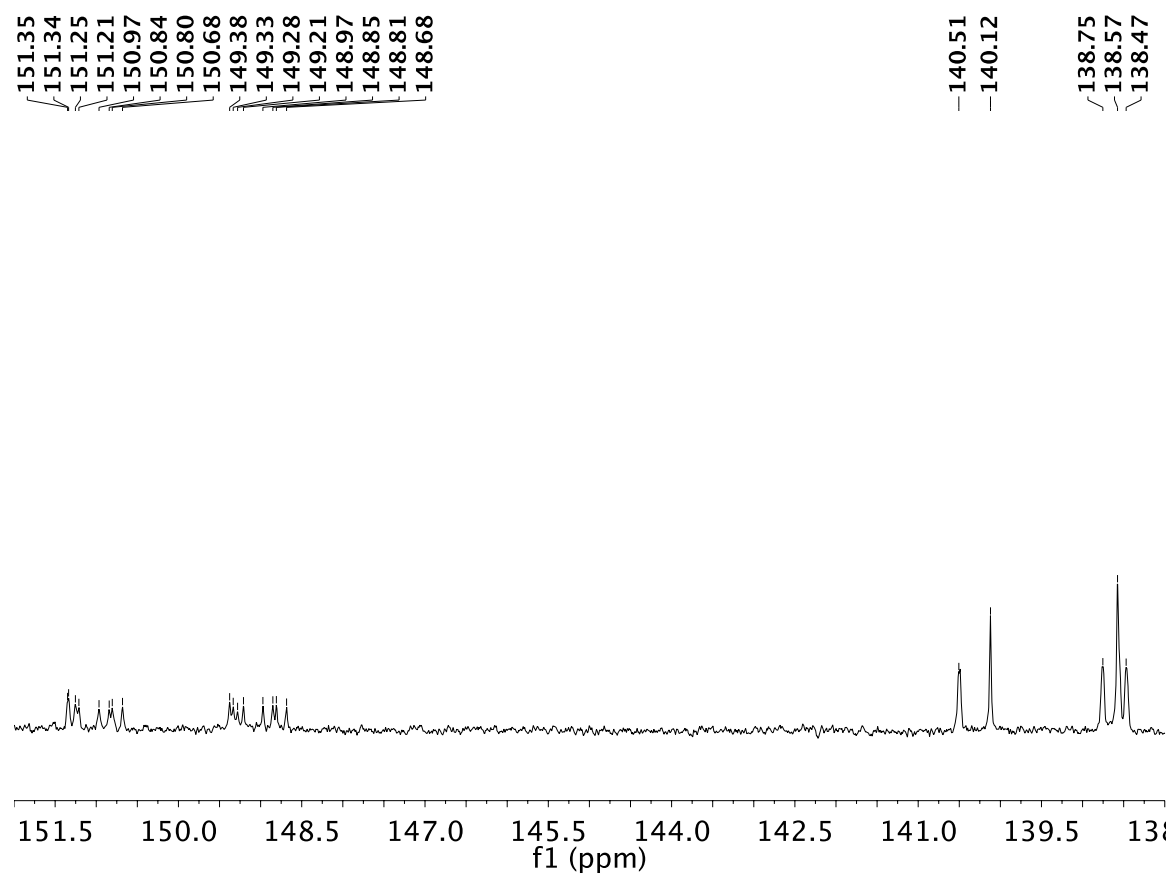
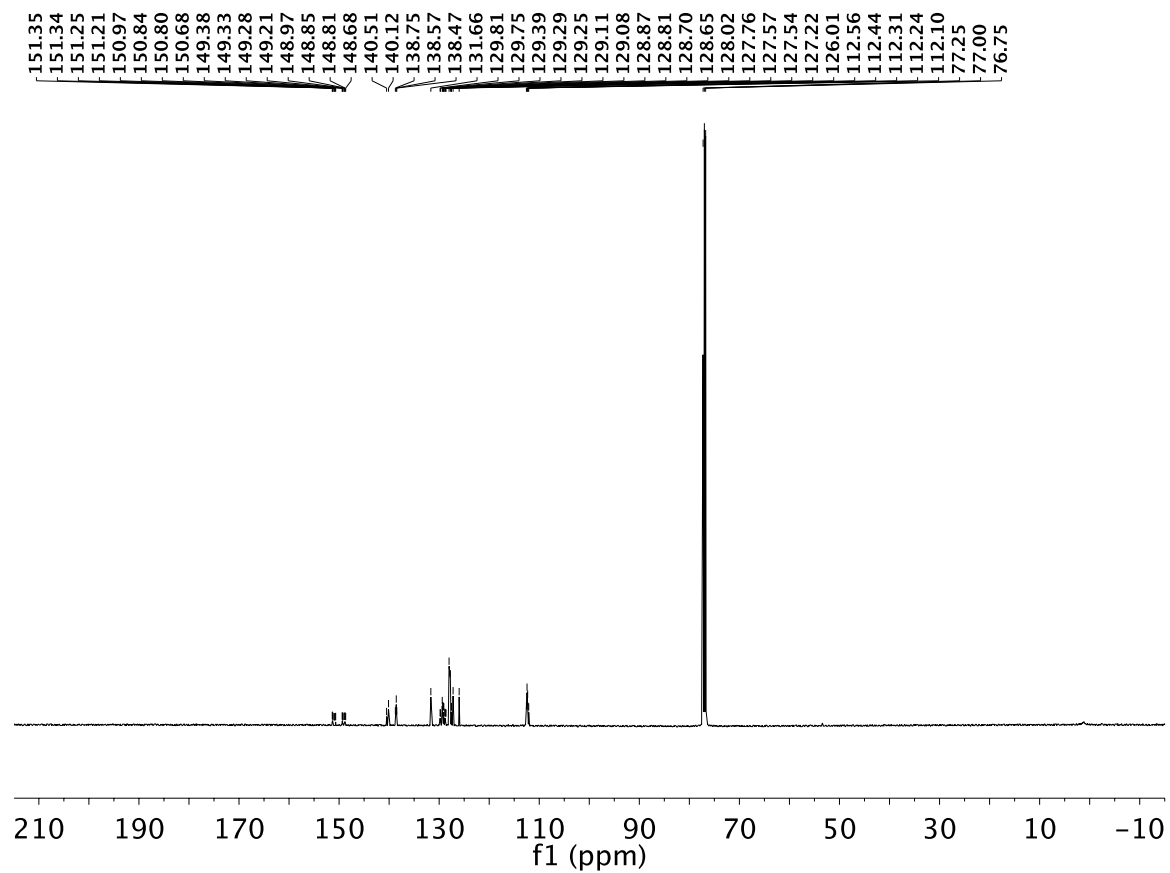


Figure S43. ^{13}C NMR (125 MHz) spectrum of **F-Ar-5** in CDCl_3 : (top) full view, (bottom) 152.0 to 138.0 ppm region.

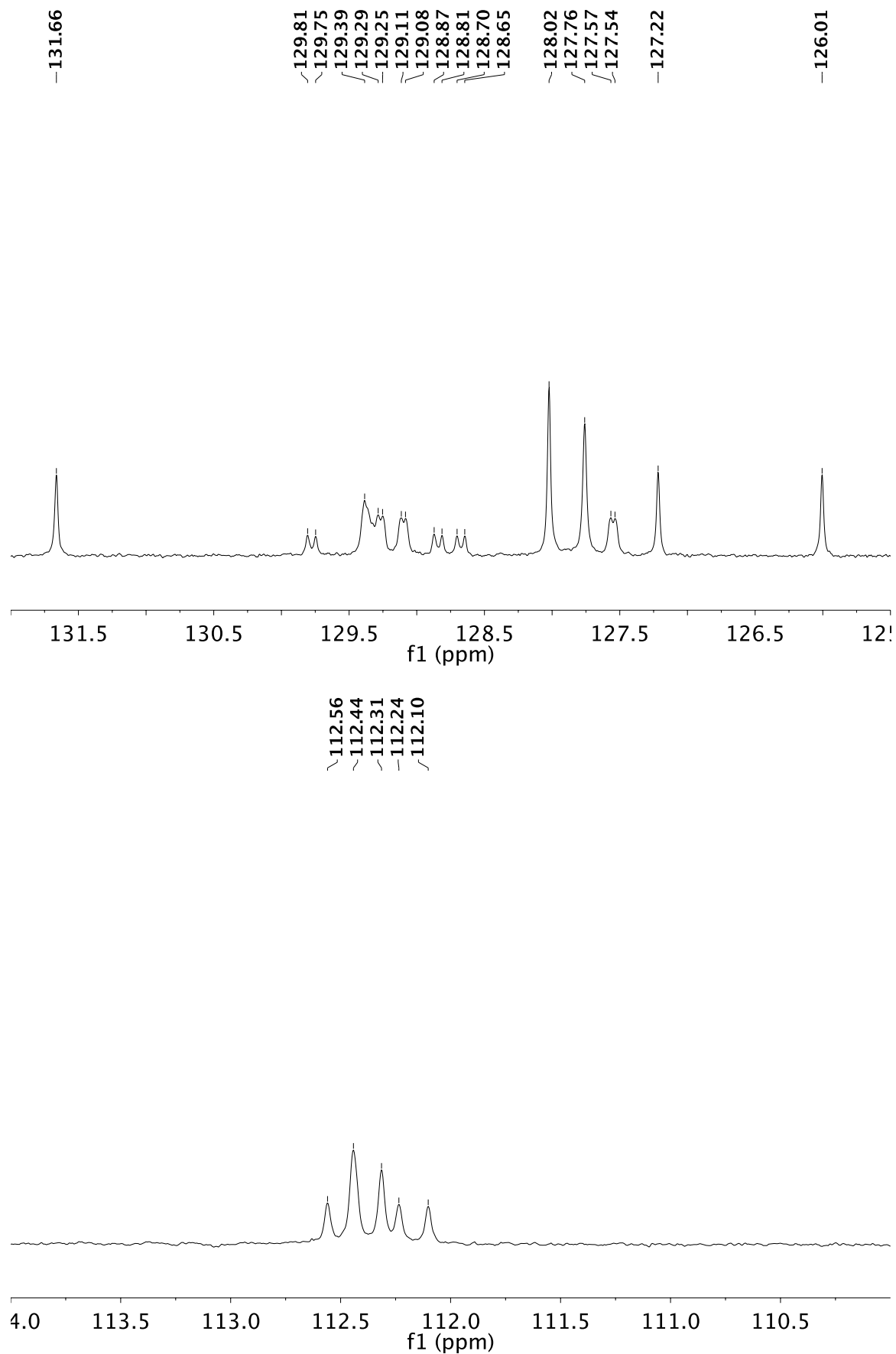


Figure S43 (continued). ^{13}C NMR (125 MHz) spectrum of **F-Ar-5** in CDCl_3 : (top) 132.0 to 125.5 ppm region, (bottom) 114.0 to 110.0 ppm region.

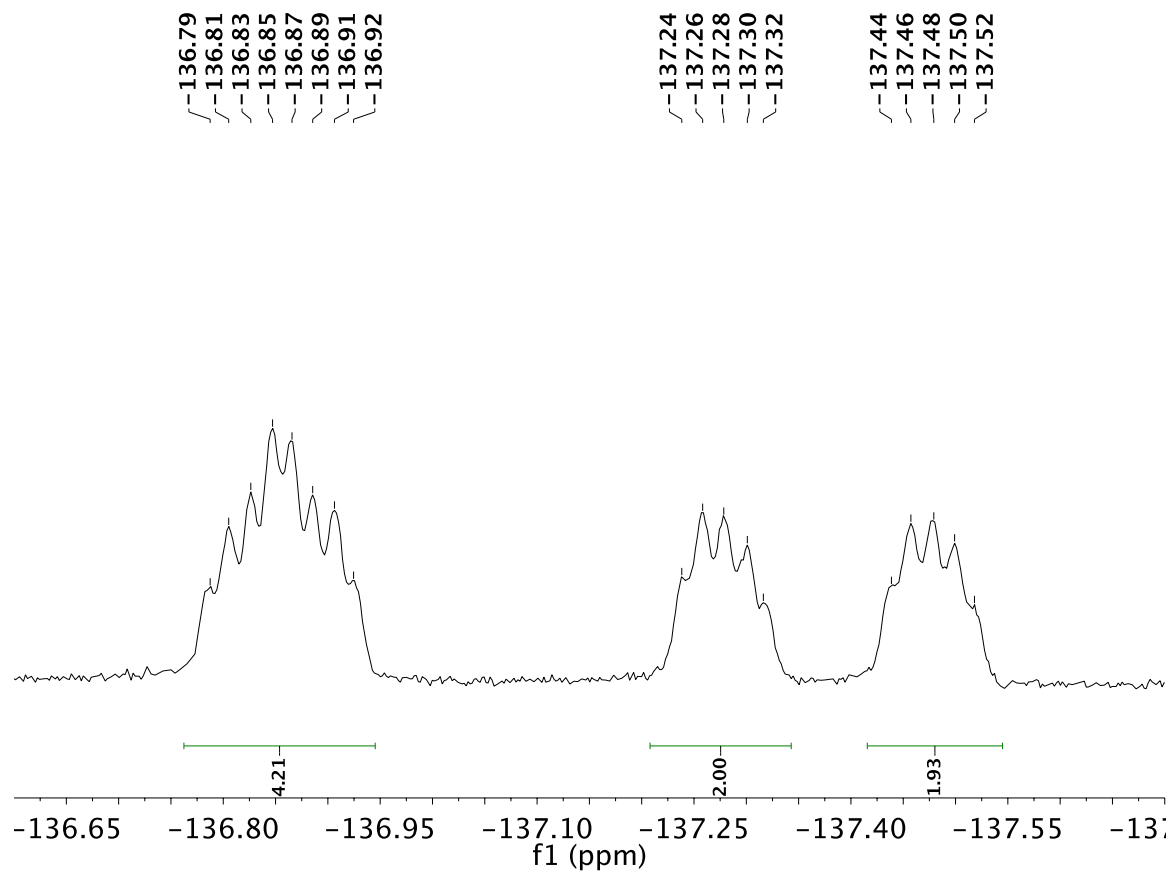
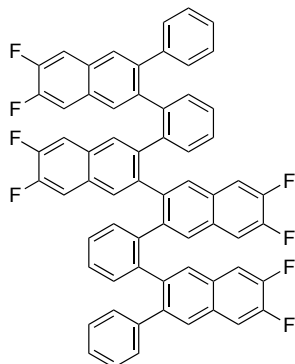


Figure S44. ^{19}F NMR (470 MHz) spectrum of **F-Ar-5** in CDCl_3 .



F-Ar-6: A solution of **6** (0.200 g, 0.497 mmol) and 2-(phenylethynyl)-4,5-difluorobenzaldehyde (0.963 g, 3.98 mmol) in 1,2-dichloroethane (10 mL), which had been deoxygenated by sparging with N₂ for 5 min, was transferred via cannula into a round bottom flask equipped with a water-cooled condenser containing Cu(OTf)₂ (0.072 g, 0.199 mmol) under a nitrogen atmosphere. TFA (0.46 mL, 0.68 g, 5.96 mmol) was immediately added. The mixture was heated in an oil bath to 100 °C for 2 h. The mixture was cooled to rt, NaHCO₃ (ca. 3 g) was added, and the mixture was filtered through a short pad of silica gel using 1:1 hexanes/CH₂Cl₂. The solvent from the filtrate was removed in vacuo. The residue was suspended in CH₂Cl₂ (ca. 15 mL) accompanied with stirring for 5 h. The mixture was filtered and the solid wash washed with CH₂Cl₂ (3 x ca. 2 mL) to afford **F-Ar-6** (0.179 g, 38%) as a white solid. *R*_f = 0.6 (50% CH₂Cl₂ in hexanes). IR (CDCl₃ cast film): 3064 (vw), 1601 (vw), 1512 (s), 1476 (w), 1445 (w), 1399 (w), 1351 (w), 1276 (w), 1243 (s), 1205 (vw), 1187 (vw), 1156 (w), 1128 (w), 905 (s), 860 (w), 785 (w), 760 (m), 751 (m), 737 (m), 701 (m) cm⁻¹. ¹H NMR (500 MHz, CDCl₃): δ 7.31 (dd, *J* = 10.7, 7.8 Hz, 2H), 7.28 (dd, *J* = 7.6, 1.3 Hz, 2H), 7.14–7.10 (s, 4H), 7.03–6.96 (m, 4H), 6.89 (t, *J* = 7.4 Hz, 2H), 6.53 (t, *J* = 7.3 Hz, 4H), 6.31 (s, 2H), 6.28 (dd, *J* = 10.5, 8.3 Hz, 2H), 6.24 (dd, *J* = 7.7, 1.1 Hz, 2H), 6.19 (dd, *J* = 10.8, 8.0 Hz, 2H), 6.15 (s, 2H), 6.06 (d, *J* = 7.2 Hz, 4H), 6.04 (s, 2H). ¹³C NMR¹³ (125 MHz, CDCl₃): δ 151.15, 151.03, 150.87, 150.72, 150.67, 150.61, 150.55, 150.47, 149.16, 149.04, 148.86, 148.71, 148.68, 148.60, 148.56, 148.47, 140.62, 140.24, 139.00, 138.98, 138.75, 138.56, 138.40, 131.54, 131.28, 130.30, 130.27, 129.19, 129.13, 129.07, 129.00, 128.95, 128.92, 128.77, 128.74, 128.70, 128.61, 128.55, 127.73, 127.41, 127.18, 127.15, 126.86, 125.94, 112.97, 112.85, 112.41, 112.28, 112.21, 112.07, 111.93, 111.92, 111.82, 111.80. ¹⁹F NMR (376 MHz, CDCl₃): δ –137.19 – –137.36 (m, 2F), –137.75 – –138.06 (m, 6F). DART HRMS *m/z* calcd. for C₆₄H₃₄F₈ (M⁺), 954.2527, found 954.2588. Crystals suitable for X-ray crystallographic analysis were obtained from solutions of **F-Ar-6** in CH₂Cl₂ that were layered with pentane and allowed to slowly evaporate at rt, for X-ray data of **F-Ar-6**, see: CCDC-1483965.

(13) The complete line list of signals for the proton decoupled ¹³C NMR is provided without interpretation of the coupling to ¹⁹F due to the complex nature of the spectrum.

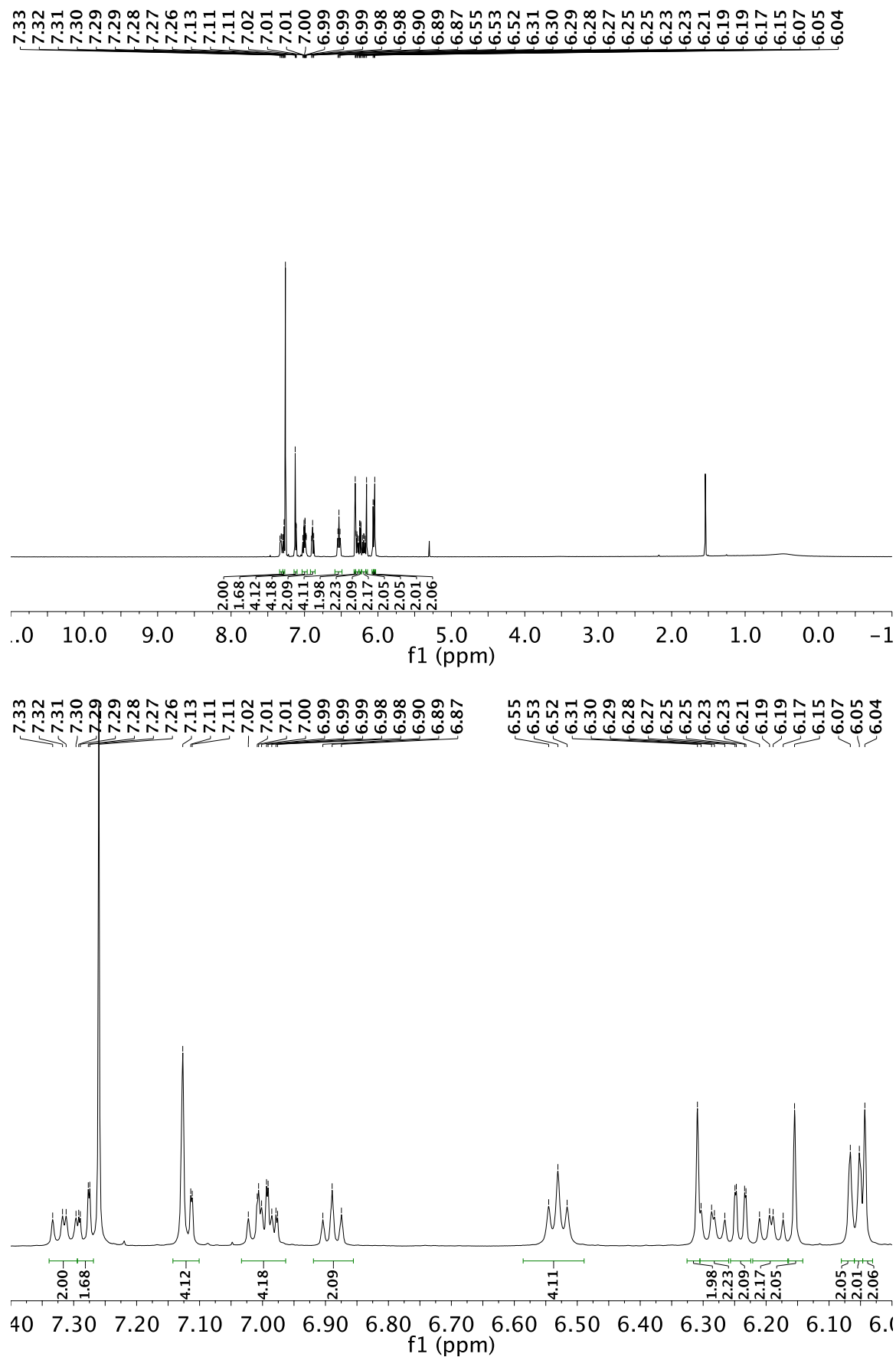


Figure S45. ^1H NMR (500 MHz) spectrum of **F-Ar-6** in CDCl_3 : (top) full view, (bottom) 7.40 to 6.00 ppm region.

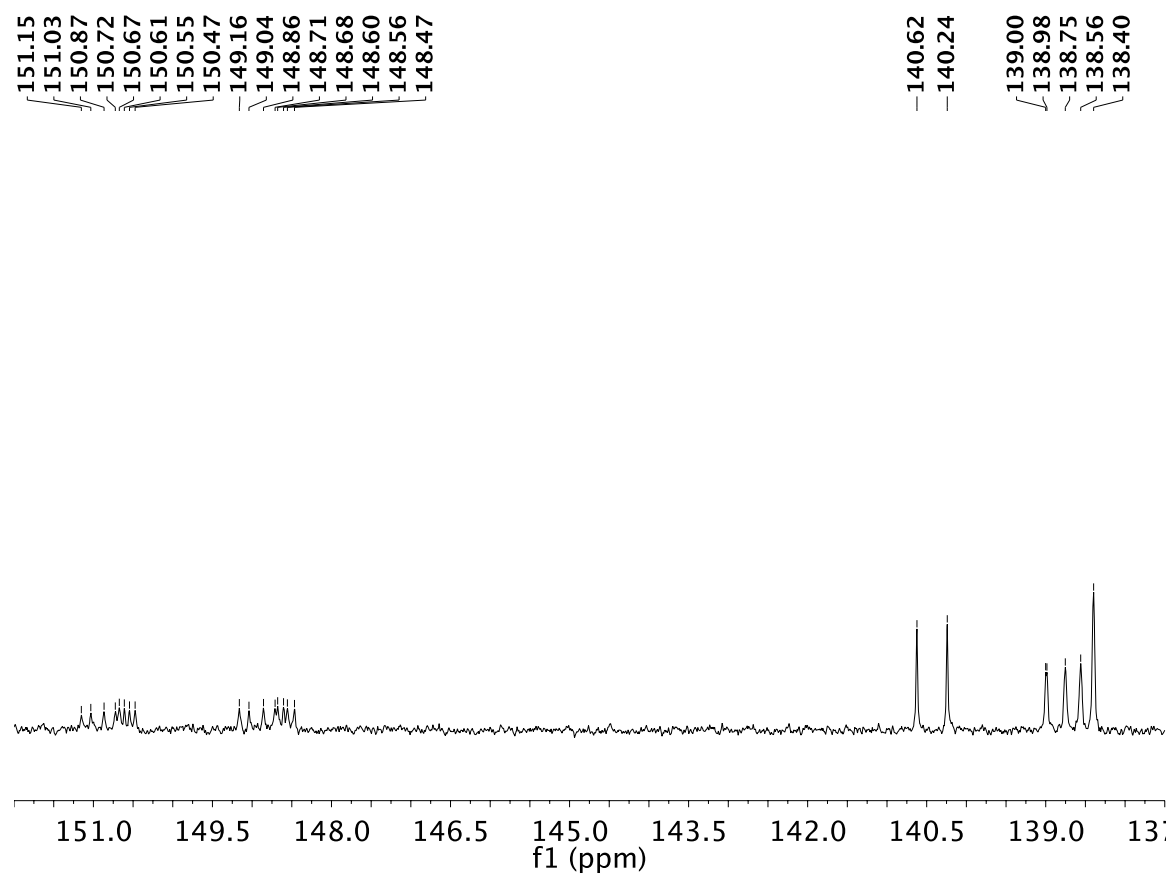
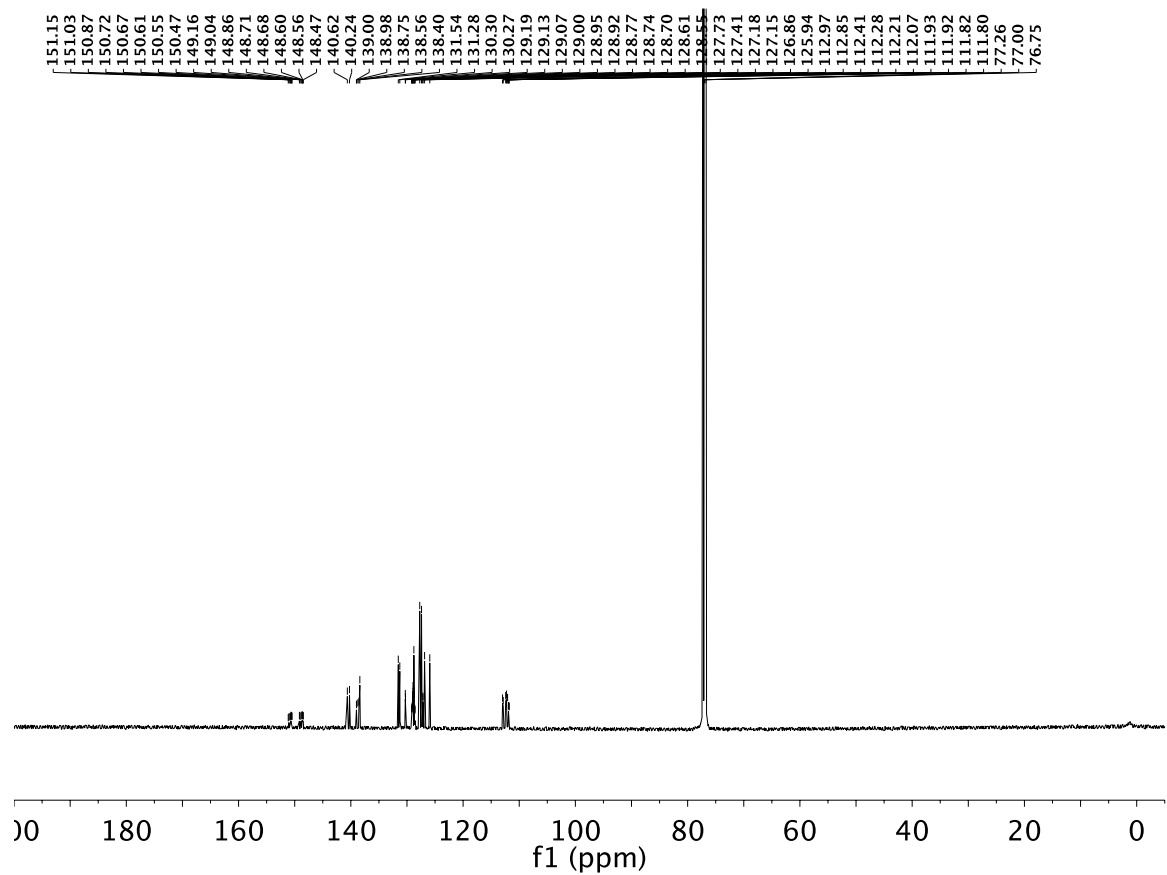


Figure S46. ^{13}C NMR (125 MHz) spectrum of **F-Ar-6** in CDCl_3 : (top) full view, (bottom) 152.0 to 137.5 ppm region.

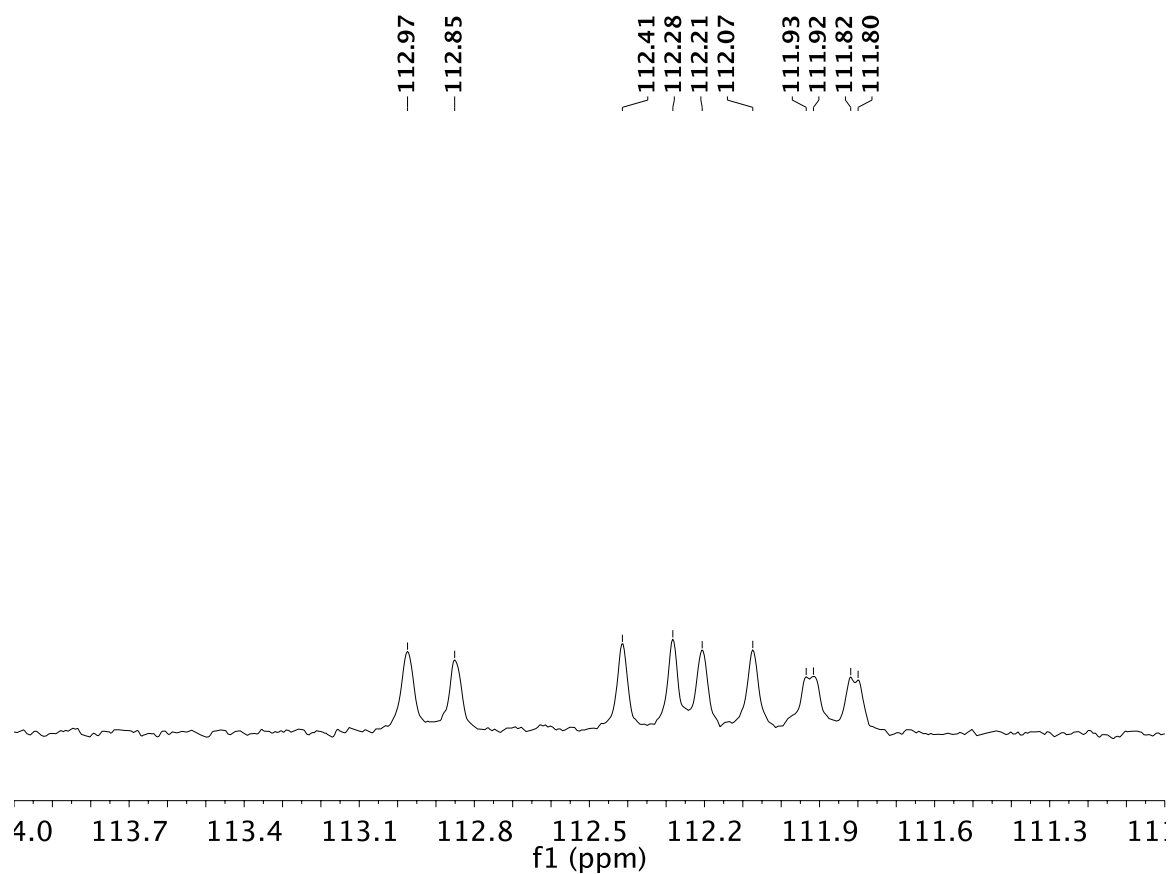
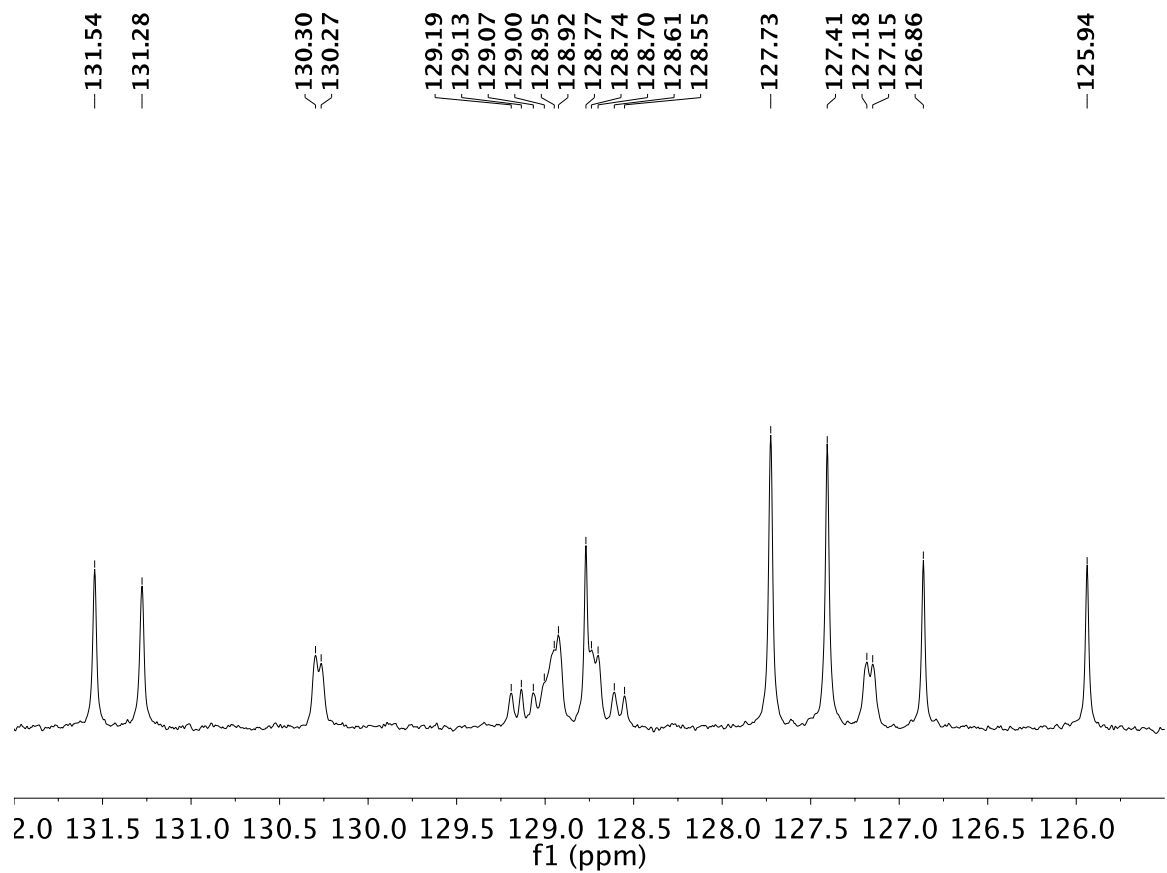


Figure S46 (continued). ^{13}C NMR (125 MHz) spectrum of **F-Ar-6** in CDCl_3 : (top) 132.0 to 125.5 ppm, (bottom) 114.0 to 111.0 ppm region.

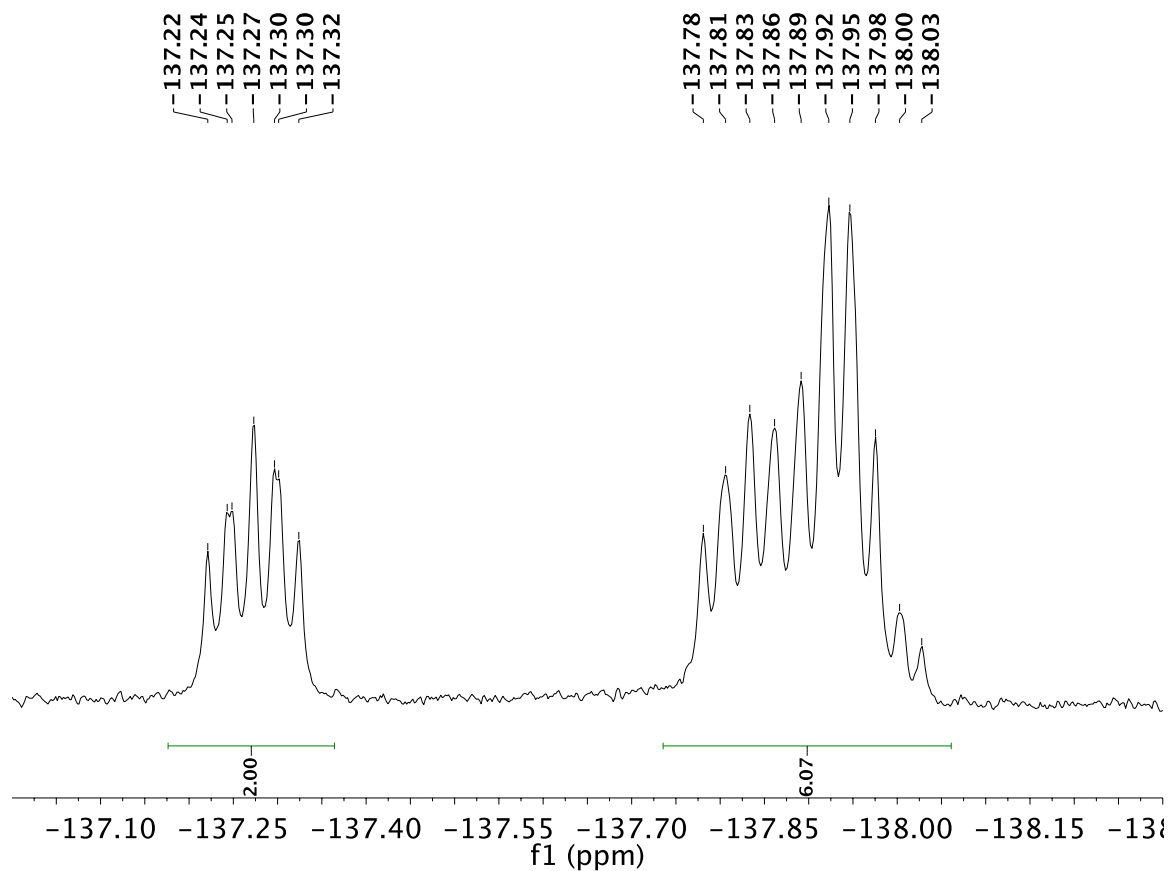


Figure S47. ^{19}F NMR (376 MHz) spectrum of **F-Ar-6** in CDCl_3 .

3. Thermoanalytical Characterization

Table S1. Summary of thermoanalytical data for *ortho*-arylene **X-Ar-1** to **X-Ar-4**.

Compound	DSC ^a		TGA ^b
	$T_{\text{sub,onset}} / ^\circ\text{C}$	$T_{\text{sub,max}} / ^\circ\text{C}$	$T_{\text{onset}} / ^\circ\text{C}$
H-Ar-1	155	253	185
F-Ar-1	133	138	171
Cl-Ar-1	123	130	201
H-Ar-2	295	>300	270
F-Ar-2	264	268	268
Cl-Ar-2	233	239	273
H-Ar-3	n.d. ^c	n.d. ^c	333
F-Ar-3	n.d. ^c	n.d. ^c	303
Cl-Ar-3	n.d. ^c	n.d. ^c	377
H-Ar-4	n.d. ^c	n.d. ^c	362
F-Ar-4	n.d. ^c	n.d. ^c	369
Cl-Ar-4	n.d. ^c	n.d. ^c	425

^a DSC run under a nitrogen atmosphere, $T_{\text{sub,onset}}$ and $T_{\text{sub,max}}$ are the onset and maxima of the first endothermic peak observed corresponding to the sublimation temperature. ^b TGA run under a nitrogen atmosphere, T_{onset} is the temperature corresponding to the onset of weight loss in which the sample weight reaches 95% of its original weight. ^c No peaks were observed within the limited temperature range available (−100 to 300 °C) for the DSC instrument utilized.

4. UV-vis Absorption and Emission Spectra

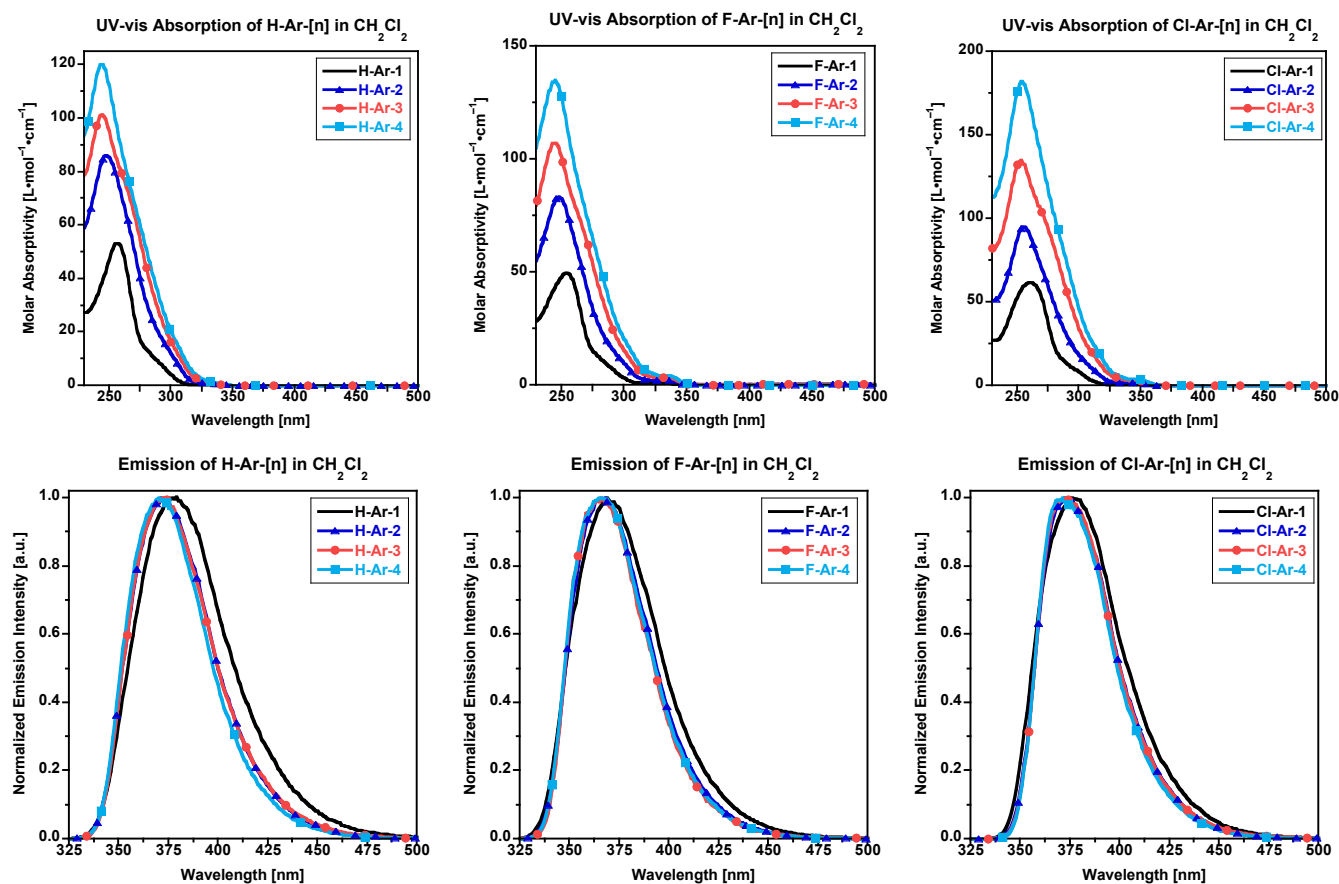


Figure S48. (Top row) UV-vis absorption and (bottom row) emission spectra of oligomeric series **X-Ar-[n]** in CH_2Cl_2 ($\lambda_{\text{exc}} = 260 \text{ nm}$): (left) **H-Ar-1** to **H-Ar-4**, (middle) **F-Ar-1** to **F-Ar-4**, and (right) **Cl-Ar-1** to **Cl-Ar-4**.

Table S2. Optical properties of *ortho*-arylene oligomers **X-Ar-1** to **X-Ar-4** in CH_2Cl_2 .

Compound	ϵ (at $\lambda_{\text{max,abs}}$) [$10^3 \text{ L} \cdot \text{mol}^{-1} \cdot \text{cm}^{-1}$]	$\lambda_{\text{max,abs}}$ [nm]	$\lambda_{\text{max,em}}^a$ [nm]	Stokes Shift [cm^{-1}]
H-Ar-1	53.3	256	375	12,400
F-Ar-1	49.7	254	368	12,200
Cl-Ar-1	61.8	261	375	11,600
H-Ar-2	86.2	248	373	13,500
F-Ar-2	83.2	248	366	13,000
Cl-Ar-2	95.2	255	372	12,300
H-Ar-3	101	244	372	14,100
F-Ar-3	107	245	366	13,500
Cl-Ar-3	135	253	372	12,600
H-Ar-4	120	244	370	14,000
F-Ar-4	135	245	365	13,400
Cl-Ar-4	182	253	371	12,600

^a Emission measured using $\lambda_{\text{exc}} = 260 \text{ nm}$.

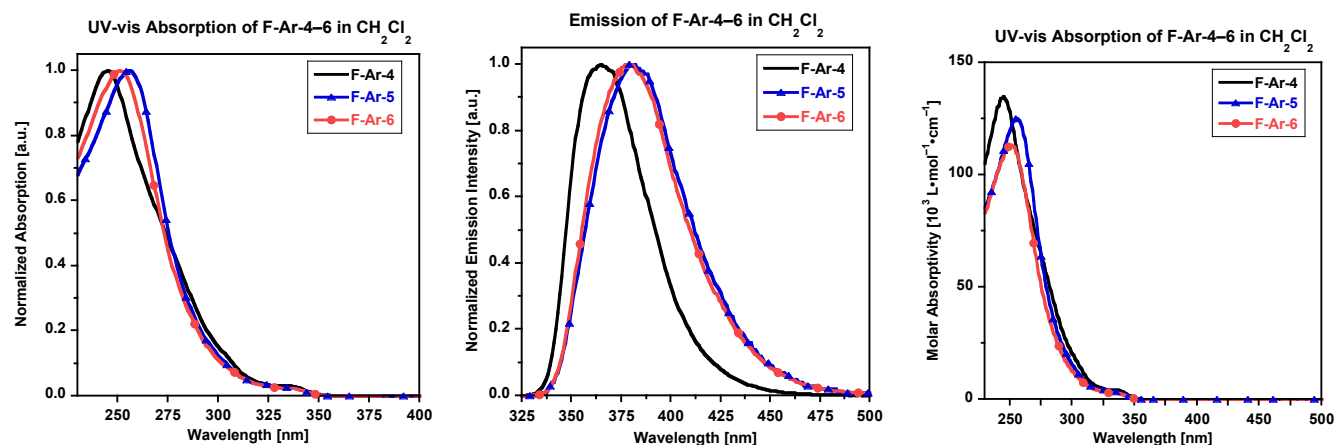


Figure S49. UV-vis absorption and emission spectra of oligomeric series **F-Ar-4** to **F-Ar-6** in CH_2Cl_2 ($\lambda_{\text{exc}} = 260$ nm): (left) normalized absorption, (middle) normalized emission, and (right) absorption in molar absorptivity.

Table S3. Optical properties of sequence-defined *ortho*-arylenes **F-Ar-4** to **F-Ar-6** in CH_2Cl_2 .

Compound	ϵ (at $\lambda_{\text{max,abs}}$) [$10^3 \text{ L} \cdot \text{mol}^{-1} \cdot \text{cm}^{-1}$]	$\lambda_{\text{max,abs}}$ [nm]	$\lambda_{\text{max,em}}^a$ [nm]	Stokes Shift [cm^{-1}]
F-Ar-4	135	245	365	13,400
F-Ar-5	111	255	382	13,000
F-Ar-6	108	251	380	13,500

^a Emission measured using $\lambda_{\text{exc}} = 260$ nm.

5. Electrochemistry

Table S4. Summary electrochemical data. Voltages reported are the onset of the oxidation (E_{ox}) processes in 0.1 M tetrabutylammonium perchlorate in MeCN supporting electrolyte.

Compound	Onset of Oxidation, E_{ox} (V vs Ag/AgClO ₄)
H-Ar-1	1.184
H-Ar-2	1.090
H-Ar-3	1.006
H-Ar-4	0.979
F-Ar-1	1.320
F-Ar-2	1.279
F-Ar-3	1.265
F-Ar-4	1.180
Cl-Ar-1	1.293
Cl-Ar-2	1.223
Cl-Ar-3	NA ^[a]
Cl-Ar-4	NA ^[a]
F-Ar-5	1.212
F-Ar-6	1.172

^[a] NA = not available due to limited solubility.

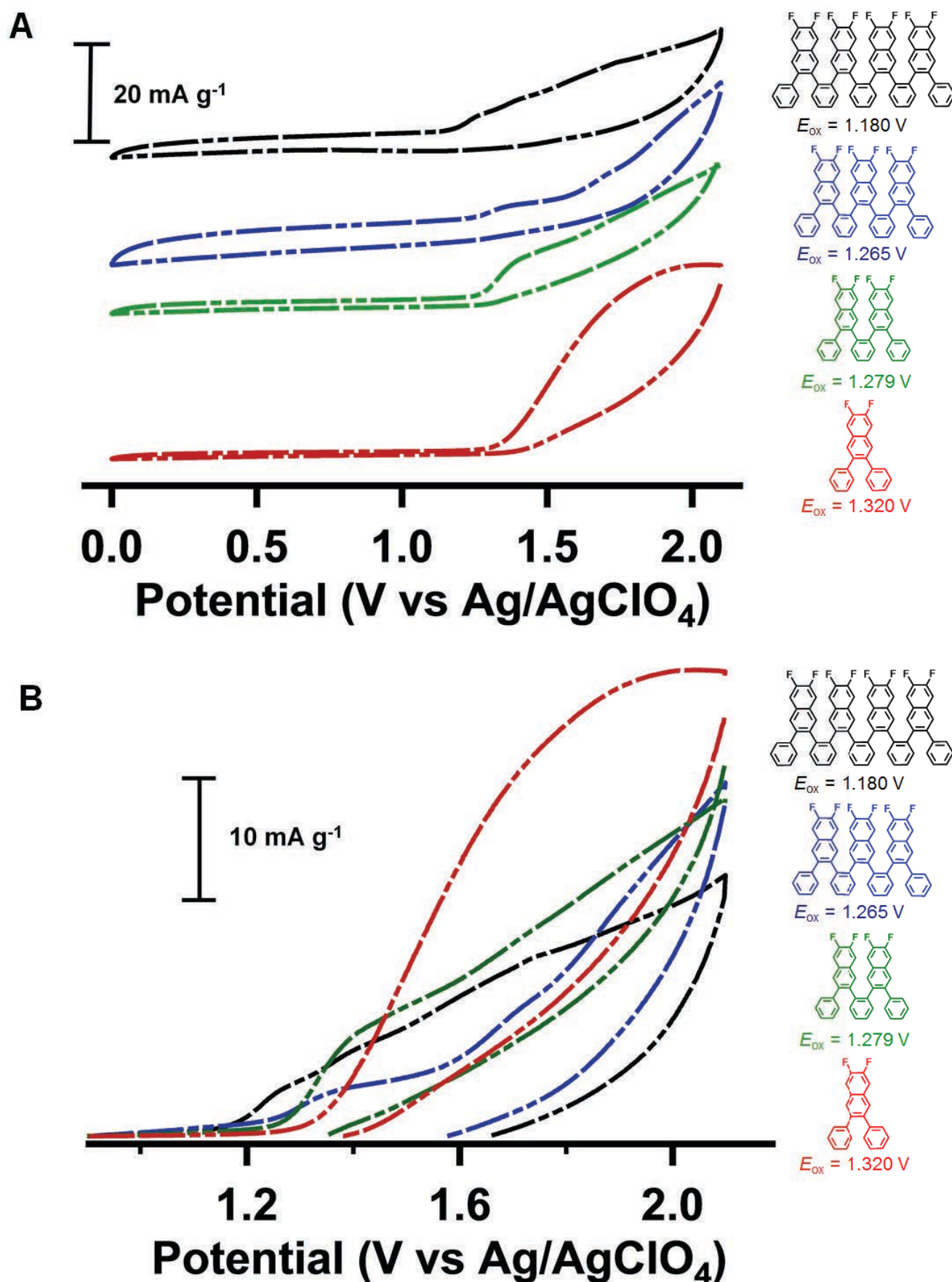


Figure S51. Cyclic voltammetric responses of fluorinated series at 50 mV s⁻¹ in 0.1 M TBAP/MeCN. (A) 0 to 2.1 V vs Ag/AgClO₄ and (B) zoom in of data in part A from 1.0 to 2.1 V vs Ag/AgClO₄.

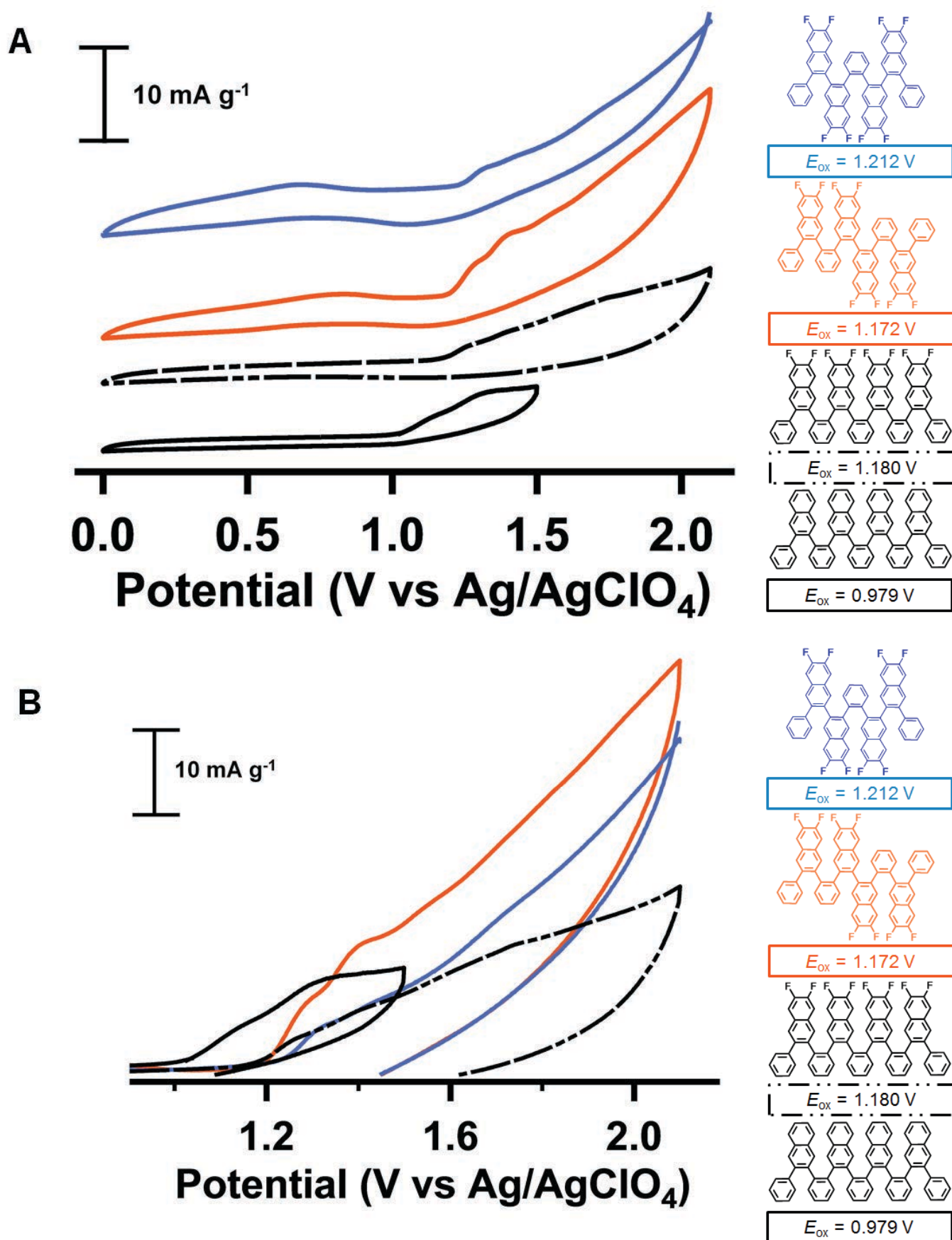


Figure S52. Cyclic voltammetric responses showing the effect of sequence on onset of oxidation at 50 mV s⁻¹ in 0.1 M TBAP/MeCN. (A) 0 to 2.1 V vs Ag/AgClO₄ and (B) zoom in of data in part A from 1.0 to 2.1 V vs Ag/AgClO₄.

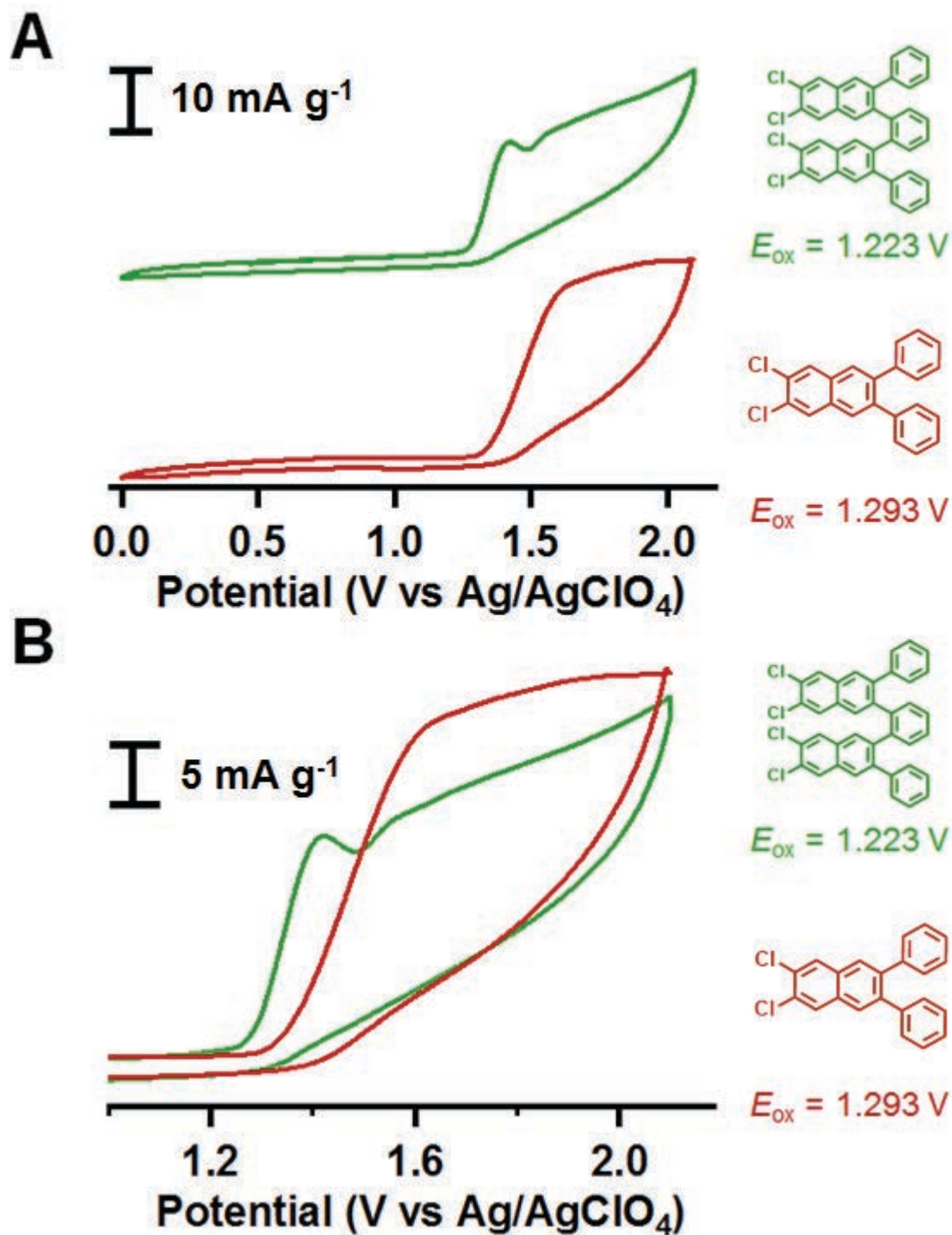


Figure S53. Cyclic voltammetric responses of chlorinated series at 50 mV s⁻¹ in 0.1 M TBAP/MeCN. (A) 0 to 2.1 V vs Ag/AgClO₄ and (B) zoom in of data in part A from 0.8 to 2.1 V vs Ag/AgClO₄.

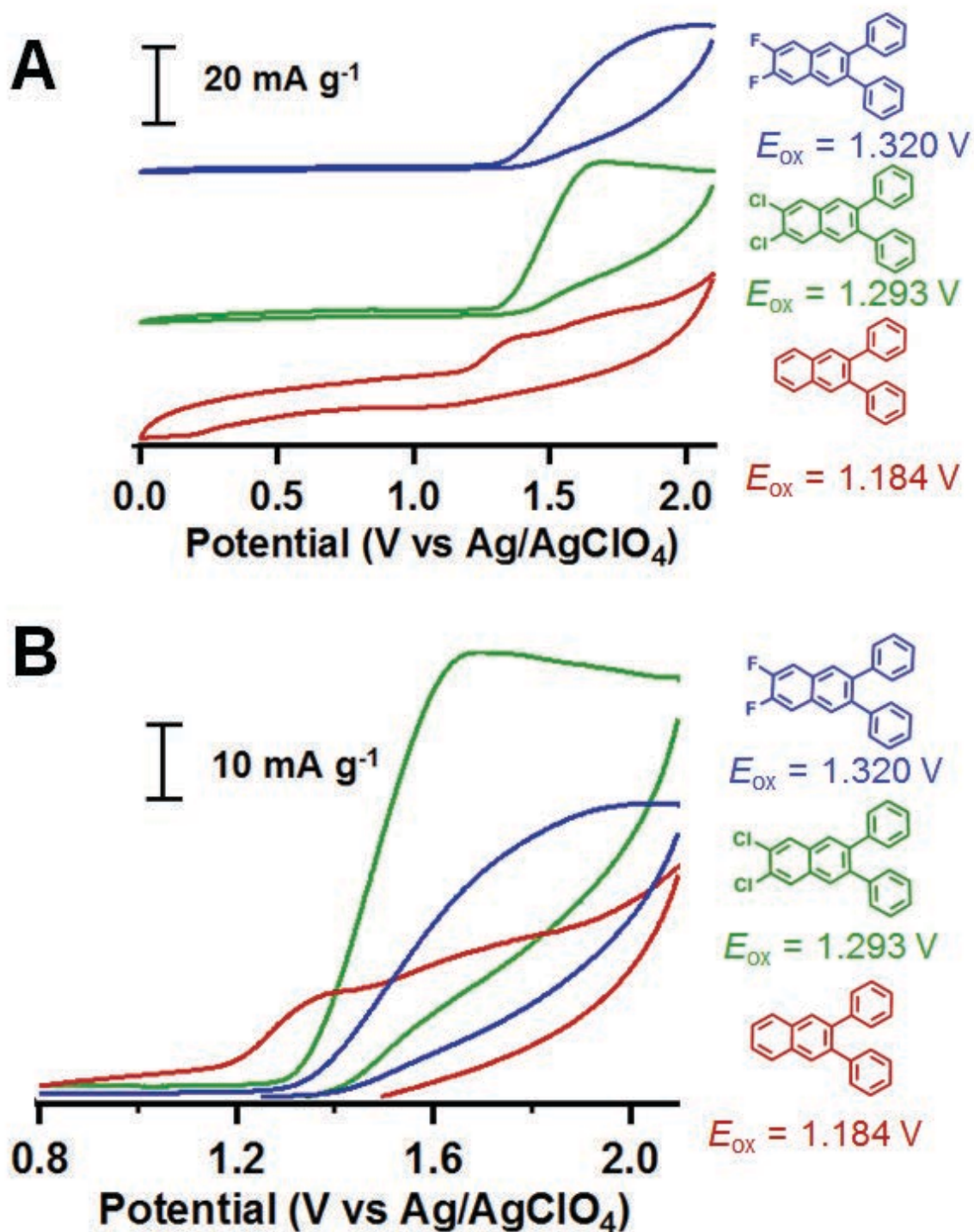


Figure S54. Cyclic voltammetric responses showing the substituent effect on onset of oxidation at 50 mV s⁻¹ in 0.1 M TBAP/MeCN. (A) 0 to 2.1 V vs Ag/AgClO₄ and (B) zoom in of data in part A from 1.0 to 2.1 V vs Ag/AgClO₄.

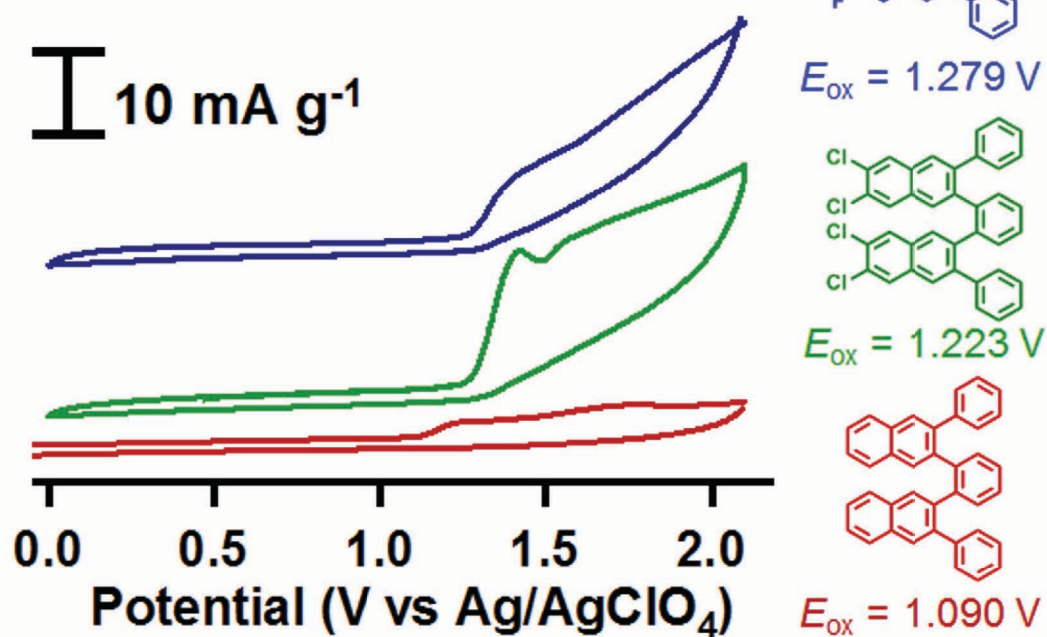
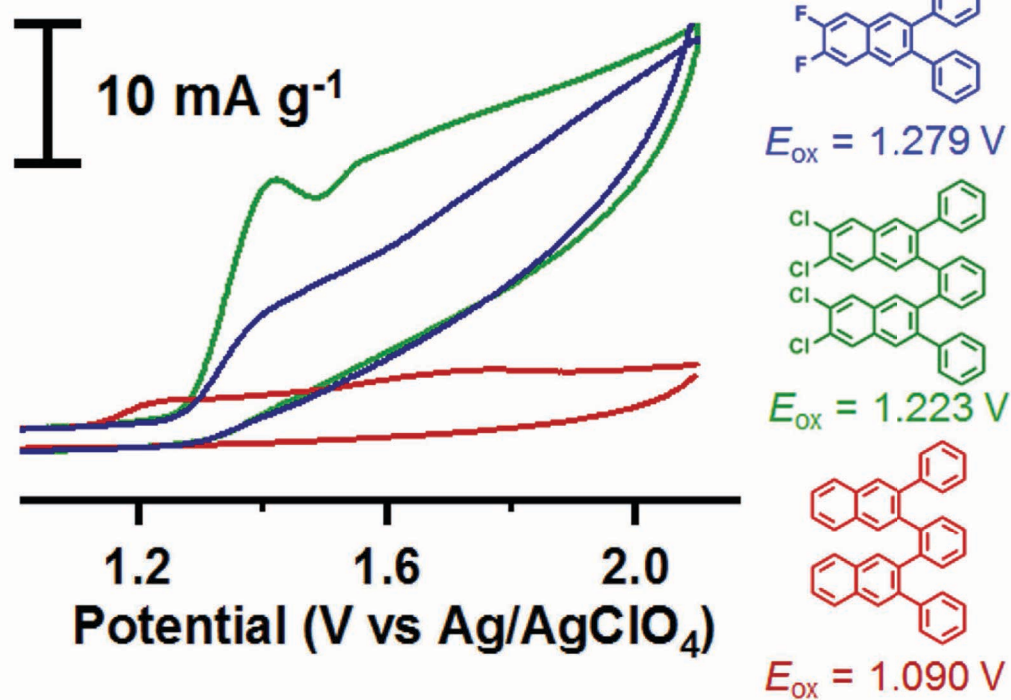
A**B**

Figure S55. Cyclic voltammetric responses showing the substituent effect on onset of oxidation at 50 mV s⁻¹ in 0.1 M TBAP/MeCN. (A) 0 to 2.1 V vs Ag/AgClO₄ and (B) zoom in of data in part A from 1.0 to 2.1 V vs Ag/AgClO₄.

6. X-ray Crystallographic Structures of Foldamers *H-Ar-[n]*, *F-Ar-[n]*, and *Cl-Ar-[n]*

See Figure 1 in the main text for an illustration of the X-ray crystallographic structure of foldamers **H-Ar-2**, **H-Ar-3**, **H-Ar-4** and **F-Ar-6** and their associated selected carbon-carbon distances.

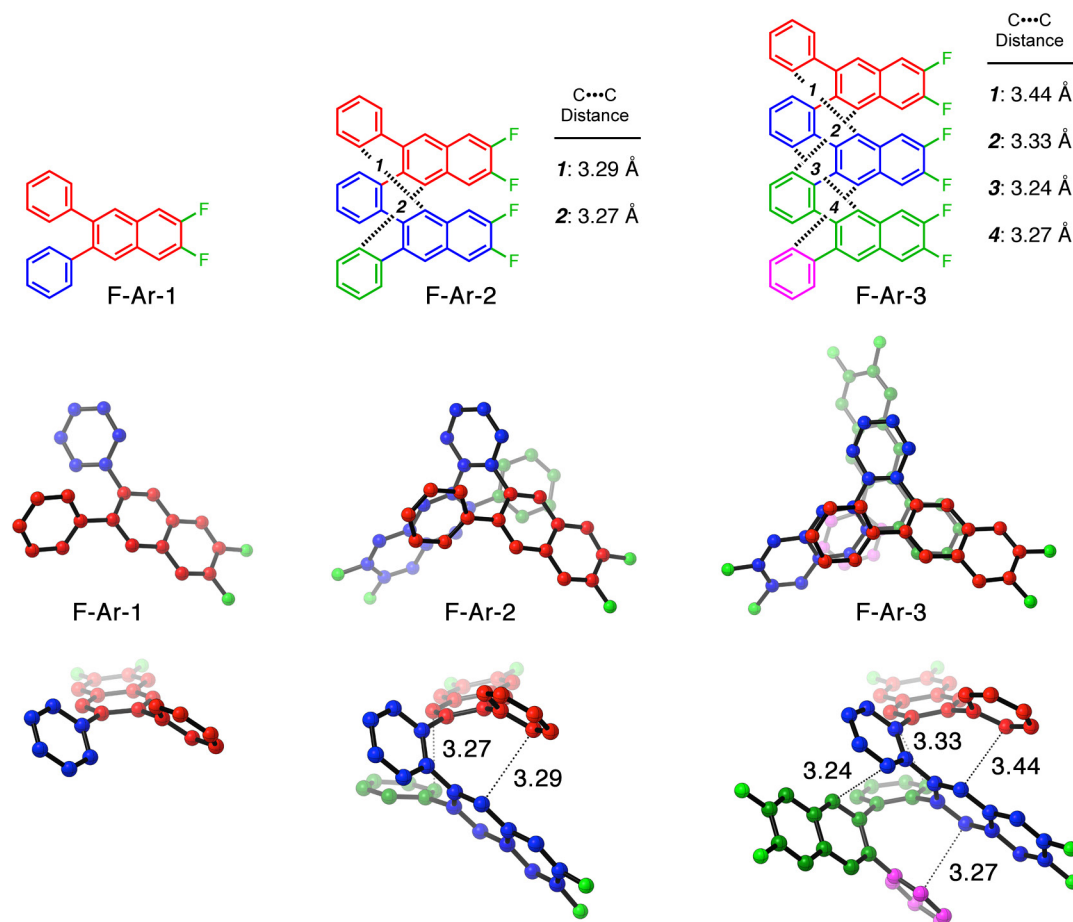


Figure S56. X-ray crystallographic structure of foldamers (left to right): **F-Ar-1**, **F-Ar-2**, and **F-Ar-3**. (Top) Line representation with selected carbon-carbon distances, (middle) top view and (bottom) side view with each repeat unit colored differently.

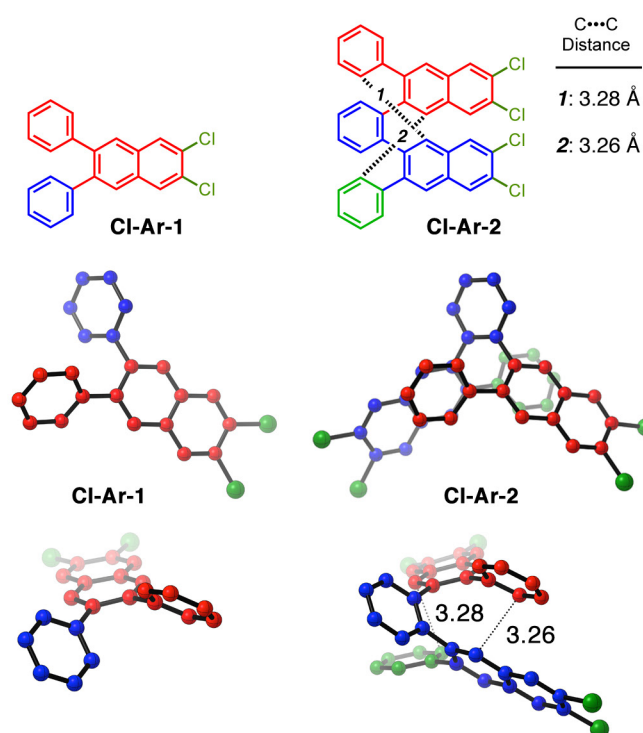


Figure S57. X-ray crystallographic structure of foldamers (left to right): **Cl-Ar-1**, and **Cl-Ar-2**. (Top) Line representation with selected carbon-carbon distances, (middle) top view and (bottom) side view with each repeat unit colored differently.

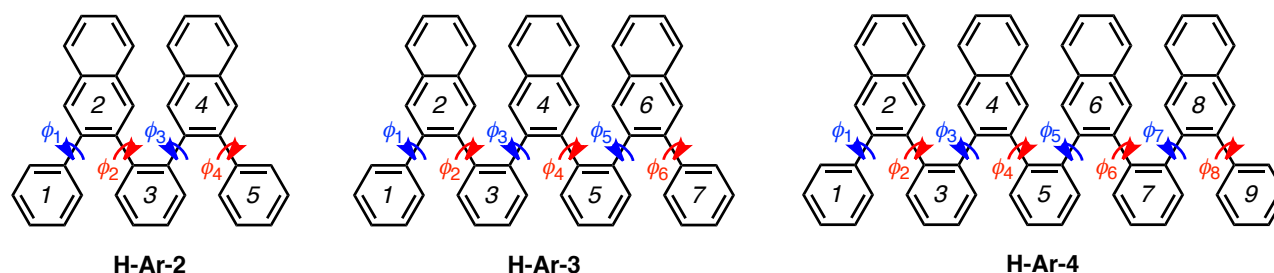


Figure S58. Definition of Dihedral Angles Summarized in Table S5.

Table S5. Dihedral angle analysis of X-ray crystallographic structures of **X-Ar-[*n*]**^[a]

Compound	ϕ_1 (°)	ϕ_2 (°)	ϕ_3 (°)	ϕ_4 (°)	ϕ_5 (°)	ϕ_6 (°)	ϕ_7 (°)	ϕ_8 (°)
F-Ar-1 (mol. 1)	-47.4,	-53.0,	–	–	–	–	–	–
F-Ar-1 (mol. 2)	49.7	50.7	–	–	–	–	–	–
Cl-Ar-1 (mol. 1)	-46.5	-50.5	–	–	–	–	–	–
Cl-Ar-1 (mol. 2)	46.5	50.5	–	–	–	–	–	–
H-Ar-2	-48.4	-63.4	-61.3	-44.9	–	–	–	–
F-Ar-2	-50.3	-67.3	-64.9	-44.4	–	–	–	–
Cl-Ar-2 (mol. 1)	-49.1,	-59.5,	-59.4,	-47.3,	–	–	–	–
Cl-Ar-2 (mol. 2)	48.9	59.5	61.7	50.0	–	–	–	–
H-Ar-3	-42.4	-58.1	-59.4	-59.4	-58.1	-42.4	–	–
F-Ar-3	-46.0	-57.3	-56.6	-58.1	-60.5	-49.5	–	–
H-Ar-4	-46.4	-59.8	-57.1	-55.6	-56.7	-55.4	-57.9	-48.1
F-Ar-6	43.9	55.1	56.7	52.4	57.6	59.4	48.2	–

^[a] See Figure S58 for definition of dihedral angles.

The numbers 1 to n above the dashed lines represent the interatomic distances d_1 to d_n .

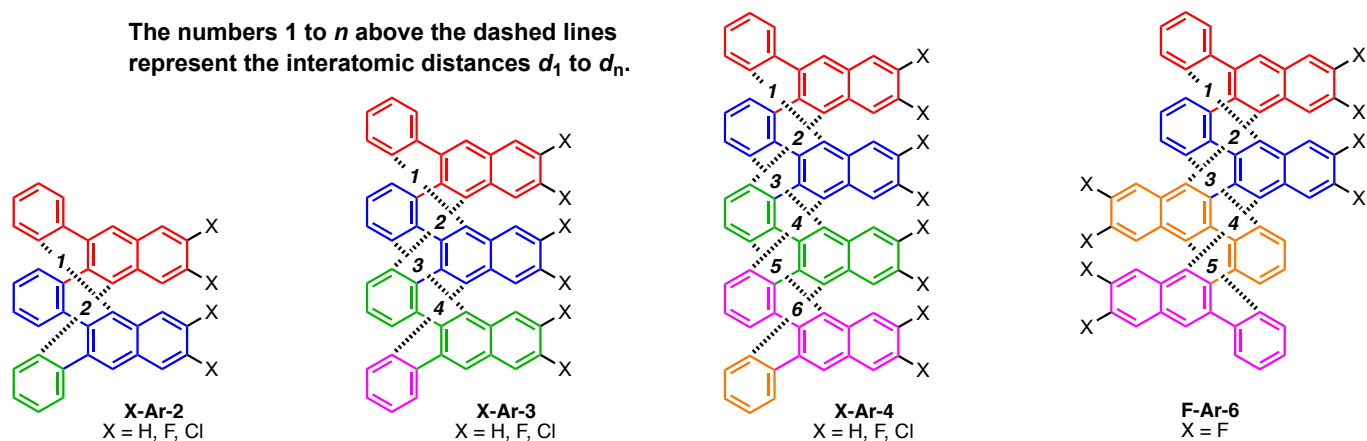


Figure S59. Definition of non-covalent interatomic distances d_1 to d_n in oligo(*ortho*-arylenes) **X-Ar-2**, **X-Ar-3**, **X-Ar-4**, and **F-Ar-6**.

Table S6. Non-covalent interatomic distances of X-ray crystallographic structures of **X-Ar-[n]**^[a]

Compound	d_1 (Å)	d_2 (Å)	d_3 (Å)	d_4 (Å)	d_5 (Å)	d_6 (Å)
H-Ar-2 (mol. 1)	3.36,	3.17,	–	–	–	–
H-Ar-2 (mol. 2)	3.36	3.17	–	–	–	–
F-Ar-2	3.29	3.27	–	–	–	–
Cl-Ar-2 (mol. 1)	3.26,	3.28,	–	–	–	–
Cl-Ar-2 (mol. 2)	3.41	3.19	–	–	–	–
H-Ar-3	3.33	3.14	3.14	3.33	–	–
F-Ar-3	3.44	3.33	3.24	3.27	–	–
H-Ar-4	3.24	3.20	3.36	3.42	3.33	3.54
F-Ar-6	3.33	3.37	3.33	3.39	3.35	–

^[a] See Figure S58 for definition of interatomic distances d_1 to d_6 .

7. DFT Computational Study

7.1 DFT Computed Conformations of Foldamers X-Ar-3

Table S7. DFT calculated energies, dipoles, and dihedral angles using M06-2X/6-31G for various folded geometries of **X-Ar-3**.^a

Folding Conformation ^b	X	E (kcal•mol ⁻¹)	Rank	Dipole (Debye)	ϕ_1 (°) ^c	ϕ_2 (°)	ϕ_3 (°)	ϕ_4 (°)	ϕ_5 (°)	ϕ_6 (°) ^c
AAAA	H	0.0	1	0.21	-46.4	-53.8	-51.0	-51.0	-53.8	-46.4
	F	0.0	1	0.47	-46.2	-53.8	-52.1	-52.1	-53.8	-46.2
	Cl	0.0	1	0.40	-45.6	-54.3	-52.4	-52.4	-54.3	-45.6
AAAB	H	+4.9	2	0.42	-44.1	-59.9	-60.7	-59.2	137.0	-48.5
	F	+5.3	2	4.95	-44.4	-60.3	-61.4	-58.5	138.8	-50.5
	Cl	+5.4	2	5.18	-43.8	-61.0	-61.1	-58.2	138.5	-52.0
AABB	H	+6.6	3	0.35	-49.6	-68.4	-67.0	134.1	127.4	-47.7
	F	+6.1	3	8.36	-48.6	-67.9	-67.3	133.8	128.3	-47.4
	Cl	+6.3	3	8.77	-47.2	-68.5	-69.4	132.2	134.1	-47.5
BAAB	H	+8.1	4	0.62	-52.5	139.0	-61.4	-61.4	139.0	-52.5
	F	+9.1	4	9.34	-52.2	138.5	-61.9	-61.9	138.5	-52.3
	Cl	+9.6	4	9.78	-52.6	138.9	-61.8	-61.8	138.9	-52.7
ABBA	H	+8.9	5	0.27	-59.4	-62.2	135.5	135.5	-62.2	-59.4
	F	+9.6	5	9.16	-59.9	-62.6	135.2	135.2	-62.6	-59.9
	Cl	+10.1	5	9.41	-62.4	-62.8	134.8	134.8	-62.8	-62.4
BABB	H	+11.5	6	0.45	-48.3	139.9	-73.4	137.7	119.5	-48.7
	F	+11.8	6	10.6	-47.2	134.9	-77.5	133.6	126.2	-49.3
	Cl	+12.8	6	11.1	-47.1	139.2	-73.0	135.8	118.3	-50.3
ABBB	H	+12.8	7	0.56	-59.2	-62.9	136.1	124.5	132.1	-48.1
	F	+13.2	7	10.0	-59.9	-63.0	135.8	124.1	131.6	-48.1
	Cl	+13.6	7	10.4	-61.1	-63.0	134.7	130.0	123.2	-47.2
Coil 1: BAAC	H	+13.3	8	0.49	-48.2	138.2	-56.9	-72.3	-103.8	56.6
	F	+13.8	8	5.47	-51.2	138.3	-57.9	-73.5	-104.3	56.5
	Cl	ND ^d	(8) ^d	–	–	–	–	–	–	–
BBBB	H	+16.1	9	0.01	-48.1	126.8	129.2	129.2	126.8	-48.1
	F	+17.0	9	7.89	-47.4	127.1	130.5	130.6	127.1	-47.4
	Cl	+17.2	9	8.48	-47.5	127.0	129.0	129.0	127.0	-47.5
AABA	H	+19.2	10	0.55	-51.7	-73.3	-86.1	140.7	-70.7	-51.3
	F	+19.8	10	7.44	-52.6	-74.5	-84.2	138.2	-71.0	-52.2
	Cl	+19.8	10	7.74	-51.7	-73.0	-85.3	140.2	-70.7	-51.9
Coil 2: ABCB	H	+22.3	11	0.39	-47.6	-69.9	149.5	-92.1	143.7	-48.1
	F	+23.3	11	9.66	-46.8	-68.7	148.9	-92.9	143.4	-48.0
	Cl	+23.7	11	10.1	-46.8	-68.1	148.5	-92.9	143.9	-49.0
Coil 3: BABC	H	+25.4	12	0.37	-48.6	140.9	-78.7	145.8	-121.2	49.2
	F	+26.5	12	10.6	-47.7	138.8	-80.3	144.3	-120.8	47.7
	Cl	+27.3	12	11.1	-47.8	139.2	-80.1	144.8	-120.4	48.2
ABAB not possible	H	NA	–	–	–	–	–	–	–	–
	F	NA	–	–	–	–	–	–	–	–
	Cl	NA	–	–	–	–	–	–	–	–

^a See Figure S58 for definition of dihedral angles. ^b Folding conformation coding for $\phi_2, \phi_3, \phi_4, \phi_5$ using A if ($0^\circ < \phi_n < -90^\circ$), B ($90^\circ < \phi_n < 180^\circ$), and C if ($-90^\circ \leq \phi_n < -180^\circ$). ^c There are two possible measurements for this dihedral angle, the one reported is the angle with the smallest absolute value. ^d Attempts to locate the BAAC conformer for **Cl-Ar-3** (analogous to that of compound **H-Ar-3** and **F-Ar-3**) with zero imaginary frequencies were unsuccessful to date.

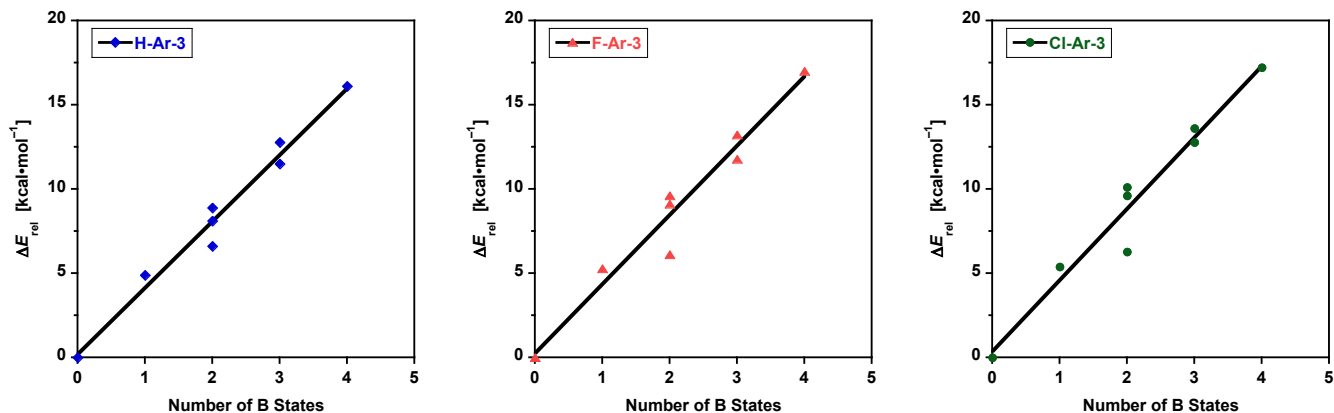


Figure S60. Electronic energy relative to lowest energy conformer (AAAA) for **X-Ar-3** calculated using M06-2X/6-31G and plotted as function of the number of B states. The slope estimates the stacking interaction energy. Left: **H-Ar-3**, middle: **F-Ar-3**, right: **Cl-Ar-3**. (Each plot omits conformation AABA, which is exceptionally high in energy due to forcing the ends of the foldamer into each other, specifically, the terminal phenyl ring and the outermost naphthalene from the other terminus).

Figure S61 illustrates the linear dependence of ΔE_{rel} on the number of B states for **X-Ar-3** ($R^2 = 0.97, 0.95$, and 0.95 for $X = \text{H}, \text{Cl}, \text{F}$, respectively). This is consistent with each B state defect eliminating exactly one cofacial π -stacking interaction. The slope of each plot corresponds to the energy associated with breaking one stacking interaction: 4.0 ± 0.3 , 4.11 ± 0.4 , and 4.23 ± 0.4 kcal/mol per B state for $X = \text{H}, \text{F}, \text{Cl}$, respectively. These energy are comparable to the energy associate with breaking a cofacial π -stacked benzene–naphthalene arene dimer (see Figure S61 below), calculated to be 4.5 kcal/mol at M06-2X/6-31G. The fact that the π -stacking interaction energies obtained from the conformational analysis plot in Figure S60 (4.0 ± 0.3 for **H-Ar-3**) is almost as large as the 4.5 kcal/mol associated with a benzene–naphthalene π -stacking interaction reveals that the foldamer backbone places these arenes in near optimal geometry for maximizing the π -stacking (achieving ca. 89% of the potential stabilization energy attainable from a phenylene–naphthalene π -stacking interaction).

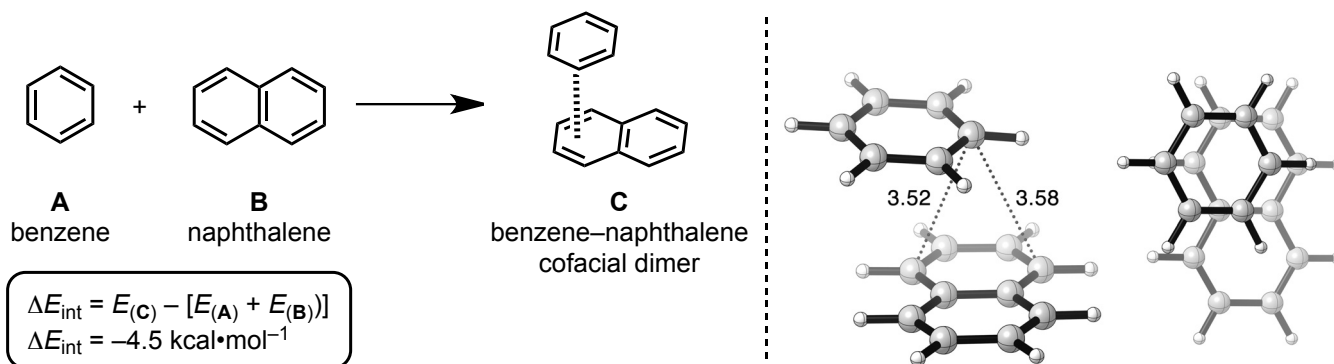


Figure S61. (Left) Reaction used to estimate the cofacial interaction energy in the absence of the foldamer architecture as a comparison to the π -stacking interaction energies obtain in foldamers **X-Ar-3** via the plots in Figure S60. (Right) DFT optimized naphthalene•••benzene cofacial π -stacked dimer calculated using M06-2X/6-31G along with selected non-covalent C•••C interatomic distances in Ångström (Å) shown from the side and top view.

Table S8. DFT optimized conformers of **H-Ar-3** calculated using M06-2X/6-31G (gas phase).

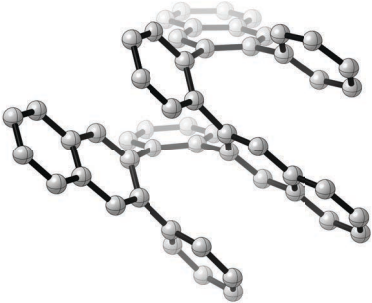
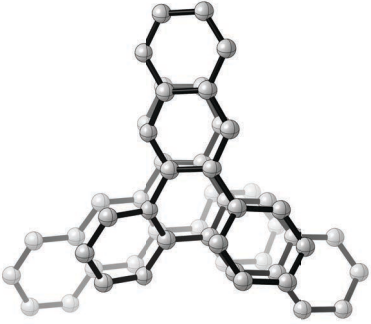
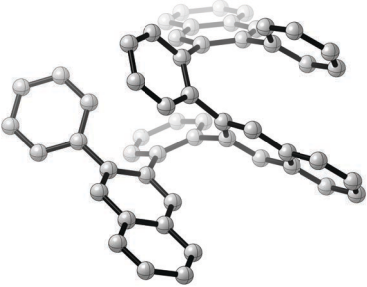
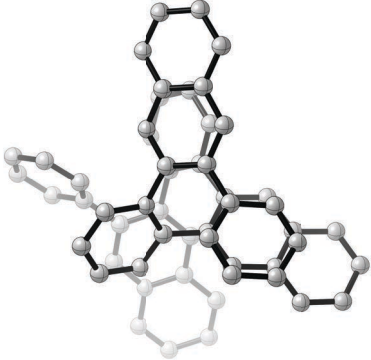
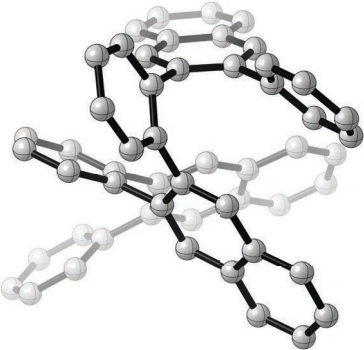
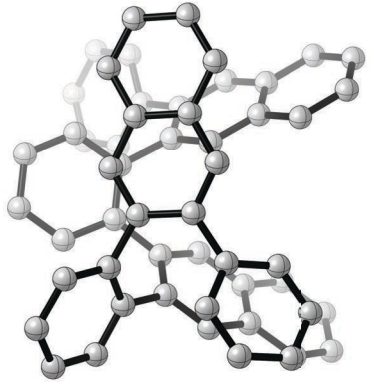
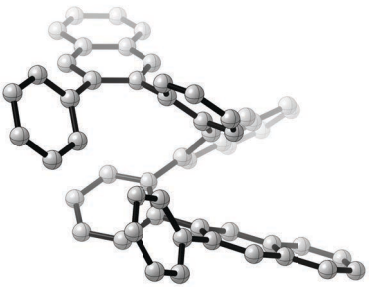
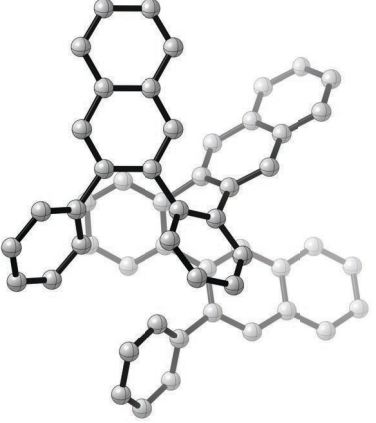
Conformer	Energy Relative to AAAA [kcal•mol ⁻¹]	Side View	Top View
AAAA	0.0 (defined)		
AAAB	+4.9		
AABB	+6.6		
BAAB	+8.1		

Table S8 (continued). DFT optimized conformers of **H-Ar-3** calculated using M06-2X/6-31G (gas phase).

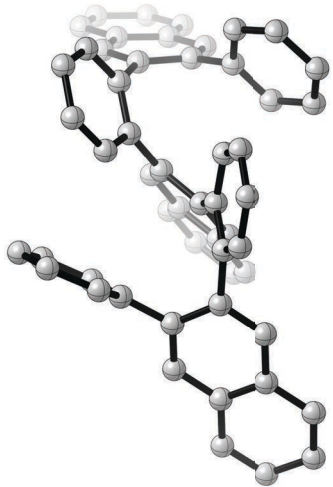
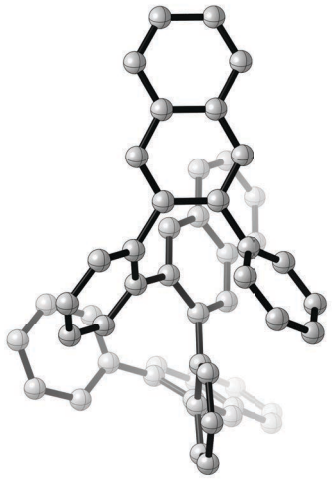
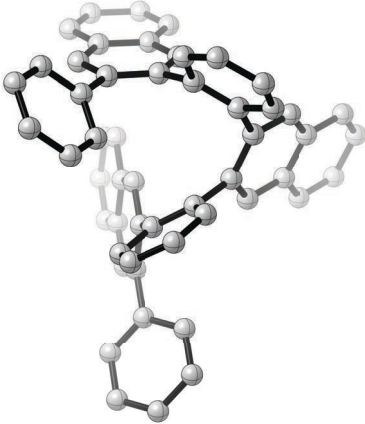
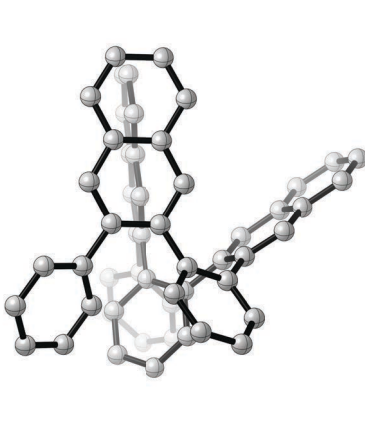
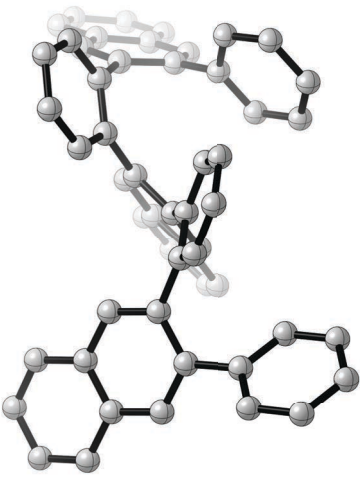
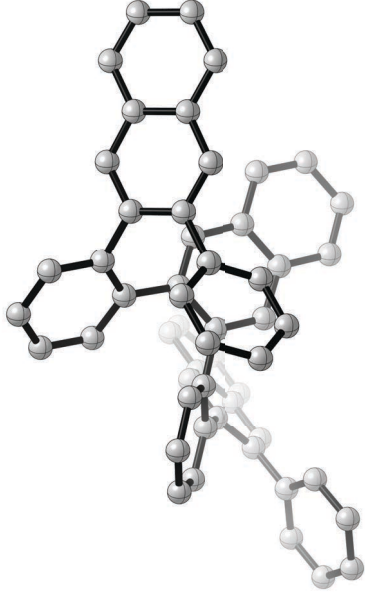
Conformer	Energy Relative to AAAA [kcal•mol ⁻¹]	Side View	Top View
ABBA	+8.9		
BABB	+11.5		
ABBB	+12.8		

Table S8 (continued). DFT optimized conformers of **H-Ar-3** calculated using M06-2X/6-31G (gas phase).

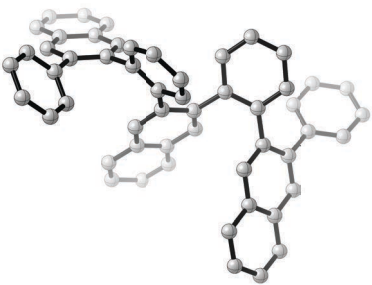
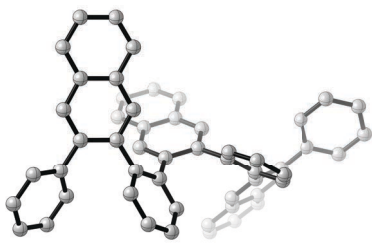
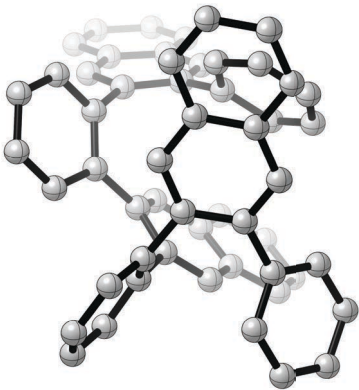
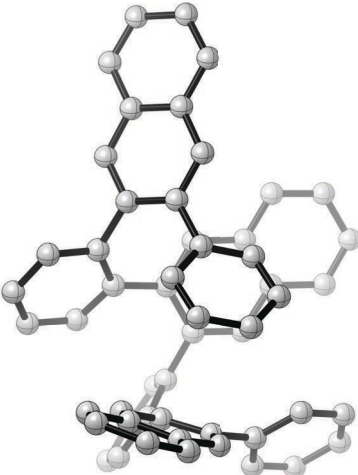
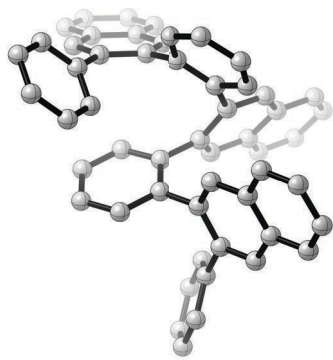
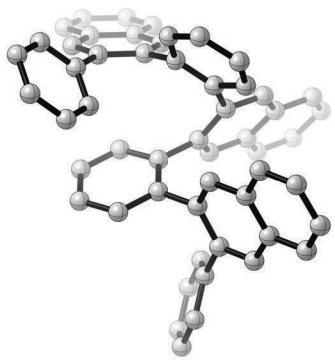
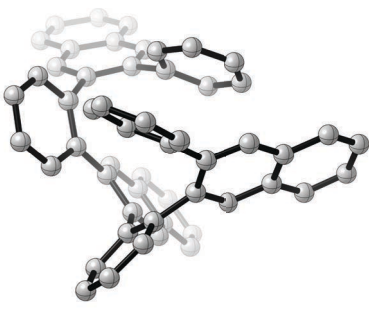
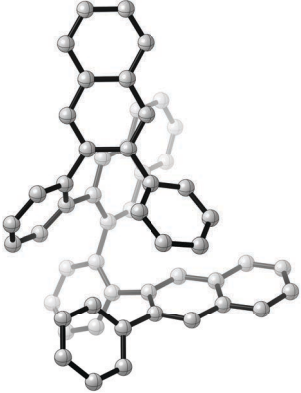
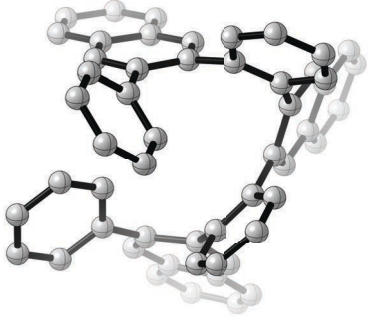
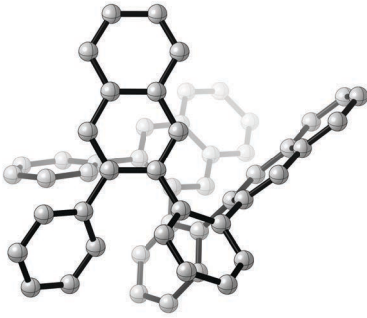
Conformer	Energy Relative to AAAA [kcal•mol ⁻¹]	Side View	Top View
BBBB	+16.1		
AABA	+19.2		

Table S8 (continued). DFT optimized conformers of **H-Ar-3** calculated using M06-2X/6-31G (gas phase).

Conformer	Energy Relative to AAAA [kcal•mol ⁻¹]	Side View	Top View
BAAC	+13.3		
ABCB	+22.3		
BABC	+25.4		

The last three entries of Table S8 illustrate conformers of **H-Ar-3** that contain a “C” dihedral angle, a new observation in *o*-arylenes, in contrast to previous conformational analysis of oligo(*o*-phenylene)s by Hartley and coworkers¹⁴ which describe only A and B dihedral angles. Dihedral angle down the backbone are defined as: A if ($0^\circ < \phi_i < -90^\circ$), B ($90^\circ < \phi_i < 180^\circ$), or C if ($-90^\circ \leq \phi_i < -180^\circ$); the opposite signs correspond to the analogous enantiomeric conformation. It is not clear whether such C dihedral angles have been overlooked in oligo(*o*-phenylene)s or whether additional conformers containing a C dihedral angle in **H-Ar-3** exist, since a more detailed computational conformational search was beyond the scope of this study. Attempts at locating an AAAC conformation were unsuccessful to date, and the relaxed dihedral angle scan shown in Figure S62 suggests that if such a conformation were to exist, its barrier to convert back to AAAA would likely be small and thus kinetically unstable.

(14) (a) J. He, J. J. L. Crase, S. H. Wadumethrige, K. Thakur, L. Dai, S. Zou, and R. Rathore and C. S. Hartley, *J. Am. Chem. Soc.* **2010**, *132*, 13848–13857. (b) C. S. Hartley and J. He. *J. Org. Chem.* **2010**, *75*, 8627–8636. (c) S. M. Mathew and C. S. Hartley, *Macromolecules* **2011**, *44*, 8425–8432. (d) S. M. Mathew, J. T. Engle, C. J. Ziegler and C. S. Hartley, *J. Am. Chem. Soc.* **2013**, *135*, 6714–6722. (e) S. M. Mathew, L. A. Crandall, C. J. Ziegler and C. S. Hartley, *J. Am. Chem. Soc.* **2014**, *136*, 16666–16675. (f) C. S. Hartley, *Acc. Chem. Res.* **2016**, *49*, 646–654.

7.2 DFT Analysis of Rotational Barrier for Interconverting AAAA and AAAB in X-Ar-3

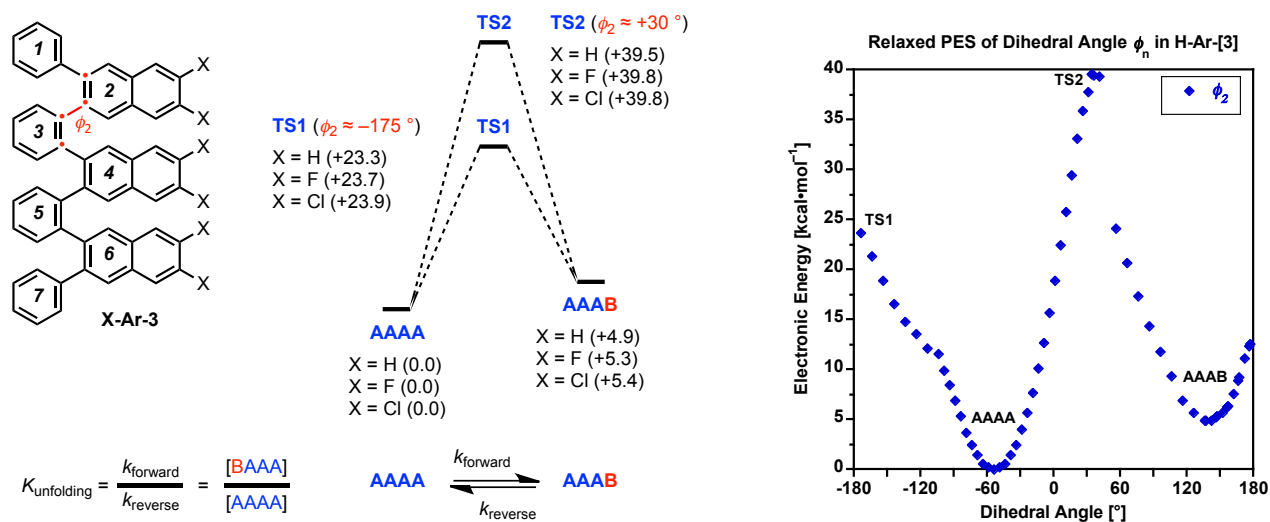
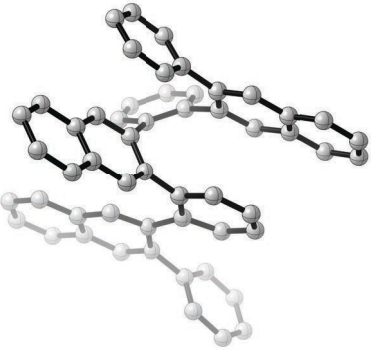
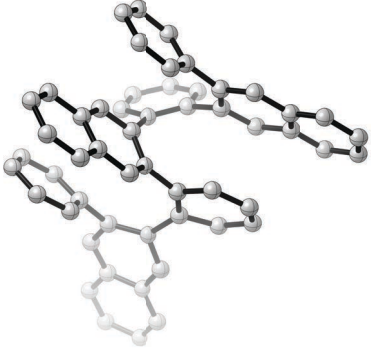
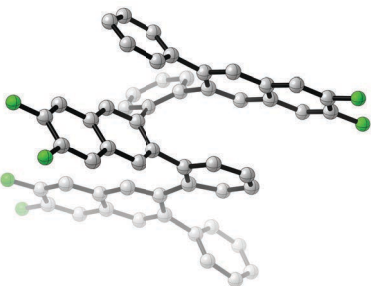
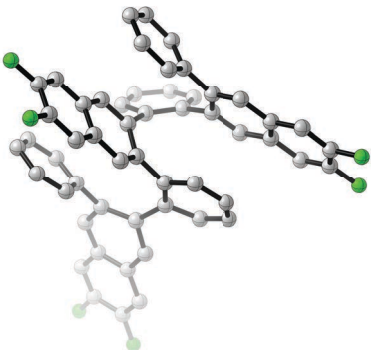
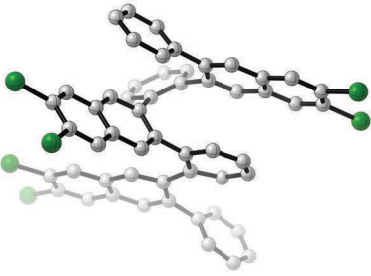
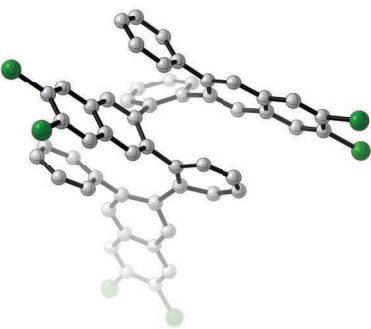


Figure S62. (Left) M06-2X/6-31G (gas phase) computed electronic energy barriers for the interconversion of conformers AAAA and AAAB in **X-Ar-3**. (Right) Relaxed dihedral angle scan for the rotation about ϕ_2 in **X-Ar-3** as computed using M06-2X/6-31G (gas phase).

Table S9. DFT optimized transition states **TS1** and **TS2** for **X-Ar-3** calculated using M06-2X/6-31G (gas phase).^[a]

Compound	TS1	TS2
H-Ar-3	 <p>$E = +23.3 \text{ kcal}\cdot\text{mol}^{-1}$ $\phi_2 = -176.3^\circ$</p>	 <p>$E = +39.5 \text{ kcal}\cdot\text{mol}^{-1}$ $\phi_2 = +33.6^\circ$</p>
F-Ar-3	 <p>$E = +23.7 \text{ kcal}\cdot\text{mol}^{-1}$ $\phi_2 = -173.6^\circ$</p>	 <p>$E = +39.8 \text{ kcal}\cdot\text{mol}^{-1}$ $\phi_2 = +33.4^\circ$</p>
Cl-Ar-3	 <p>$E = +23.9 \text{ kcal}\cdot\text{mol}^{-1}$ $\phi_2 = -174.5^\circ$</p>	 <p>$E = +39.8 \text{ kcal}\cdot\text{mol}^{-1}$ $\phi_2 = +29.8^\circ$</p>

^[a] Electronic energies are relative to those of conformer AAAA.

7.3 DFT Computed Conformations AA...A and AA...AB of Foldamers X-Ar-4, F-Ar-5 and F-Ar-6

Table S10. DFT Computed Conformations AA...A and AA...AB of foldamers **X-Ar-4**, **F-Ar-5** and **F-Ar-6** using M06-2X/6-31G.^a

Compound	Folding Conformation ^b	Relative E (kcal•mol ⁻¹)
H-Ar-4	AAAAA	0.0 (defined)
	AAAAB	+4.8
F-Ar-4	AAAAA	+0.0
	AAAAB	+5.1
Cl-Ar-4	AAAAA	0.0 (defined)
	AAAAB	+6.0
F-Ar-5	AAAA	0.0 (defined)
	AAAB	+6.5
F-Ar-6	AAAAA	0.0 (defined)
	AAAAB	+7.2

^a See Figure S58 for definition of dihedral angles. ^b Folding conformation coding for $\phi_2, \phi_3, \phi_4, \phi_5, \phi_6$ using A if ($0^\circ < \phi_n < -90^\circ$) and B ($90^\circ < \phi_n < 180^\circ$).

Table S11. DFT optimized conformers AA...A and AA...AB of **X-Ar-4**, **F-Ar-5** and **F-Ar-6** calculated using M06-2X/6-31G (gas phase).

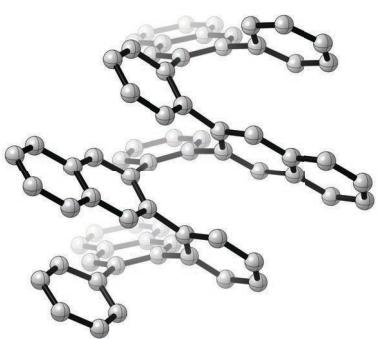
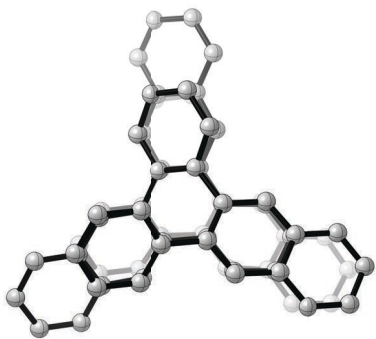
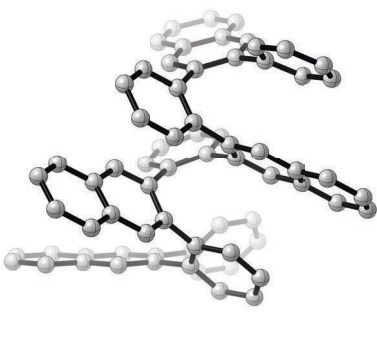
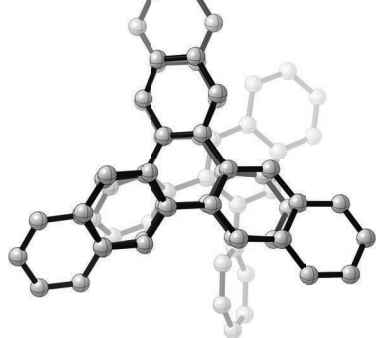
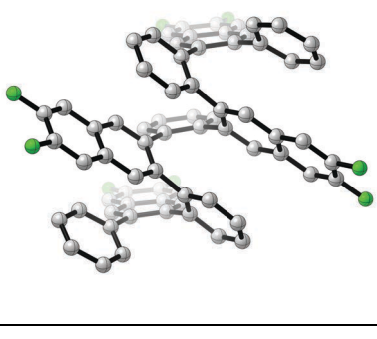
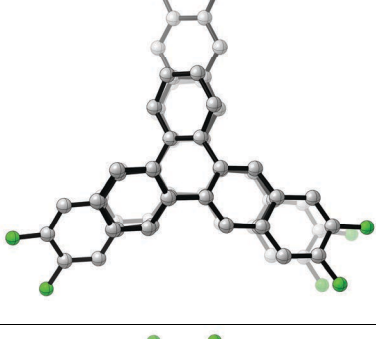
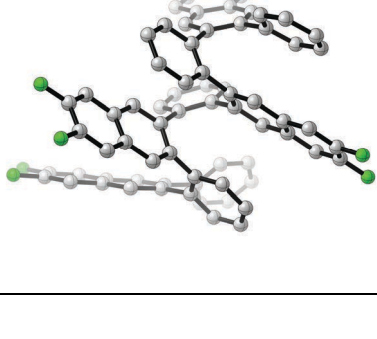
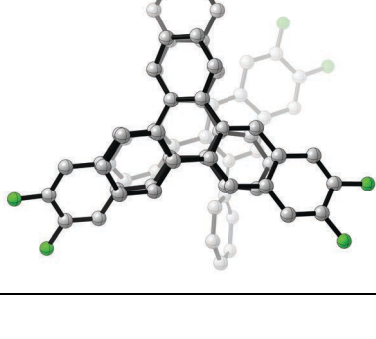
Compound / Conformer	Energy Relative to AA...A [kcal•mol ⁻¹]	Side View	Top View
H-Ar-4 / AAAAA	0.0 (defined)		
H-Ar-4 / AAAAB	+4.8		
F-Ar-4 / AAAAA	0.0 (defined)		
F-Ar-4 / AAAAB	+5.1		

Table S11 (continued). DFT optimized conformers AA...A and AA...AB of **X-Ar-4**, **F-Ar-5** and **F-Ar-6** calculated using M06-2X/6-31G (gas phase).

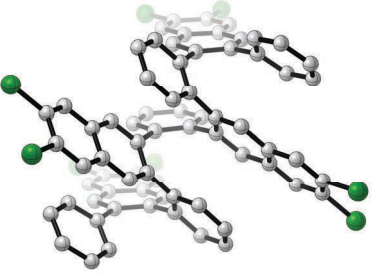
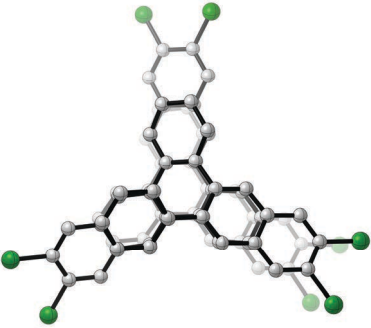
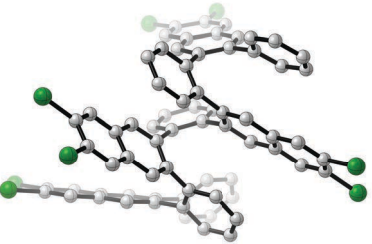
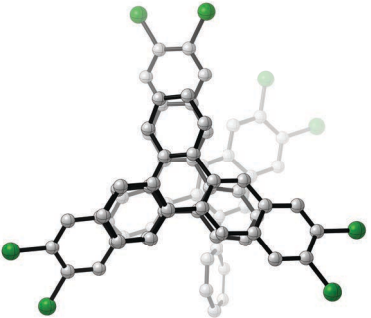
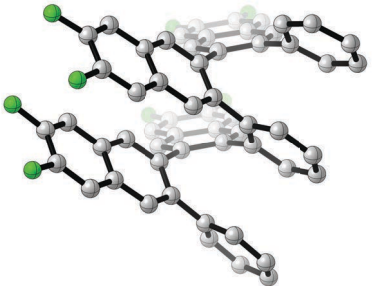
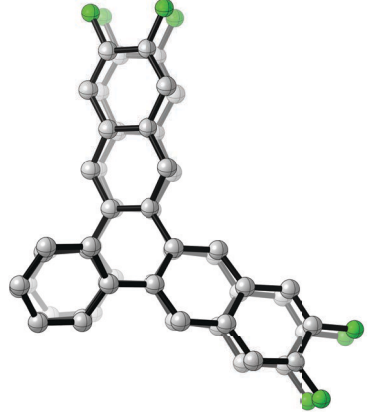
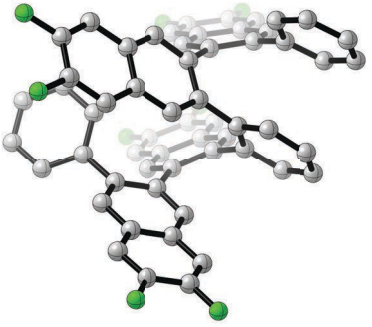
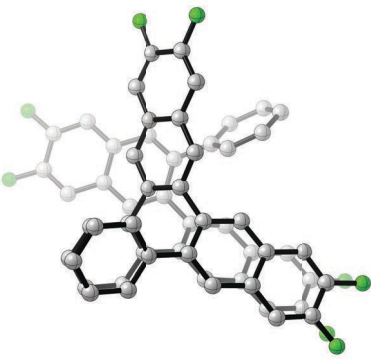
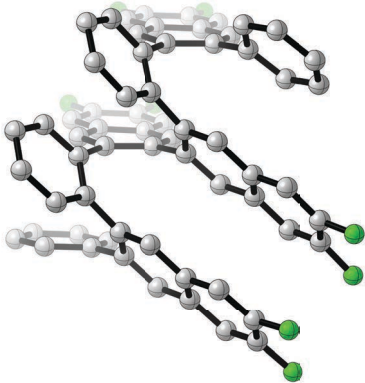
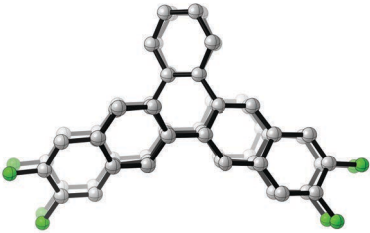
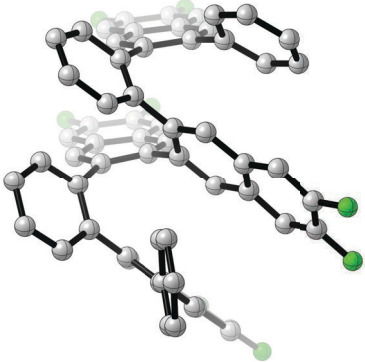
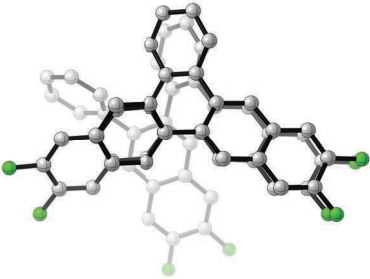
Conformer	Energy Relative to AAAA [kcal•mol ⁻¹]	Side View	Top View
Cl-Ar-4 / AAAAB	0.0 (defined)		
Cl-Ar-4 / AAAAB	+5.1		
F-Ar-5 / AAAA	0.0 (defined)		
F-Ar-5 / AAAB	+5.1		

Table S11 (continued). DFT optimized conformers AA...A and AA...AB of **X-Ar-4**, **F-Ar-5** and **F-Ar-6** calculated using M06-2X/6-31G (gas phase).

Conformer	Energy Relative to AAAA [kcal•mol ⁻¹]	Side View	Top View
F-Ar-6 / AAAAA	0.0 (defined)		
F-Ar-6 / AAAAB	+5.1		

7.4 DFT Computed Structures and Properties Graphene Nanoribbons X-GNR-[*n*]

Table S12. Summary of DFT results for **X-GNR-[*n*]** calculated using M06-2X/6-31G (gas phase).^[a]

Compound	Energy Relative to Lowest Conformation [kcal•mol ⁻¹]	Dipole Moment [Debye]	HOMO [eV]	LUMO [eV]
H-GNR-1	0.0	0.0	-6.67	-0.69
F-GNR-1	0.0	4.3	-7.05	-1.06
Cl-GNR-1	0.0	4.7	-7.07	-1.18
H-GNR-2	0.0	0.1	-5.88	-1.51
F-GNR-2	0.0	7.8	-6.42	-1.95
Cl-GNR-2	0.0	7.8	-6.47	-2.09
H-GNR-3- <i>planar</i>	0.0	0.1	-5.51	-1.95
F-GNR-3- <i>wagging</i>	0.0	11.1	-6.10	-2.44
F-GNR-3- <i>helical</i>	+2.5	10.9	-6.12	-2.41
Cl-GNR-3- <i>wagging</i>	0.0	10.8	-6.14	-2.59
Cl-GNR-3- <i>helical</i>	+7.8	10.3	-6.17	-2.51
H-GNR-4- <i>planar</i>	0.0	0.1	-5.28	-2.22
F-GNR-4- <i>wagging</i>	0.0	14.4	-5.92	-2.74
F-GNR-4- <i>helical</i>	+5.8	13.8	-5.94	-2.69
Cl-GNR-4- <i>wagging</i>	0.0	13.7	-5.95	-2.88
Cl-GNR-4- <i>helical</i>	+17.2	12.5	-5.99	-2.76

^[a] HOMO and LUMO levels are calculated vs vacuum. See Table S13–S16 for conformations.

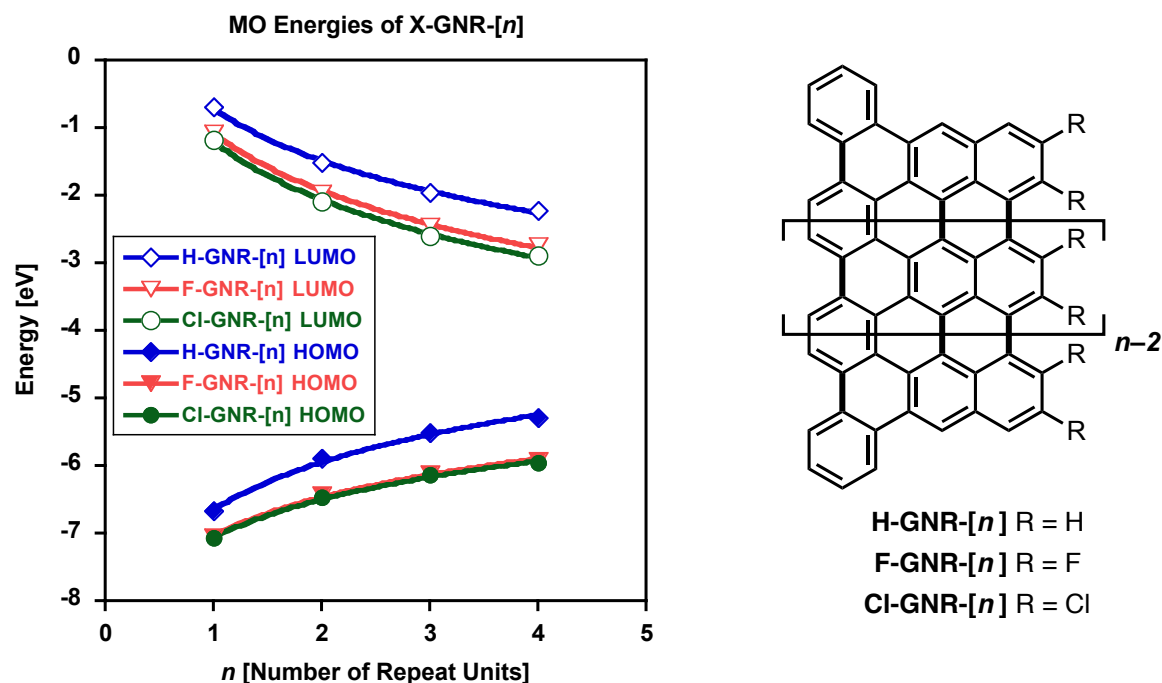


Figure S63. Plot of molecular orbital energies as a function of repeat of **X-GNR-[*n*]** as calculated by DFT using M06-2X/6-31G (gas phase). The results are based on the lowest energy conformation of **X-GNR-[*n*]** as determined by DFT (see Table S15–S16).

Table S13. DFT optimized structures of **X-GNR-1** illustrating the top, side and eclipsed view calculated using M06-2X/6-31G (gas phase).

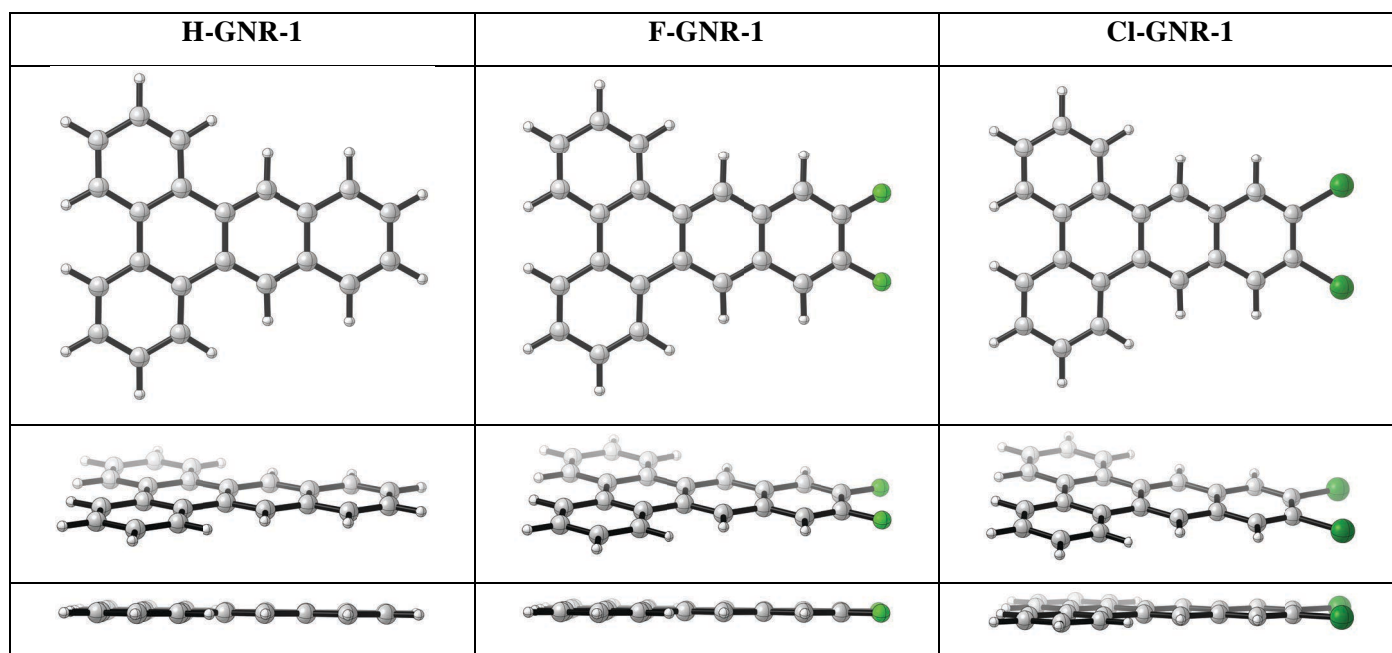


Table S14. DFT optimized structures of **X-GNR-2** illustrating the top, side and eclipsed view calculated using M06-2X/6-31G (gas phase).

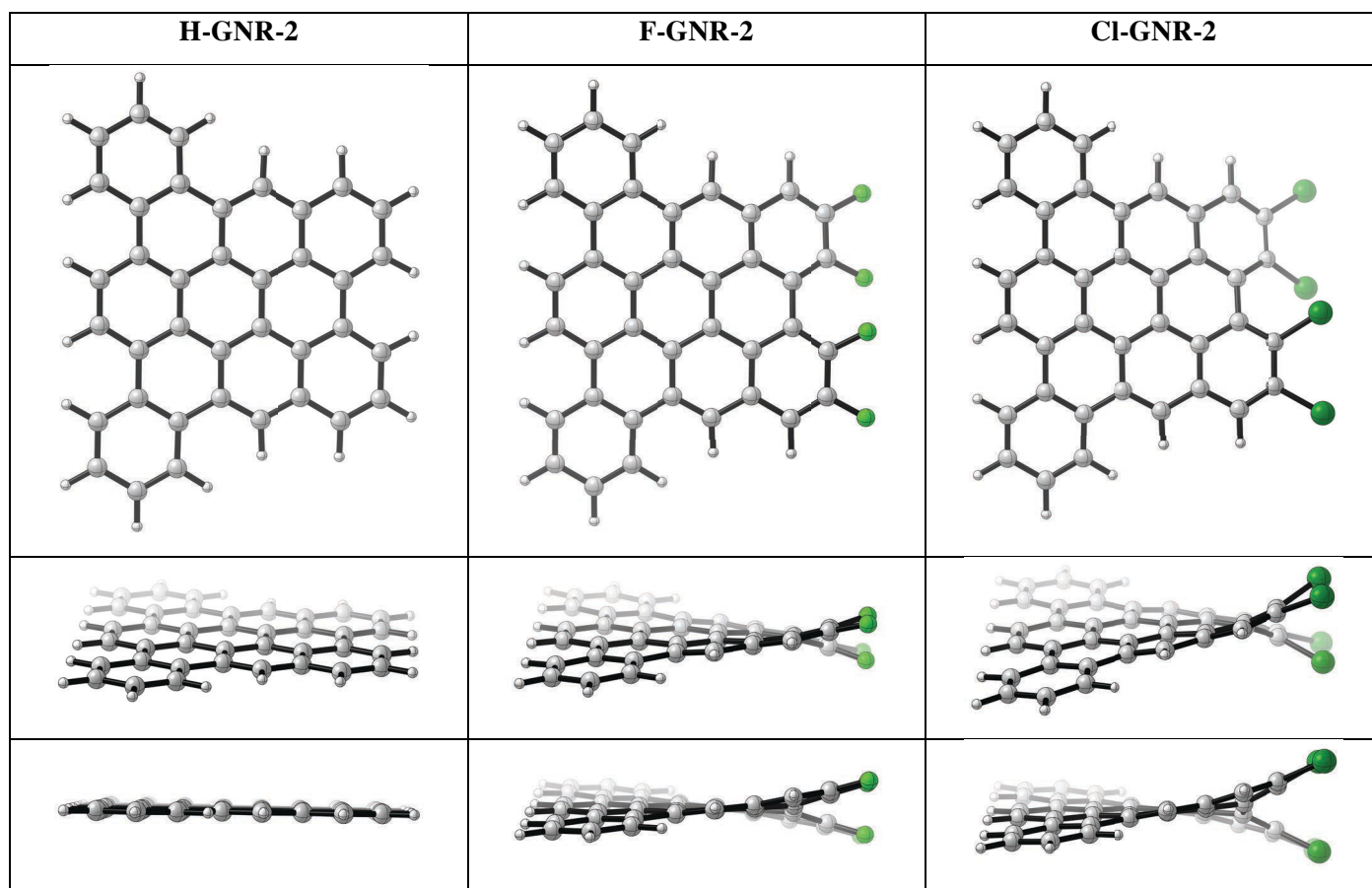


Table S15. DFT optimized structures of **X-GNR-3** illustrating the top, side and eclipsed view calculated using M06-2X/6-31G (gas phase). (Conformation legend: *h* = helical, *w* = wagging, *p* = planar)

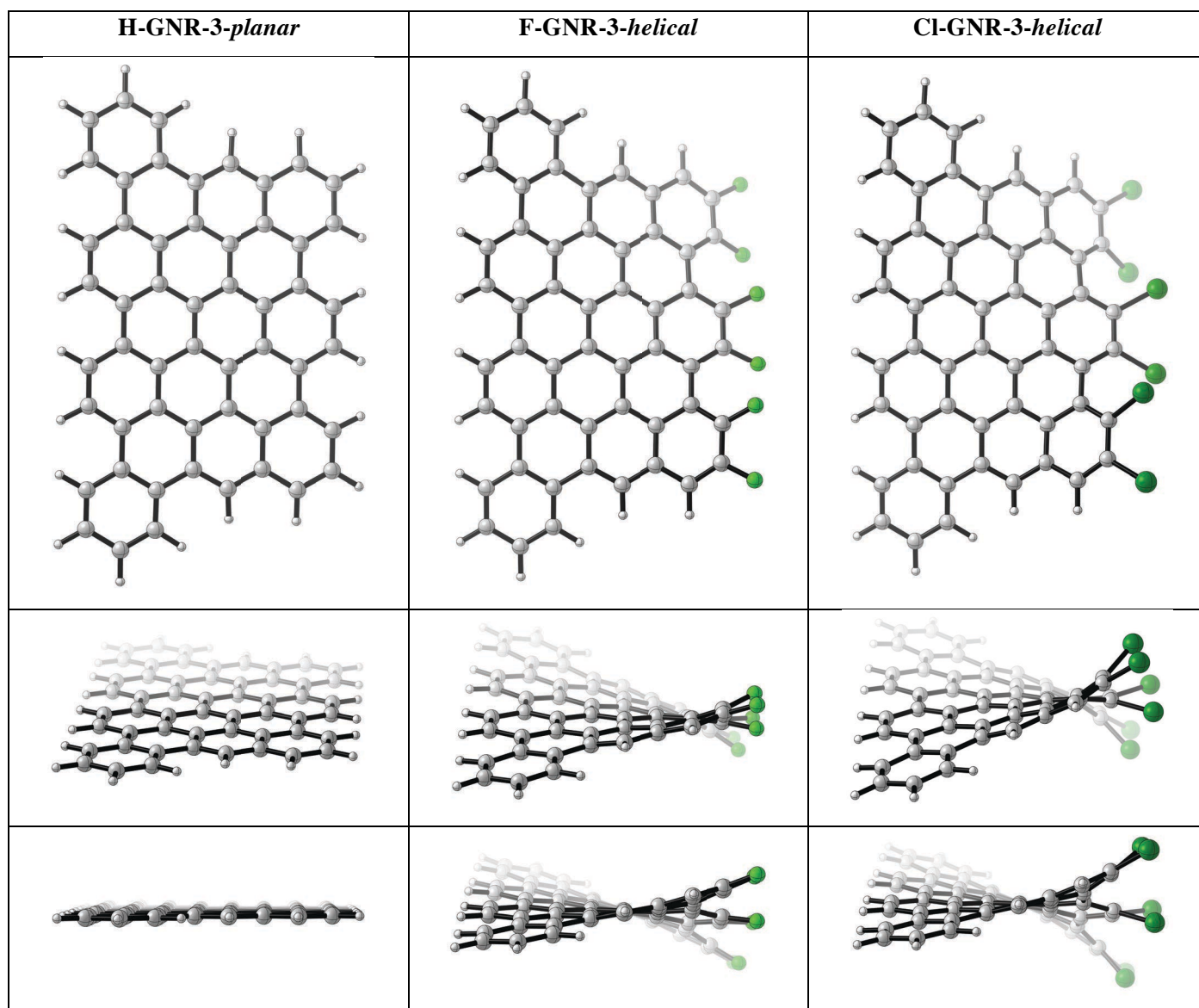


Table S15 (continued). DFT optimized structures of **X-GNR-3** illustrating the top, side and eclipsed view calculated using M06-2X/6-31G (gas phase). (Conformation legend: *h* = helical, *w* = wagging, *p* = planar)

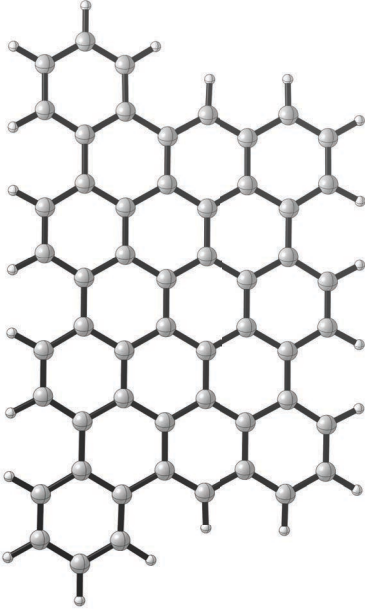
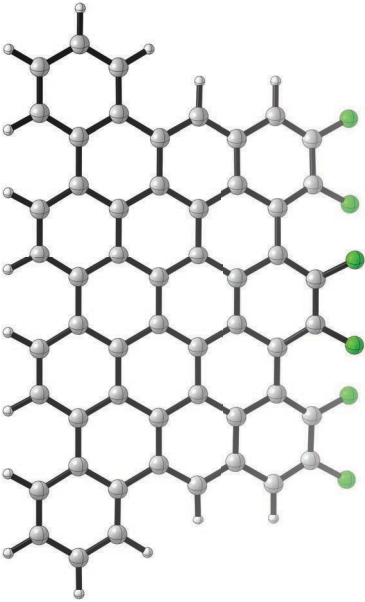
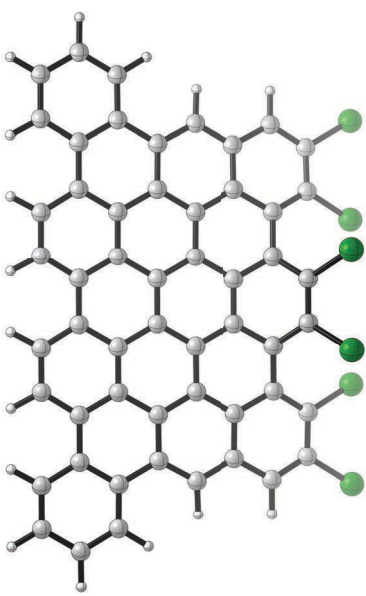
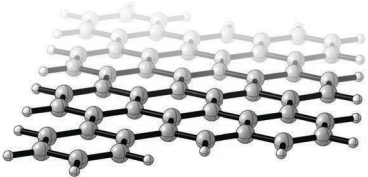
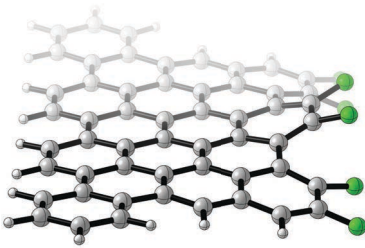
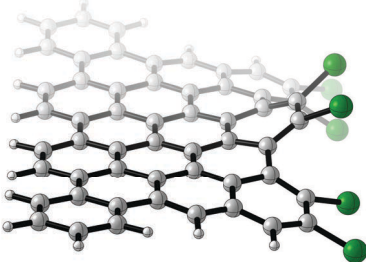



H-GNR-3- <i>planar</i>	F-GNR-3- <i>wagging</i>	Cl-GNR-3- <i>wagging</i>
		
		
		

Table S16. DFT optimized structures of **X-GNR-4** illustrating the top, side and eclipsed view calculated using M06-2X/6-31G (gas phase). (Conformation legend: *h* = helical, *w* = wagging, *p* = planar)

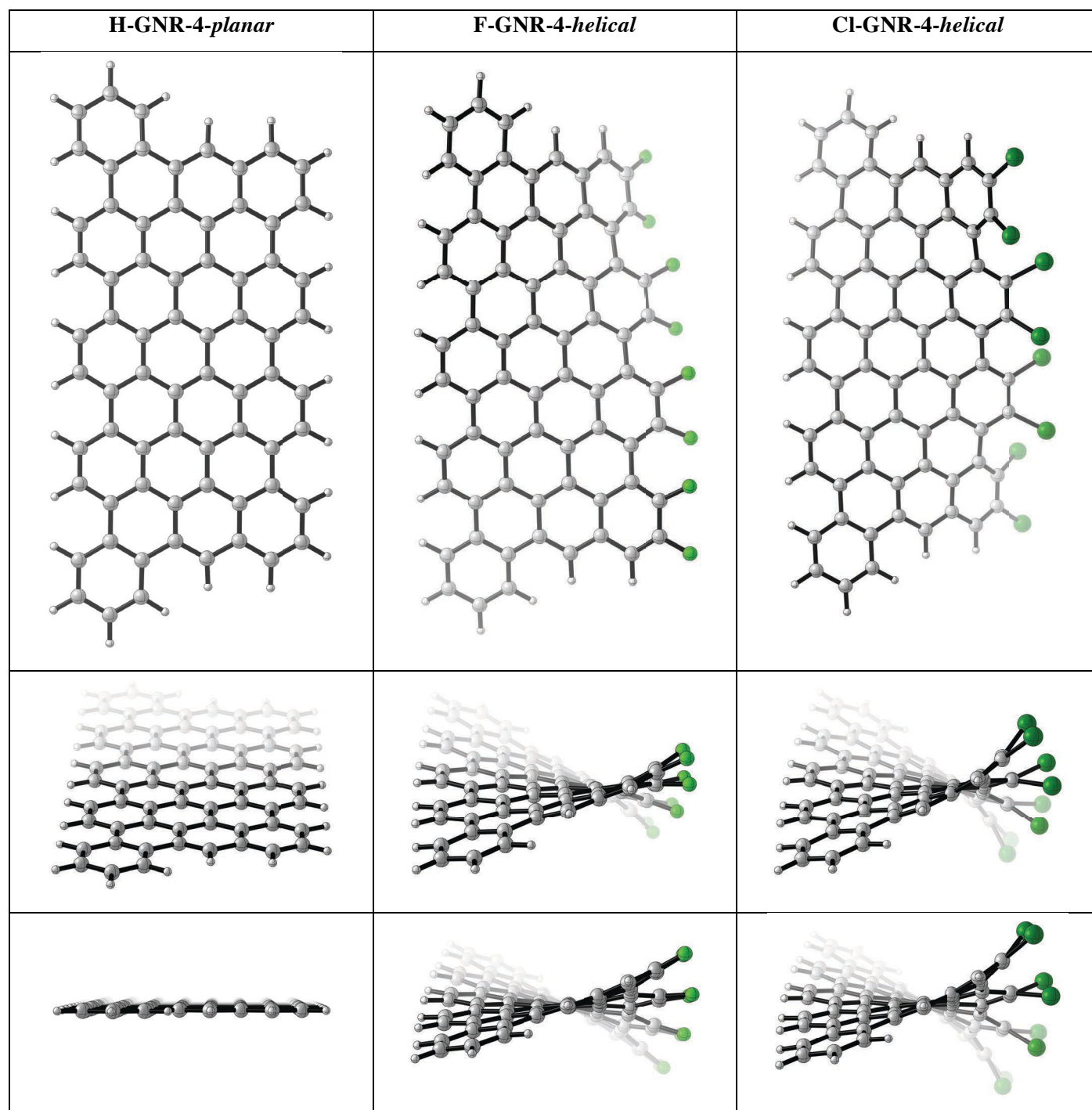
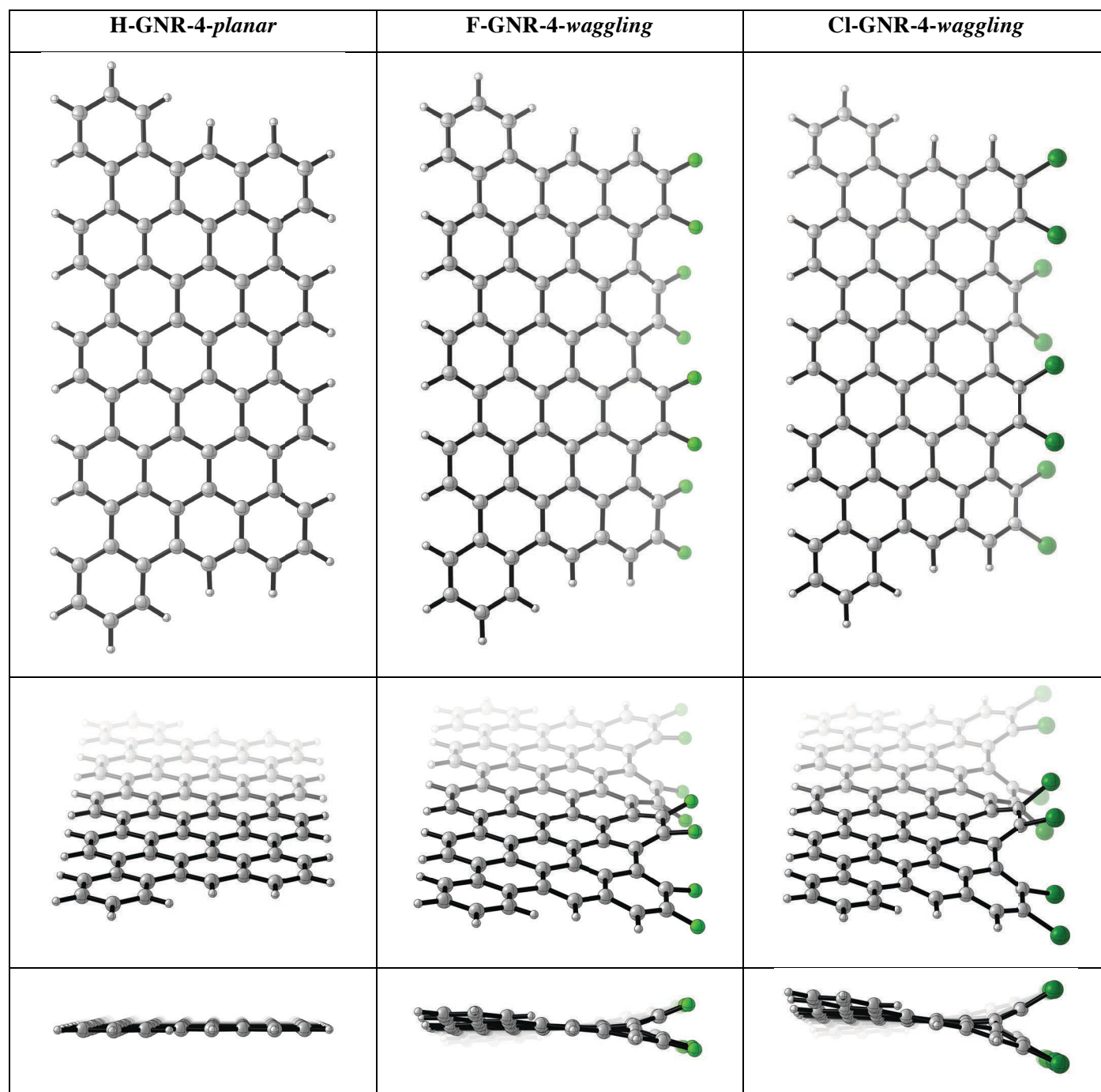


Table S16 (continued). DFT optimized structures of **X-GNR-4** illustrating the top, side and eclipsed view calculated using M06-2X/6-31G (gas phase). (Conformation legend: *h* = helical, *w* = wagging, *p* = planar)



8. Determination of Thermodynamic Parameters for the Interconversion of Conformers AAAA and AAAB of X-Ar-3

8.1 Determination of the Equilibrium Constants and van 't Hoff Analysis

The unfolding equilibrium constant ($K_{\text{unfolding}}$) associated with the process of converting conformer AAAA to AAAB in **X-Ar-3** was determined by ^1H NMR spectroscopy by taking the ratio of twice the signal integration of the H17 associated with AAAB ($I_{(\text{H17-AAAB})}$) and the H17 signal integration of AAAA ($I_{(\text{H17-AAAA})}$). The factor is 2 is used to correct for the loss of symmetry as H17 in AAAA affords both H17 and H28 in conformer AAAB.

$$K_{\text{unfolding}} = [\text{AAAB}]/[\text{AAAA}] = 2 \cdot I_{(\text{H17-AAAB})} / I_{(\text{H17-AAAA})}$$

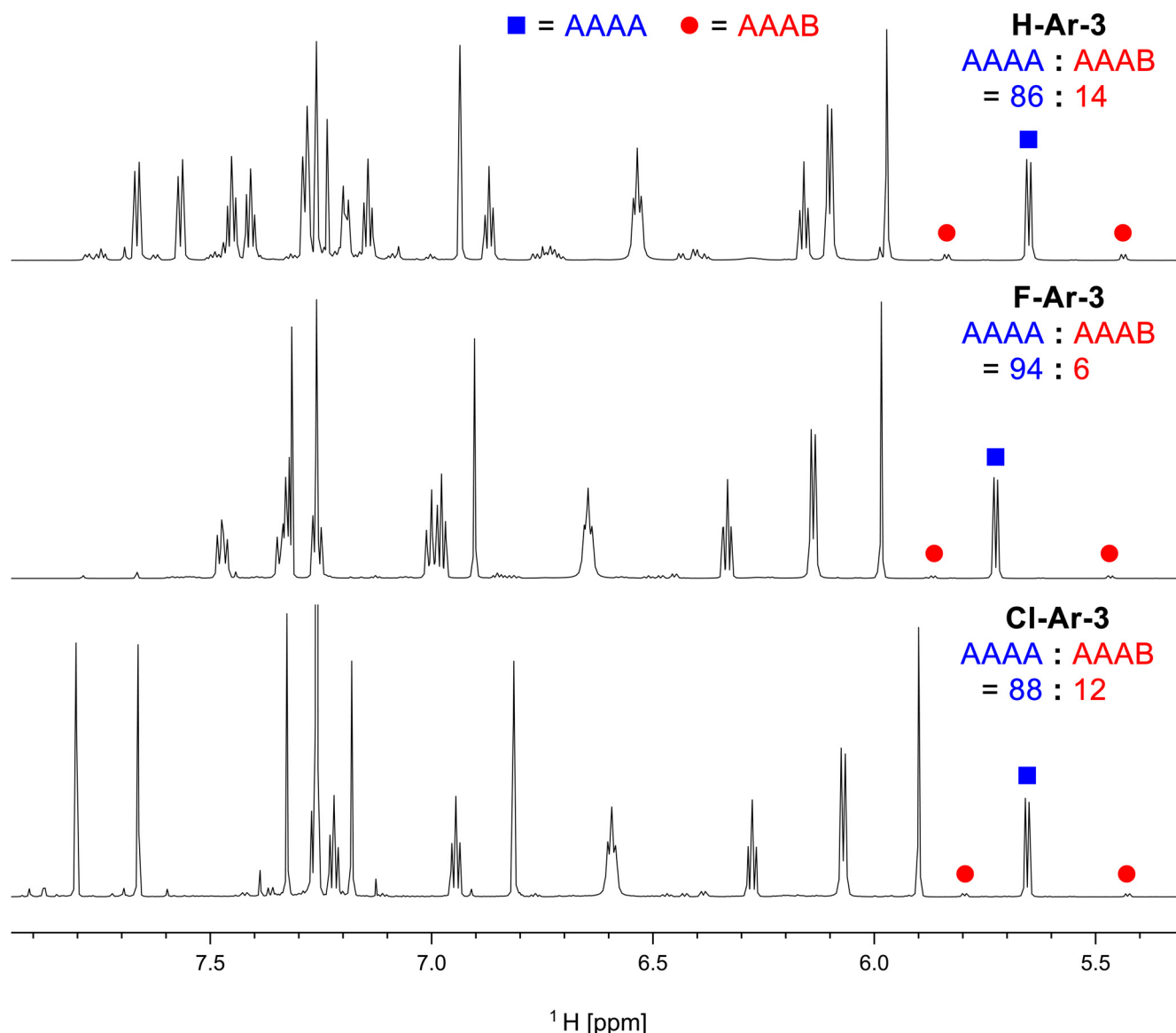
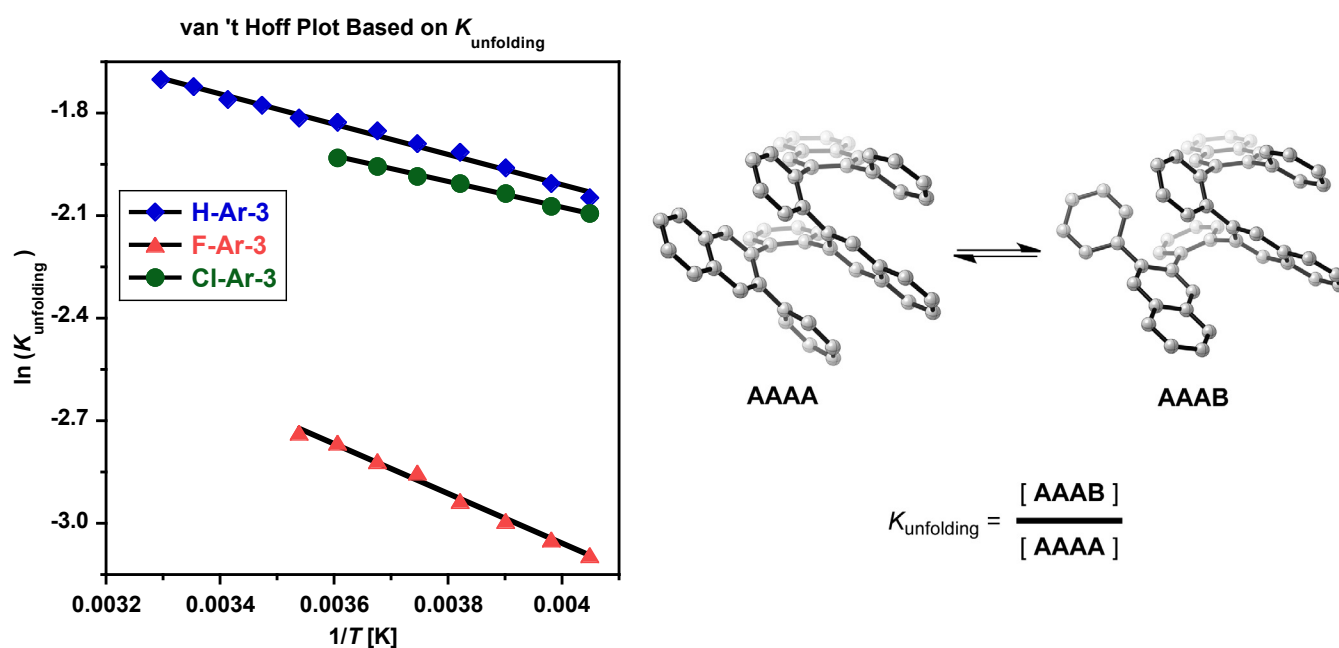


Figure S64. ^1H NMR spectra (800 MHz) of (top): **H-Ar-3**, **F-Ar-3**, **Cl-Ar-3** in CDCl_3 at $0\text{ }^\circ\text{C}$ illustrating the hydrogen signal used for determining the ratio and kinetics for the equilibrium and exchange between conformer AAAA and AAAB, respectively. Signals from right to left: H17-AAAB, H17-AAAA, H28-AAAB.

Table S17. $K_{\text{unfolding}}$ for **X-Ar-3** in CDCl_3 as a function of temperature as determined of by NMR spectroscopy.^[a]

H-Ar-3		F-Ar-3		Cl-Ar-3	
1/T [K ⁻¹]	$K_{\text{unfolding}}$	1/T [K ⁻¹]	$K_{\text{unfolding}}$	1/T [K ⁻¹]	$K_{\text{unfolding}}$
0.0040475	-2.0460	0.0040475	-3.0897	0.0040475	-2.0933
0.0039801	-2.0047	0.0039801	-3.0453	0.0039801	-2.0720
0.0038989	-1.9567	0.0038989	-2.9905	0.0038989	-2.0331
0.0038210	-1.9137	0.0038210	-2.9332	0.0038210	-2.0055
0.0037461	-1.8889	0.0037461	-2.8481	0.0037461	-1.9812
0.0036741	-1.8513	0.0036741	-2.8154	0.0036741	-1.9529
0.0036048	-1.8249	0.0036048	-2.7633	0.0036048	-1.9273
0.0035381	-1.8105	0.0035381	-2.7342	–	–
0.0034738	-1.7753	–	–	–	–
0.0034118	-1.7587	–	–	–	–
0.0033519	-1.7197	–	–	–	–
0.0032942	-1.7013	–	–	–	–

^[a] Temperature was calibrated using MeOH signals in ¹H NMR. $K_{\text{unfolding}} = [\text{AAAB}]/[\text{AAAA}]$.

**Figure S65.** (Left) van 't Hoff plot associated with the unfolding process (AAAA to AAAB) of **X-Ar-3** in CDCl_3 determined by ¹H NMR. (Right) DFT structures illustrating the equilibrium process studied in the van 't Hoff plot.**Table S18.** Parameters obtained from least-square linear fit to data in van 't Hoff plot (Figure S65) for $K_{\text{unfolding}}$ of **X-Ar-3**.

Compound	Slope	Intercept	R ²
H-Ar-3	-440.8 ± 37.2	-0.244 ± 0.136	0.992
F-Ar-3	-729.3 ± 77.5	-0.139 ± 0.294	0.993
Cl-Ar-3	-376.7 ± 22.3	-0.568 ± 0.086	0.998

^[a] Error range calculated by reporting the magnitude of three standard errors.

A van 't Hoff plot based on the data in **Table S17** allows the data to be fit to the following equation:

$$\ln(K_{\text{unfolding}}) = (-\Delta H_{\text{unfolding}}/R)(1/T) + (\Delta S_{\text{unfolding}}/R)$$

Where $K_{\text{unfolding}} = [\text{AAAB}]/[\text{AAAA}]$, R is the ideal gas constant ($1.9858775 \times 10^{-3} \text{ kcal}\cdot\text{mol}^{-1}$), T is the temperature, $\Delta H_{\text{unfolding}}$ and $\Delta S_{\text{unfolding}}$ are the enthalpy and entropy for the unfolding process from AAAA to AAAB. The values presented in Table S19 are derived using the following relationships: $K_{\text{folding}} = 1 / K_{\text{unfolding}} = [\text{AAAA}]/[\text{AAAB}]$, $\Delta G_{\text{folding}} = -\Delta G_{\text{unfolding}}$, $\Delta H_{\text{folding}} = -\Delta H_{\text{unfolding}}$, $\Delta S_{\text{folding}} = -\Delta S_{\text{unfolding}}$.

Table S19. Thermochemistry values determined from the van 't Hoff analysis.^[a]

Compound	$\Delta G_{\text{folding}}$ at 272 K [kcal•mol ⁻¹]	$\Delta H_{\text{folding}}$ [kcal•mol ⁻¹]	$\Delta S_{\text{folding}}$ [kcal•mol ⁻¹]	K_{folding} at 272 K
H-Ar-3	-1.0 ± 0.1	-0.88 ± 0.07	-0.5 ± 0.3	6.4
F-Ar-3	-1.5 ± 0.3	-1.5 ± 0.2	$+0.3 \pm 0.6$	17
Cl-Ar-3	-1.1 ± 0.1	-0.75 ± 0.04	$+1.1 \pm 0.2$	7.0

^[a] Error range calculated by reporting the magnitude of three standard errors.

8.2 Determination of the Rate and Activation Parameters for Unfolding Process

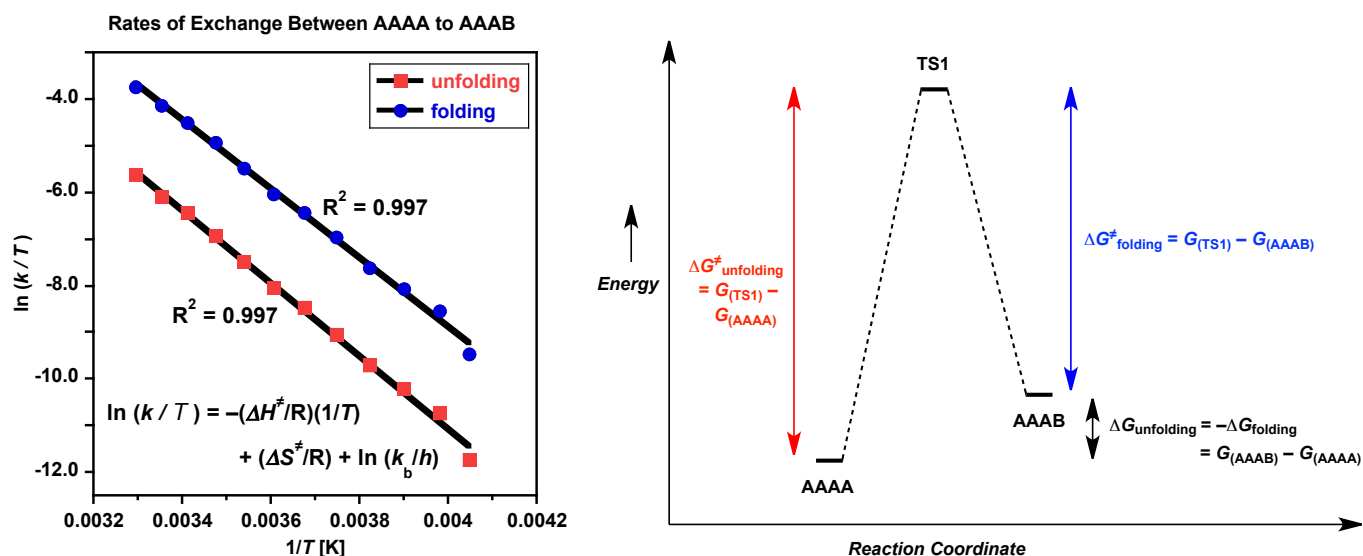


Figure S67. (Left) Eyring plot based on the folding (AAAB to AAAA) and unfolding (AAAA to AAAB) rates measured by EXSY NMR at various temperatures (ca. -24°C to 30°C) for solutions of **H-Ar-3** in CDCl_3 . (Right) Energy diagram illustrating various parameters associated with the measurements obtained from the Eyring plot.

An Eyring plot based on the data in **Table S20** allows the data to be fit to the following equation:

$$\ln(k_{\text{unfolding}}/T) = (-\Delta H_{\text{unfolding}}^\ddagger/R)(1/T) + (\Delta S_{\text{unfolding}}^\ddagger/R) + \ln(k_b/h)$$

Where $k_{\text{unfolding}}$ is the rate of unfolding from AAAA to AAAA, T is the temperature, R is the ideal gas constant ($1.9858775 \times 10^{-3} \text{ kcal}\cdot\text{mol}^{-1}$), k_b is the Boltzmann distribution constant ($3.299892916 \times 10^{-24} \text{ cal}\cdot\text{K}^{-1}$), h is Planck's constant ($1.58366875 \times 10^{-34} \text{ cal}\cdot\text{s}^{-1}$), $\Delta H_{\text{unfolding}}^\ddagger$ and $\Delta S_{\text{unfolding}}^\ddagger$ are the enthalpy and entropy of activation for the unfolding process from AAAA to AAAB. The values presented in Table S21 are derived using the following relationships:

$$\Delta G_{\text{unfolding}}^\ddagger = -\Delta H_{\text{unfolding}}^\ddagger - T\Delta S_{\text{unfolding}}^\ddagger$$

Table S20. $k_{\text{unfolding}}$ for **X-Ar-3** in CDCl_3 as a function of temperature as determined of by EXSY.^[a]

$1/T$ [K^{-1}]	$\ln(k_{\text{unfolding}}/T)$	$\ln(k_{\text{folding}}/T)$
0.0040475	-11.72	-9.473
0.0039801	-10.73	-8.553
0.0038989	-10.20	-8.060
0.0038210	-9.702	-7.611
0.0037461	-9.029	-6.969
0.0036741	-8.462	-6.422
0.0036048	-8.039	-6.026
0.0035381	-7.493	-5.479
0.0034738	-6.920	-4.914
0.0034118	-6.439	-4.504
0.0033519	-6.086	-4.128
0.0032942	-5.606	-3.739

^[a] Temperature was calibrated using MeOH signals in ^1H NMR. k_{folding} is the rate associated with the process of going from AAAB to AAAA. $k_{\text{unfolding}}$ is the rate associated with the process of going from AAAA to AAAB.

Table S21. Relative rate and activation parameters associated with the unfolding and folding between AAAA and AAAB for **X-Ar-3**.^[a]

Compound	$\Delta G^\ddagger_{\text{unfolding}}$ at 272 K [$\text{kcal}\cdot\text{mol}^{-1}$]	$\Delta H^\ddagger_{\text{unfolding}}$ [$\text{kcal}\cdot\text{mol}^{-1}$]	$\Delta S^\ddagger_{\text{unfolding}}$ [$\text{cal}\cdot\text{mol}^{-1}$]	$k_{\text{unfolding}}$ [relative] at 272 K
H-Ar-3	17.5 ± 1.7	15.5 ± 0.9	-7.1 ± 3.2	1.00 ^[b]
F-Ar-3	ND	ND	ND	0.25
Cl-Ar-3	ND	ND	ND	0.22

^[a] Error range calculated by reporting the magnitude of three standard errors. ND = not determined.

^[b] Relative rate defined to 1.00 for **H-Ar-3a**, all other rates in the column are measured relative to this rate.

In order to probe whether the exchange between AAAB and BAAA proceeds via a direct exchange mechanism (connected only via a transition state and no intermediate) or via an indirect exchange mechanism (connected via an intermediate, such as AAAA), the EXSY cross-peak volume integrals of conformers AAAA and AAAB of **H-Ar-3** were plotted as a function of mixing time. The plot clearly illustrates that degenerate exchange between conformers AAAB and BAAA proceeds via an intermediate state based on the negative curvature in the dashed trace, in contrast to the unfolding process of AAAA to AAAB that proceeds via direct exchange based on the positive curvature of the solid line in the plot below.

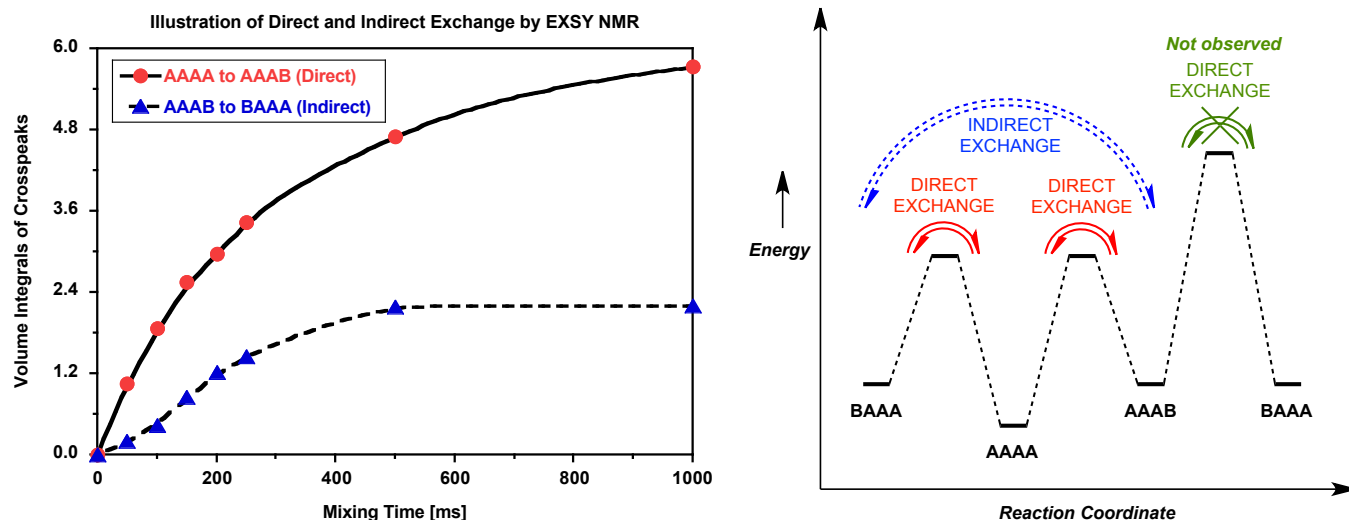


Figure S67. (Left) EXSY cross-peak volume integrals of **H-Ar-3** as a function of mixing time illustrating that degenerate exchange between conformers AAAB and BAAA must proceed via an intermediate state (indirect exchange), in contrast to the unfolding process of AAAA to AAAB (direct exchange). (Right) Potential energy surface (not drawn to scale) illustrating the difference between direct and indirect exchange pathways for the interconversion of conformers BAAA, AAAA, and AAAB.

9. 2-D NMR Data and Solution-Structure Assignment of X-Ar-3, X-Ar-4, F-Ar-5, and F-Ar-6

9.1 NMR Assignment of Conformers AAAA and AAAB of X-Ar-3

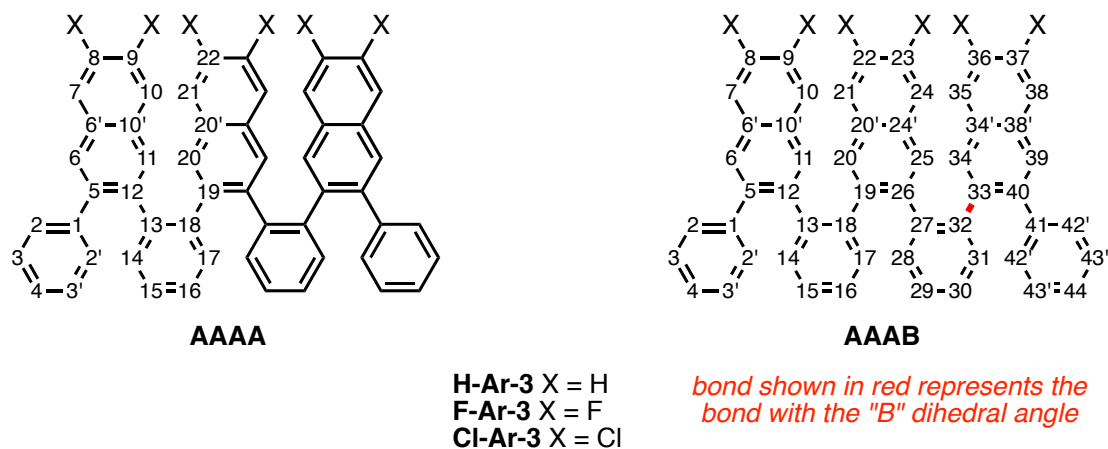


Figure S68. Atom numbering of **X-Ar-3** for conformers AAAA and AAAB.

For the atom numbering scheme associated with the NMR spectral assignment, see Figure S68.

Table S22. Assignment of ^1H and ^{13}C Chemical Shifts for **X-Ar-3-AAAA** in CDCl_3 at 0°C .^[a]

Atom #	H-Ar-3-AAAA		F-Ar-3-AAAA		Cl-Ar-3-AAAA	
	δ_{C} [ppm]	δ_{H} [ppm]	δ_{C} [ppm]	δ_{H} [ppm]	δ_{C} [ppm]	δ_{H} [ppm]
1	141.03	–	140.33	–	140.14	–
2	128.13	6.13	127.94	6.08	127.90	6.07
2'	128.13	6.13	127.94	6.08	127.90	6.07
3	127.30	6.56	127.45	6.59	127.55	6.59
3'	127.30	6.56	127.45	6.59	127.55	6.59
4	125.54	6.89	125.92	6.92	126.18	6.95
5	138.60	–	138.72	–	139.59	–
6	128.04	7.28	127.41	7.20	127.05	7.18
6'	132.40	–	129.08	–	131.28	–
7	127.42	7.69	113.05	7.42	128.40	7.80
8	125.61	7.43	149.80 ^[b]	–	129.78	–
9	125.34	7.48	149.80 ^[b]	–	129.56	–
10	128.48	7.59	113.78	7.28	129.12	7.66
10'	132.95	–	129.70	–	131.84	–
11	130.70	6.96	129.82	6.85	129.49	6.81
12	139.03	–	139.14	–	140.02	–
13	139.16	–	138.64	–	138.49	–
14	131.56	7.31	131.71	7.27	131.69	7.27
15	126.62	7.17	127.1	7.20	127.33	7.22
16	127.42	6.18	127.6	6.28	127.86	6.28
17	131.80	5.68	131.49	5.67	131.44	5.65
18	141.11	–	140.49	–	140.29	–
19	138.55	–	138.63	–	139.52	–
20	130.24	6.00	129.58	5.93	129.33	5.90
20'	132.31	–	128.94	–	131.10	–
21	128.04	7.22	113.27	6.94	128.77	7.33
22	124.55	7.31	149.28	–	128.88	–

[a] The carbon-hydrogen connectivity was established via HSQC NMR. [b] Assignment of C8 and C9 could not be made unambiguously and may be reversed.

Table S23. Assignment of ^1H and ^{13}C Chemical Shifts for **X-Ar-3-AAAB** in CDCl_3 at 0°C .^[a]

Atom #	H-Ar-3-AAAB		F-Ar-3-AAAB		Cl-Ar-3-AAAB	
	δ_{C} [ppm]	δ_{H} [ppm]	δ_{C} [ppm]	δ_{H} [ppm]	δ_{C} [ppm]	δ_{H} [ppm]
1	140.98	–	140.31	–	140.10	–
2	128.64	6.43	128.46	6.39	128.48	6.39
2'	128.64	6.43	128.46	6.39	128.48	6.39
3	127.56	6.76	127.73	6.79	127.82	6.81
3'	127.56	6.76	127.73	6.79	127.82	6.81
4	125.94	7.03	126.41	7.07	126.65	7.11
5	139.07	–	139.23	–	140.08	–
6	128.22	7.50	127.58	7.42	127.23	7.39
6'	132.75	–	129.49	–	131.63	–
7	127.59	7.80	113.32	7.53	128.62	7.91
8	126.02	7.51	150.08 ^[c]	–	130.31 ^[c]	–
9	125.77	7.52	150.08 ^[c]	–	130.06 ^[c]	–
10	128.28	7.65	113.66	7.33	128.89	7.70
10'	132.29	–	129.05	–	131.11	–
11	132.21	7.10	131.46	6.95	131.04	6.91
12	138.50	–	138.63	–	139.45	–
13	141.13	–	140.53	–	140.36	–
14	131.19	7.47	131.22	7.42	131.20	7.42
15	128.02	7.19	128.55	7.20	128.68	7.21
16	127.52	6.74	127.94	6.75	128.09	6.77
17	131.52	5.46	131.24	5.41	131.18	5.43
18	140.84	–	140.07	–	139.86	–
19	138.25	–	138.52	–	139.27	–
20	131.42	6.01	130.74	5.93	130.54	5.90
20'	132.39	–	129.03	–	131.15	–
21	128.80	7.27	114.14	7.00	129.63	7.37
22	124.96	7.42	149.59 ^[c]	–	130.15 ^[c]	–
23	125.58	7.48	150.01 ^[c]	–	129.57 ^[c]	–
24	127.05	7.78	112.69	7.50	128.08	7.88
24'	132.31	–	128.87	–	131.06	–
25	130.62	7.47	129.87	7.39	129.50	7.36
26	139.52	–	139.73	–	140.60	–
27	140.97	–	140.26	–	140.06	–
28	132.50	5.86	132.13	5.81	132.36	5.80
29	125.65	6.41	125.80	6.45	126.06	6.47
30	125.54	6.76	126.03	6.77	126.21	6.80
31	132.07	6.46	132.15	6.43	132.23	6.43
32	136.96	–	136.57	–	136.41	–
33	136.11	–	136.26	–	137.26	–
34	131.17	6.77	130.14	6.59	129.75	6.60
34'	131.55	–	128.16	–	130.36	–
35	127.66	6.79	112.91	6.51	128.15	6.96
36	125.58	7.11	149.78 ^[c]	–	129.94 ^[c]	–
37	125.93	7.34	150.13 ^[c]	–	130.34 ^[c]	–
38	127.23	7.77	112.97	7.48	128.28	7.87
38'	131.89	–	128.64	–	130.85	–
39	129.24	7.72	128.57	7.61	128.31	7.60
40	139.89	–	138.73	–	141.20	–
41	141.36	–	140.56	–	ND	–
42	130.38	6.30 (br)	130.16	6.21	130.09	6.21
42'	130.38	6.30 (br)	130.16	6.21	ND	ND
43	127.23	7.23	127.90	7.23	ND	ND
43'	127.23	7.23	127.90	7.23	ND	6.65
44	126.33	7.28	126.78	7.27	126.95	7.29

[a] C–H connectivity established via HSQC NMR. [c] Assignment may be reversed between C8 & C9, similarly for C22 & C23, and similarly for C36 & C37.

Table S24. Summary of 2D NMR data for **H-Ar-3-AAAA** and **H-Ar-3-AAAB** in CDCl₃ at 0 °C.^[a]

Atom #	H-Ar-3-AAAA				H-Ar-3-AAAB			
	δ_c [ppm]	δ_H [ppm]	COSY	HMBC ^[b]	δ_c [ppm]	δ_H [ppm]	COSY	HMBC ^[b]
1	141.03	–	–	3', 3, 4, 6	140.98	–	–	3', 3, 6
2	128.13	6.13	3, 4	2', 3, 4	128.64	6.43	3, 4	2', 3, 4
2'	128.13	6.13	3', 4	2, 3', 4	128.64	6.43	3', 4	2, 3', 4
3	127.30	6.56	2, 4	3', 4	127.56	6.76	2, 4	3'
3'	127.30	6.56	2', 4	3, 4	127.56	6.76	2', 4	3
4	125.54	6.89	2, 2', 3, 3'	2, 2', 3, 3'	125.94	7.03	2, 2', 3, 3'	2, 2'
5	138.60	–	–	2, 2', 11	139.07	–	–	2, 2', 11
6	128.04	7.28	7, 10, 11	7, 11	128.22	7.50	11	7
6'	132.40	–	–	6, 8, 10, 11	132.75	–	–	8, 10, 11
7	127.42	7.69	6, 8, 9, 10, 11	6, 9, 10	127.59	7.80	8, 9, 11	6, 9
8	125.61	7.43	7, 9, 10, 11	10	126.02	7.51	7, 10	10
9	125.34	7.48	7, 8, 10, 11	7	125.77	7.52	7, 10	7
10	128.48	7.59	6, 7, 8, 9, 11	8, 11	128.28	7.65	8, 9	8, 11
10'	132.95	–	–	6, 7, 9, 11	132.29	–	–	6, 7, 9
11	130.70	6.96	6, 7, 8, 9, 10	10	132.21	7.10	6, 7	10
12	139.03	–	–	6, 14	138.50	–	–	6, 14
13	139.16	–	–	11, 15, 16, 17	141.13	–	–	11, 15, 17
14	131.56	7.31	15, 16, 17	15, 16	131.19	7.47	15, 16	16
15	126.62	7.17	14, 16, 17	16, 17	128.02	7.19	14, 16, 17	17
16	127.42	6.18	14, 15, 17	14	127.52	6.74	14, 15, 17	14
17	131.80	5.68	14, 15, 16	15, 16	131.52	5.46	15, 16	15
18	141.11	–	–	14, 16, 20	140.84	–	–	14, 16, 20
19	138.55	–	–	17, 20	138.25	–	–	17, 25
20	130.24	6.00	21	20, 21	131.42	6.01	24, 25	21
20'	132.31	–	–	20, 21, 22	132.39	–	–	22, 24, 25
21	128.04	7.22	20, 22	20, 22	128.80	7.27	22, 23	20, 23
22	124.55	7.31	21	21	124.96	7.42	21, 24	24
23	–	–	–	–	125.58	7.48	21, 24	21
24	–	–	–	–	127.05	7.78	20, 22, 23	22, 25
24'	–	–	–	–	132.31	–	–	20, 21, 23
25	–	–	–	–	130.62	7.47	20	24
26	–	–	–	–	139.52	–	–	20, 28
27	–	–	–	–	140.97	–	–	25, 29, 31
28	–	–	–	–	132.50	5.86	29, 30	30
29	–	–	–	–	125.65	6.41	28, 30, 31	31
30	–	–	–	–	125.54	6.76	28, 29, 31	28
31	–	–	–	–	132.07	6.46	29, 30	29
32	–	–	–	–	136.96	–	–	28, 30, 34
33	–	–	–	–	136.11	–	–	31, 39
34	–	–	–	–	131.17	6.77	38, 39	35
34'	–	–	–	–	131.55	–	–	36, 38, 39
35	–	–	–	–	127.66	6.79	36, 37, 39	34, 37
36	–	–	–	–	125.58	7.11	35, 37, 38	38
37	–	–	–	–	125.93	7.34	35, 36, 38	35
38	–	–	–	–	127.23	7.77	34, 36, 37	36, 39
38'	–	–	–	–	131.89	–	–	34, 35, 37
39	–	–	–	–	129.24	7.72	34, 35	38
40	–	–	–	–	139.89	–	–	34
41	–	–	–	–	141.36	–	–	39, 43, 43'
42	–	–	–	–	130.38	6.30 (br)	ND	44
42'	–	–	–	–	130.38	6.30 (br)	ND	44
43	–	–	–	–	127.23	7.23	ND	43'
43'	–	–	–	–	127.23	7.23	ND	43
44	–	–	–	–	126.33	7.28	ND	ND

^[a] ND = not determined. ^[b] Numbers indicate the hydrogen(s) that is/are correlated to the carbon signal in the row.

Table S25. Summary of 2D NMR data for **F-Ar-3-AAAA** and **F-Ar-3-AAAB** in CDCl₃ at 0 °C.^[a]

Atom #	F-Ar-3-AAAA				F-Ar-3-AAAB			
	δ_c [ppm]	δ_H [ppm]	COSY	HMBC ^[b]	δ_c [ppm]	δ_H [ppm]	COSY	HMBC ^[b]
1	140.33	–	–	3, 4, 6	140.31	–	–	3', 3, 6
2	127.94	6.08	3, 4	2', 4	128.46	6.39	3', 4	2', 4, 5
2'	127.94	6.08	3', 4	2, 4	128.46	6.39	3', 4	2, 4, 5
3	127.45	6.59	2, 4	3'	127.73	6.79	4	3'
3'	127.45	6.59	2', 4	3	127.73	6.79	2'	3
4	125.92	6.92	2, 2', 3, 3'	2, 2'	126.41	7.07	2', 3	2, 2'
5	138.72	–	–	2, 2', 11	139.23	–	–	2, 2', 11
6	127.41	7.20	7, 10, 11	7	127.58	7.42	7, 10, 11	7
6'	129.08	–	–	10, 11	129.49	–	–	10
7	113.05	7.42	6, 11	6, 10	113.32	7.53	6, 11	6
8	149.80	–	–	10	150.08 ^[c]	–	–	7, 10
9	149.80	–	–	7	150.08 ^[c]	–	–	7, 10
10	113.78	7.28	6, 11	7, 11	113.66	7.33	6, 11	11
10'	129.70	–	–	6, 7	129.05	–	–	6, 7
11	129.82	6.85	6, 7, 10	10	131.46	6.95	6, 7, 10, 11	10
12	139.14	–	–	6, 14, 17	138.63	–	–	6
13	138.64	–	–	11, 15	140.53	–	–	11, 17
14	131.71	7.27	15, 16, 17	15, 16, 17	131.22	7.42	16, 17	16
15	127.1	7.20	14, 16, 17	17	128.55	7.20	17	17
16	127.6	6.28	14, 15, 17	14, 17	127.94	6.75	14, 17	14
17	131.49	5.67	14, 15, 16	14, 16	131.24	5.41	14, 15, 16	–
18	140.49	–	–	14, 16, 20	140.07	–	–	14, 16, 20
19	138.63	–	–	17, 20	138.52	–	–	17, 25
20	129.58	5.93	21	21	130.74	5.93	21, 24, 25	21
20'	128.94	–	–	20, 21	129.03	–	–	24, 25
21	113.27	6.94	20	20, 21	114.14	7.00	20, 25	20
22	149.28	–	–	21	149.59 ^[c]	–	–	21, 24
23	–	–	–	–	150.01 ^[c]	–	–	21, 24
24	–	–	–	–	112.69	7.50	25, 20	25
24'	–	–	–	–	128.87	–	–	21
25	–	–	–	–	129.87	7.39	20, 21, 24	24
26	–	–	–	–	139.73	–	–	20, 28
27	–	–	–	–	140.26	–	–	25, 29, 31
28	–	–	–	–	132.13	5.81	29, 30	30
29	–	–	–	–	125.80	6.45	28, 30, 31	31
30	–	–	–	–	126.03	6.77	28, 29, 31	28
31	–	–	–	–	132.15	6.43	29, 30	29
32	–	–	–	–	136.57	–	–	28, 30, 34
33	–	–	–	–	136.26	–	–	31, 39
34	–	–	–	–	130.14	6.59	35, 38, 39	35
34'	–	–	–	–	128.16	–	–	34, 38, 39
35	–	–	–	–	112.91	6.51	34, 39	34
36	–	–	–	–	149.78 ^[c]	–	–	35, 38
37	–	–	–	–	150.13 ^[c]	–	–	35, 38
38	–	–	–	–	112.97	7.48	34, 39	39
38'	–	–	–	–	128.64	–	–	34, 35
39	–	–	–	–	128.57	7.61	34, 35, 38	38
40	–	–	–	–	138.73	–	–	34
41	–	–	–	–	140.56	–	–	39
42	–	–	–	–	130.16	6.21	–	44
42'	–	–	–	–	130.16	6.21	–	44
43	–	–	–	–	127.90	7.23	–	–
43'	–	–	–	–	127.90	7.23	–	–
44	–	–	–	–	126.78	7.27	–	42, 42'

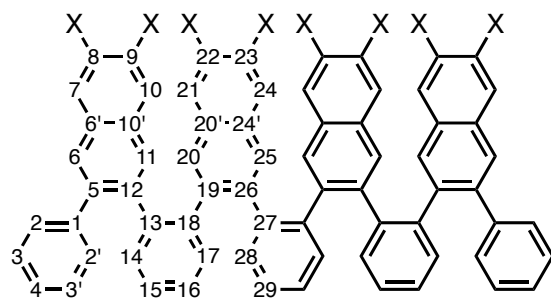
^[a] ND = not determined. ^[b] Numbers indicate the hydrogen(s) that is/are correlated to the carbon signal in the row.^[c] Assignment may be reversed between C8 & C9, similarly for C22 & C23, and similarly for C36 & C37.

Table S26. Summary of 2D NMR data for **Cl-Ar-3-AAAA** and **Cl-Ar-3-AAAB** in CDCl₃ at 0 °C.^[a]

Atom #	Cl-Ar-3-AAAA				Cl-Ar-3-AAAB			
	δ_c [ppm]	δ_H [ppm]	COSY	HMBC ^[b]	δ_c [ppm]	δ_H [ppm]	COSY	HMBC ^[b]
1	140.14	–	–	3, 4, 6	140.10	–	–	3', 3, 6
2	127.90	6.07	3, 4	2', 4	128.48	6.39	3, 4	2', 4
2'	127.90	6.07	3', 4	2, 4	128.48	6.39	3', 4	2, 4
3	127.55	6.59	2, 4	3'	127.82	6.81	2, 4	3'
3'	127.55	6.59	2', 4	3	127.82	6.81	2', 4	3
4	126.18	6.95	2, 2', 3, 3'	2, 2'	126.65	7.11	2, 2', 3, 3'	2, 2'
5	139.59	–	–	2, 2', 11	140.08	–	–	2, 2', 11
6	127.05	7.18	7, 10, 11	7	127.23	7.39	7, 10, 11	7
6'	131.28	–	–	6, 10, 11	131.63	–	–	8', 10, 11
7	128.40	7.80	6, 10, 11	6, 10, 11	128.62	7.91	6, 10, 11	6, 9'
8	129.78	–	–	7, 10	130.31 ^[c]	–	–	7, 10
9	129.56	–	–	7, 10	130.06 ^[c]	–	–	7, 10
10	129.12	7.66	6, 7, 11	7, 11	128.89	7.70	6, 7, 11	11
10'	131.84	–	–	6, 7, 11	131.11	–	–	6, 7, 9'
11	129.49	6.81	6, 7, 10	6, 10	131.04	6.91	6, 7, 10	10
12	140.02	–	–	6, 14	139.45	–	–	6, 14
13	138.49	–	–	11, 15, 16, 17	140.36	–	–	11, 15, 17
14	131.69	7.27	15, 16, 17	15, 16	131.20	7.42	15, 16	12, 18
15	127.33	7.22	14, 16, 17	17	128.68	7.21	14, 16, 17	–
16	127.86	6.28	14, 15, 17	14	128.09	6.77	14, 15, 17	–
17	131.44	5.65	14, 15, 16	15, 16	131.18	5.43	15, 16	–
18	140.29	–	–	14, 16, 20	139.86	–	–	14, 16
19	139.52	–	–	17, 20	139.27	–	–	25
20	129.33	5.90	21	20, 21	130.54	5.90	21, 24, 25	21
20'	131.10	–	–	20, 21	131.15	–	–	24, 25
21	128.77	7.33	20	20	129.63	7.37	20, 24	20
22	128.88	–	–	21	130.15 ^[c]	–	–	21, 24
23	–	–	–	–	129.57 ^[c]	–	–	21, 24
24	–	–	–	–	128.08	7.88	20, 21, 25	25
24'	–	–	–	–	131.06	–	–	21
25	–	–	–	–	129.50	7.36	20, 24	–
26	–	–	–	–	140.60	–	–	20, 28
27	–	–	–	–	140.06	–	–	25
28	–	–	–	–	132.36	5.80	29, 30, 31	29
29	–	–	–	–	126.06	6.47	28, 30, 31	31
30	–	–	–	–	126.21	6.80	28, 29, 31	28
31	–	–	–	–	132.23	6.43	28, 29, 30	29, 30
32	–	–	–	–	136.41	–	–	28, 34
33	–	–	–	–	137.26	–	–	39
34	–	–	–	–	129.75	6.60	38, 39	35
34'	–	–	–	–	130.36	–	–	38, 39
35	–	–	–	–	128.15	6.96	38, 39	34
36	–	–	–	–	129.94 ^[c]	–	–	35, 38
37	–	–	–	–	130.34 ^[c]	–	–	35, 38
38	–	–	–	–	128.28	7.87	34, 35, 39	39
38'	–	–	–	–	130.85	–	–	34, 35
39	–	–	–	–	128.31	7.60	34, 35, 38	–
40	–	–	–	–	141.20	–	–	34
41	–	–	–	–	ND	–	–	39
42	–	–	–	–	130.09	6.21	43'	44
42'	–	–	–	–	ND	ND	–	–
43	–	–	–	–	ND	ND	–	–
43'	–	–	–	–	ND	6.65	42'	–
44	–	–	–	–	126.95	7.29	–	42'

^[a] ND = not determined. ^[b] Numbers indicate the hydrogen(s) that is/are correlated to the carbon signal in the row.^[c] Assignment may be reversed between C8 & C9, similarly for C22 & C23, and similarly for C36 & C37.

9.2 NMR Assignment of Conformers AAAA of X-Ar-4



H-Ar-4 X = H

F-Ar-4 X = F

Cl-Ar-4 X = Cl

Figure S69. Atom numbering of **X-Ar-4** for conformers AAAA.

Table S27. Summary of 2D NMR data for **H-Ar-4-AAAA** in CDCl₃ at 0 °C.^[a]

Atom #	δ_c [ppm]	δ_H [ppm]	COSY	HMBC ^[b]	NOE
1	141.00	–	–	3, 3', 6	–
2	128.08	6.05	3, 4	2', 4	6
2'	128.08	6.05	3', 4	2, 4	6
3	127.23	6.52	2, 4	3'	–
3'	127.23	6.52	2', 4	3	–
4	125.45	6.86	2, 2', 3, 3'	2, 2'	–
5	138.32	–	–	2, 2', 11	–
6	127.82	7.19	7	–	2, 2', 7
6'	132.22	–	–	6, 11	–
7	127.28	7.63	6, 8, 11	6	6
8	125.35	7.36	7	10	–
9	125.03	7.35	–	7	–
10	128.51	7.35	–	11	11
10'	132.75	–	–	6, 7, 11	–
11	130.26	6.61	7	–	10, 14
12	138.80	–	–	6, 14	–
13	138.51	–	–	11, 15, 17	–
14	131.20	7.08	15, 16, 17	16	11
15	126.23	6.89	14, 16, 17	17	–
16	127.19	5.74	14, 15, 17	14	–
17	131.03	5.51	14, 15, 16	15	20
18	140.96	–	–	14, 16, 20	–
19	138.22	–	–	17, 25	17, 21
20	130.37	5.92	21, 24, 25	21	–
20'	132.37	–	–	20, 25	–
21	128.19	7.21	20, 23, 25	20	20
22	124.36	7.31	21	24	–
23	124.60	7.36	21	21	–
24	127.97	7.36	20	22, 25	–
24'	132.84	–	–	20, 21, 25	25
25	129.77	6.46	20, 21	–	24, 28
26	139.51	–	–	20, 28	–
27	139.23	–	–	25, 28	–
28	131.61	5.67	29	29	25
29	126.69	5.83	28	28	–

^[a] ND = not determined. ^[b] Numbers indicate the hydrogen(s) that is/are correlated to the carbon signal in the row.

Table S28. Summary of 2D NMR data for **F-Ar-4-AAAA** in CDCl₃ at 0 °C.^[a]

Atom #	δ_c [ppm]	δ_H [ppm]	COSY	HMBC ^[b]	NOE
1	140.30	–	–	3, 3', 6	–
2	127.90	6.00	3	2', 4	6
2'	127.90	6.00	3'	2, 4	6
3	127.41	6.55	2, 4	3'	–
3'	127.41	6.55	2', 4	3	–
4	125.87	6.89	3, 3'	2, 2'	–
5	138.36	–	–	2, 2', 11	–
6	127.23	7.12	7, 10, 11	7	2, 2', 7
6'	128.90	–	–	10, 11	–
7	112.92	7.35	6, 11	6	6
8	149.62	–	–	7, 10	–
9	149.75	–	–	7, 10	–
10	113.72	7.05	6, 11	11	11
10'	129.47	–	–	6, 7	–
11	129.35	6.50	6, 7, 10	10	10
12	138.78	–	–	6, 14	–
13	138.09	–	–	11, 15, 17	–
14	131.39	7.05	15, 16	16	–
15	126.74	6.94	14, 16, 17	17	–
16	127.34	5.89	14, 15, 17	14	–
17	130.84	5.51	15, 16	15	20
18	140.26	–	–	14, 16, 20	–
19	138.26	–	–	17, 25	–
20	129.80	5.85	21, 24, 25	21	17, 21
20'	128.99	–	–	24, 25	–
21	113.39	6.93	20, 25	20	–
22	149.21	–	–	21, 24	–
23	149.38	–	–	21, 24	–
24	113.16	7.09	20, 25	25	25
24'	129.41	–	–	20, 21	–
25	128.92	6.36	20, 21, 24	24	24, 28
26	139.42	–	–	20, 28	–
27	138.82	–	–	25, 28, 29	–
28	131.53	5.65	29	29	25
29	126.83	5.94	–	28	–

^[a] ND = not determined. ^[b] Numbers indicate the hydrogen(s) that is/are correlated to the carbon signal in the row.

Table S29. Summary of 2D NMR data for **Cl-Ar-4-AAAA** in CDCl₃ at 0 °C.^[a]

Atom #	δ_c [ppm]	δ_H [ppm]	COSY	HMBC ^[b]	NOE
1	140.15	–	–	3, 3', 6	–
2	127.88	6.01	3, 4	2', 4	6, 14
2'	127.88	6.01	3', 4	2, 4	6, 14
3	127.52	6.58	2, 4	3'	
3'	127.52	6.58	2', 4	3	
4	126.14	6.94	2, 2', 3, 3'	2, 2'	
5	139.27	–	–	2, 2', 11	–
6	127.00	7.11	7, 10, 11	7	2, 2', 7
6'	131.12	–	–	10, 11	–
7	128.30	7.75	6, 10, 11	6	6
8	129.72	–	–	7, 10	–
9	129.52	–	–	7, 10	–
10	128.98	7.46	6, 7, 11	11	11, 29
10'	131.59	–	–	6, 7	–
11	128.96	6.48	6, 7, 10	10	10, 14, 28
12	139.64	–	–	6, 14	–
13	137.93	–	–	11, 15, 17	–
14	131.45	7.06	15, 16	16	2, 2', 11
15	127.00	6.96	14, 16, 17	17	
16	127.63	5.89	14, 15, 17	14	
17	130.70	5.52	15, 16	15	20
18	140.05	–	–	14, 16, 20	–
19	139.13	–	–	17, 25	–
20	129.56	5.84	21, 24, 25	21	17, 21
20'	131.18	–	–	24, 25	–
21	128.94	7.34	20, 24, 25	20	20
22	128.78	–	–	21, 24	–
23	129.04	–	–	21, 24	–
24	128.73	7.51	20, 21, 25	25	25
24'	131.61	–	–	20, 21	–
25	128.73	6.37	20, 21, 24	24	24, 28
26	140.35	–	–	20, 28	–
27	138.74	–	–	25, 28, 29	–
28	131.54	5.68	29	29	11, 25, 29
29	127.17	6.02	28	28	10, 28

^[a] ND = not determined. ^[b] Numbers indicate the hydrogen(s) that is/are correlated to the carbon signal in the row.

9.3 NMR Assignment of Folded Conformer (AAA...A) of F-Ar-5 and F-Ar-6

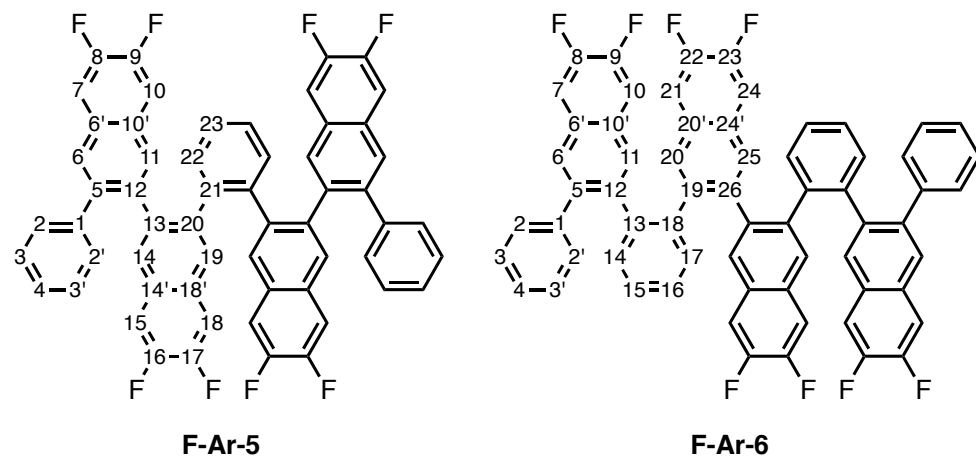


Figure S70. Atom numbering of **X-Ar-4**, **F-Ar-5**, and **F-Ar-6** for conformers AAAA.

Table S30. Summary of 2D NMR data for **F-Ar-5-AAAA** in CDCl₃ at 0 °C.^[a]

Atom #	δ_c [ppm]	δ_H [ppm]	COSY	HMBC ^[b]	NOE
1	140.07	–	–	3, 6	–
2	127.99	6.27	3, 4	2', 4	6, 14
2'	127.99	6.27	3', 4	2, 4	6, 14
3	217.81	6.80	2, 4	3'	–
3'	127.81	6.80	2', 4	3	–
4	126.03	6.98	2, 2', 3, 3'	2, 2'	–
5	138.36	–	–	11	–
6	127.56	7.32	7, 10, 11	7	2, 2', 7
6'	128.77	–	–	10, 11	–
7	112.53	7.43	6, 11	6	6
8	150.20	–	–	7, 10	–
9	149.65	–	–	7, 10	–
10	112.13	6.43	6, 11	11	11
10'	129.36	–	6, 7, 10	6, 7	–
11	129.10	–	–	10	10, 14
12	138.72	–	–	6, 14	–
13	138.48	–	–	11, 19	–
14	129.27	7.63	18, 19	15	2, 2', 15, 11
14'	128.62	–	–	18, 19	–
15	112.41	7.54	19	14	14
16	150.24	–	–	15, 18	–
17	149.85	–	–	15, 18	–
18	112.34	6.36	14, 19	19	19
18'	129.78	–	–	14, 15	–
19	129.32	6.19	14, 15, 18	18	18, 22
20	140.47	–	–	14, 22	–
21	138.50	–	–	19, 22	–
22	131.59	5.70	23	23	19, 23
23	127.26	6.64	22	22	22

^[a] ND = not determined. ^[b] Numbers indicate the hydrogen(s) that is/are correlated to the carbon signal in the row.

Table S31. Summary of 2D NMR data for **F-Ar-6-AAAAA** in CDCl₃ at 0 °C.^[a]

Atom #	δ_c [ppm]	δ_H [ppm]	COSY	HMBC ^[b]	NOE
1	140.17	–		6	–
2	127.66	6.05	3, 4	2', 4	6
2'	127.66	6.05	3', 4	2	6
3	127.45	6.52	2, 4		–
3'	127.45	6.52	2', 4		–
4	125.94	6.88	2, 2', 3, 3'	2	–
5	138.27	–		2, 11	–
6	127.16	7.13	7, 10, 11	7	2, 2', 7
6'	128.48	–		10, 11	–
7	112.37	7.32	6, 11	6	6
8	149.54	–		7, 10	–
9	149.98	–		7, 10	–
10	112.07	6.19	6, 11	11	11
10'	129.15	–		6, 7	–
11	128.92	6.31	6, 7, 10	10	10, 14, 17
12	138.95	–		6, 14	–
13	138.23	–		15, 17	–
14	131.52	7.12	15, 16	15, 16	11
15	126.89	7.27	14, 16, 17	17	–
16	128.81	6.99	14, 15, 17	14	–
17	131.19	6.23	15, 16	15	11, 20
18	140.54	–	–	14, 16, 20	–
19	138.48	–	–	17, 25	–
20	130.21	6.14	21, 24, 25	21	17, 21
20'	128.90	–	–	24, 25	–
21	112.89	7.00	20, 25	20	20
22	149.44	–	–	21, 24'	–
23	149.68	–	–	21, 24	–
24	111.79	6.27	20, 25	25	25
24'	128.99	–	–	21	–
25	128.62	6.03	20, 21, 24	24	24
26	138.66	–	–	20, 25	–

^[a] ND = not determined. ^[b] Numbers indicate the hydrogen(s) that is/are correlated to the carbon signal in the row.

9.4 *n*Oe Correlations Illustrated on DFT Computed 3-D Structures for X-Ar-3

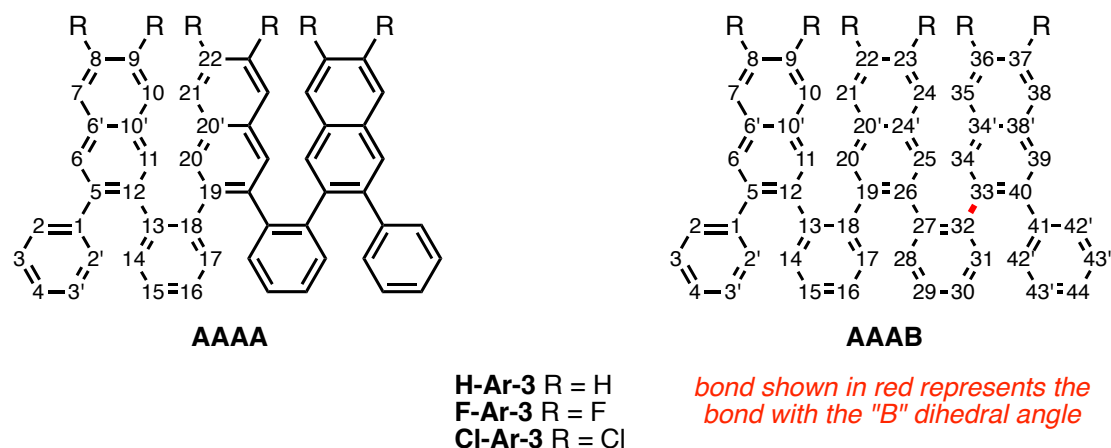


Figure S71. Atom numbering of **X-Ar-3** for conformers AAAA and AAAB.

Table S32. Selected Interatomic Distance in M06-2X/6-31G Optimized Structures Relevant to ROSEY Analysis.

Structure	Selected Interatomic Distance in M06-2X/6-31G Optimized Structures [Å]					
	H(11)–H(14)	H(11)–(20)	H(17)–H(20)	H(25)–H(28)	H(25)–H(34)	H(31)–H(34)
H-Ar-3-AAAA	2.48 [✓]	6.25 [✗]	2.38 [✓]	NA	NA	NA
F-Ar-3-AAAA	2.47 [✓]	6.25 [✗]	2.40 [✓]	NA	NA	NA
Cl-Ar-3-AAAA	2.49 [✓]	6.24 [✗]	2.41 [✓]	NA	NA	NA
H-Ar-3-AAAB	2.60 [✓]	6.15 [✗]	2.65 [✓]	2.65 [✓]	3.06 [✓]	4.25 [ND]
F-Ar-3-AAAB	2.60 [✓]	6.14 [ND]	2.63 [✓]	2.61 [✓]	3.07 [✓]	4.27 [✗]
Cl-Ar-3-AAAB	2.61 [✓]	6.13 [✗]	2.64 [✓]	2.59 [✓]	3.11 [✓]	4.28 [✗]

[✓] = observed associated signal in ROSEY spectra.

[✗] = did not observe associated signal in ROSEY spectra.

[ND] = absence or presence of signal in ROSEY spectra could not be determined due to overlapping neighboring signal.

NA = not applicable.

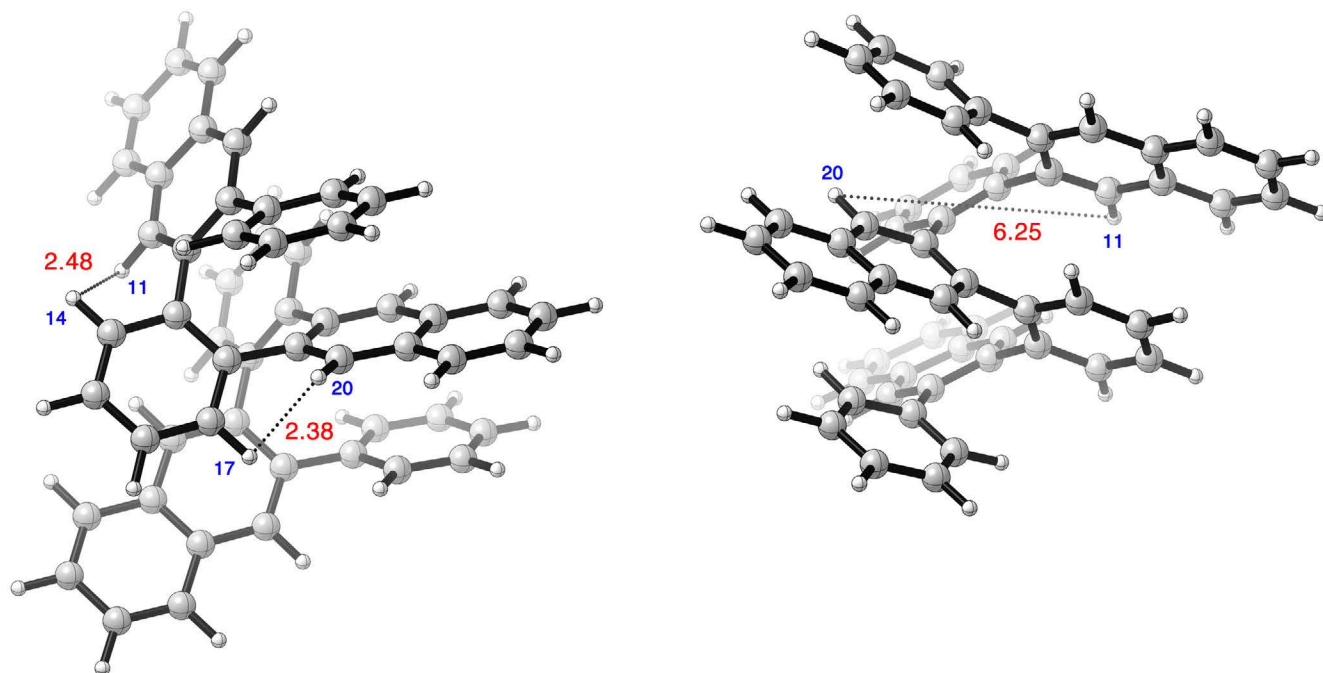


Figure S73. Conformer AAAA of **H-Ar-3** from M06-2X/6-31G calculations illustrating selected non-bonding distances (in Å, numbers in red) associated with nOe signals that are: (left) observed, (right) not observed. Numbers in blue corresponding to the atom numbering scheme illustrated in Figure S71.

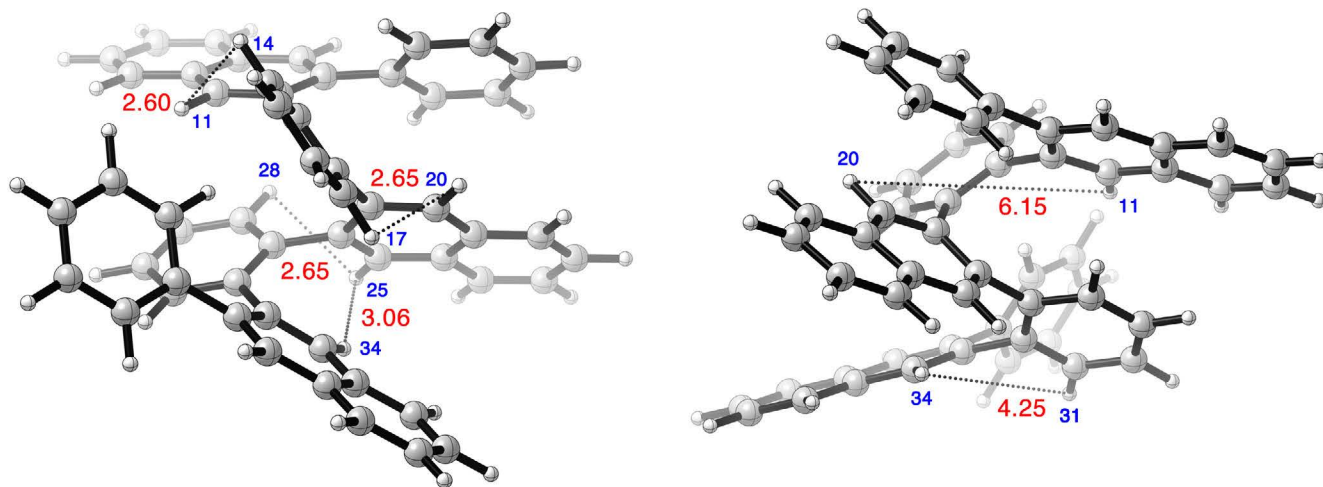


Figure S74. Conformer AAAB of **H-Ar-3** from M06-2X/6-31G calculations illustrating selected non-bonding distances (in Å, numbers in red) associated with nOe signals that are: (left) observed and (right) not observed. Numbers in blue corresponding to the atom numbering scheme illustrated in Figure S71.

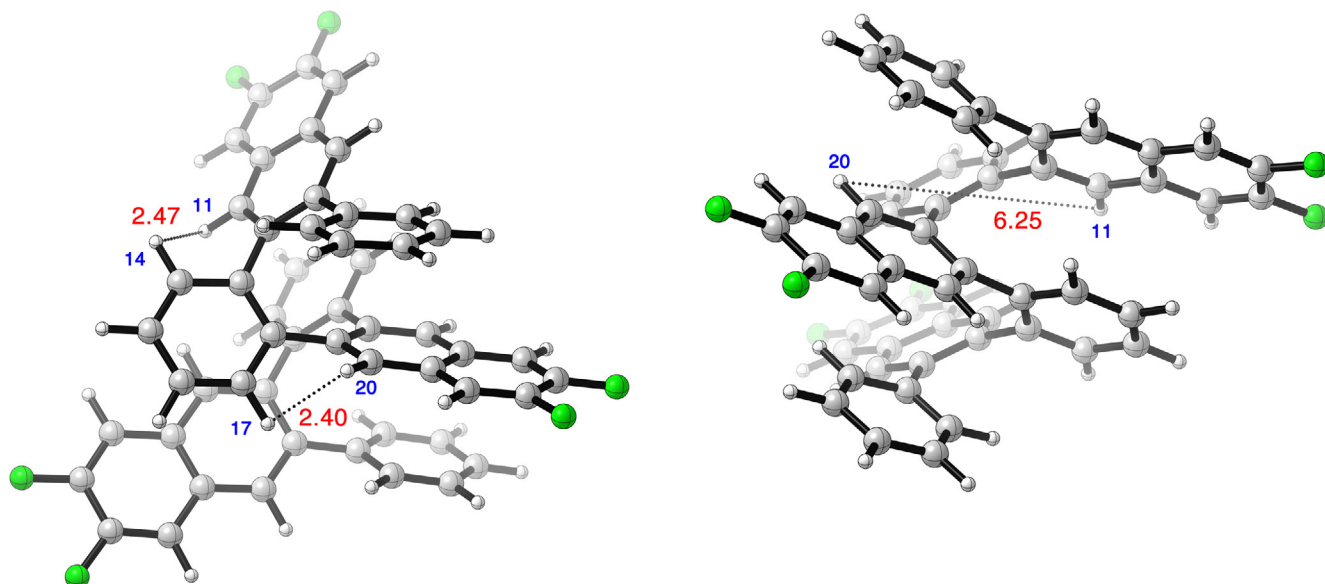


Figure S75. Conformer AAAA of **F-Ar-3** from M06-2X/6-31G calculations illustrating selected non-bonding distances (in Å, numbers in red) associated with nOe signals that are: (left) observed and (right) not observed. Numbers in blue corresponding to the atom numbering scheme illustrated in Figure S71.

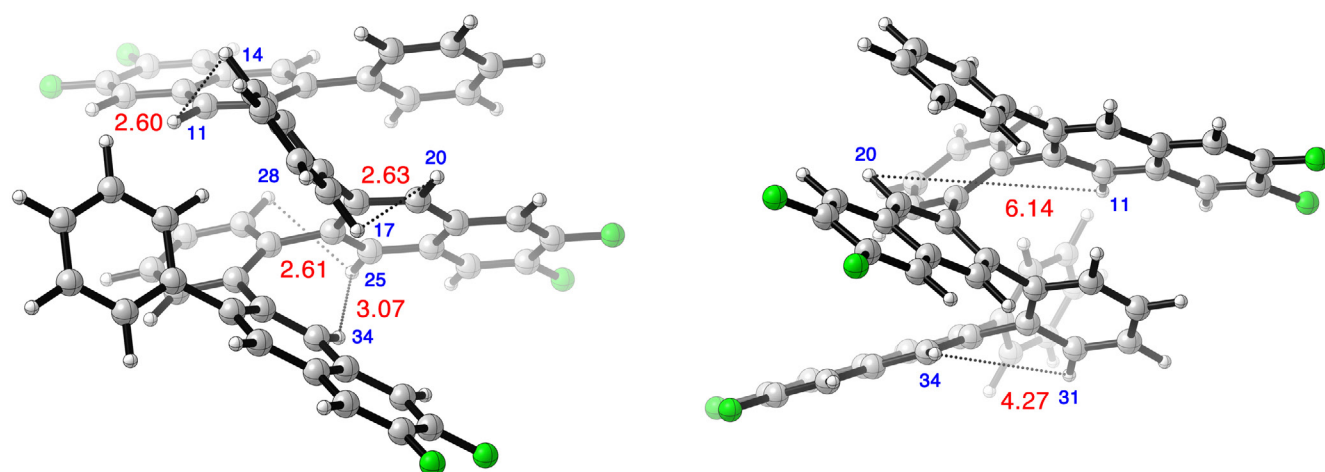


Figure S76. Conformer AAAB of **F-Ar-3** from M06-2X/6-31G calculations illustrating selected non-bonding distances (in Å, numbers in red) associated with nOe signals that are: (left) observed and (right) not observed. Numbers in blue corresponding to the atom numbering scheme illustrated in Figure S71.

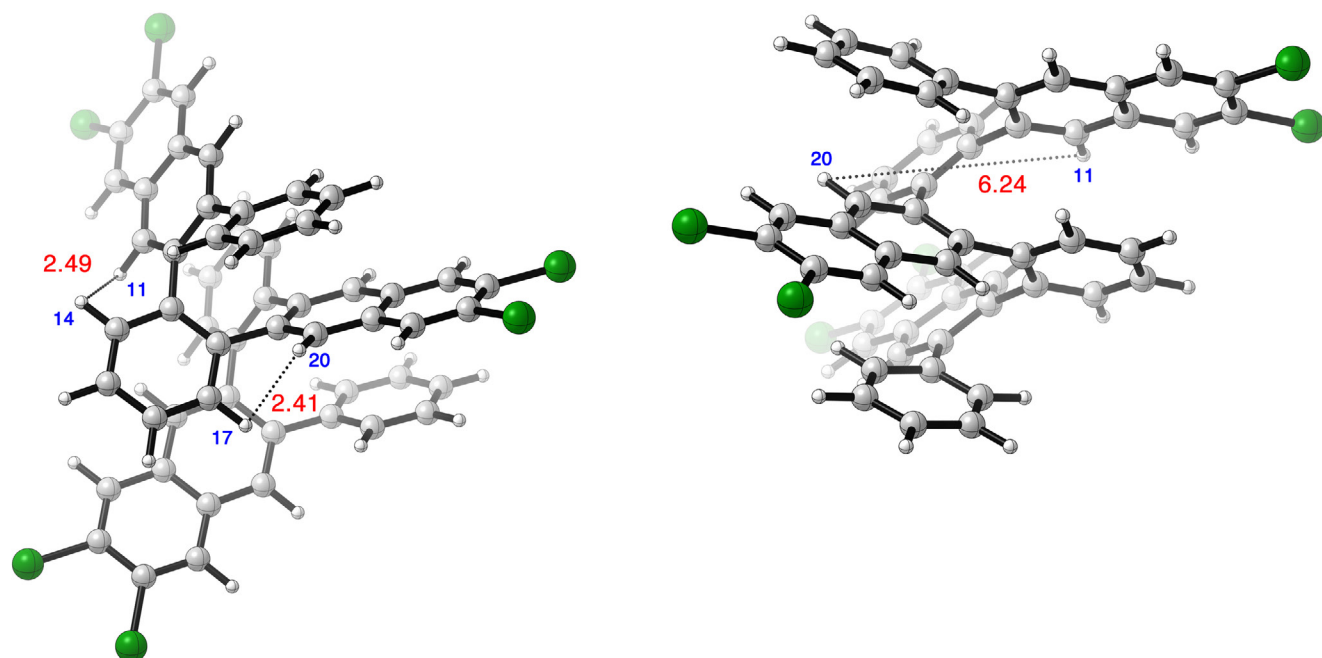


Figure S77. Conformer AAAA of **Cl-Ar-3** from M06-2X/6-31G calculations illustrating selected non-bonding distances (in Å, numbers in red) associated with nOe signals that are: (left) observed and (right) not observed. Numbers in blue corresponding to the atom numbering scheme illustrated in Figure S71.

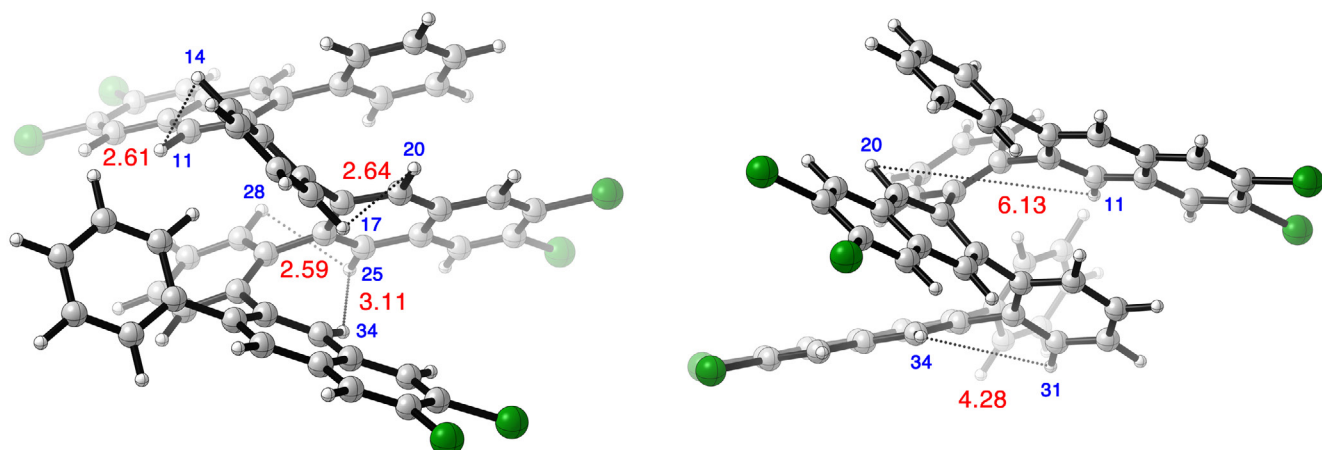


Figure S78. Conformer AAAB of **Cl-Ar-3** from M06-2X/6-31G calculations illustrating selected non-bonding distances (in Å, numbers in red) associated with nOe signals that are: (left) observed and (right) not observed. Numbers in blue corresponding to the atom numbering scheme illustrated in Figure S71.

9.4.1 ROSEY NMR Spectra of X-Ar-3 Relevant to Conformational Assignment

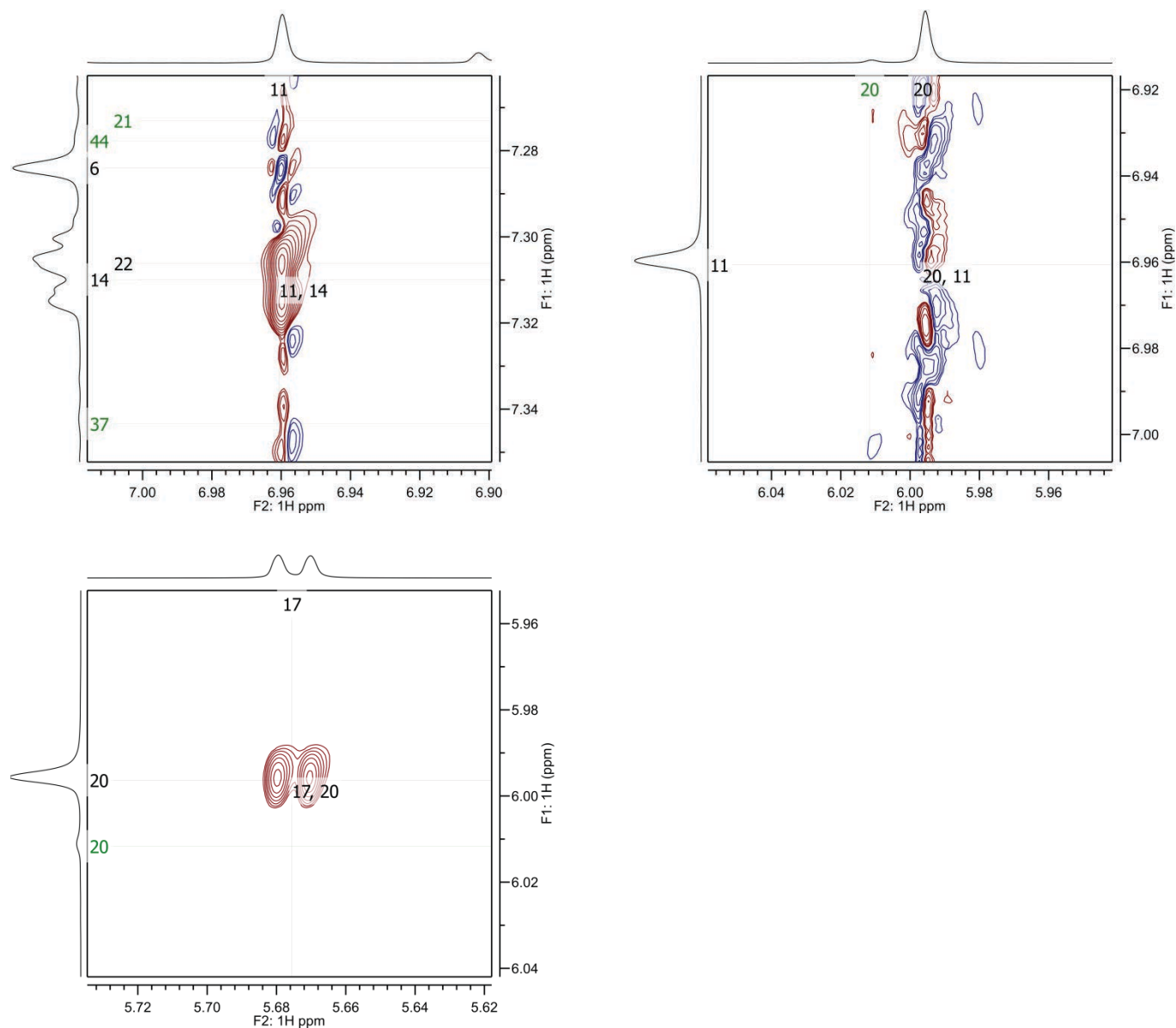


Figure S78. Selected expansions of the ROSEY NMR spectra (800 MHz) of **H-Ar-3** illustrating presence or absence of correlations listed in Table S31 for conformer AAAA. The numbers in black and green correspond to the atom numbers of the major and minor conformers, respectively, as defined in Figure S71.

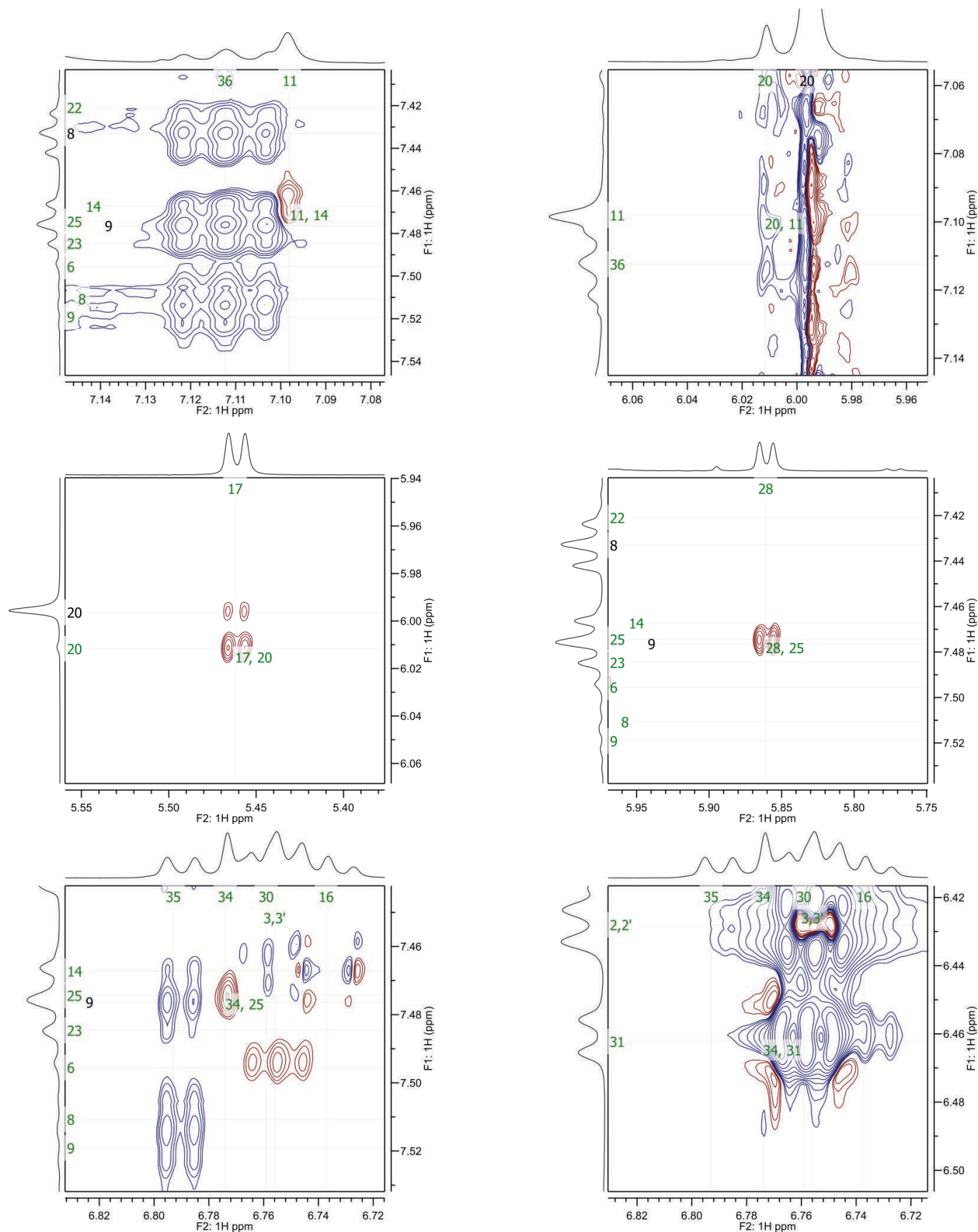


Figure S80. Selected expansions of the ROSEY NMR spectra (800 MHz) of **H-Ar-3** illustrating presence or absence of correlations listed in Table S31 for conformer AAAB. The numbers in black and green correspond to the atom numbers of the major and minor conformers, respectively, as defined in Figure S71.

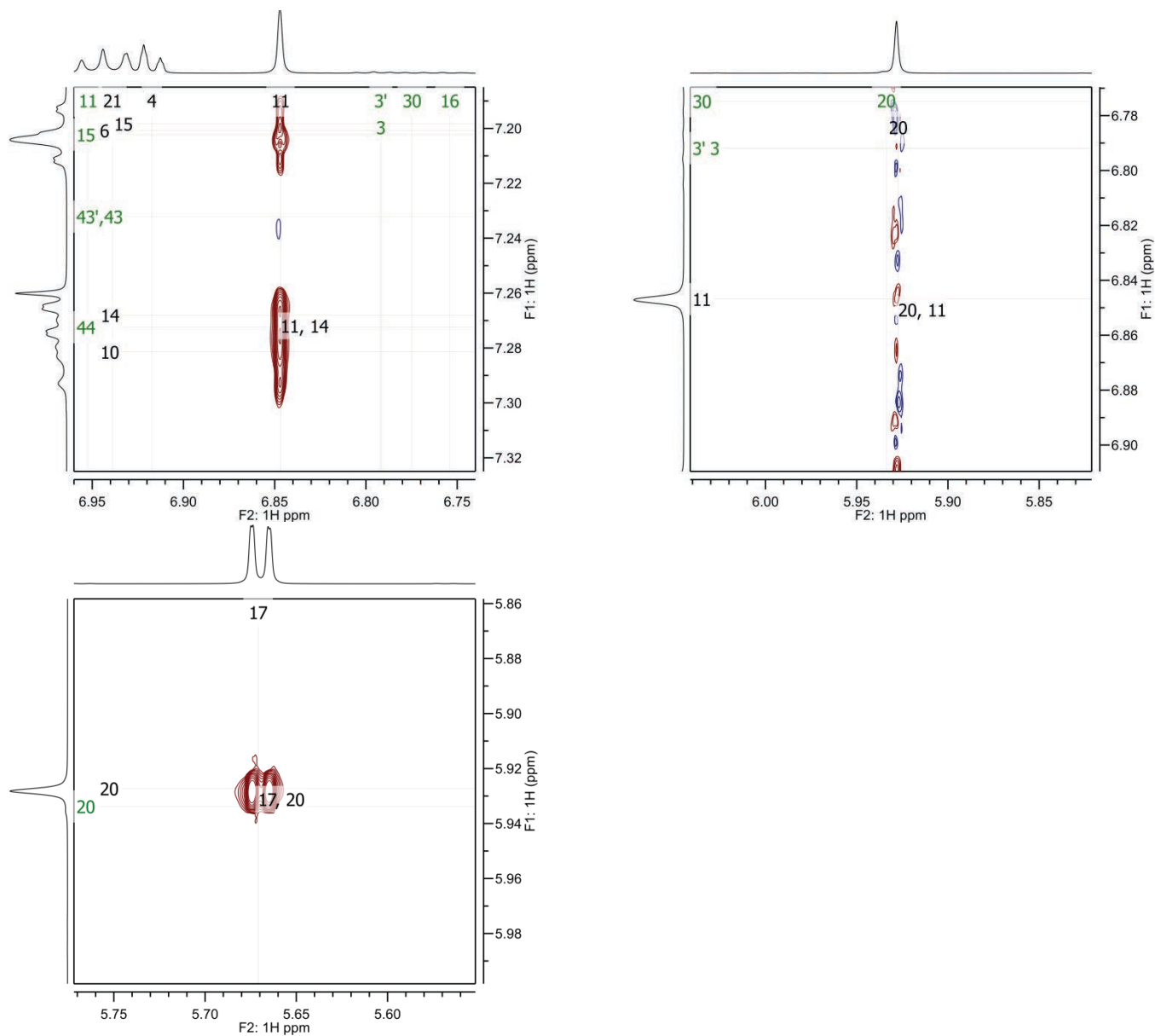


Figure S81. Selected expansions of the ROSEY NMR spectra (800 MHz) of **F-Ar-3** illustrating presence or absence of correlations listed in Table S31 for conformer AAAA. The numbers in black and green correspond to the atom numbers of the major and minor conformers, respectively, as defined in Figure S71.

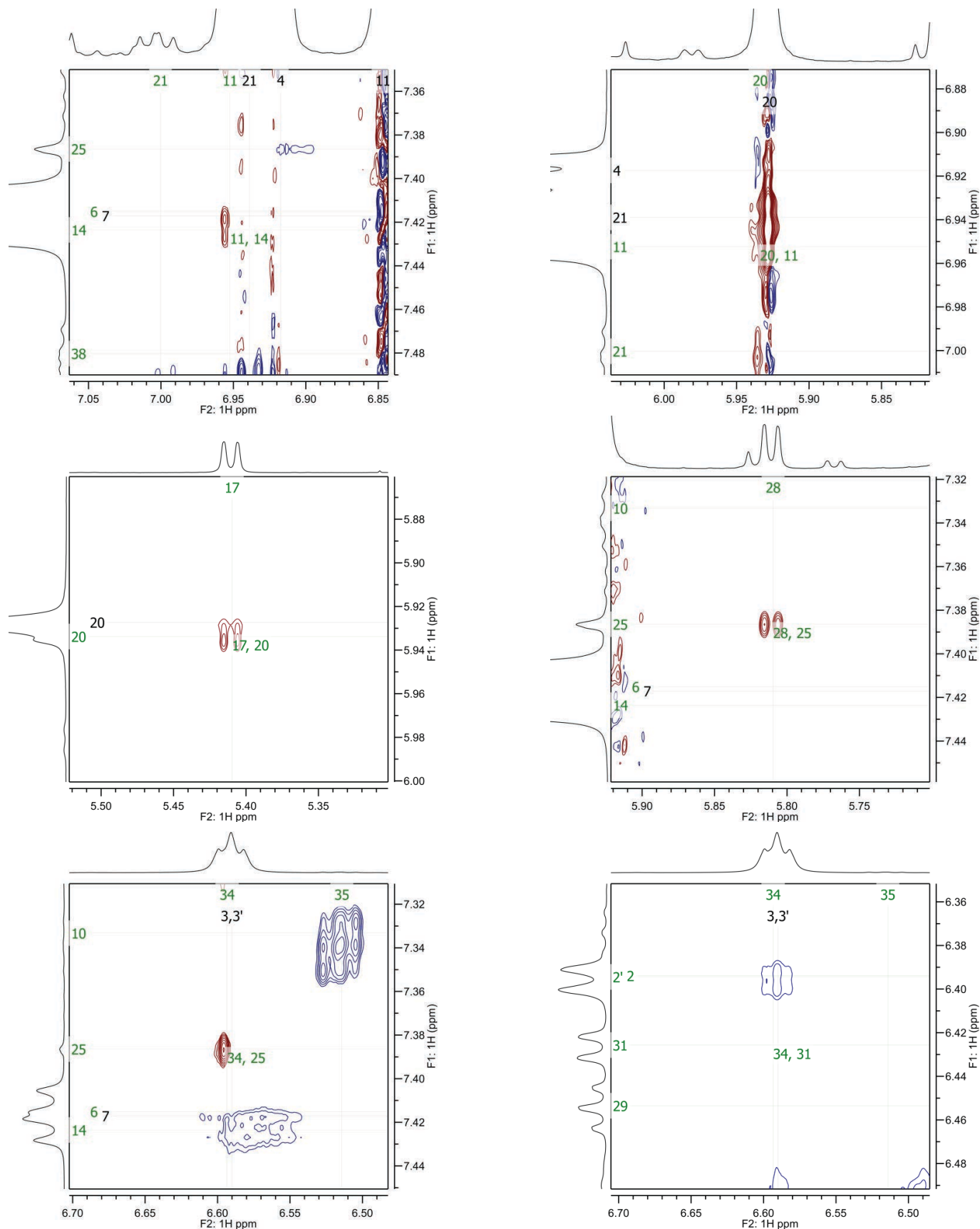


Figure S82. Selected expansions of the ROSEY NMR spectra (800 MHz) of **F-Ar-3** illustrating presence or absence of correlations listed in Table S31 for conformer AAAB. The numbers in black and green correspond to the atom numbers of the major and minor conformers, respectively, as defined in Figure S71.

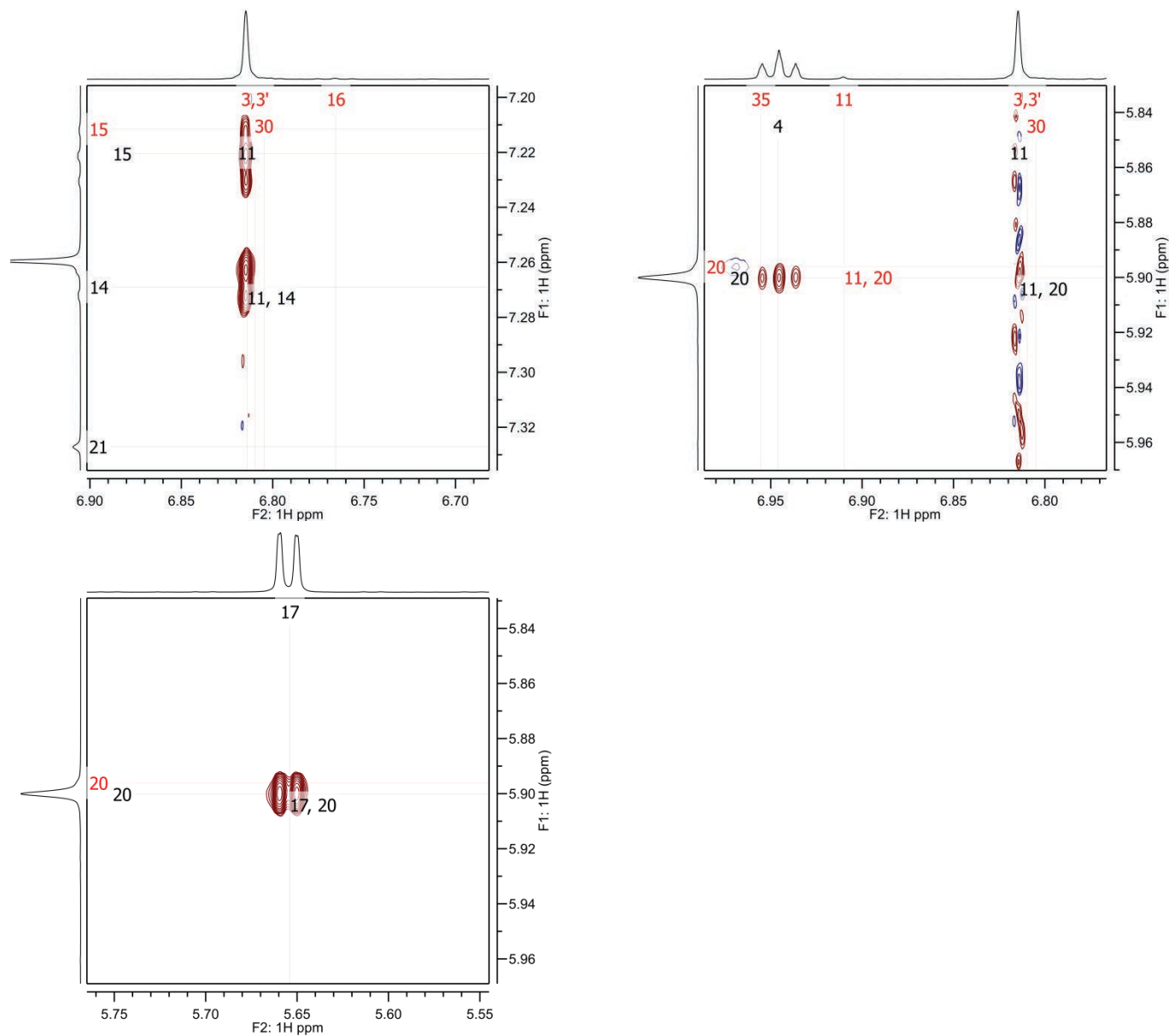


Figure S83. Selected expansions of the ROSEY NMR spectra (800 MHz) of **Cl-Ar-3** illustrating presence or absence of correlations listed in Table S31 for conformer AAAA. The numbers in black and red correspond to the atom numbers of the major and minor conformers, respectively, as defined in Figure S71.

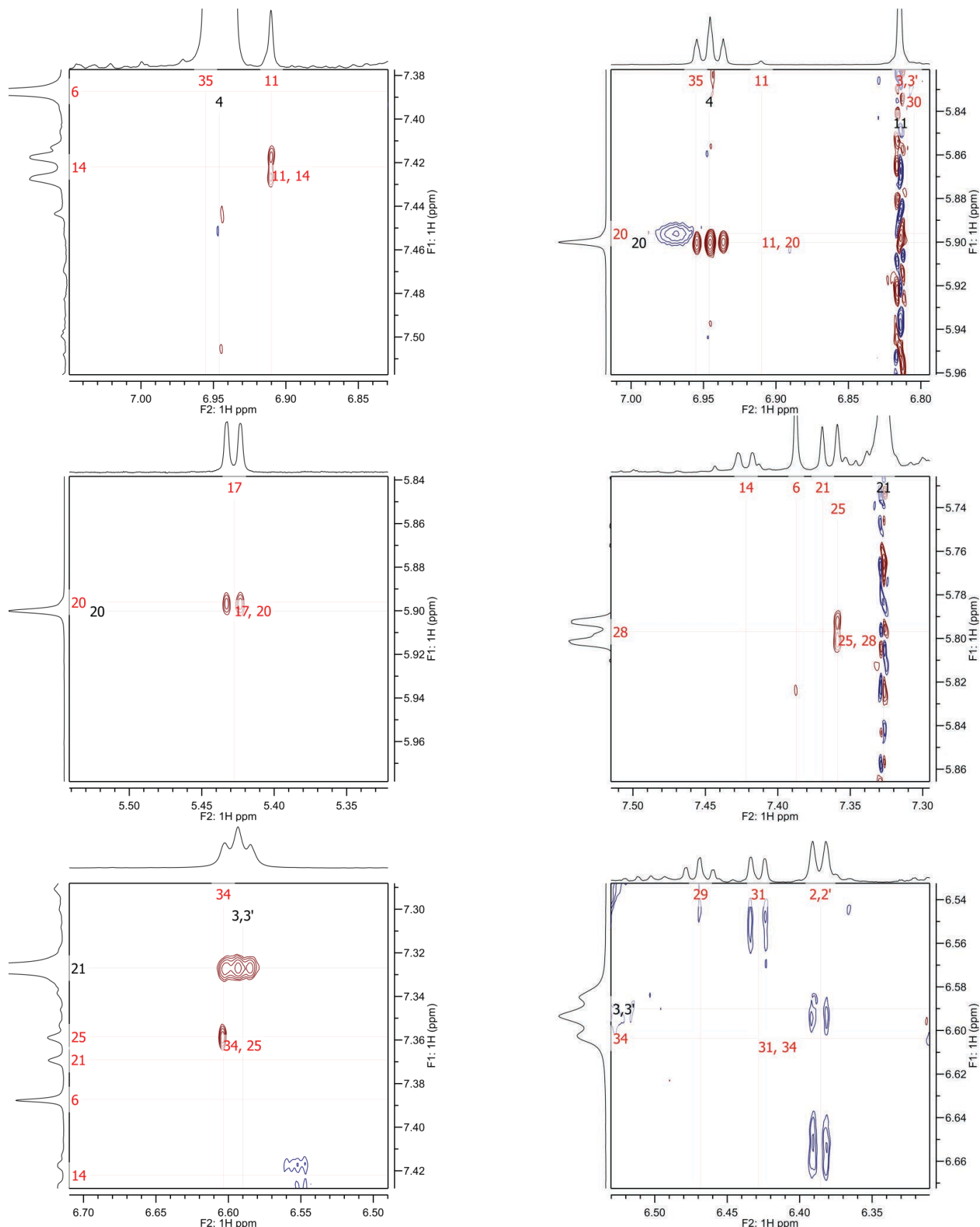


Figure S84. Selected expansions of the ROSEY NMR spectra (800 MHz) of **Cl-Ar-3** illustrating presence or absence of correlations listed in Table S31 for conformer AAAB. The numbers in black and red correspond to the atom numbers of the major and minor conformers, respectively, as defined in Figure S71.

9.5 nOe Correlations Illustrated on DFT Computed 3-D Structures for X-Ar-4

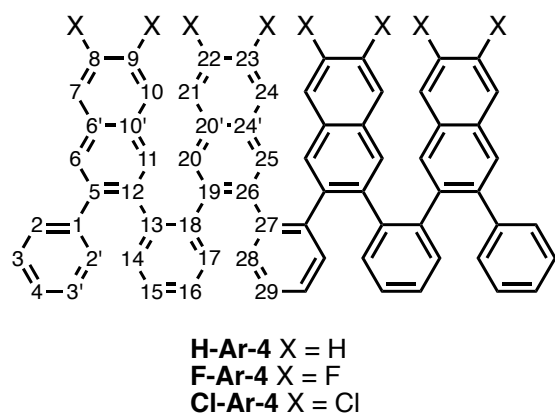


Figure S84. Atom numbering of **X-Ar-4** for conformers AAAA.

Table S33. Selected Interatomic Distance in M06-2X/6-31G Optimized Structures Relevant to ROSEY Analysis.

Structure	Selected Interatomic Distance in M06-2X/6-31G Optimized Structures [Å]			
	H(11)–H(14)	H(11)–(20)	H(17)–H(20)	H(25)–H(28)
H-Ar-4-AAAAA	2.48 [✓]	6.24 [✗]	2.43 [✓]	2.40 [✓]
F-Ar-4-AAAAA	2.47 [ND]	6.24 [✗]	2.42 [✓]	2.40 [✓]
Cl-Ar-4-AAAAA	2.47 [✓]	6.24 [✗]	2.43 [✓]	2.40 [✓]

[✓] = observed associated signal in ROSEY spectra.

[✗] = did not observe associated signal in ROSEY spectra.

[ND] = absence or presence of signal in ROSEY spectra could not be determined due to overlapping neighboring signal.

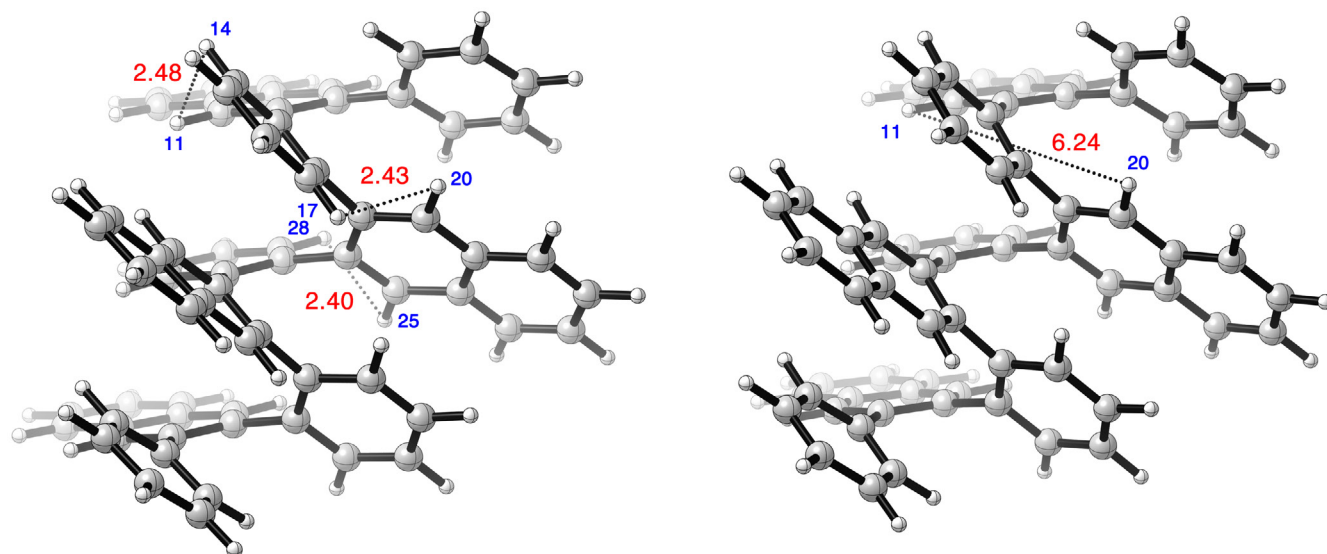


Figure S85. Conformer AAAA of **H-Ar-4** from M06-2X/6-31G calculations illustrating selected non-bonding distances (in Å, numbers in red) associated with nOe signals that are: (left) observed and (right) not observed. Numbers in blue corresponding to the atom numbering scheme illustrated in Figure S84.

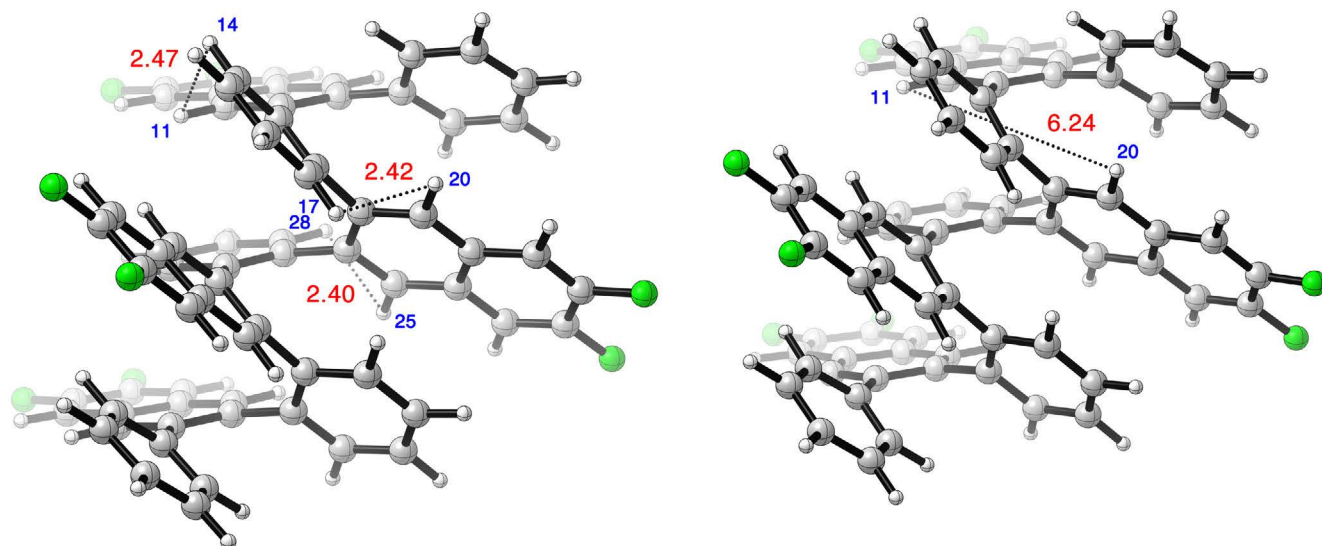


Figure S86. Conformer AAAAA of **F-Ar-4** from M06-2X/6-31G calculations illustrating selected non-bonding distances (in Å, numbers in red) associated with nOe signals that are: (left) observed and (right) not observed. Numbers in blue corresponding to the atom numbering scheme illustrated in Figure S84.

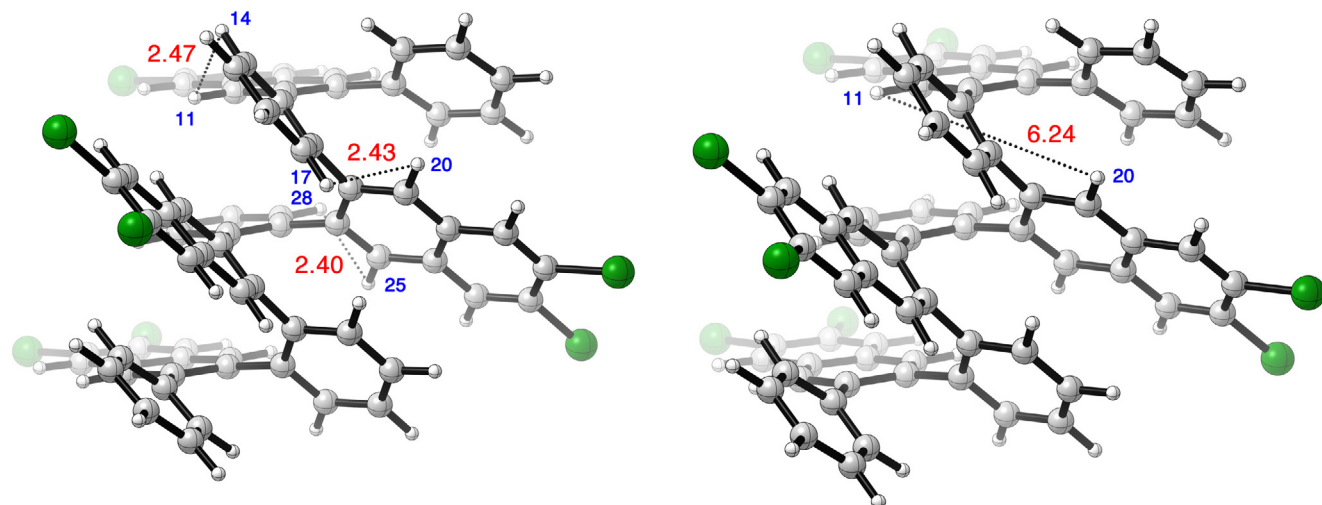


Figure S87. Conformer AAAAA of **Cl-Ar-4** from M06-2X/6-31G calculations illustrating selected non-bonding distances (in Å, numbers in red) associated with nOe signals that are: (left) observed and (right) not observed. Numbers in blue corresponding to the atom numbering scheme illustrated in Figure S84.

9.6 nOe Correlations Illustrated on DFT Computed 3-D Structures for F-Ar-5 and F-Ar-6

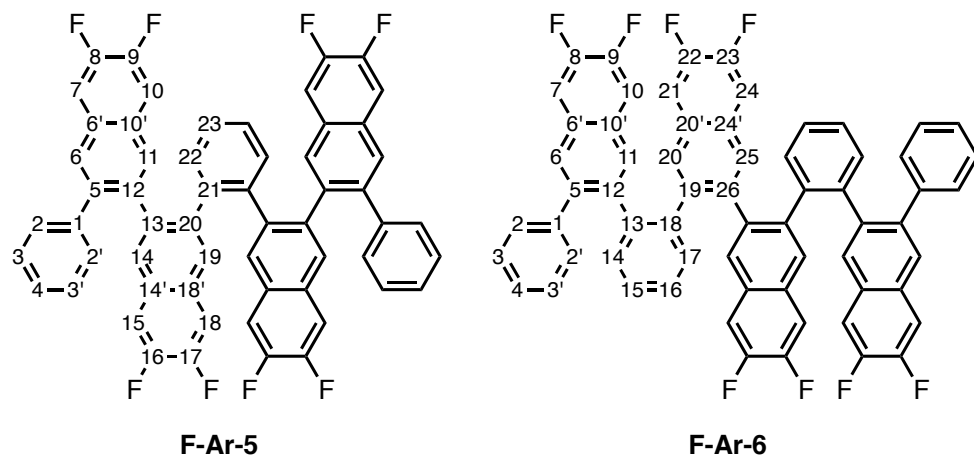


Figure S88. Atom numbering of **F-Ar-5**, and **F-Ar-6** for conformers AAAA and AAAAA, respectively.

Table S34. Selected Interatomic Distance in M06-2X/6-31G Optimized Structures Relevant to ROSEY Analysis.

Structure	Selected Interatomic Distance in M06-2X/6-31G Optimized Structures [Å]				
	H(11)–H(14)	H(11)–(20)	H(11)–(22)	H(19)–H(22)	H(17)–H(20)
F-Ar-5-AAAA	2.47 [✓]	NA	6.27 [✗]	2.40 [✓]	NA
F-Ar-6-AAAAA	2.48 [✓]	6.24 [✗]	NA	NA	2.42 [✓]

[✓] = observed associated signal in ROSEY spectra.

[✗] = did not observe associated signal in ROSEY spectra.

[ND] = absence or presence of signal in ROSEY spectra could not be determined due to overlapping neighboring signal.

NA = not applicable.

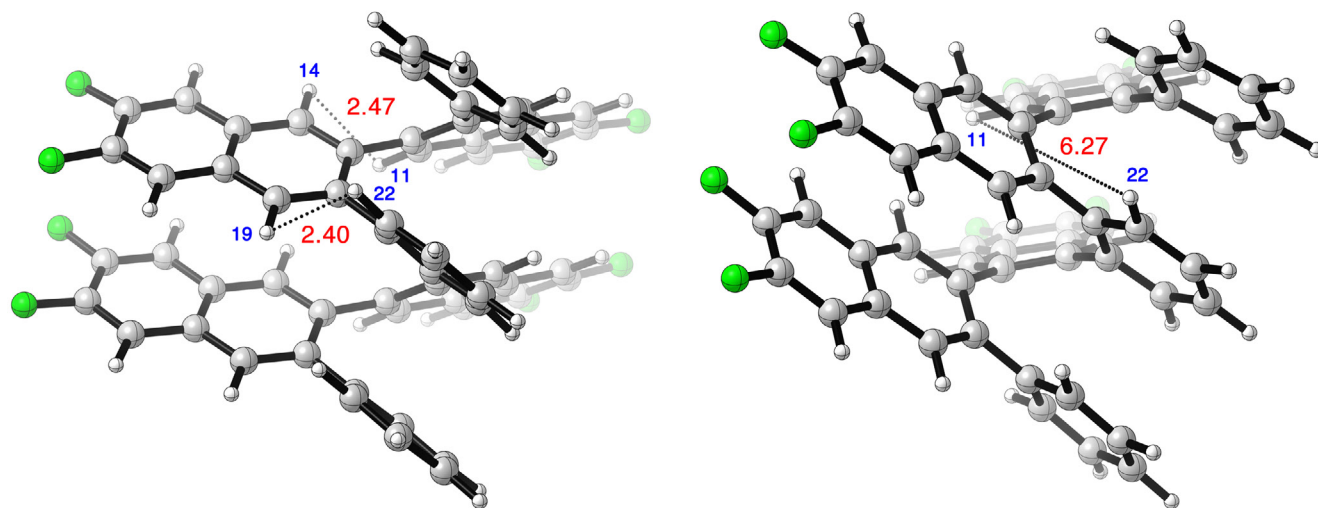


Figure S89. Conformer AAAAA of **F-Ar-5** from M06-2X/6-31G calculations illustrating selected non-bonding distances (in Å, numbers in red) associated with nOe signals that are: (left) observed and (right) not observed. Numbers in blue corresponding to the atom numbering scheme illustrated in Figure S88.

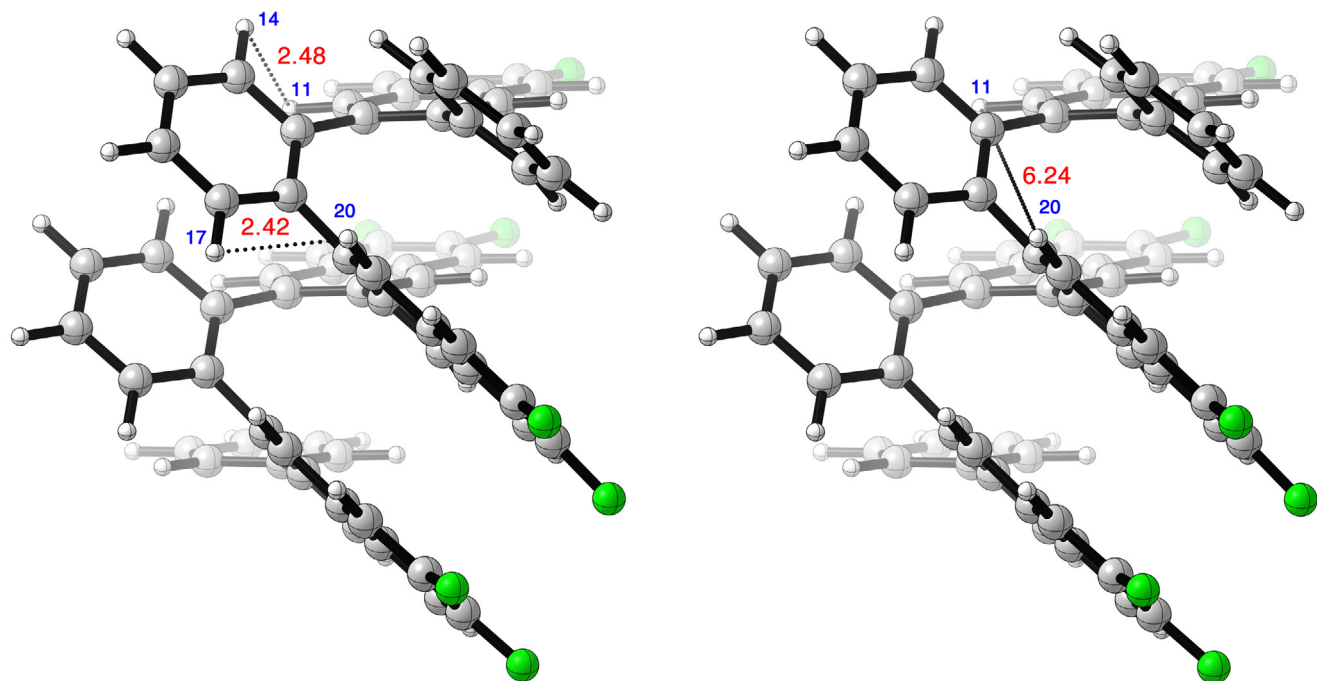


Figure S90. Conformer AAAAA of **F-Ar-6** from M06-2X/6-31G calculations illustrating selected non-bonding distances (in Å, numbers in red) associated with nOe signals that are: (left) observed and (right) not observed. Numbers in blue corresponding to the atom numbering scheme illustrated in Figure S88.

9.7 1-D and 2-D NMR Spectra of X-Ar-3

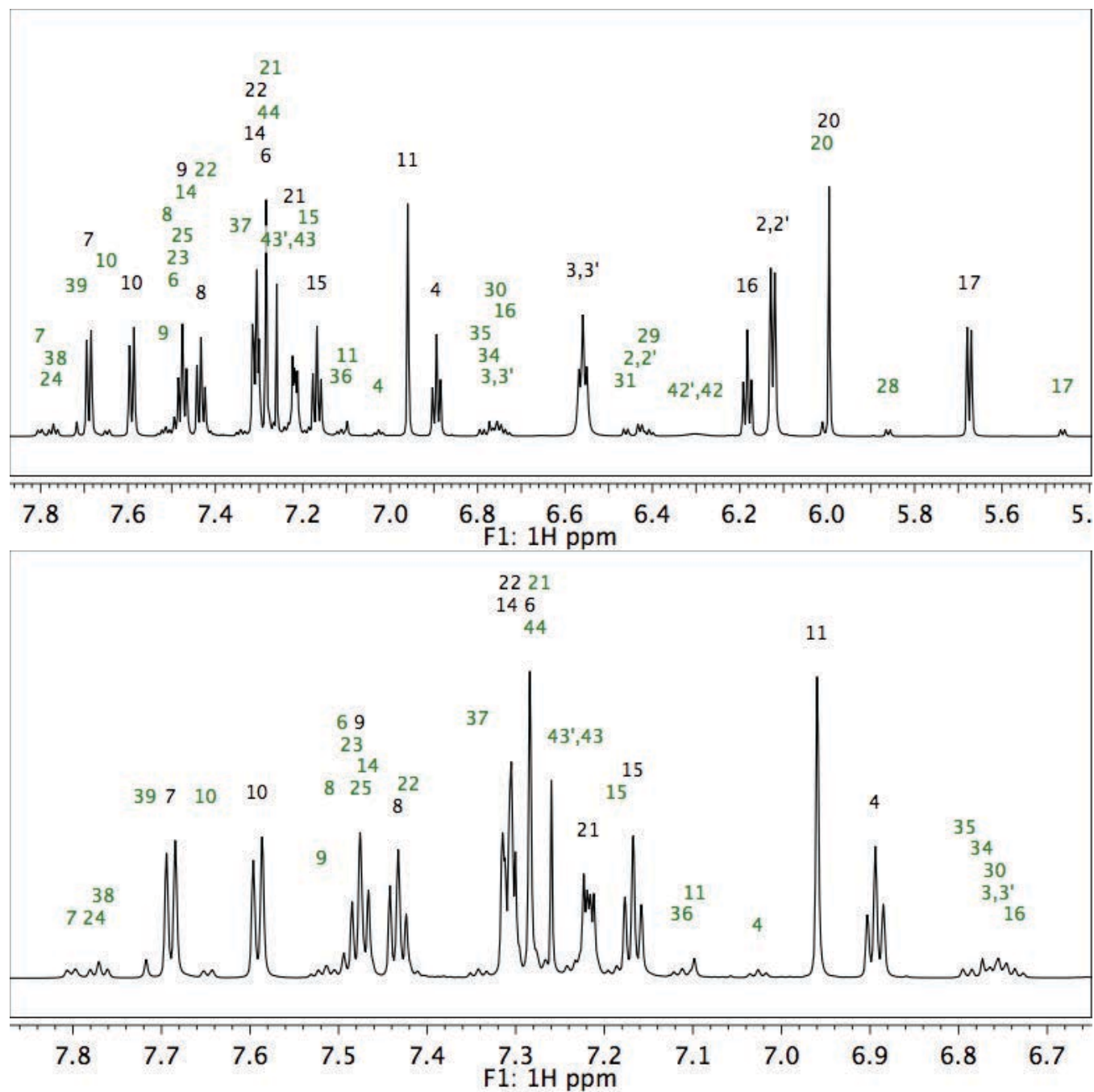


Figure S91. ¹H NMR (800 MHz) spectrum of **H-Ar-3** in CDCl₃ at 0 °C: (top) full view, (bottom) 7.75 to 6.65 ppm region. The numbers in black and green correspond to the atom numbers of the major and minor conformers, respectively, as defined in Figure S68.

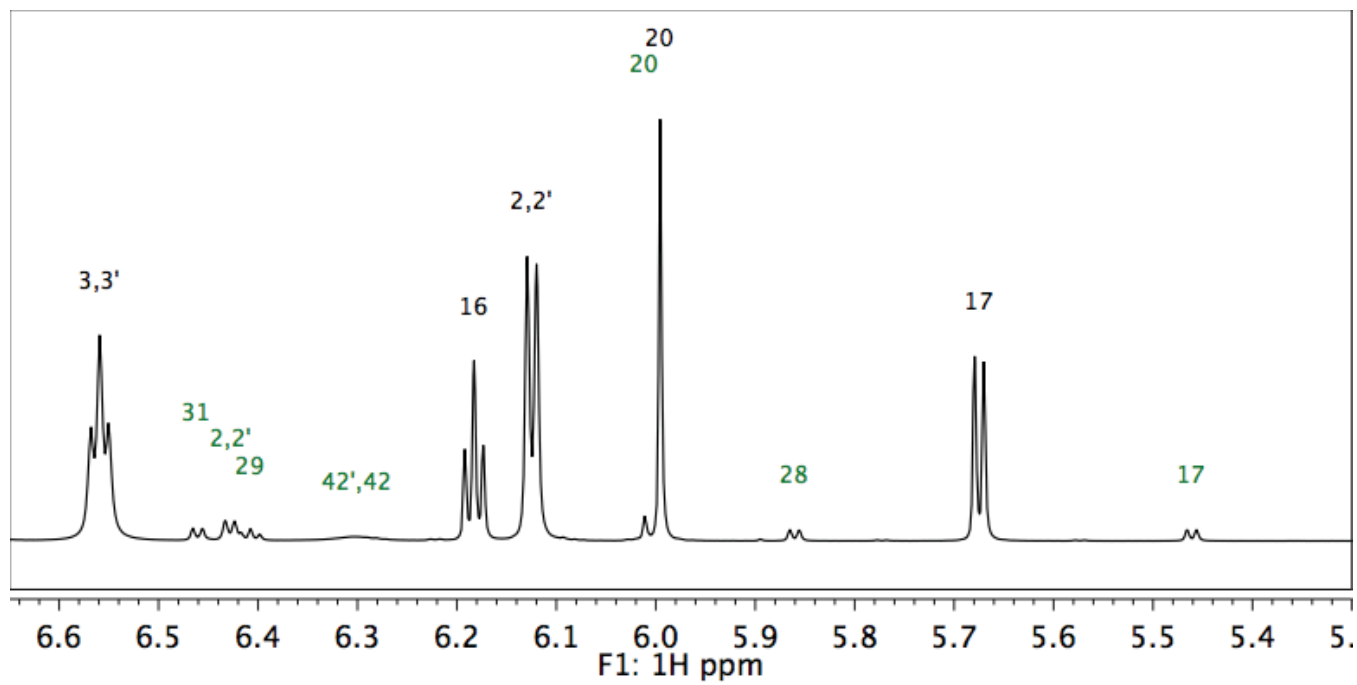


Figure S91 (continued). ^1H NMR (800 MHz) spectrum of **H-Ar-3** in CDCl_3 at 0°C , 6.70 to 5.25 ppm region. The numbers in black and green correspond to the atom numbers of the major and minor conformers, respectively, as defined in Figure S68.

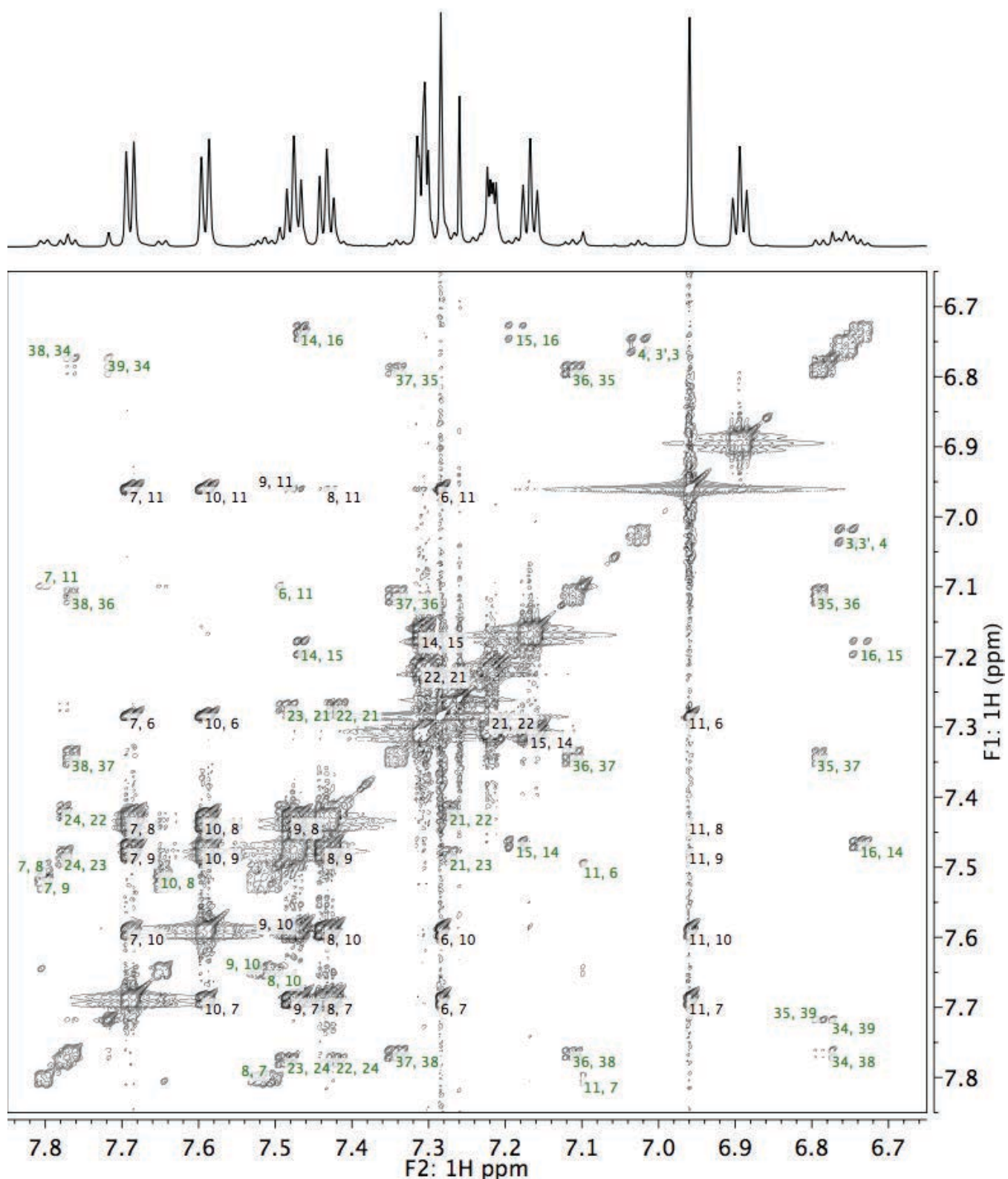


Figure S93. COSY NMR (800 MHz) spectrum of **H-Ar-3** in CDCl₃ at 0 °C, 7.85 to 6.65 ppm region. The numbers in black and green correspond to the atom numbers of the major and minor conformers, respectively, as defined in Figure S68.

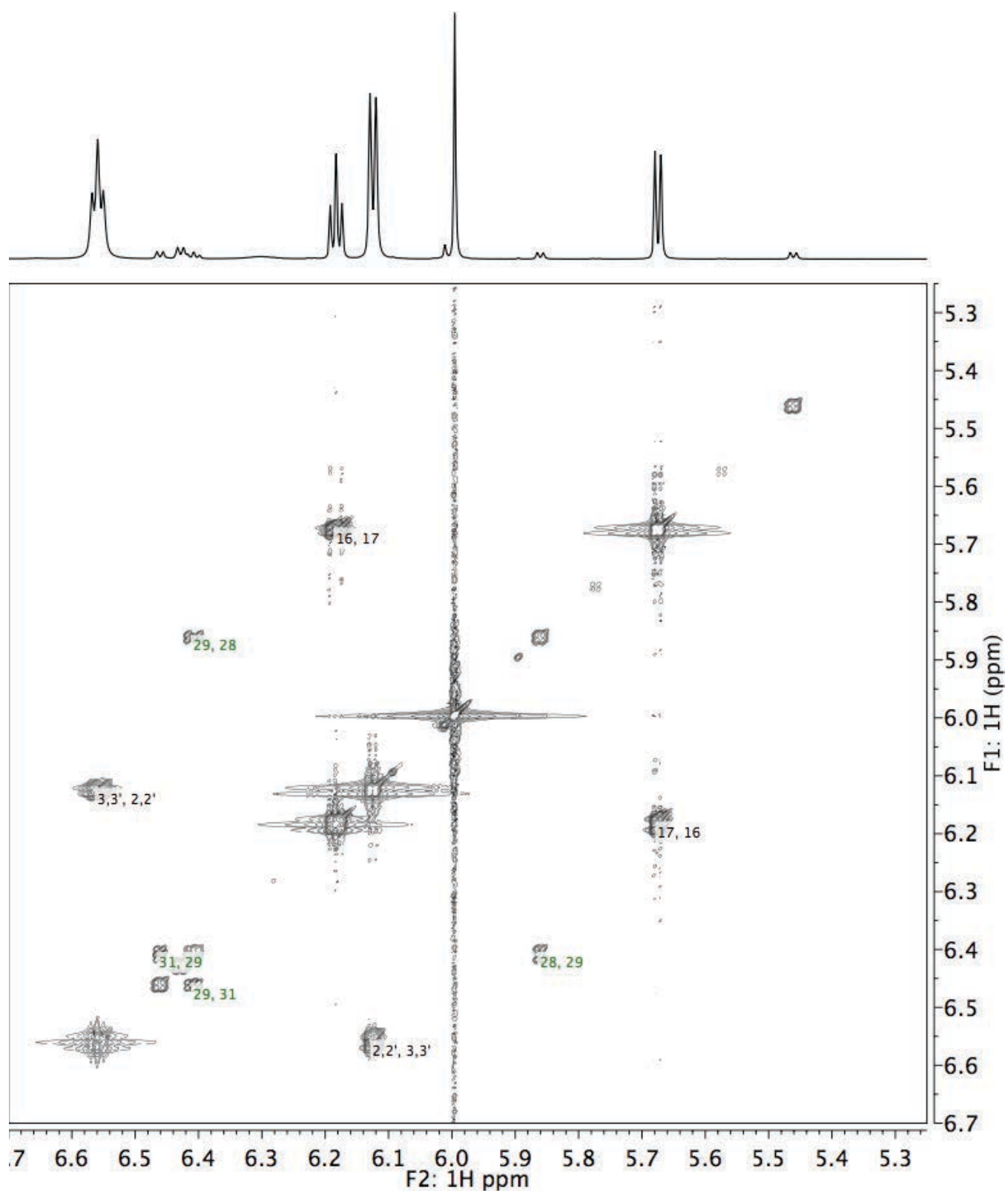


Figure S94. COSY NMR (800 MHz) spectrum of **H-Ar-3** in CDCl_3 at 0 $^\circ\text{C}$, 6.70 to 5.25 ppm region. The numbers in black and green correspond to the atom numbers of the major and minor conformers, respectively, as defined in Figure S68.

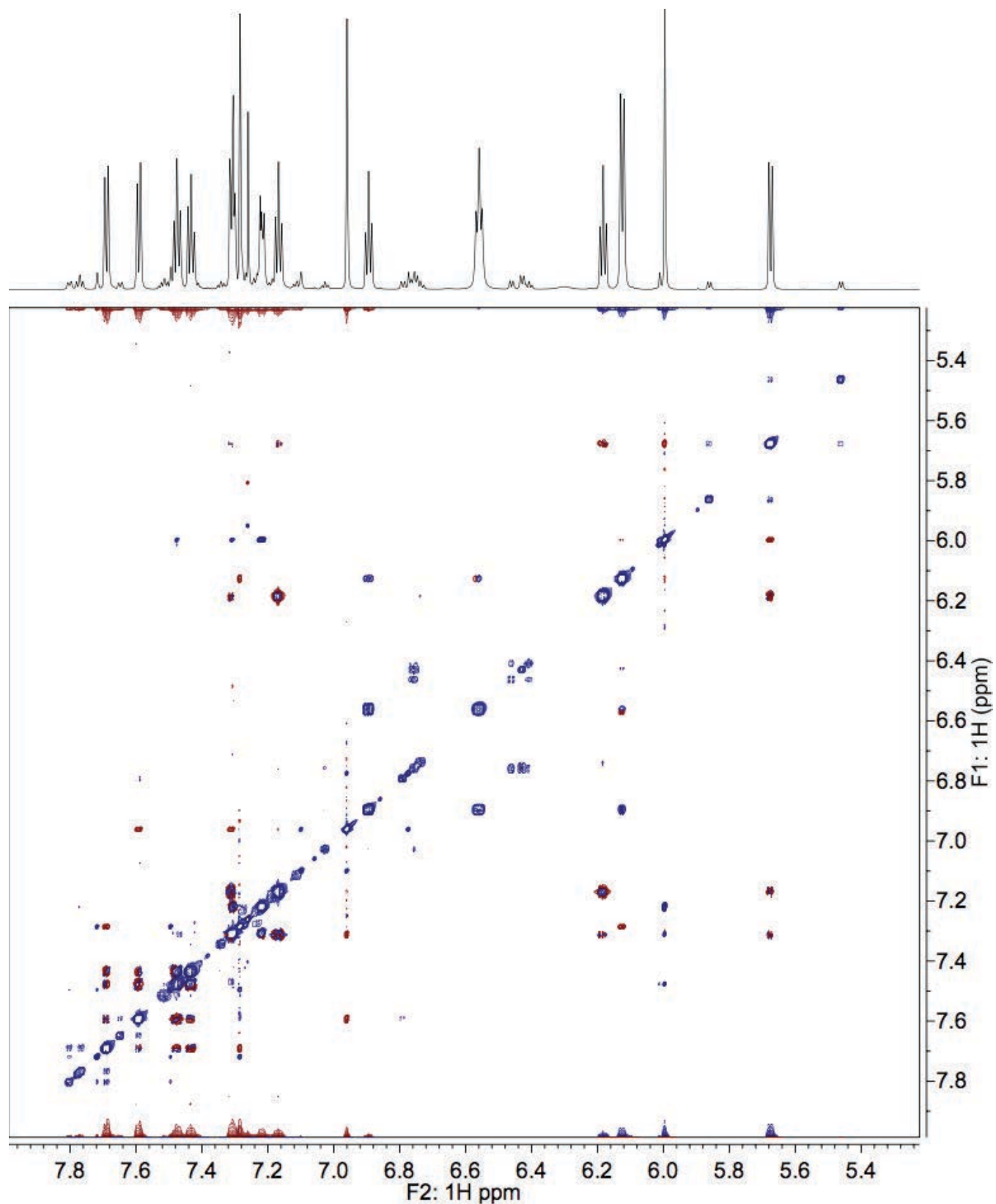


Figure S95. ROSEY NMR (800 MHz) spectrum of **H-Ar-3** in CDCl_3 at 0 °C (spectral expansions are shown in the ROSEY NMR assignment section).

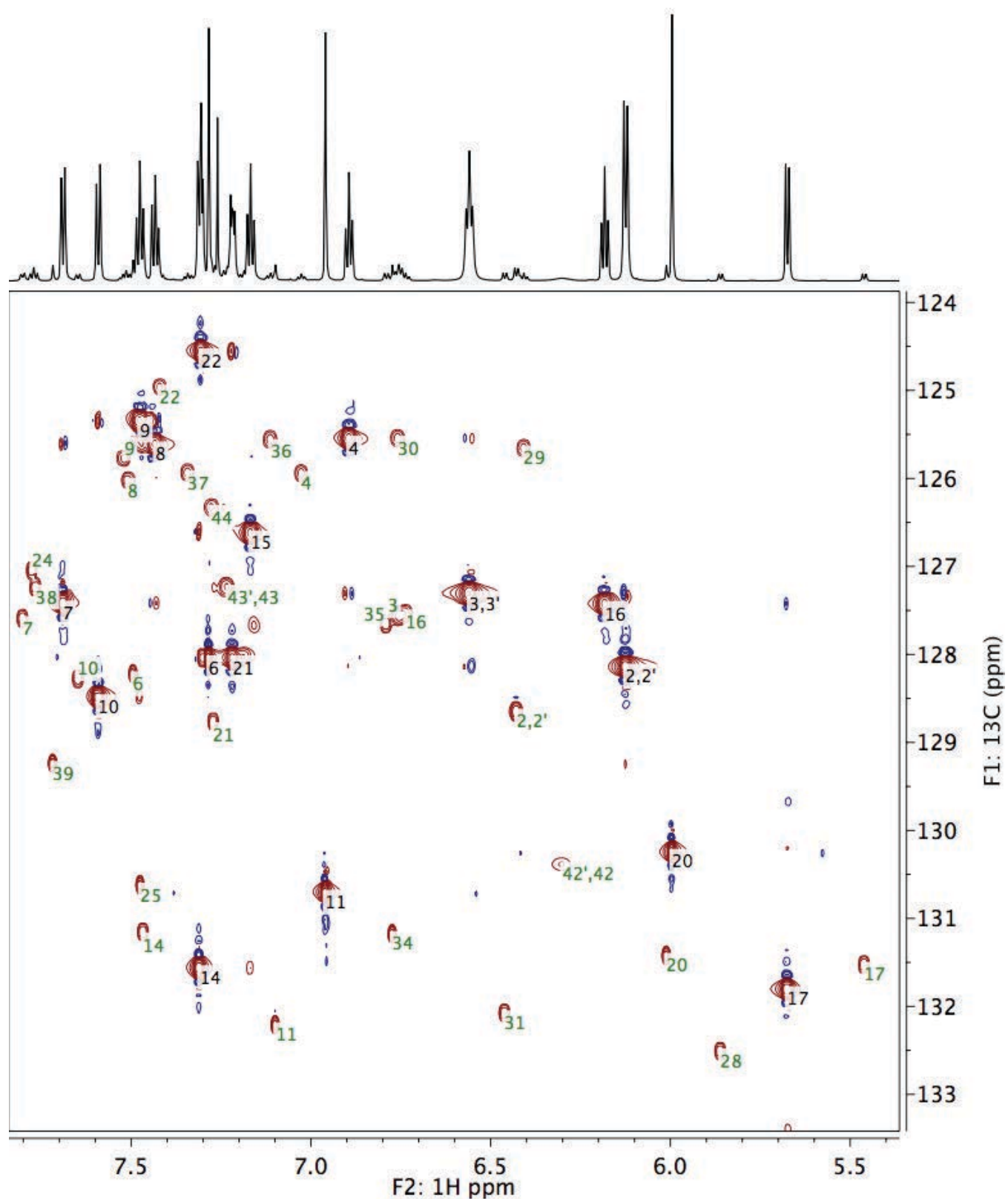


Figure S96. HSQC NMR (800 MHz) spectrum of **H-Ar-3** in CDCl_3 at 0 °C. The numbers in black and green correspond to the atom numbers of the major and minor conformers, respectively, as defined in Figure S68.

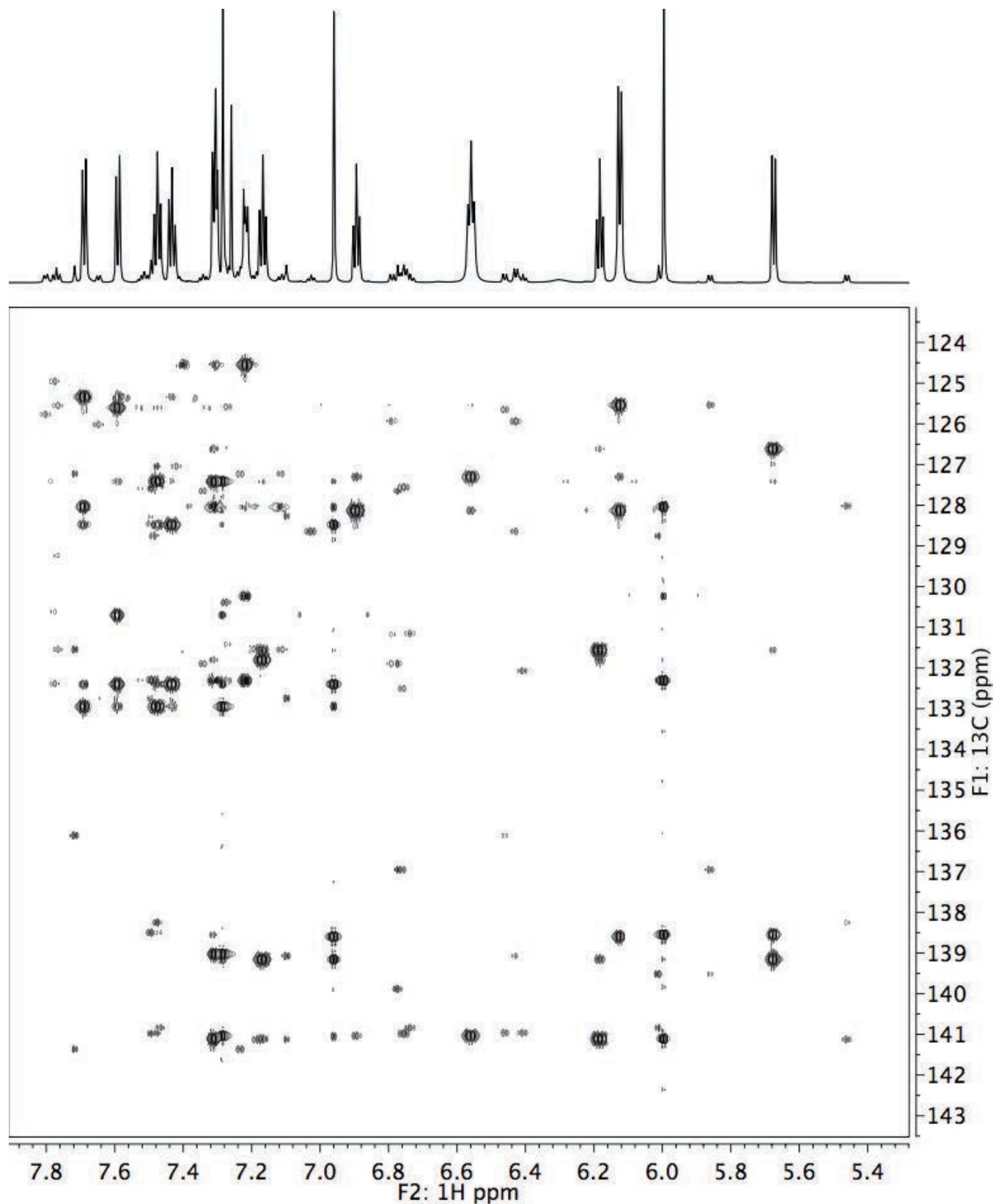


Figure S97. HMBC NMR (800 MHz) spectrum of **H-Ar-3** in CDCl_3 at 0°C , full view.

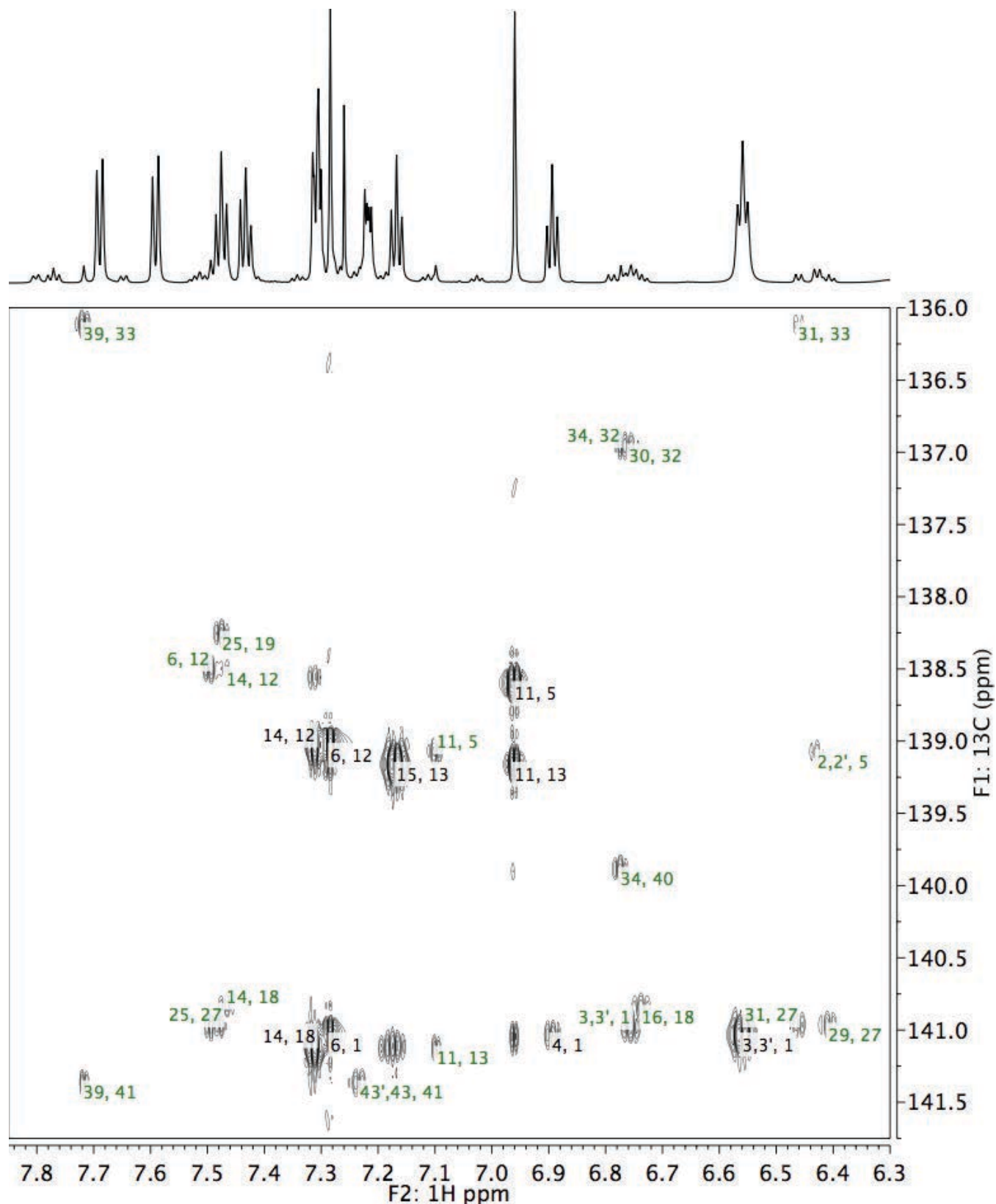


Figure S98. HMBC NMR (800 MHz) spectrum of **H-Ar-3** in CDCl_3 at 0°C , δ_{H} 7.85 to 6.30 ppm and δ_{C} 141.75 to 136.0 ppm region. The numbers in black and green correspond to the atom numbers of the major and minor conformers, respectively, as defined in Figure S68.

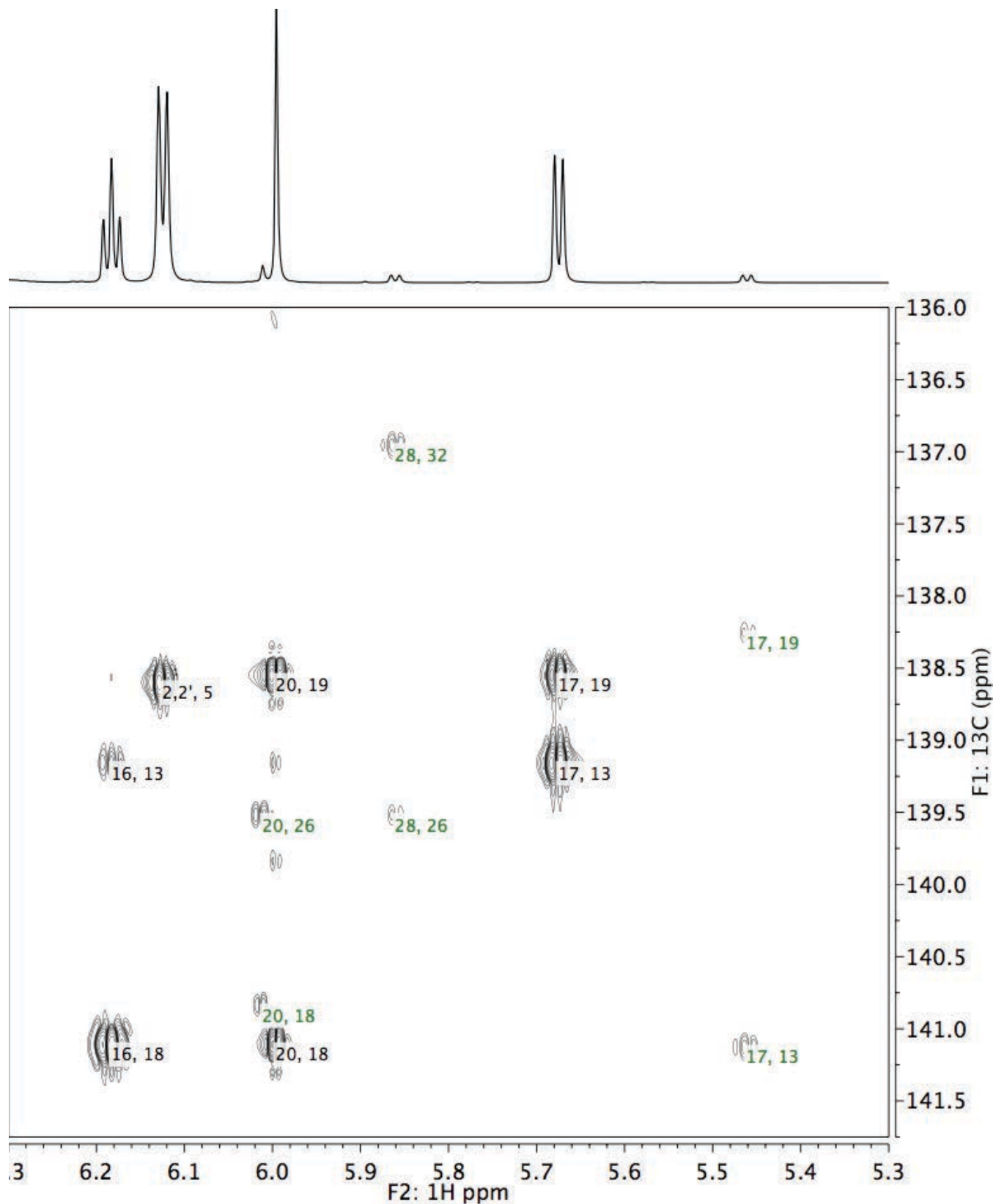


Figure S99. HMBC NMR (800 MHz) spectrum of **H-Ar-3** in CDCl_3 at 0 °C, δ_{H} 6.30 to 5.30 ppm and δ_{C} 141.75 to 136.0 ppm region. The numbers in black and green correspond to the atom numbers of the major and minor conformers, respectively, as defined in Figure S68.

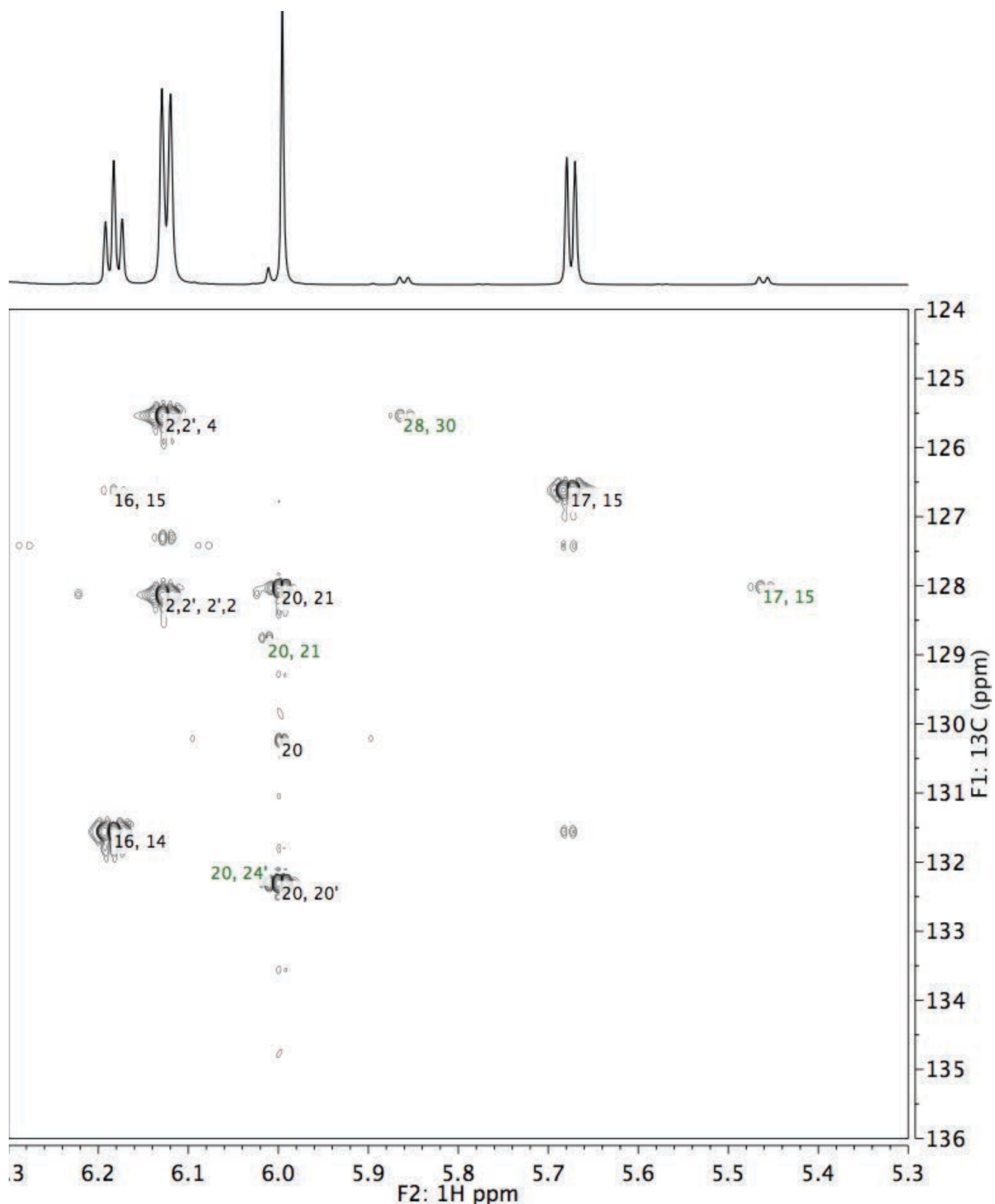


Figure S100. HMBC NMR (800 MHz) spectrum of **H-Ar-3** in CDCl₃ at 0 °C, δ_{H} 6.30 to 5.30 ppm and δ_{C} 136.0 to 124.0 ppm region. The numbers in black and green correspond to the atom numbers of the major and minor conformers, respectively, as defined in Figure S68.

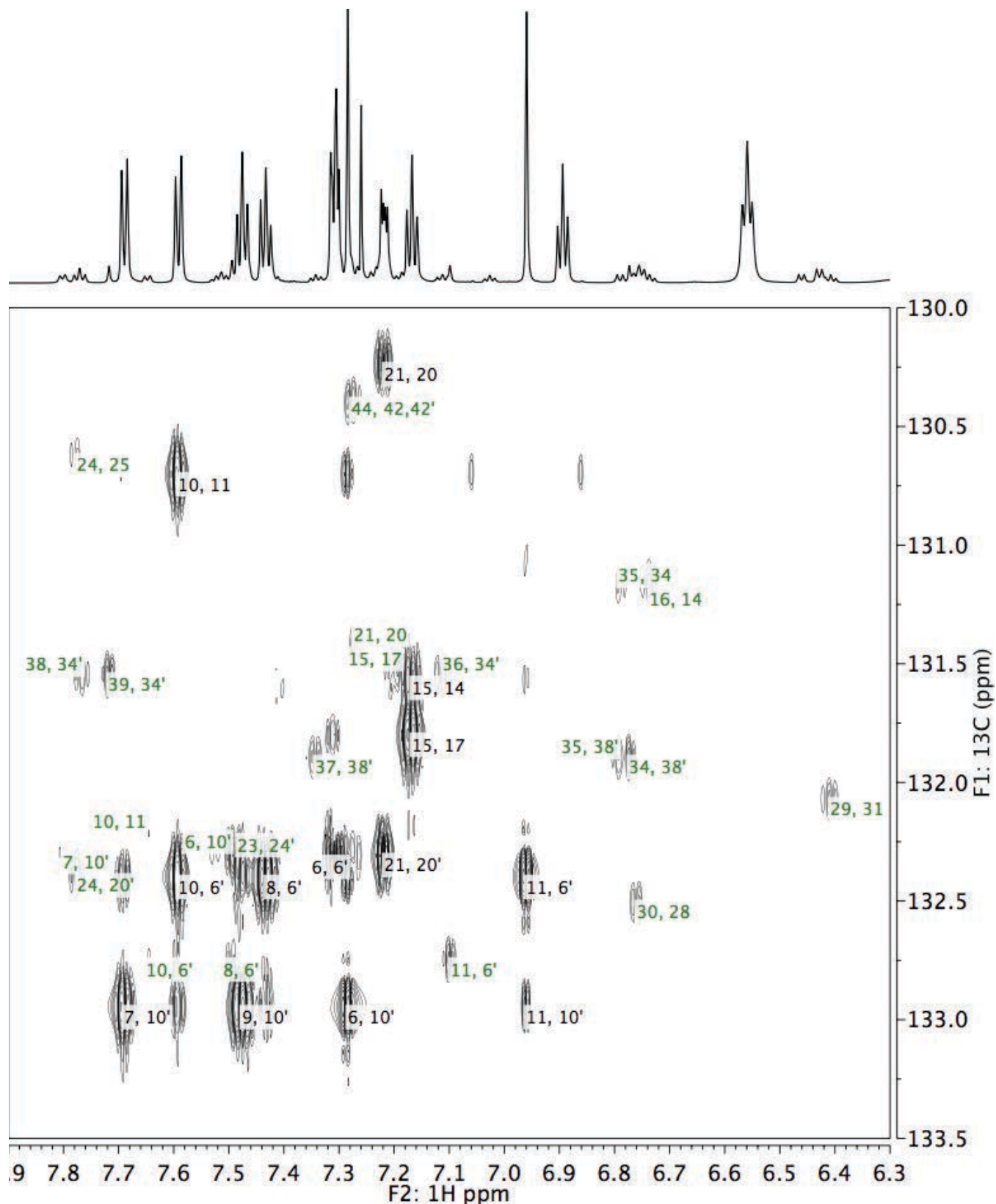


Figure S102. HMBC NMR (800 MHz) spectrum of **H-Ar-3** in CDCl_3 at 0 $^\circ\text{C}$, δ_{H} 7.90 to 6.30 ppm and δ_{C} 133.5 to 130.0 ppm region. The numbers in black and green correspond to the atom numbers of the major and minor conformers, respectively, as defined in Figure S68.

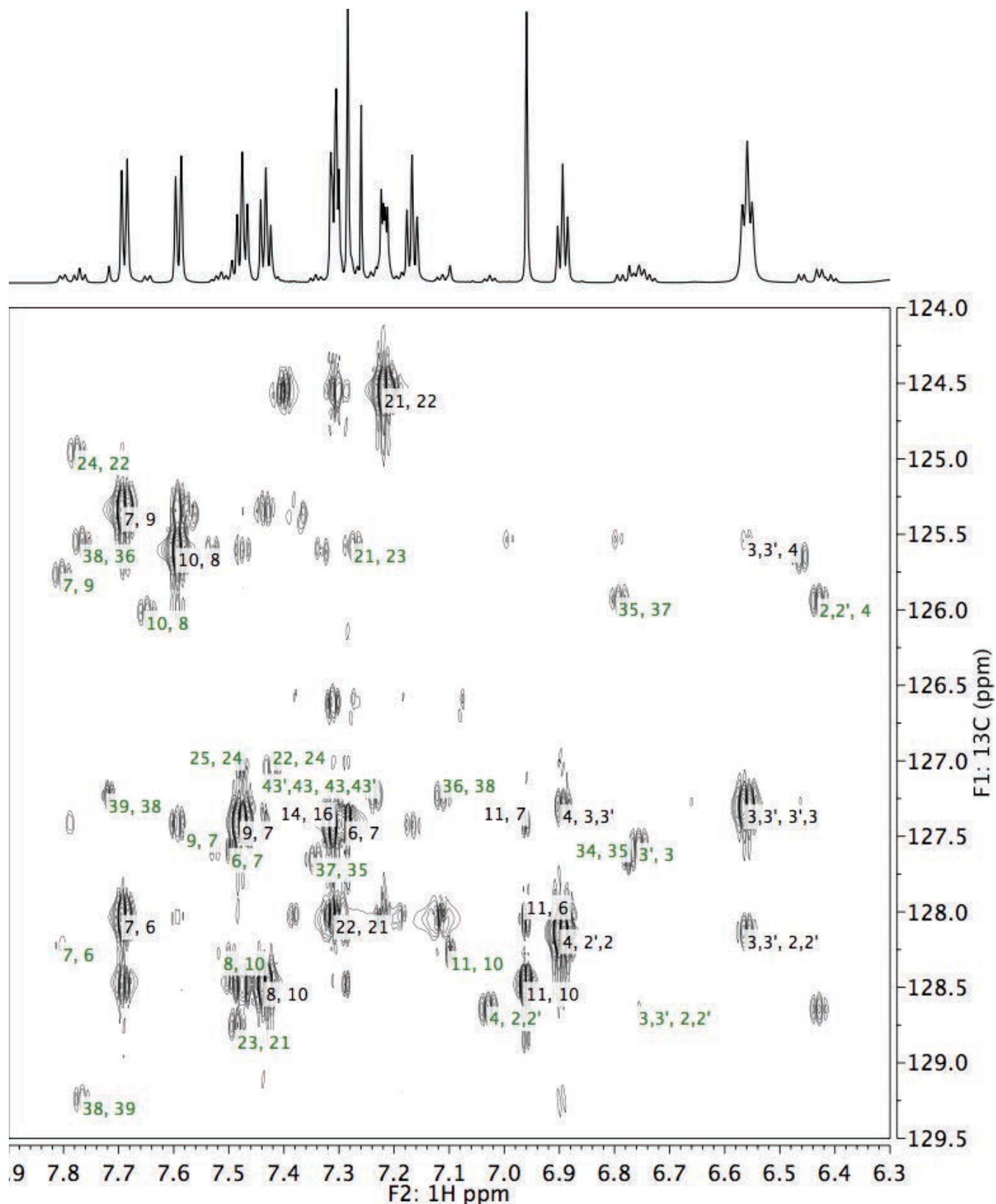


Figure S103. HMBC NMR (800 MHz) spectrum of **F-Ar-3** in CDCl_3 at 0°C , δ_{H} 7.90 to 6.30 ppm and δ_{C} 129.5 to 124.0 ppm region. The numbers in black and green correspond to the atom numbers of the major and minor conformers, respectively, as defined in Figure S68.

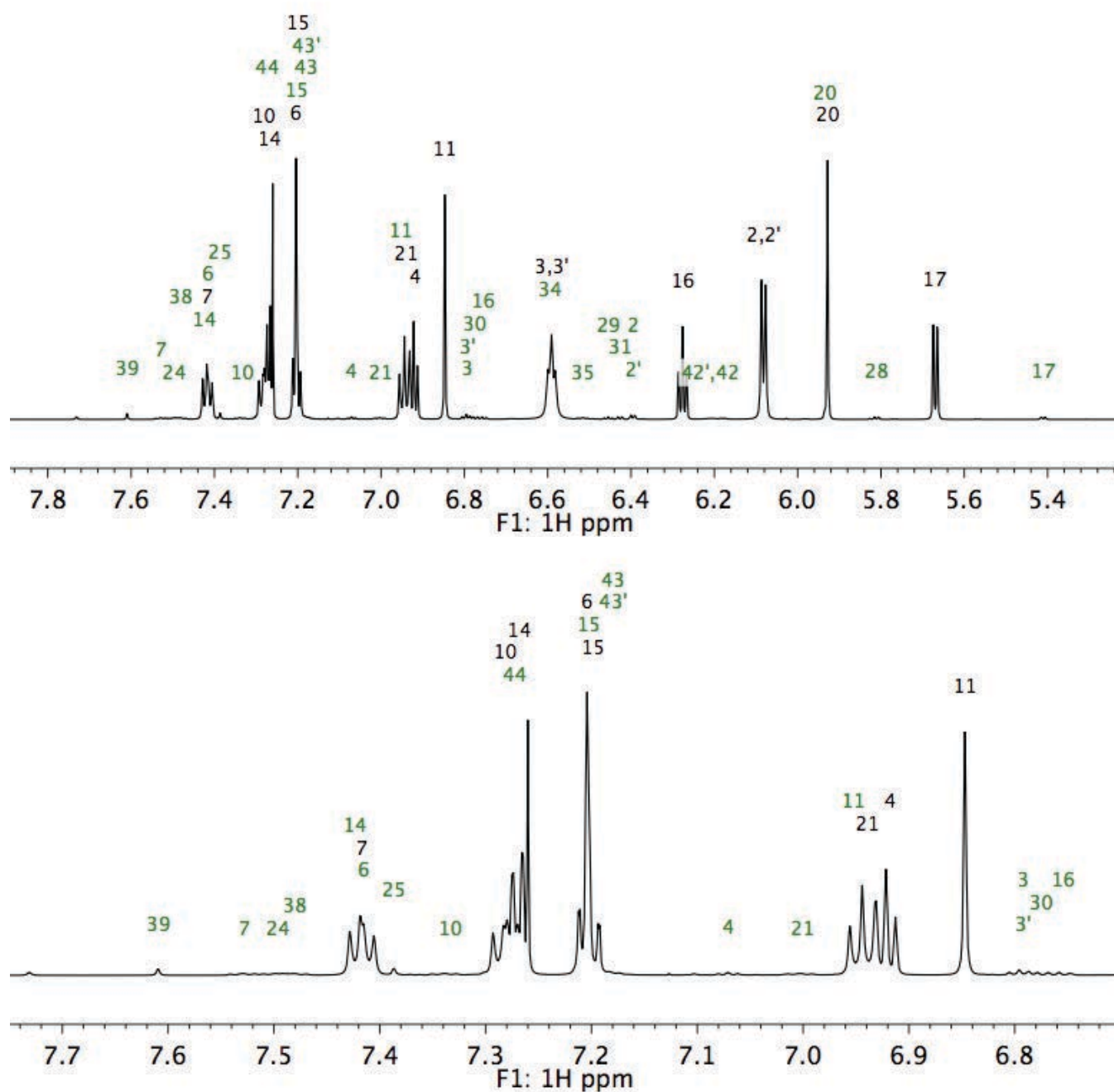


Figure S104. ¹H NMR (800 MHz) spectrum of **F-Ar-3** in CDCl₃ at 0 °C: (top) full view, (bottom) 7.75 to 6.70 ppm region. The numbers in black and green correspond to the atom numbers of the major and minor conformers, respectively, as defined in Figure S68.

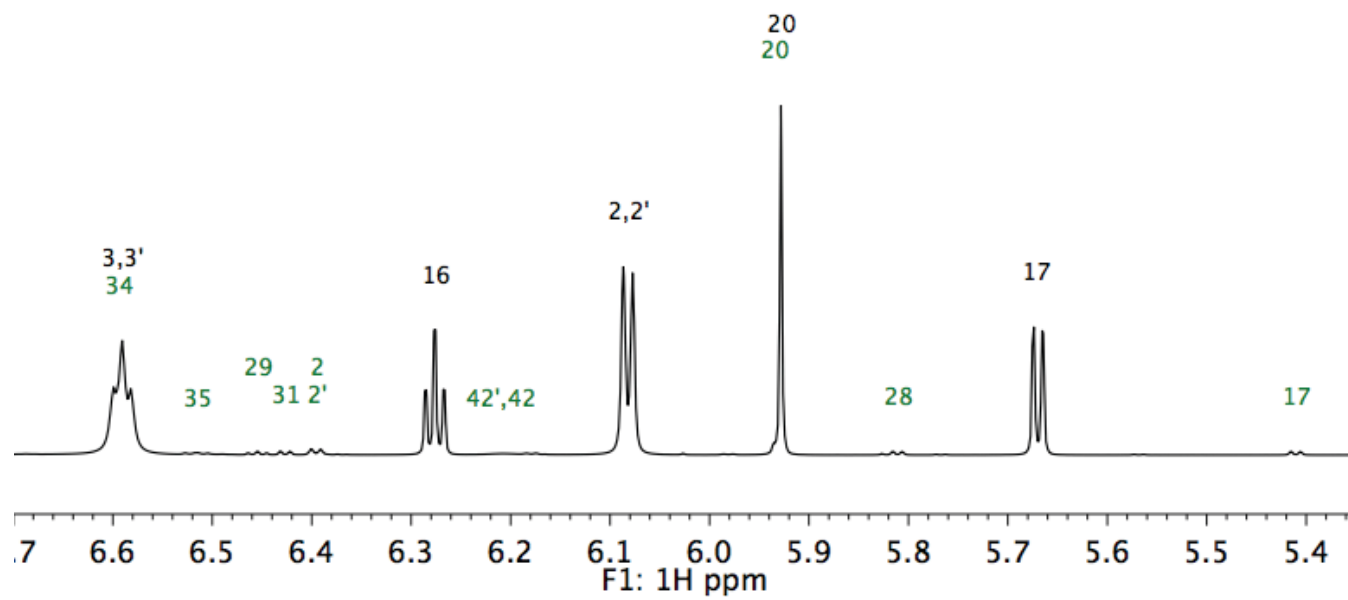


Figure S104 (continued). ^1H NMR (800 MHz) spectrum of **F-Ar-3** in CDCl_3 at $0\text{ }^\circ\text{C}$: 6.70 to 5.35 ppm region. The numbers in black and green correspond to the atom numbers of the major and minor conformers, respectively, as defined in Figure S68.

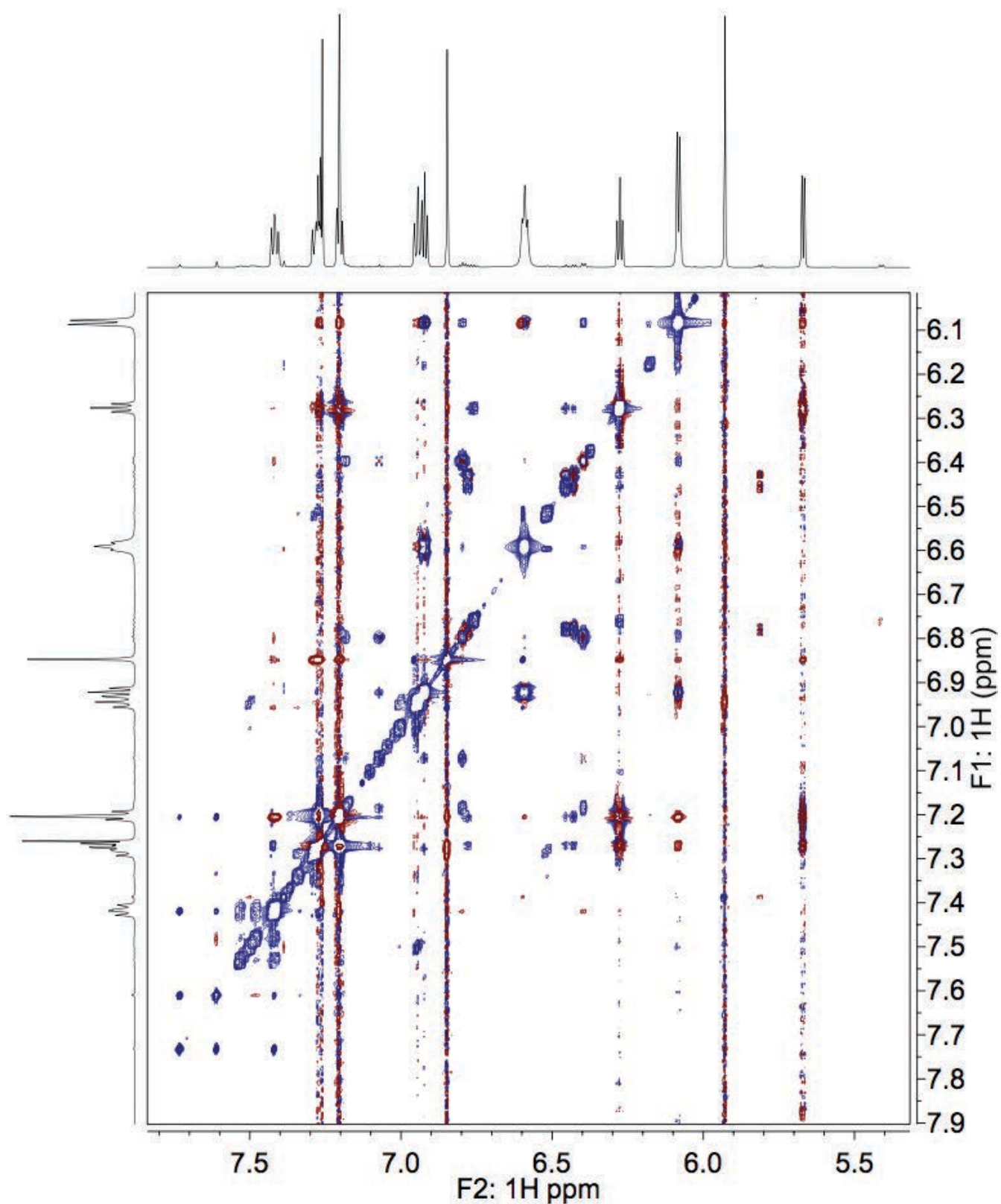


Figure S105. ROSEY NMR (800 MHz) spectrum of **F-Ar-3** in CDCl_3 at 0 °C (spectral expansions are shown in the ROSEY NMR assignment section).

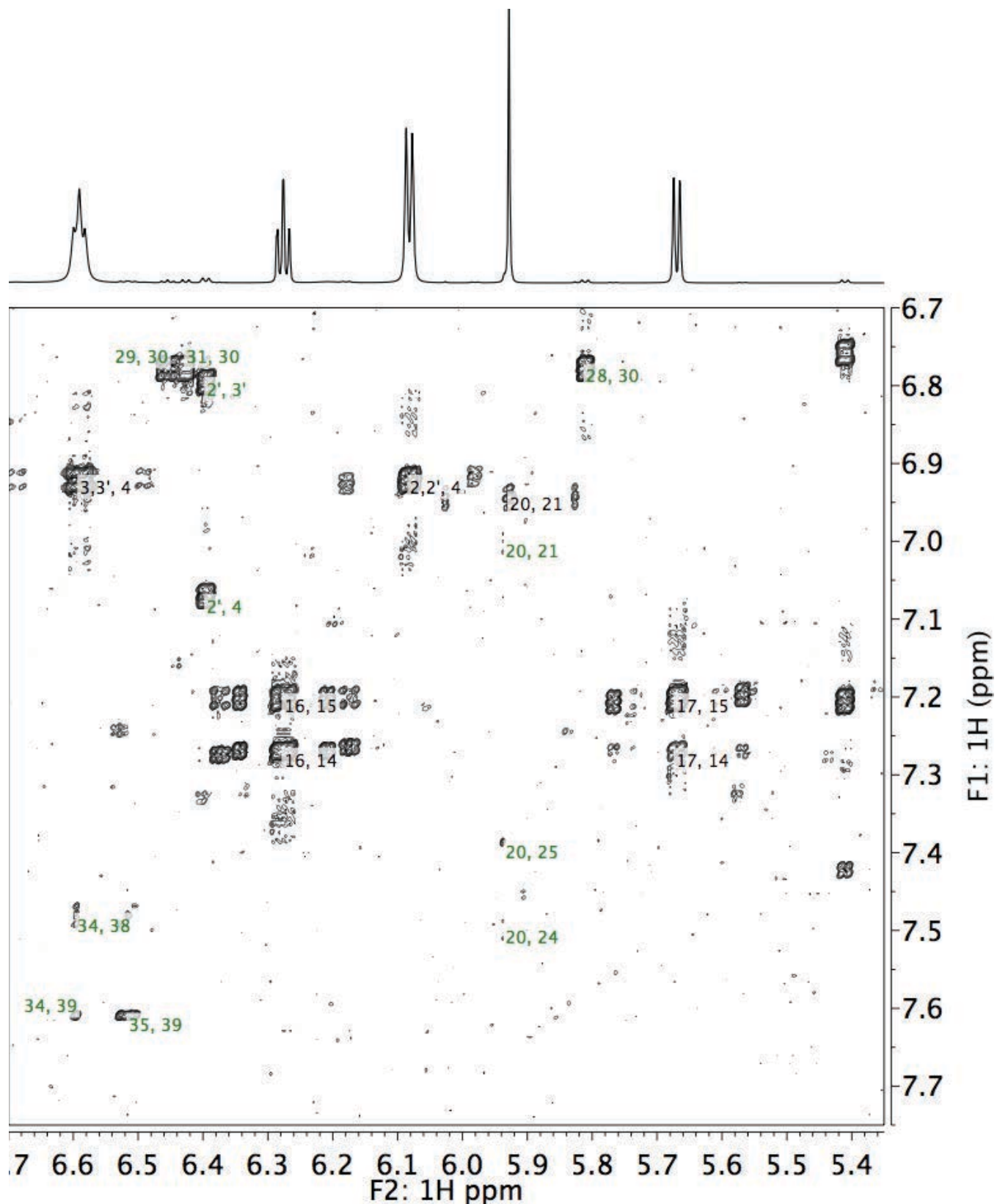


Figure S107. COSY NMR (800 MHz) spectrum of **F-Ar-3** in CDCl_3 at 0°C ; F2: 6.70 to 5.35 vs F1: 7.75 to 6.70 ppm region. The numbers in black and green correspond to the atom numbers of the major and minor conformers, respectively, as defined in Figure S68.

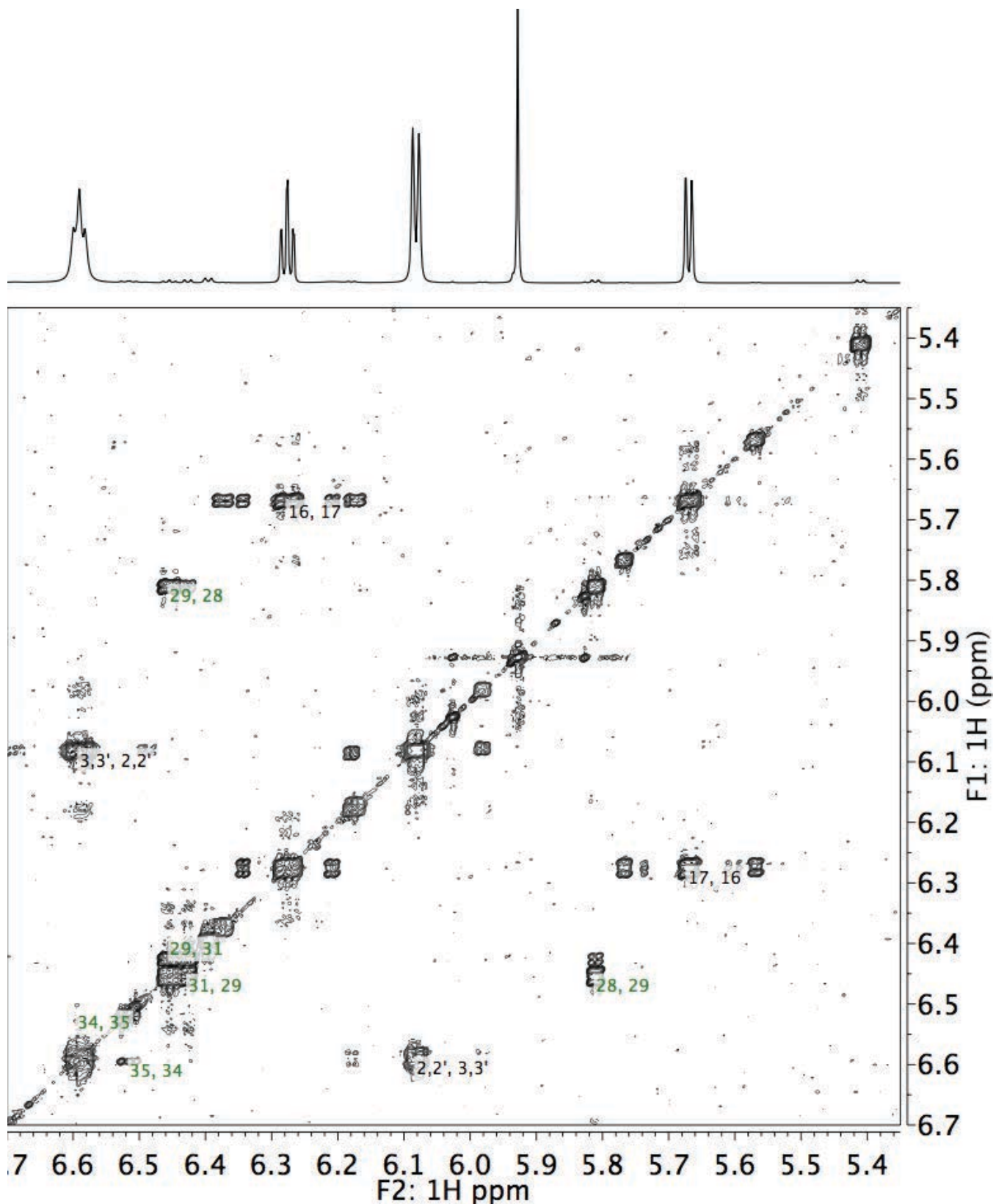


Figure S108. COSY NMR (800 MHz) spectrum of **F-Ar-3** in CDCl_3 at $0\text{ }^\circ\text{C}$; F2: 6.70 to 5.35 vs F1: 6.70 to 5.35 ppm region. The numbers in black and green correspond to the atom numbers of the major and minor conformers, respectively, as defined in Figure S68.

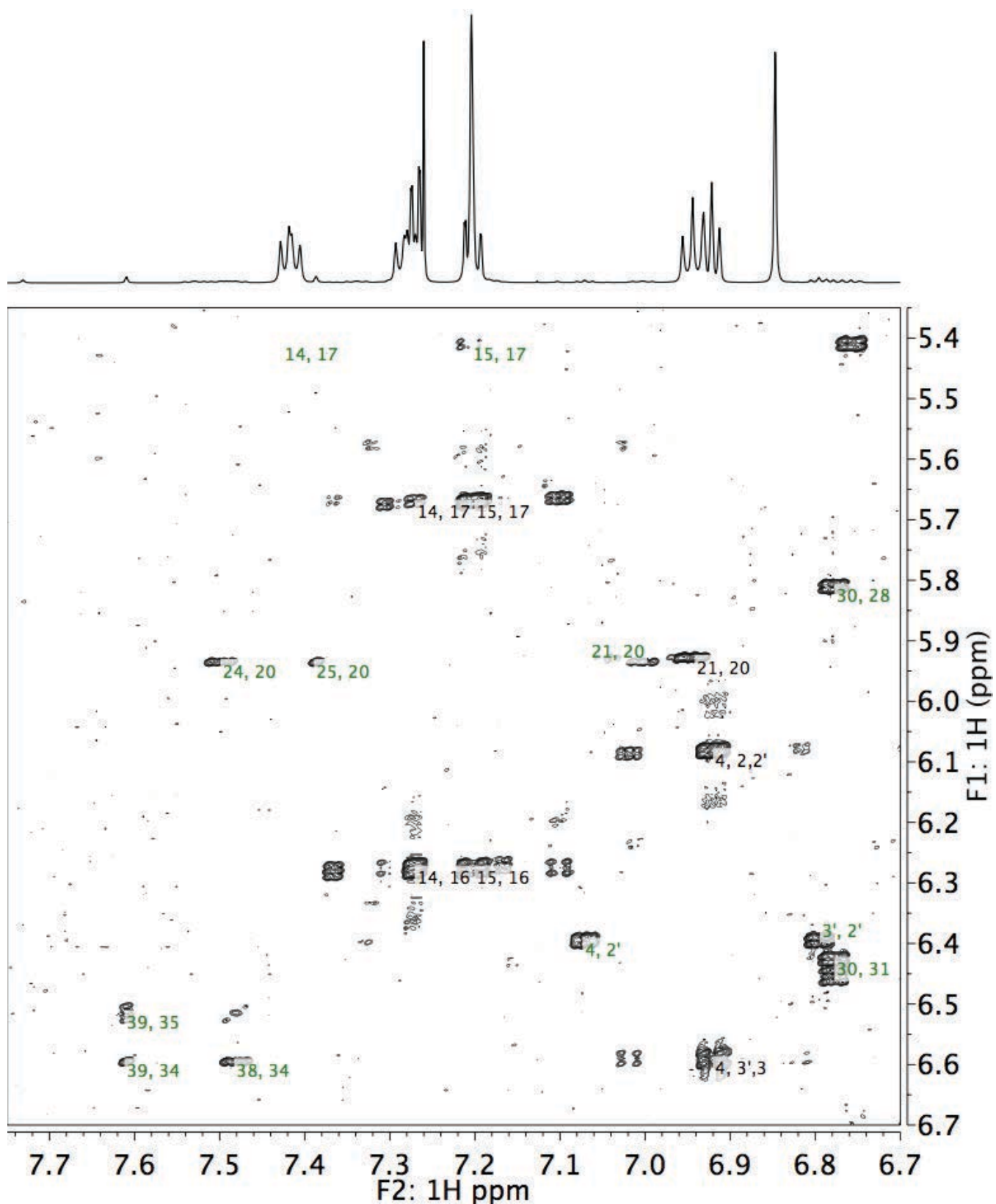


Figure S109. COSY NMR (800 MHz) spectrum of **F-Ar-3** in CDCl_3 at 0 °C; F2: 7.75 to 6.70 vs F1: 6.70 to 5.35 ppm region. The numbers in black and green correspond to the atom numbers of the major and minor conformers, respectively, as defined in Figure S68.

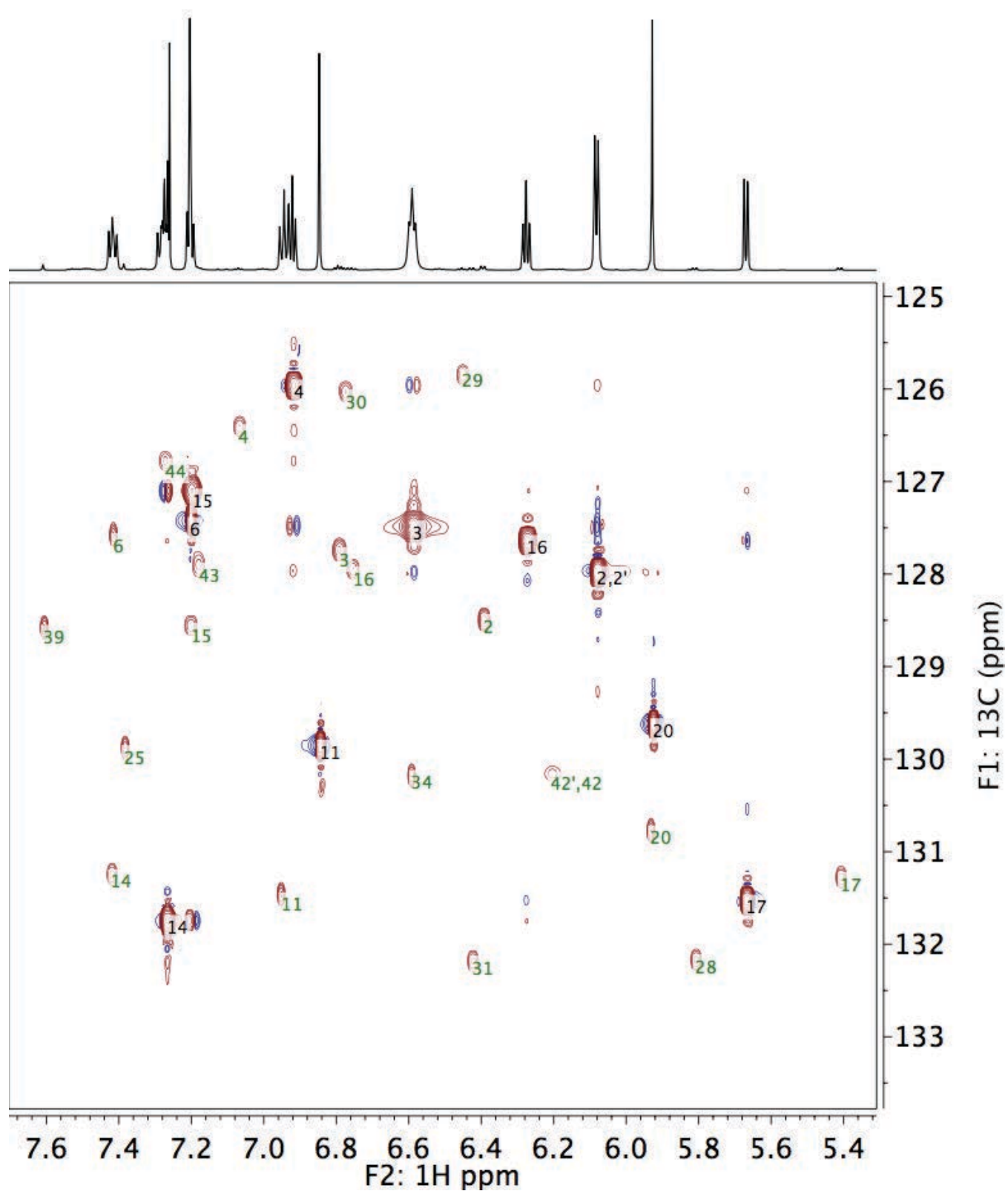


Figure S109. HSQC NMR (800 MHz) spectrum of F-Ar-3 in CDCl_3 at 0 $^\circ\text{C}$. The numbers in black and green correspond to the atom numbers of the major and minor conformers, respectively, as defined in Figure S68.

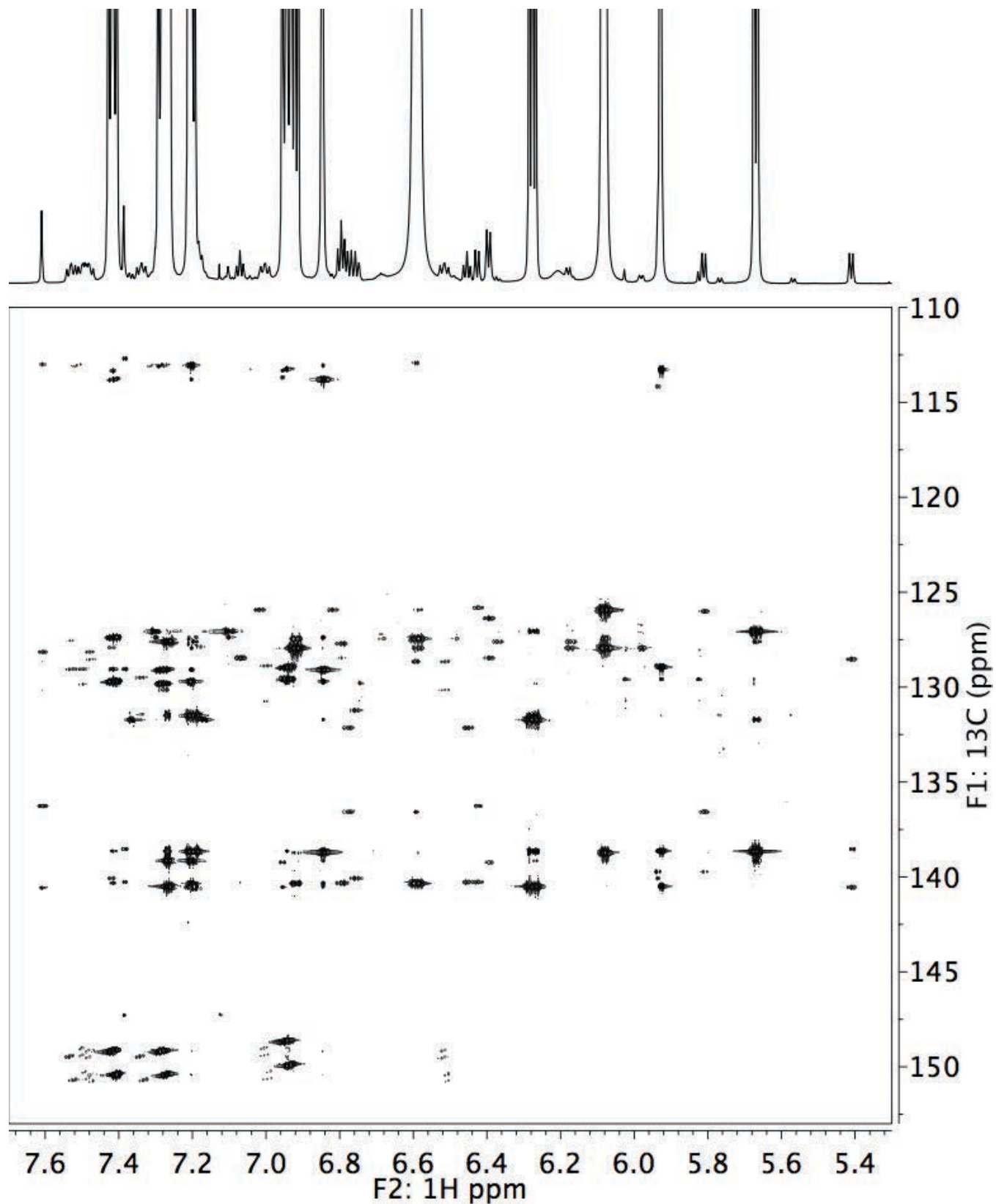


Figure S110. HMBC NMR (800 MHz) spectrum of **F-Ar-3** in CDCl_3 at 0 °C, full view.

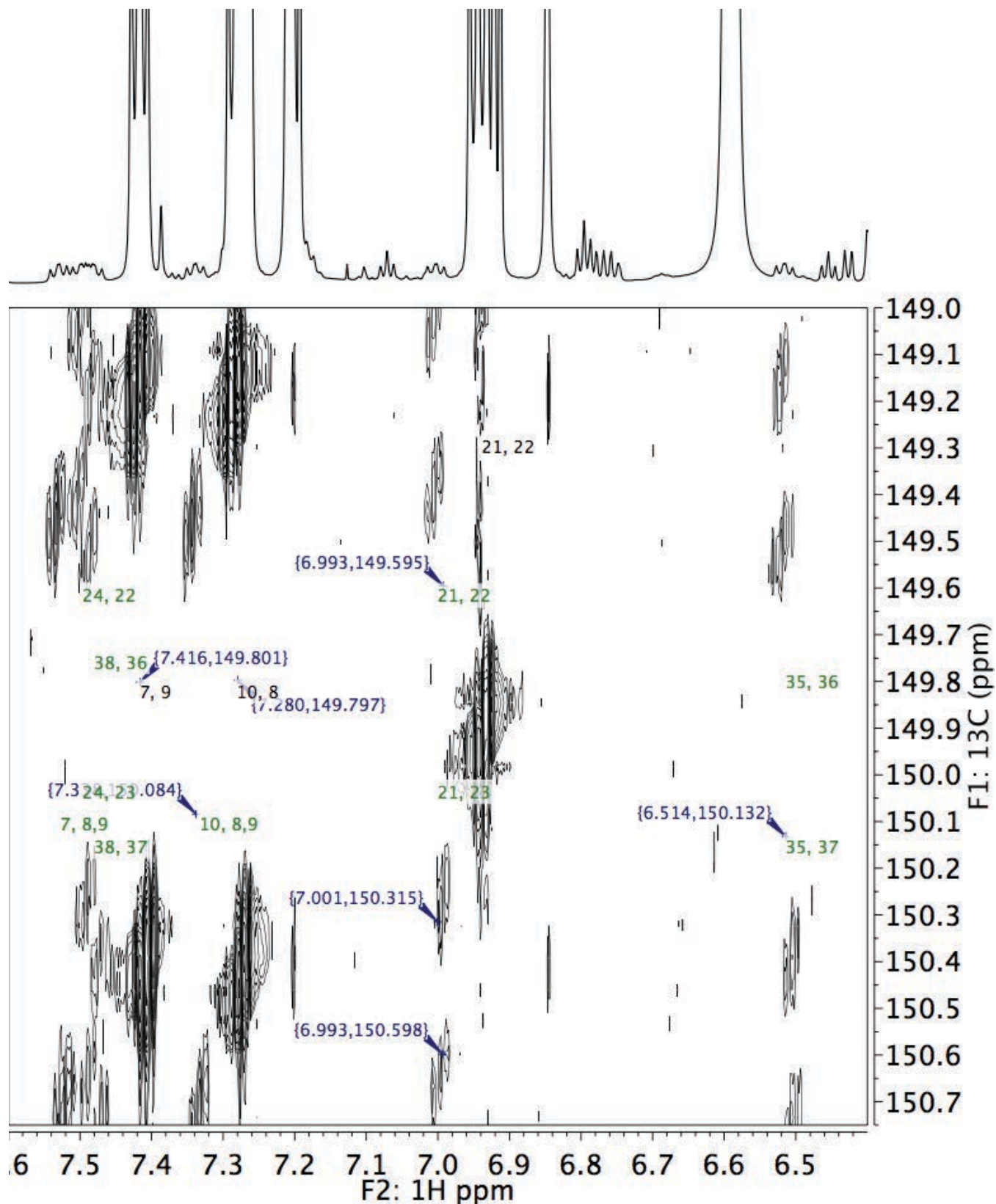


Figure S111. HMBC NMR (800 MHz) spectrum of **F-Ar-3** in CDCl_3 at 0°C ; F2: 7.60 to 6.40 vs F1: 150.75 to 149.0 ppm region. The numbers in black and green correspond to the atom numbers of the major and minor conformers, respectively, as defined in Figure S68.

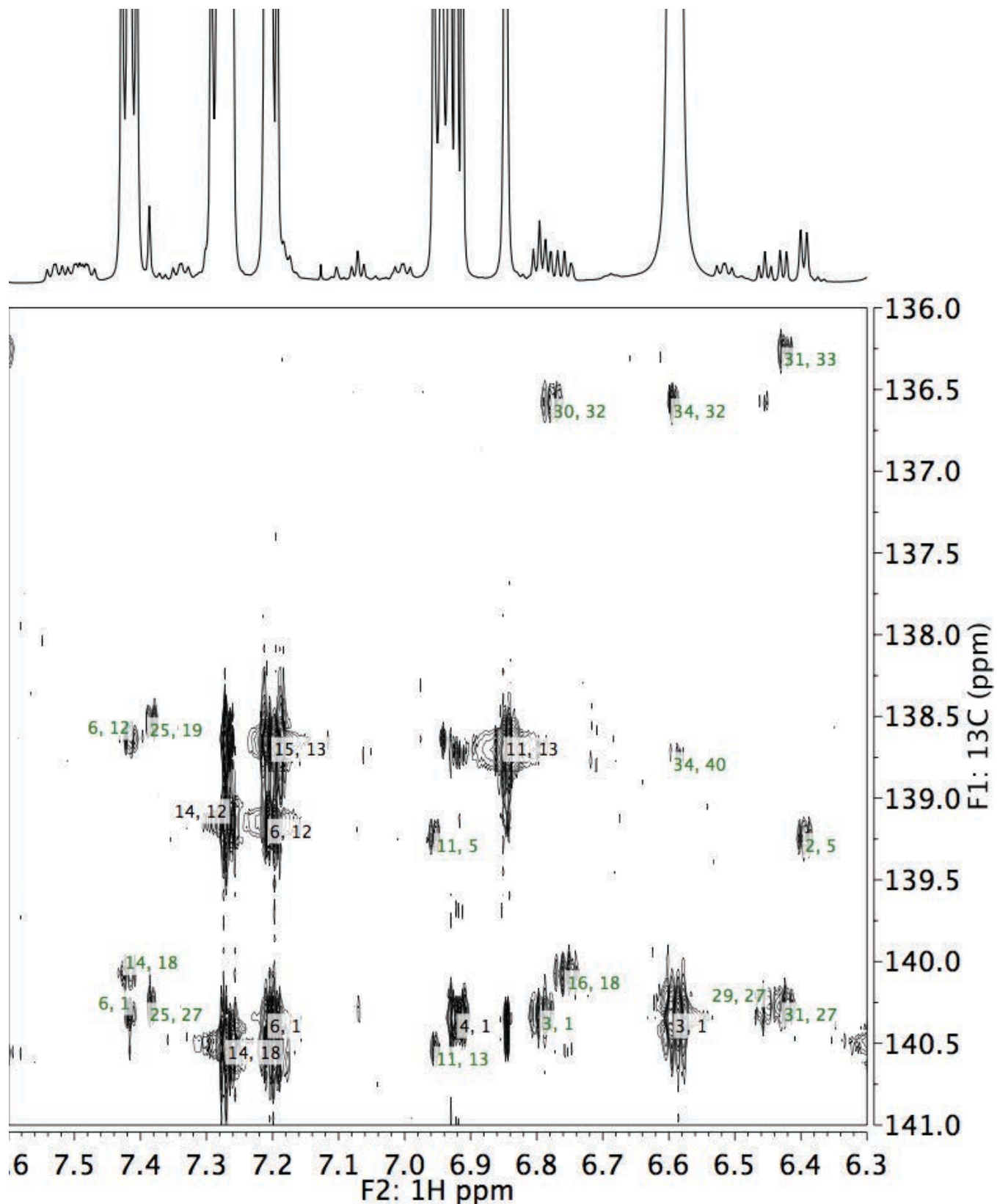


Figure S112. HMBC NMR (800 MHz) spectrum of **F-Ar-3** in CDCl_3 at 0 °C; F2: 7.60 to 6.30 vs F1: 141.0 to 136.0 ppm region. The numbers in black and green correspond to the atom numbers of the major and minor conformers, respectively, as defined in Figure S68.

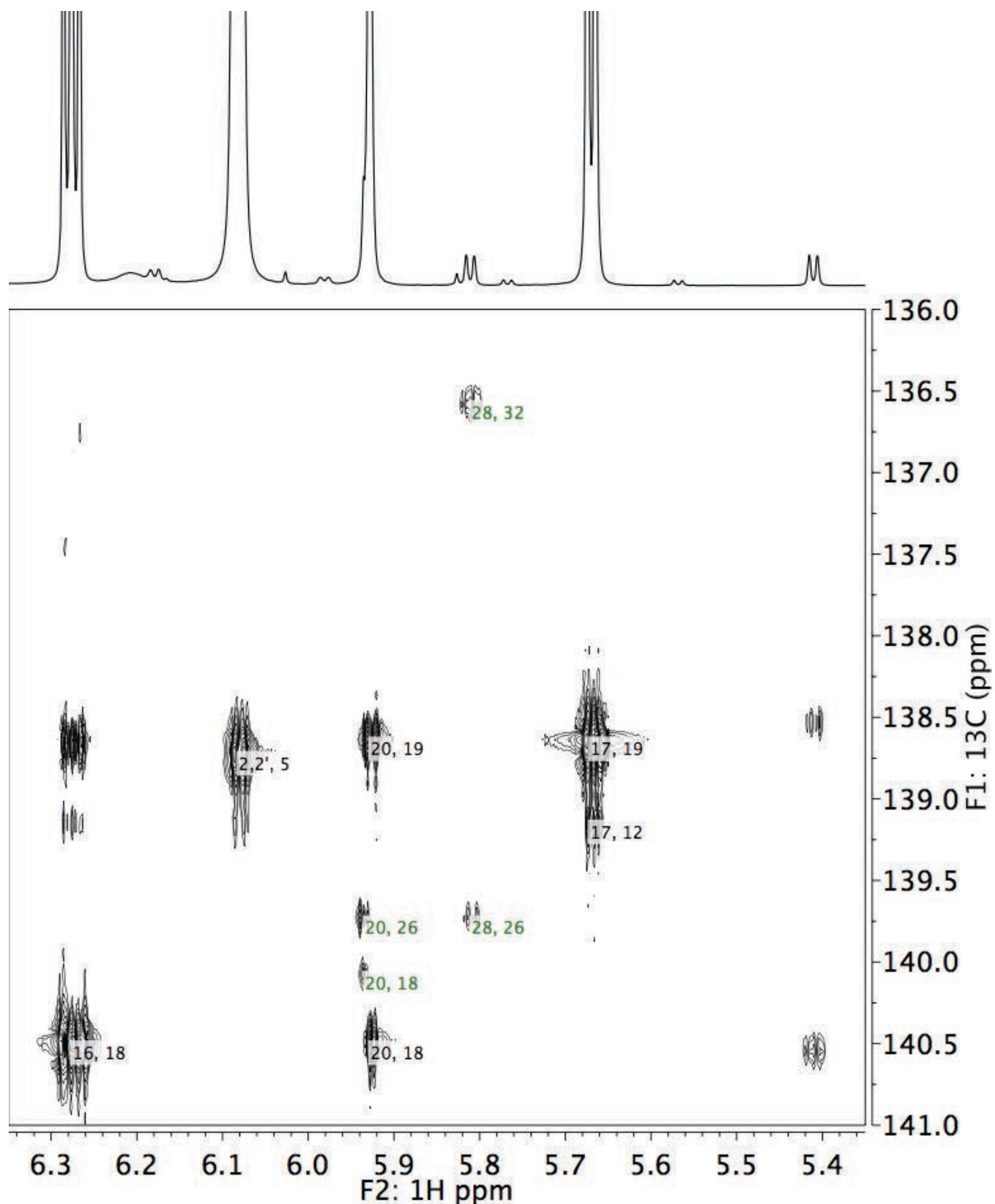


Figure S113. HMBC NMR (800 MHz) spectrum of **F-Ar-3** in CDCl_3 at 0°C ; F2: 7.60 to 6.30 vs F1: 141.0 to 136.0 ppm region. The numbers in black and green correspond to the atom numbers of the major and minor conformers, respectively, as defined in Figure S68.

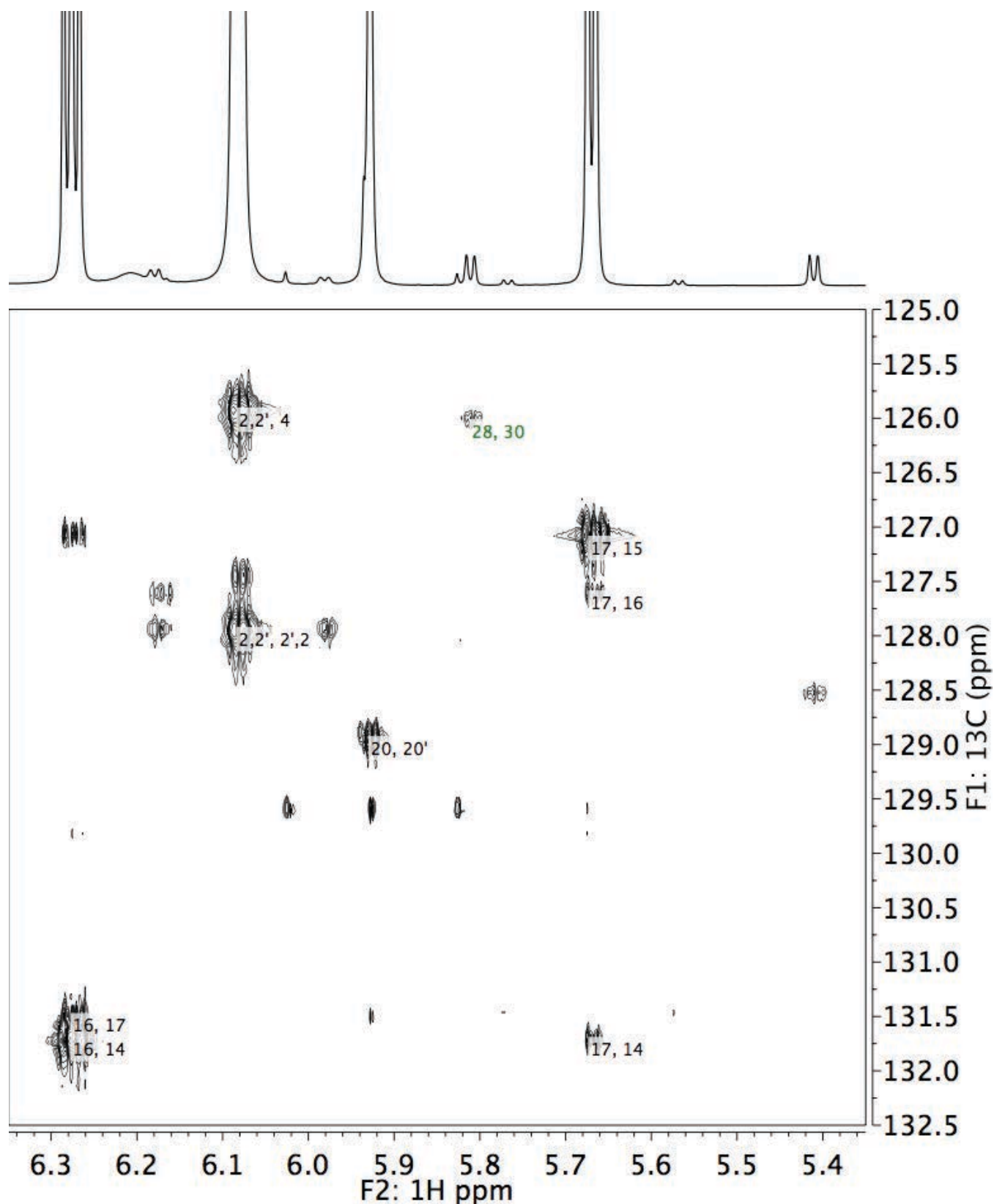


Figure S114. HMBC NMR (800 MHz) spectrum of **F-Ar-3** in CDCl_3 at 0 °C; F2: 6.35 to 5.35 vs F1: 132.5 to 125.0 ppm region. The numbers in black and green correspond to the atom numbers of the major and minor conformers, respectively, as defined in Figure S68.

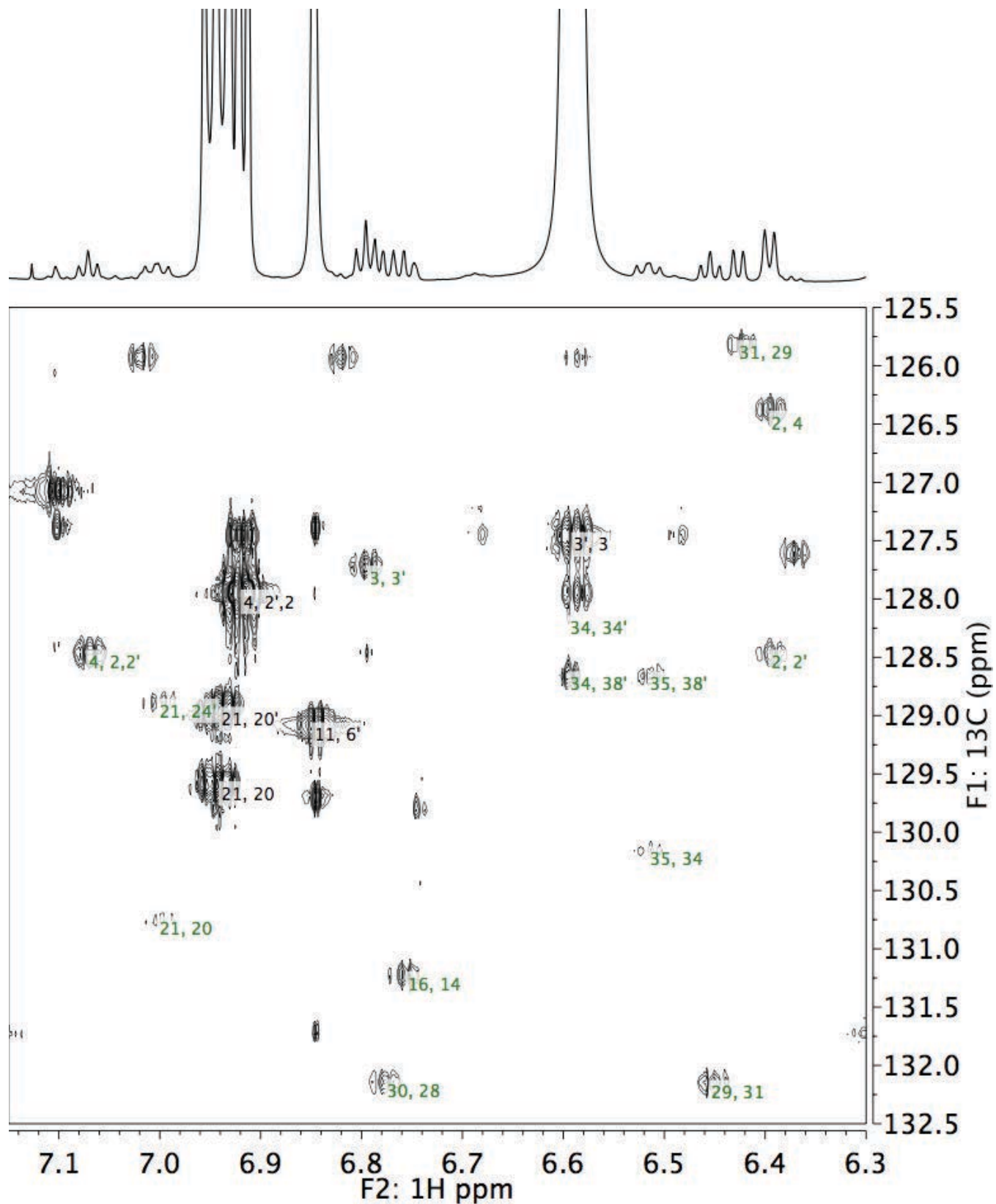


Figure S115. HMBC NMR (800 MHz) spectrum of **F-Ar-3** in CDCl_3 at 0 °C; F2: 7.15 to 6.30 vs F1: 132.5 to 125.5 ppm region. The numbers in black and green correspond to the atom numbers of the major and minor conformers, respectively, as defined in Figure S68.

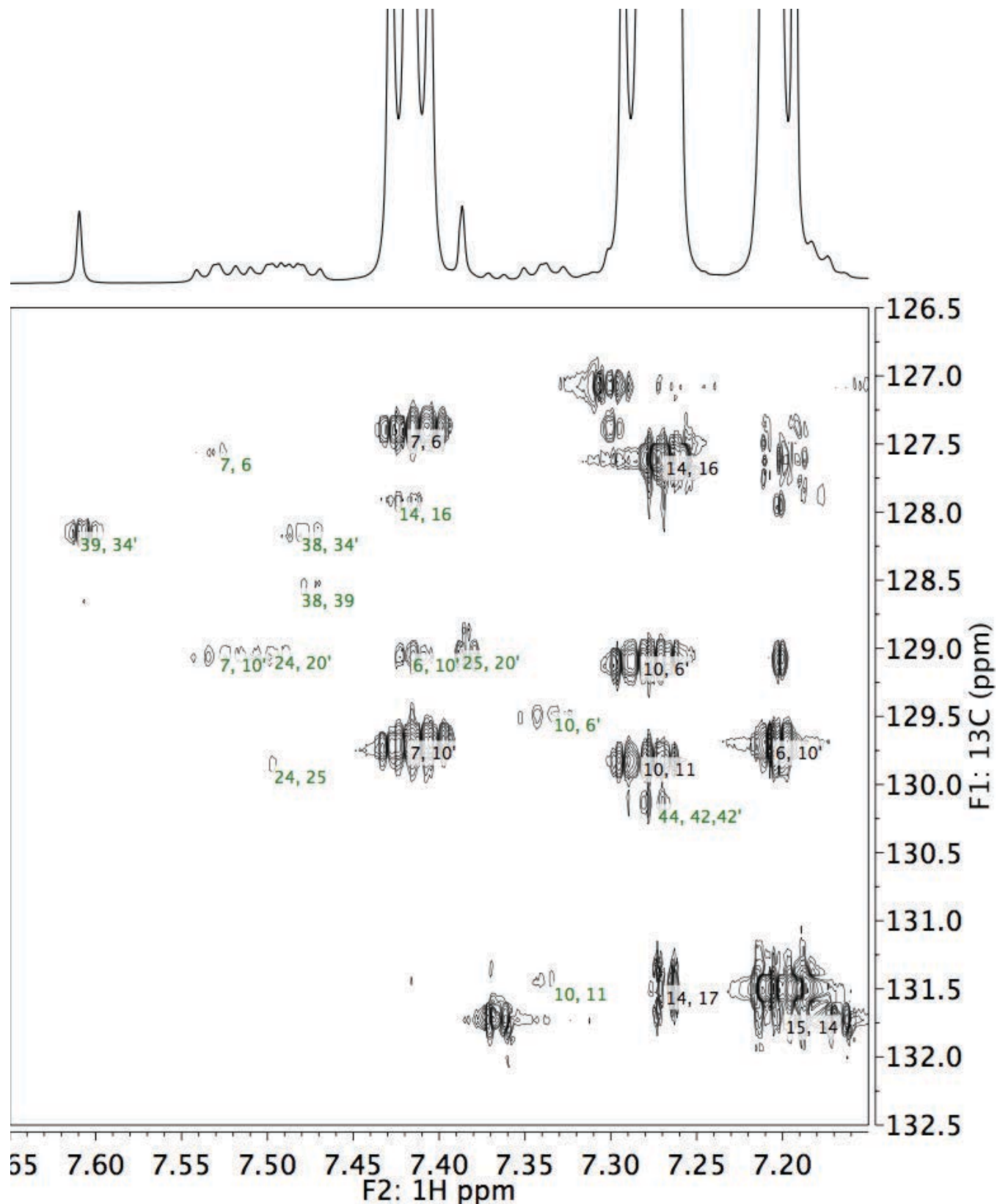


Figure S116. HMBC NMR (800 MHz) spectrum of **F-Ar-3** in CDCl_3 at 0 °C; F2: 7.65 to 7.15 vs F1: 132.5 to 126.5 ppm region. The numbers in black and green correspond to the atom numbers of the major and minor conformers, respectively, as defined in Figure S68.

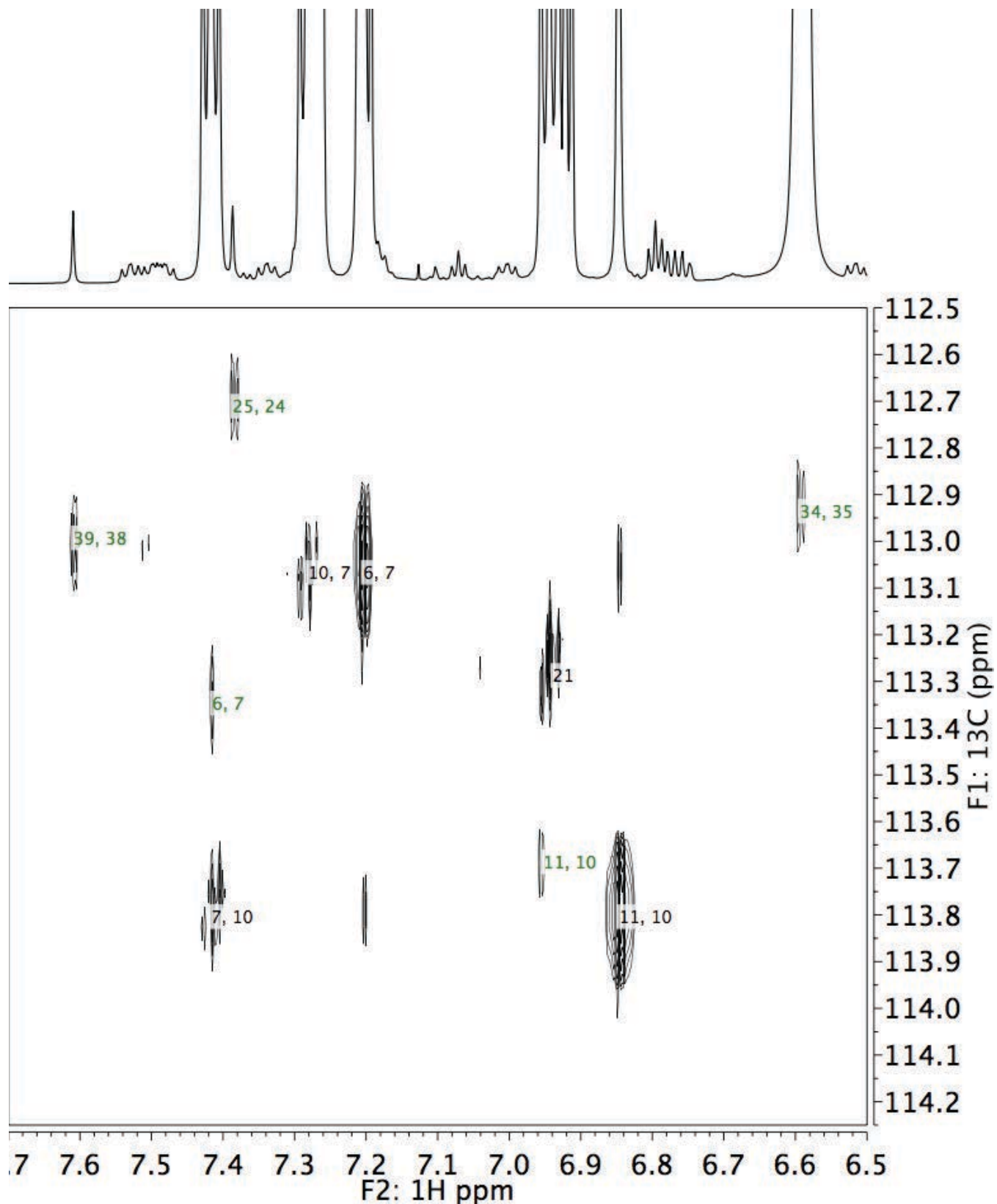


Figure S117. HMBC NMR (800 MHz) spectrum of **F-Ar-3** in CDCl₃ at 0 °C; F2: 7.570 to 6.50 vs F1: 114.25 to 112.50 ppm region. The numbers in black and green correspond to the atom numbers of the major and minor conformers, respectively, as defined in Figure S68.

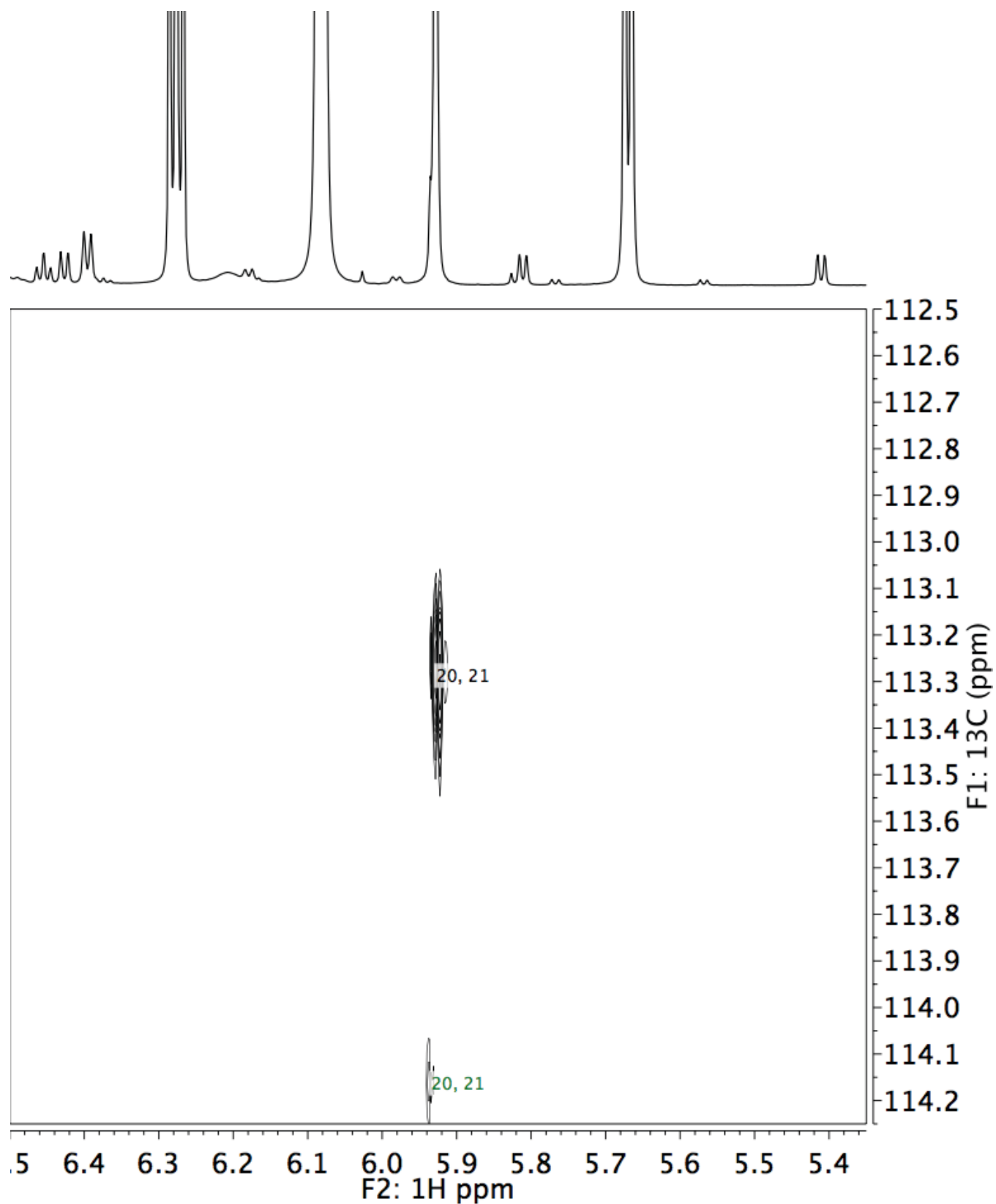


Figure S118. HMBC NMR (800 MHz) spectrum of **F-Ar-3** in CDCl_3 at 0 °C; F2: 6.50 to 5.35 vs F1: 114.25 to 112.50 ppm region. The numbers in black and green correspond to the atom numbers of the major and minor conformers, respectively, as defined in Figure S68.

9.8 1-D and 2-D NMR Spectra of X-Ar-4

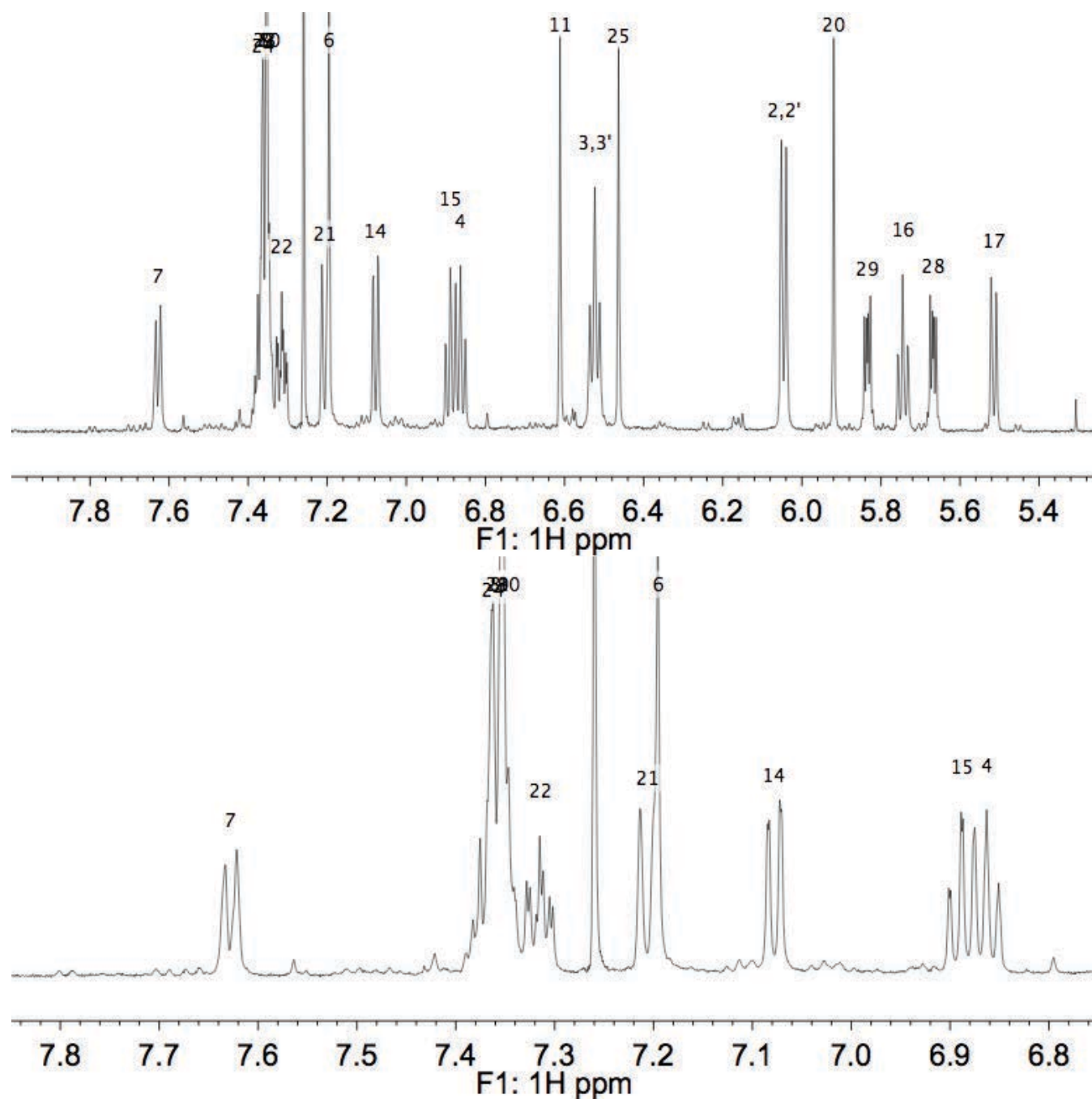


Figure S119. ¹H NMR (600 MHz) spectrum of **H-Ar-4** in CDCl₃ at 0 °C: (top) full view, (bottom) 8.00 to 6.75 ppm region. The numbers in black numbers correspond to the atom numbers of the major conformer as defined in Figure S69.

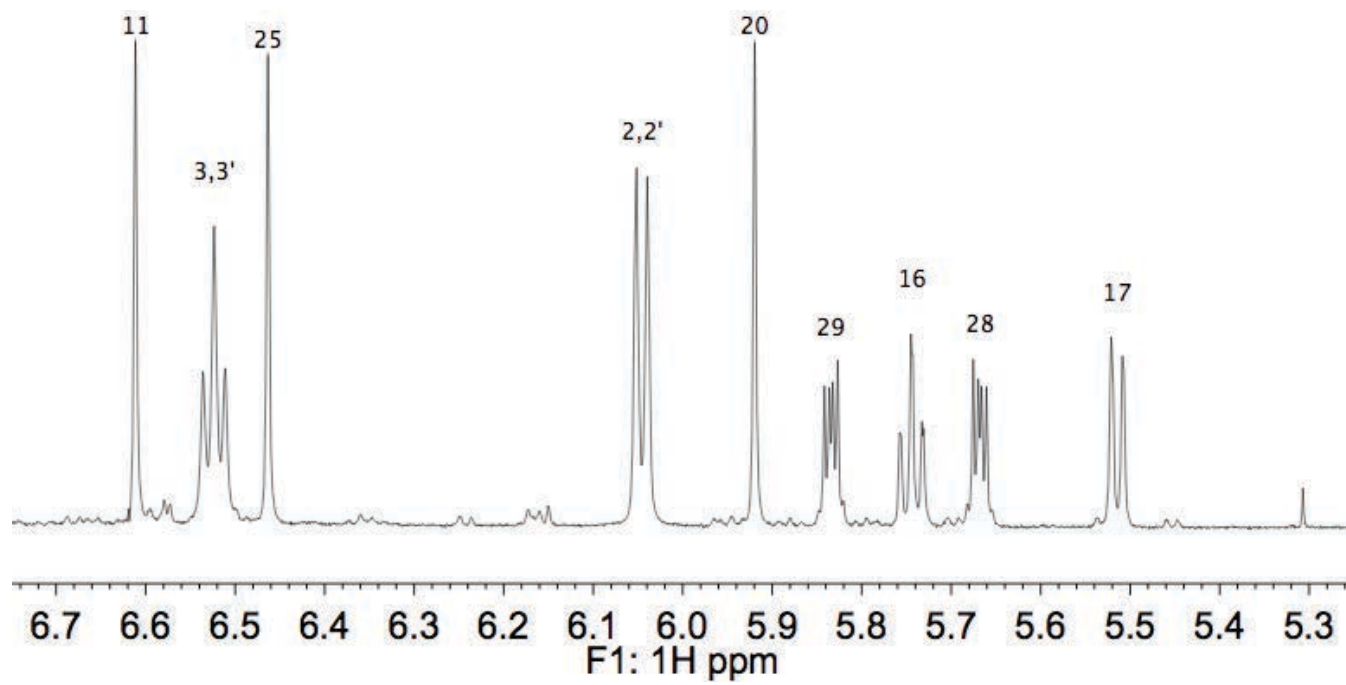


Figure S119 (continued). ¹H NMR (600 MHz) spectrum of **H-Ar-4** in CDCl₃ at 0 °C, 6.75 to 5.25 ppm region. The numbers in black correspond to the atom numbers of the major conformer as defined in Figure S69.

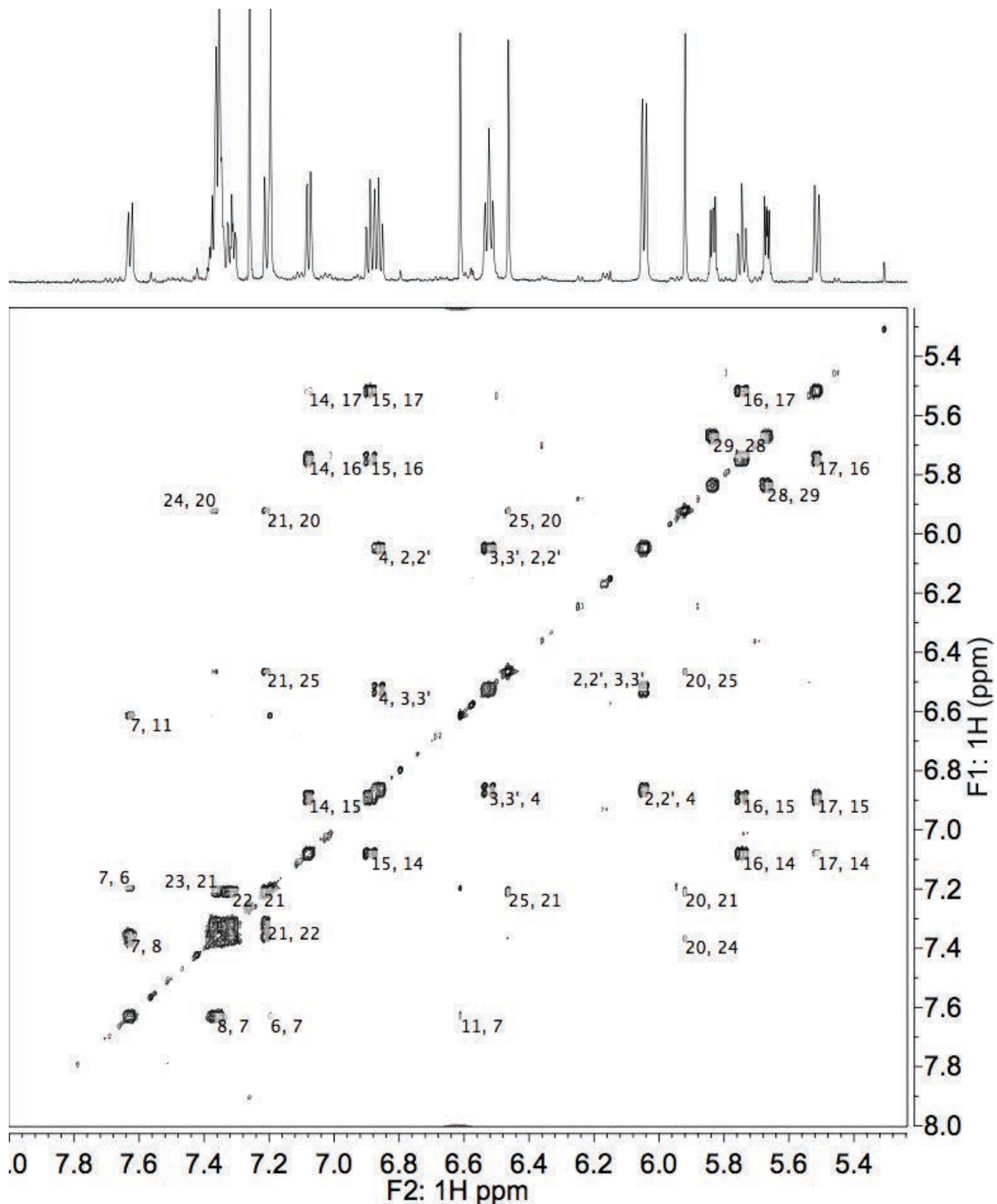


Figure S120. COSY NMR (600 MHz) spectrum of **H-Ar-4** in CDCl_3 at 0 °C, full view. The numbers in black correspond to the atom numbers of the major conformer as defined in Figure S69.

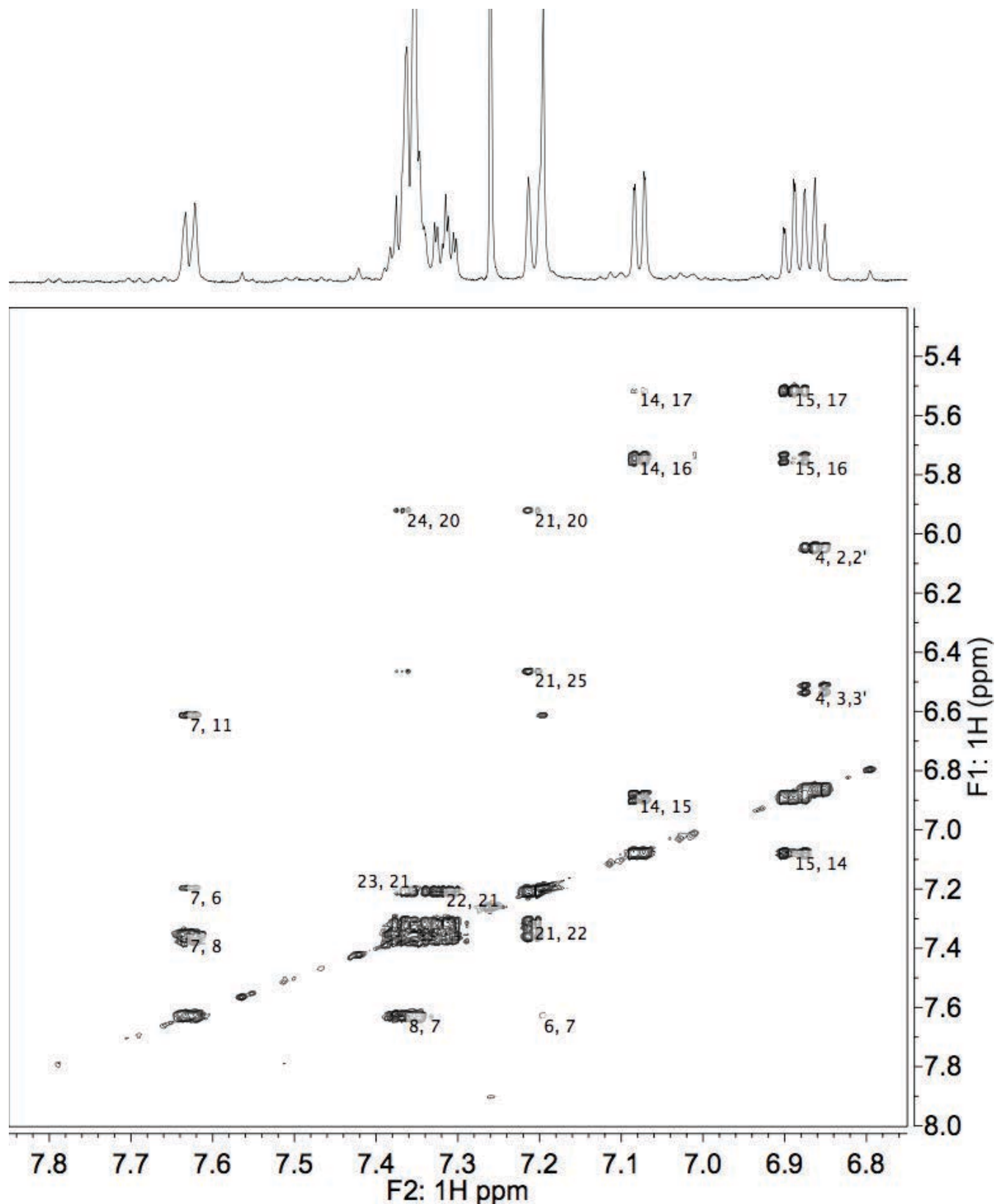


Figure S121. COSY NMR (600 MHz) spectrum of **H-Ar-4** in CDCl₃ at 0 °C, 7.85 to 6.75 ppm region. The numbers in black correspond to the atom numbers of the major conformer as defined in Figure S69.

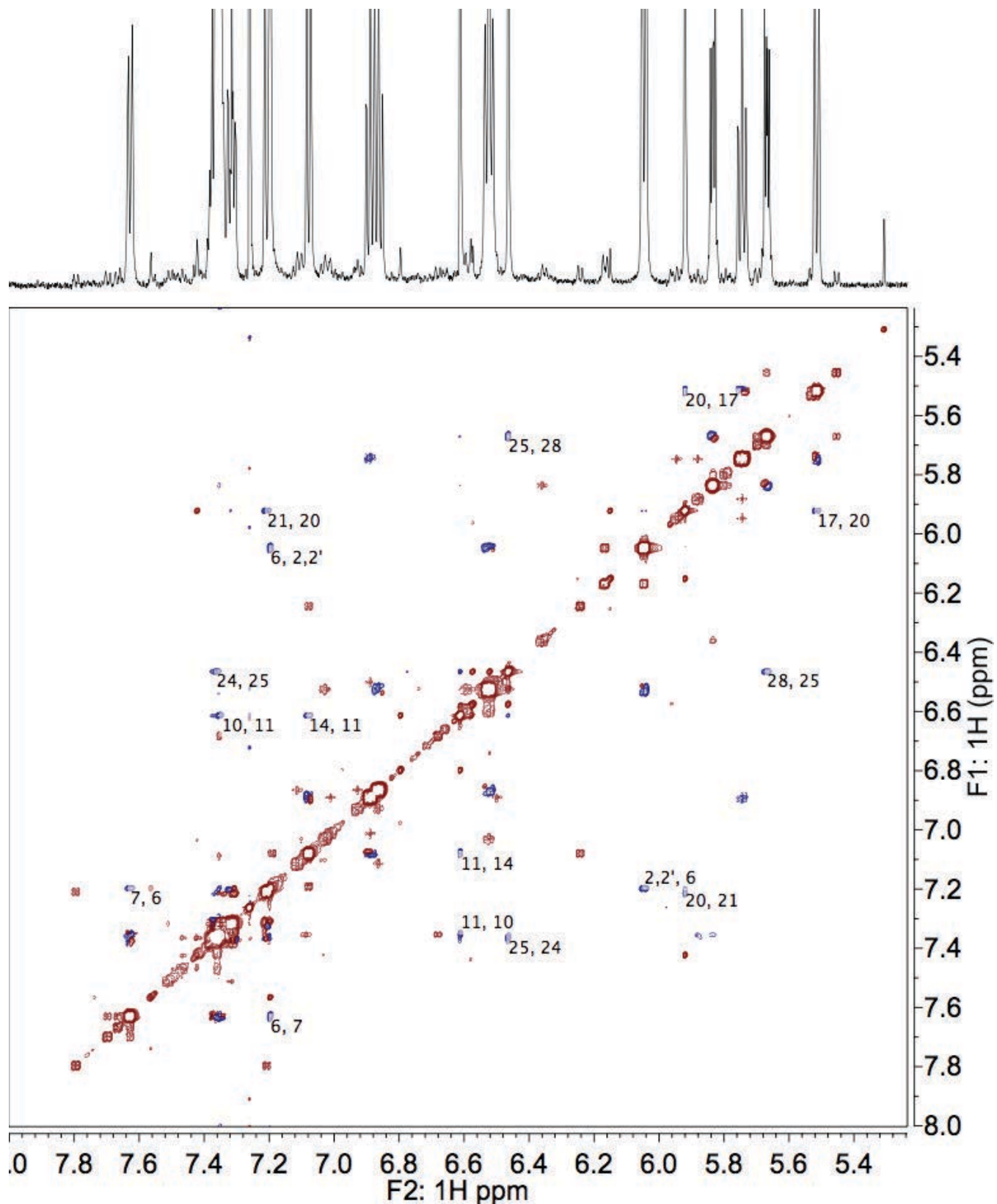


Figure S122. NOESY NMR (600 MHz) spectrum of **H-Ar-4** in CDCl_3 at 0°C (spectral expansions are shown in the ROSEY NMR assignment section).

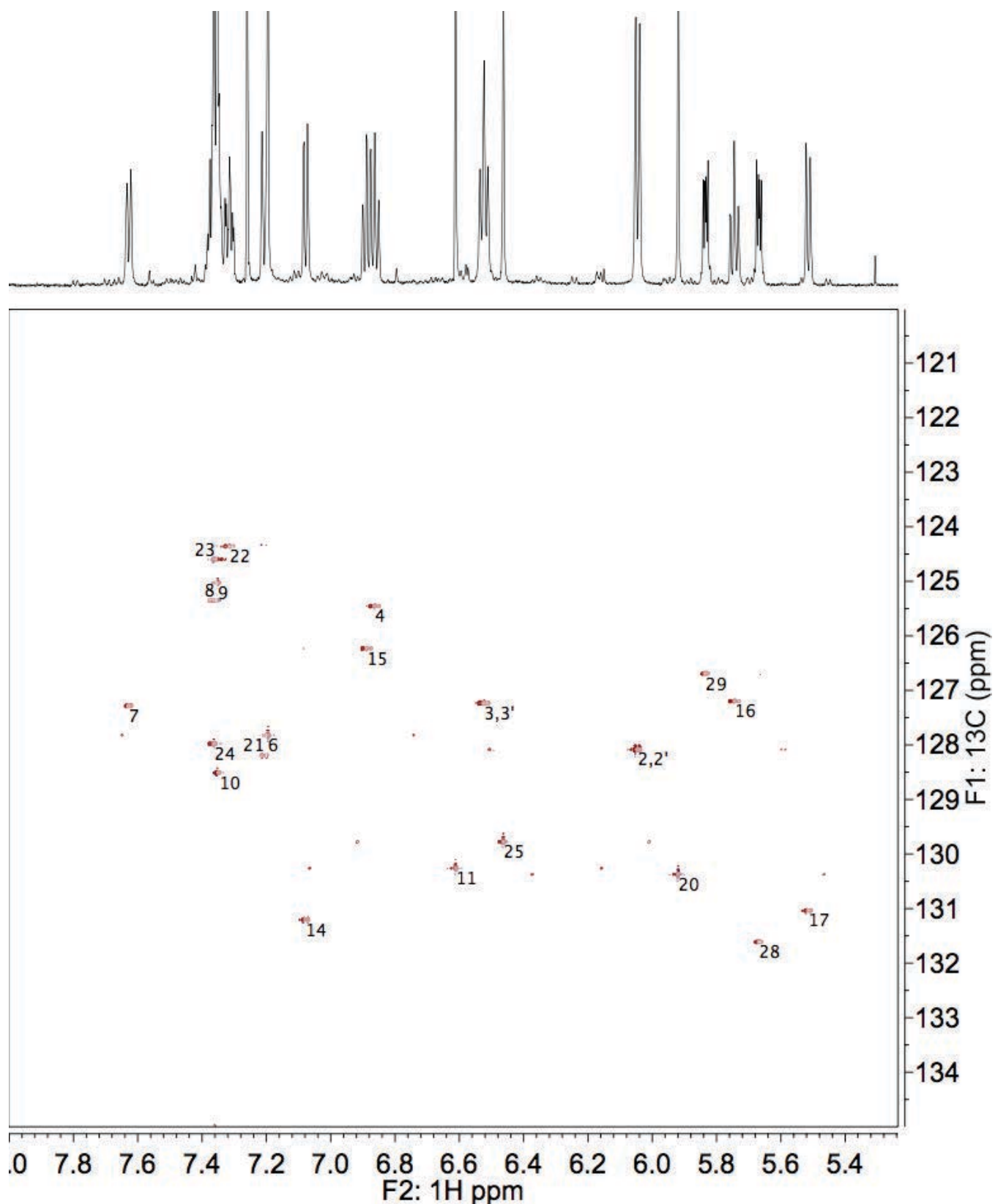


Figure S123. HSQC NMR (800 MHz) spectrum of **H-Ar-4** in CDCl_3 at 0 °C. The numbers in black correspond to the atom numbers of the major conformers, as defined in Figure S69.

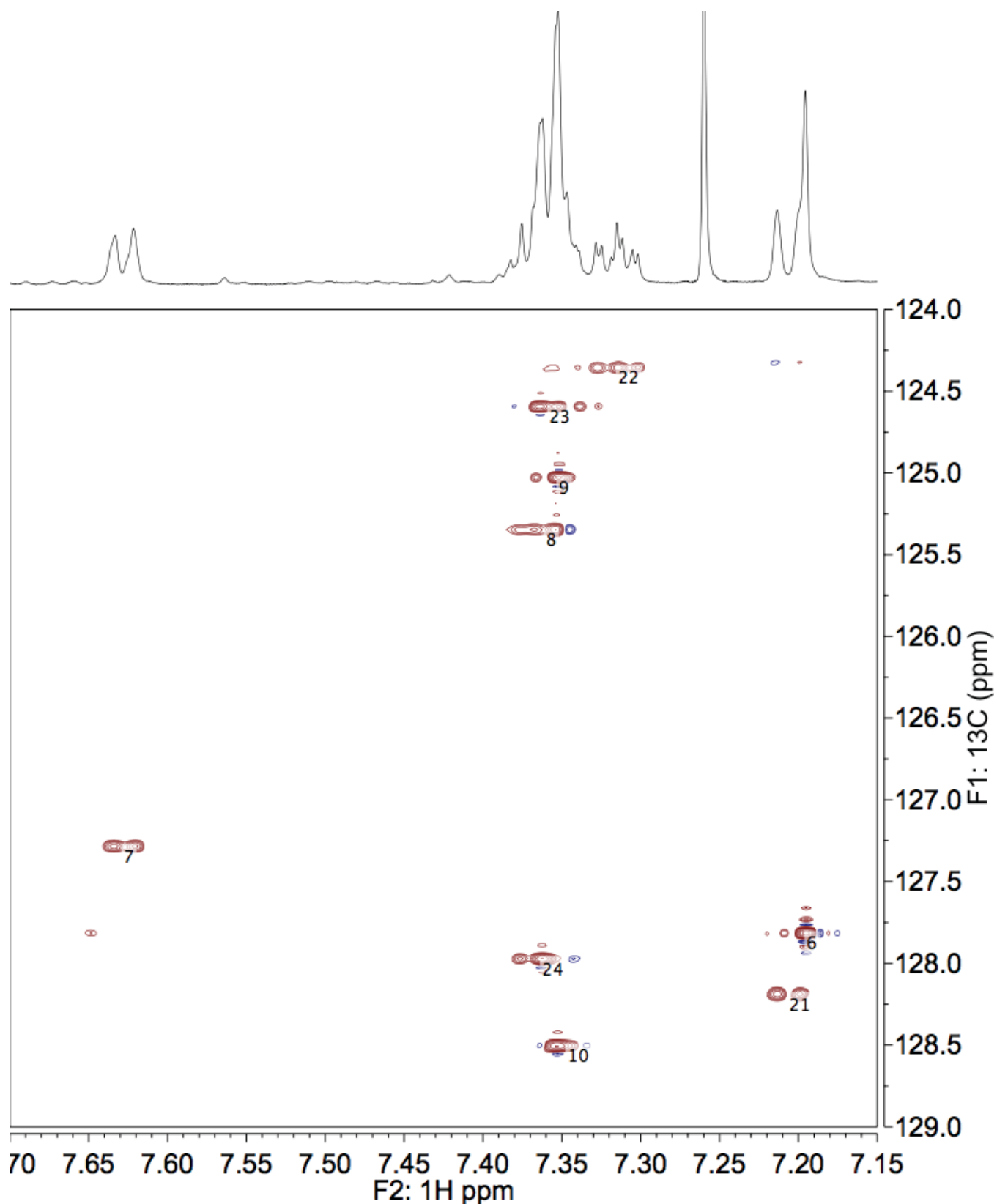


Figure S124. HSQC NMR (800 MHz) spectrum of **H-Ar-4** in CDCl_3 at 0 °C, F2: 7.85 to 7.15 ppm, F1: 124.0 to 129.0 ppm region. The numbers in black correspond to the atom numbers of the major conformers, as defined in Figure S69.

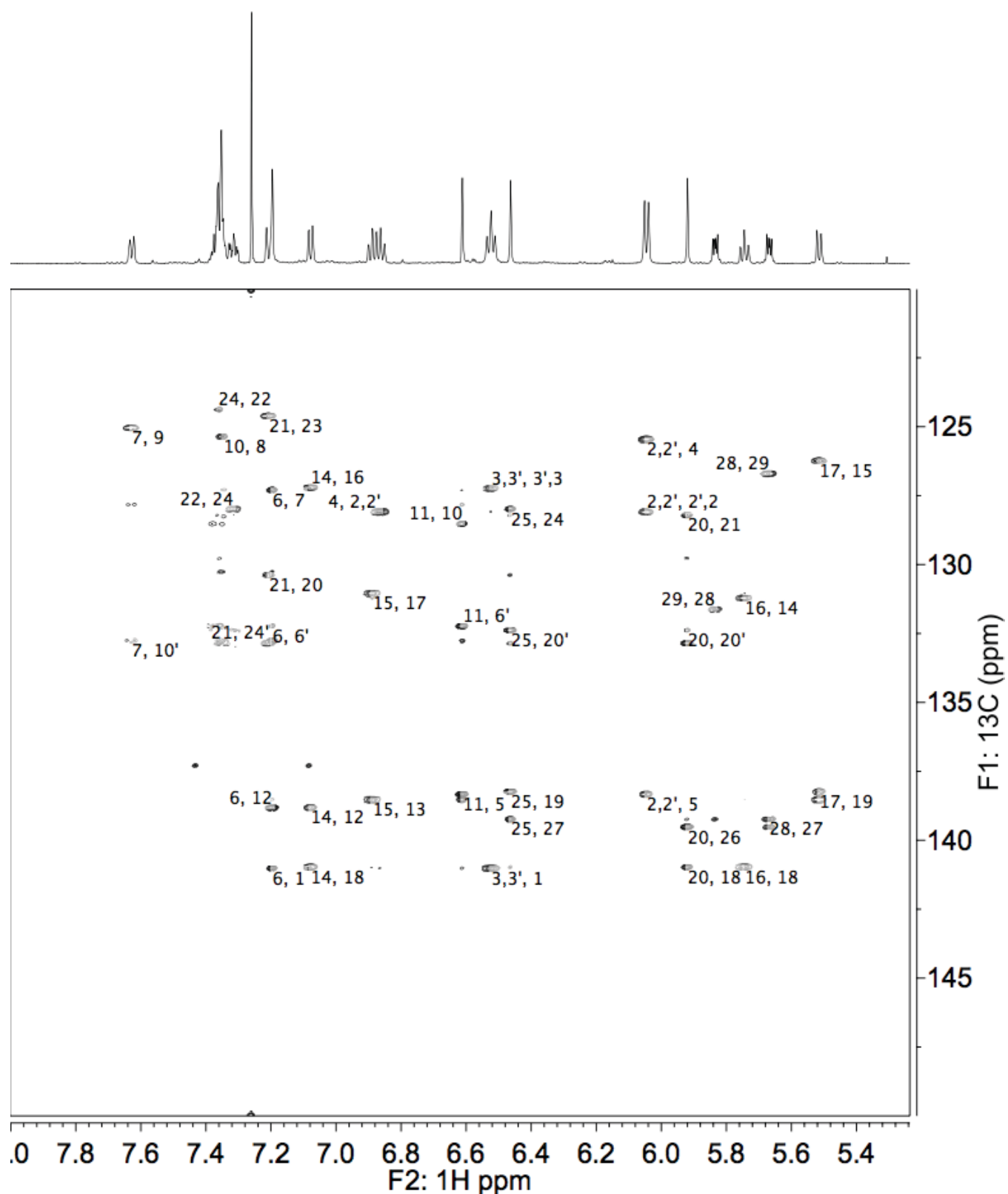


Figure S125. HMBC NMR (800 MHz) spectrum of **H-Ar-4** in CDCl_3 at 0°C , full view.

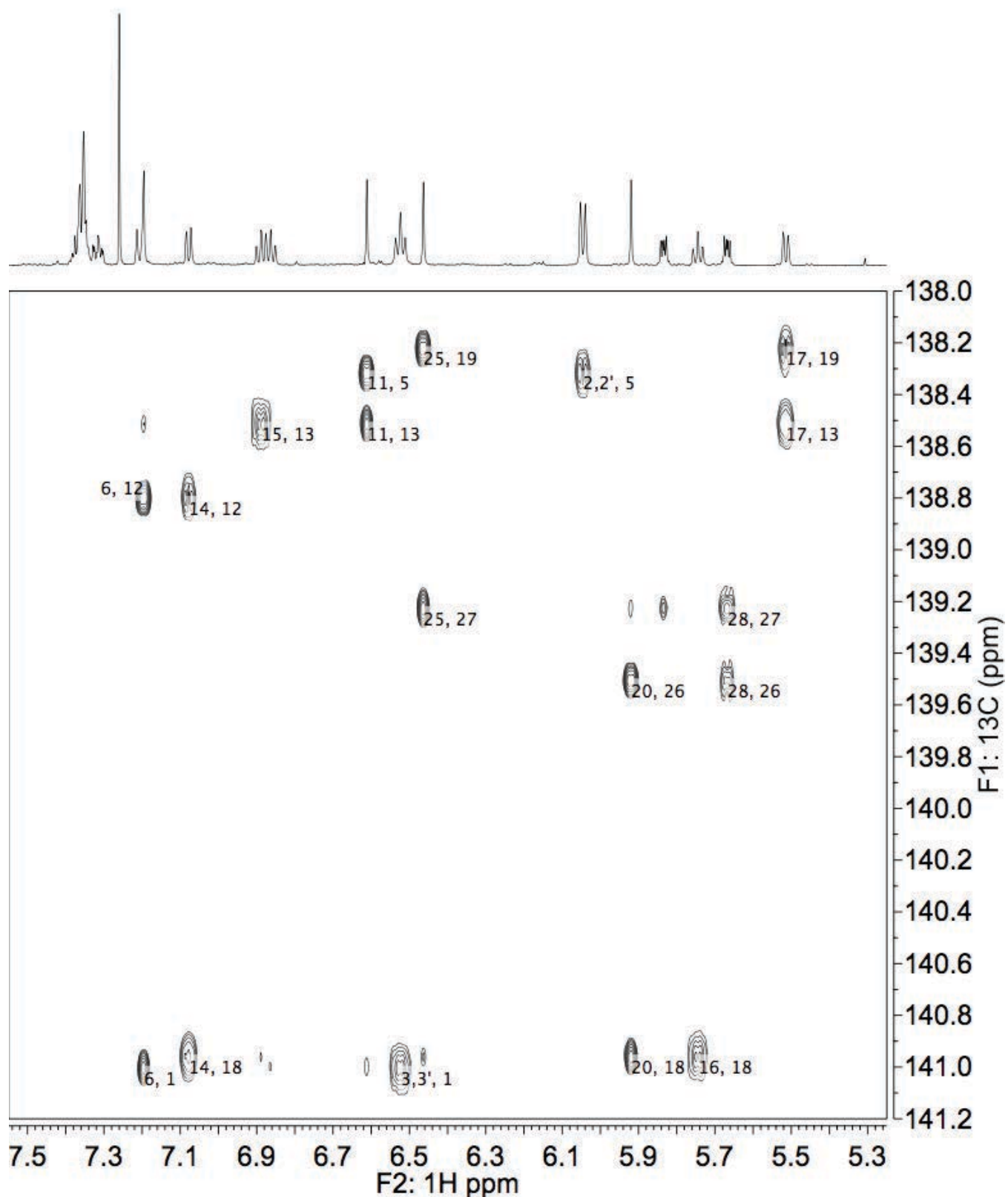


Figure S126. HMBC NMR (800 MHz) spectrum of **H-Ar-4** in CDCl_3 at 0 °C, δ_{H} 7.55 to 5.25 ppm and δ_{C} 141.2 to 138.0 ppm region. The numbers in black correspond to the atom numbers of the major conformer as defined in Figure S69.

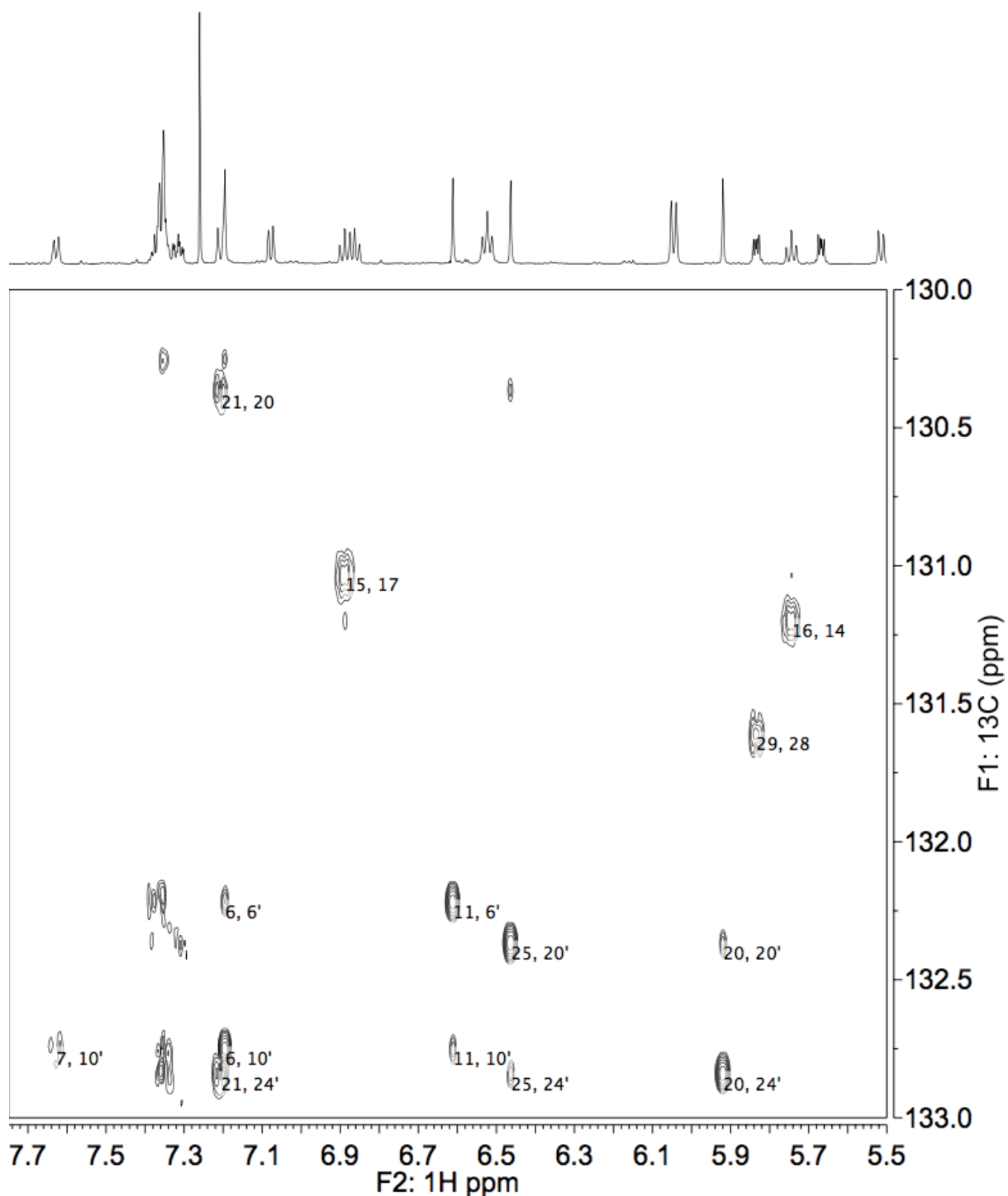


Figure S127. HMBC NMR (800 MHz) spectrum of **H-Ar-4** in CDCl₃ at 0 °C, δ_{H} 7.75 to 5.55 ppm and δ_{C} 133.0 to 130.0 ppm region. The numbers in black correspond to the atom numbers of the major conformer as defined in Figure S69.

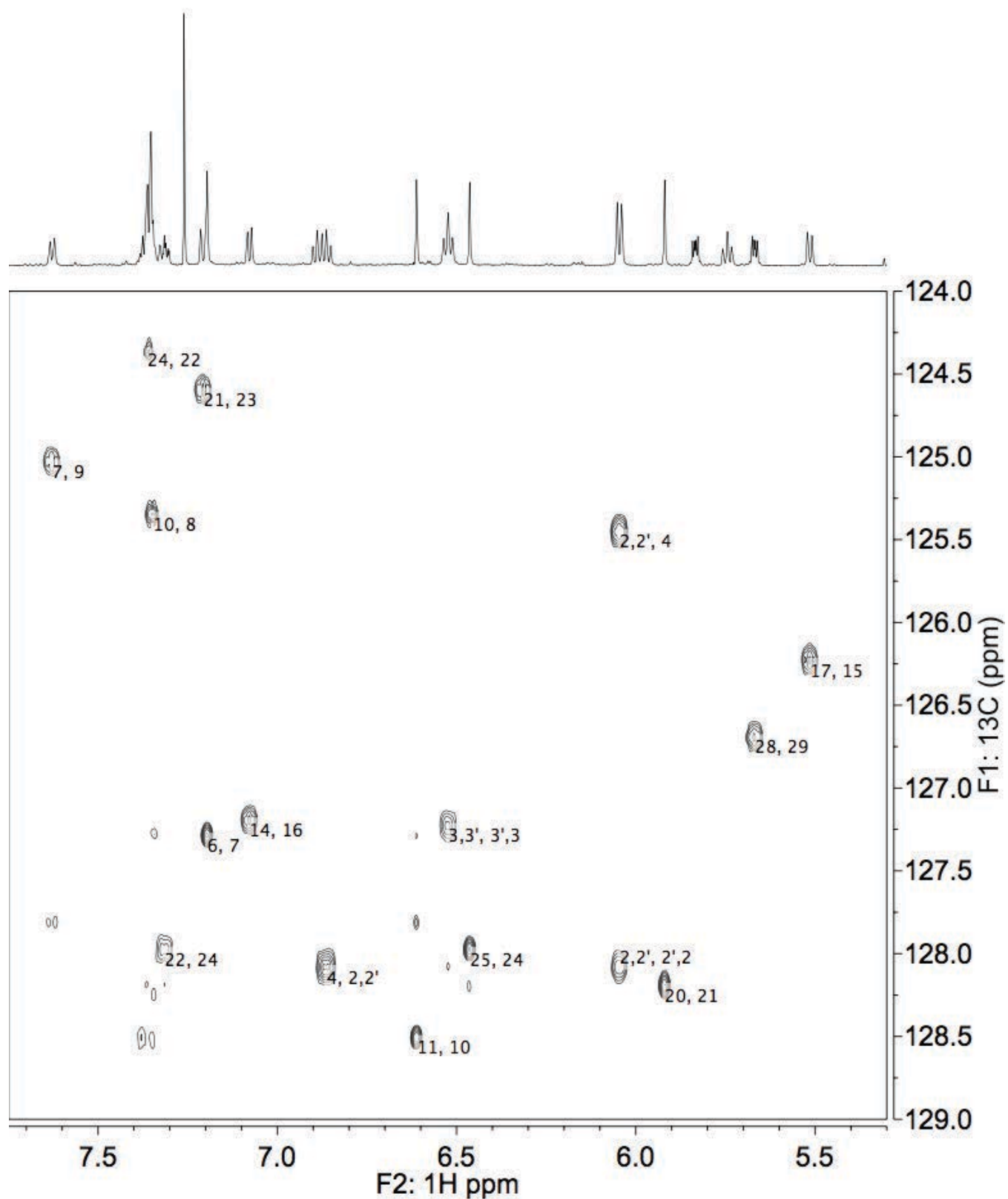


Figure S128. HMBC NMR (800 MHz) spectrum of **H-Ar-4** in CDCl_3 at 0 °C, δ_{H} 7.75 to 5.30 ppm and δ_{C} 129.0 to 124.0 ppm region. The numbers in black correspond to the atom numbers of the major conformer as defined in Figure S69.

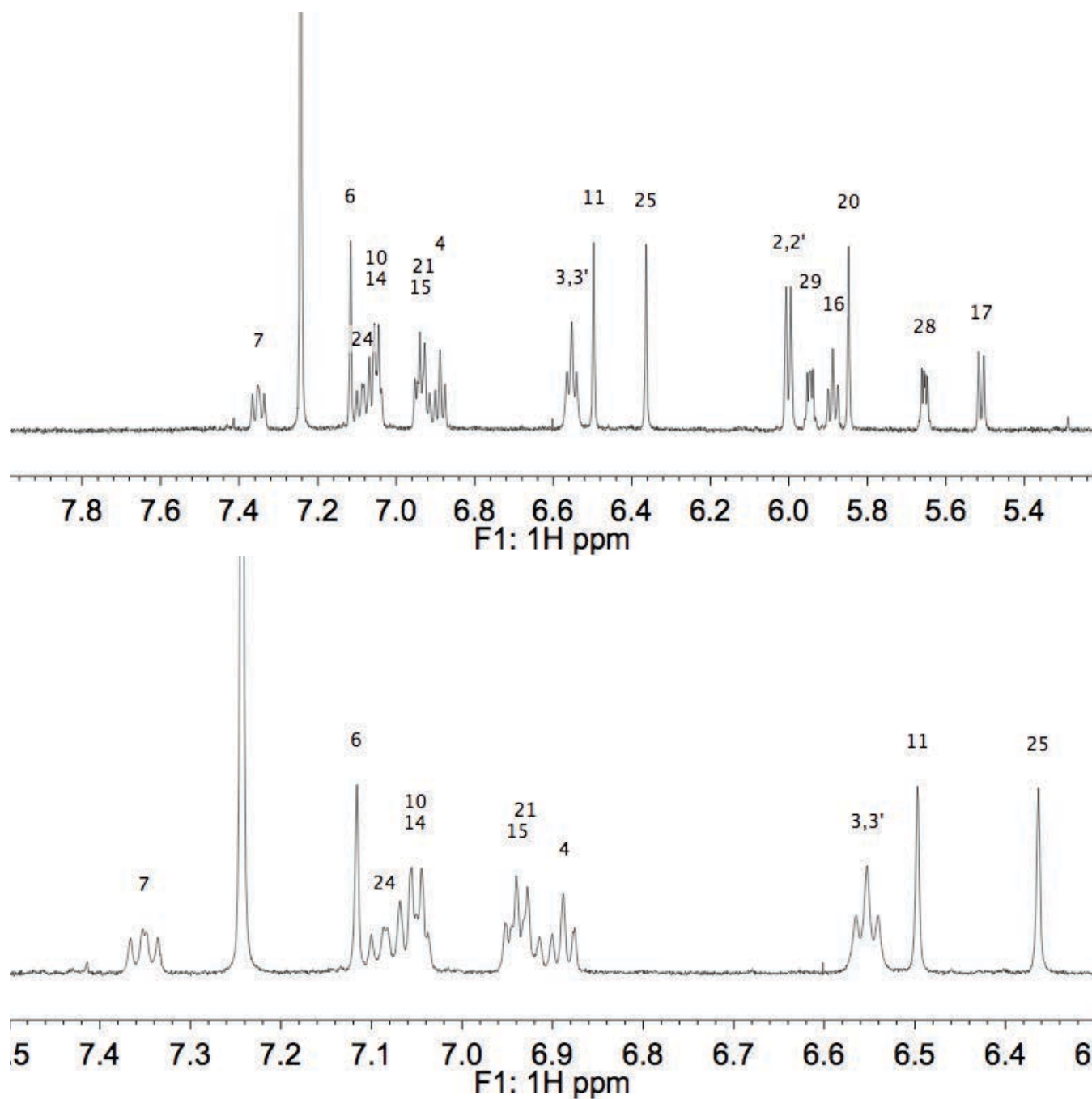


Figure S129. ^1H NMR (600 MHz) spectrum of F-Ar-4 in CDCl_3 at 0 °C: (top) full view, (bottom) 7.50 to 6.30 ppm region. The numbers in black numbers correspond to the atom numbers of the major conformer as defined in Figure S69.

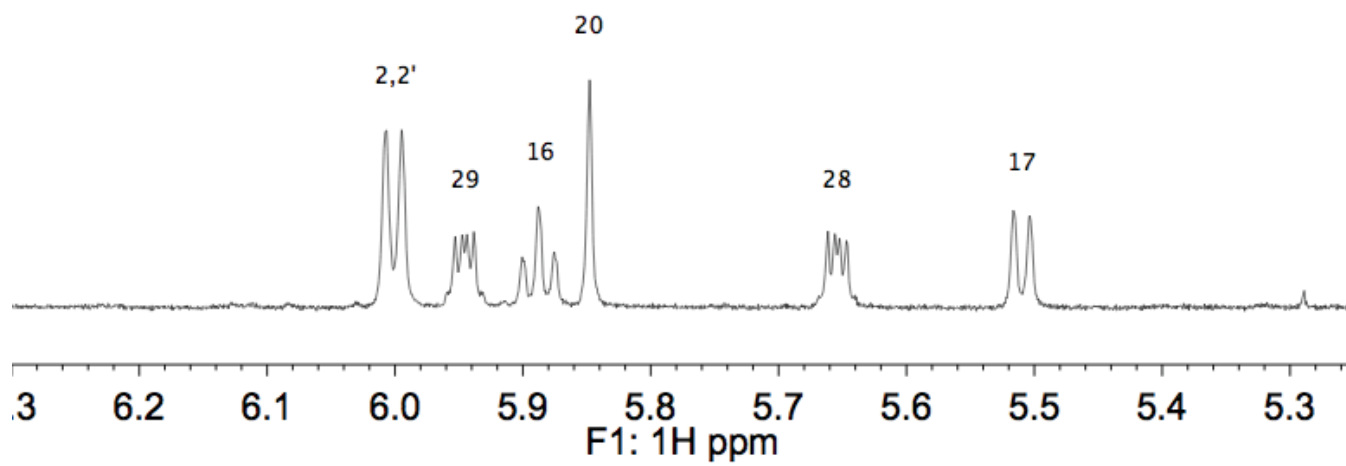


Figure S129 (continued). ¹H NMR (600 MHz) spectrum of **F-Ar-4** in CDCl₃ at 0 °C, 6.30 to 5.25 ppm region. The numbers in black correspond to the atom numbers of the major conformer as defined in Figure S69.

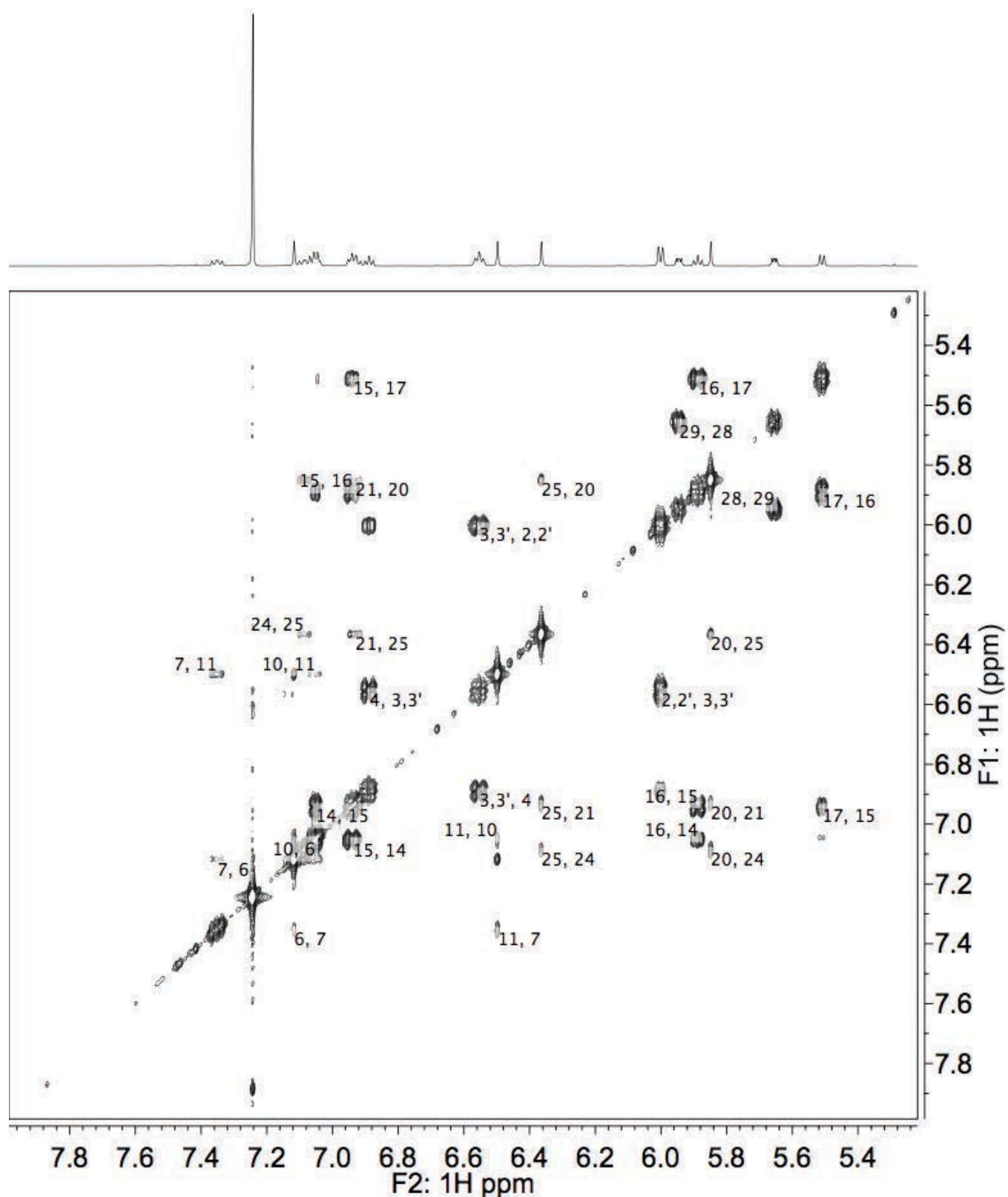


Figure S130. COSY NMR (600 MHz) spectrum of F-Ar-4 in CDCl₃ at 0 °C, full view. The numbers in black correspond to the atom numbers of the major conformer as defined in Figure S69.

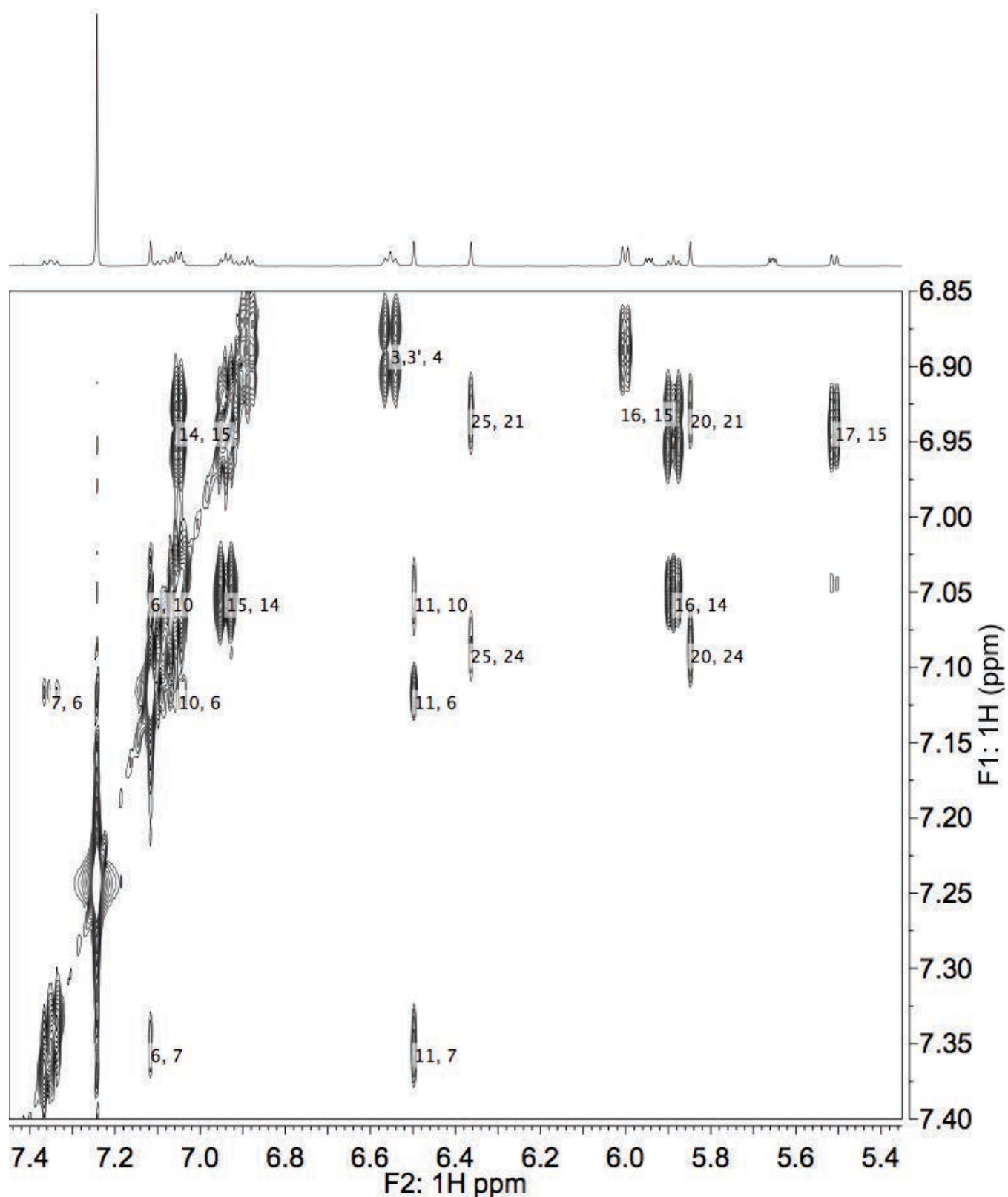


Figure S131. COSY NMR (600 MHz) spectrum of **F-Ar-4** in CDCl₃ at 0 °C, F2: 7.45 to 7.35 ppm, F1: 7.40 to 6.85 ppm region. The numbers in black correspond to the atom numbers of the major conformer as defined in Figure S69.

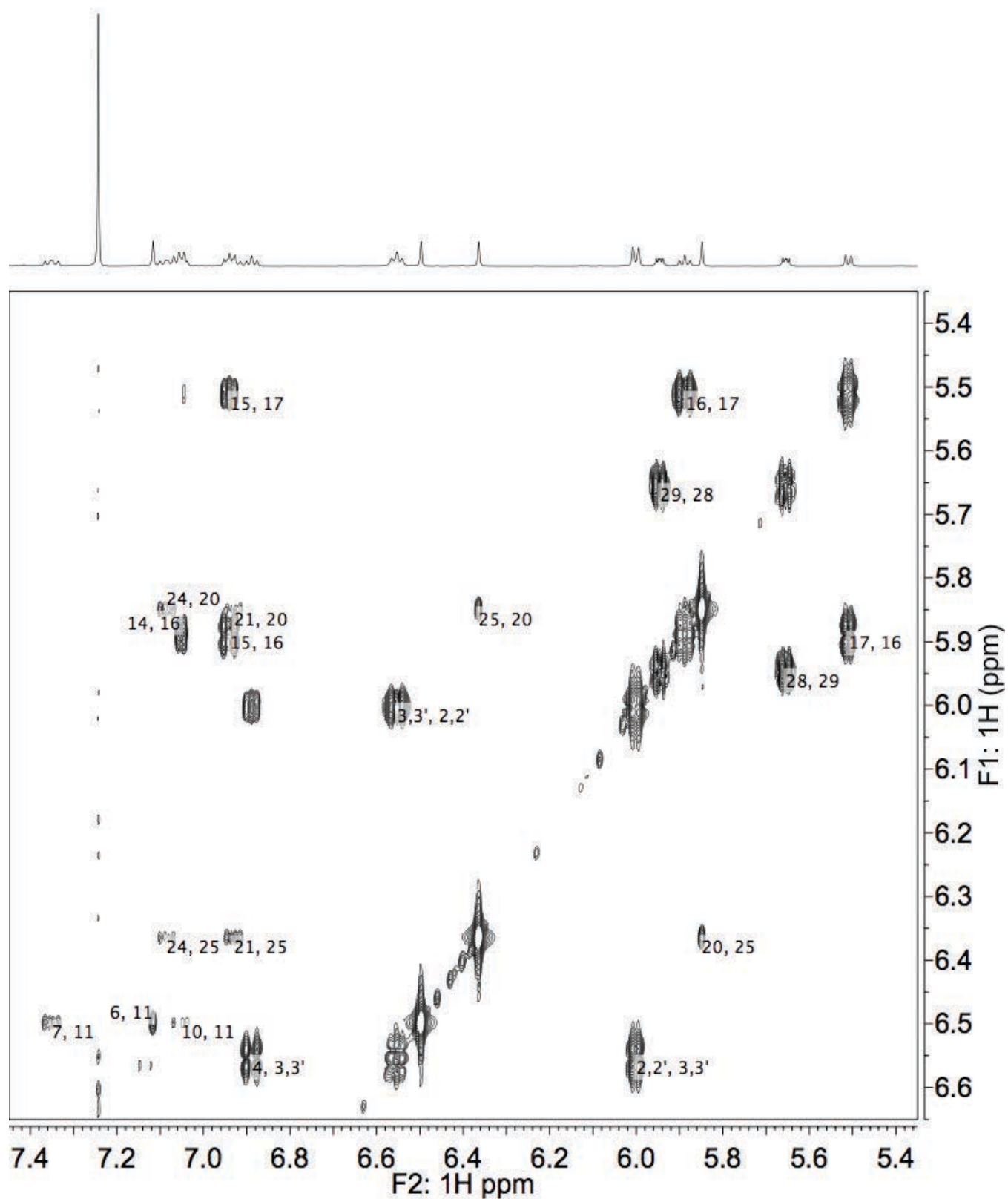


Figure S132. COSY NMR (600 MHz) spectrum of **F-Ar-4** in CDCl_3 at 0 °C, F2: 7.45 to 7.35 ppm, F1: 6.65 to 5.35 ppm region. The numbers in black correspond to the atom numbers of the major conformer as defined in Figure S69.

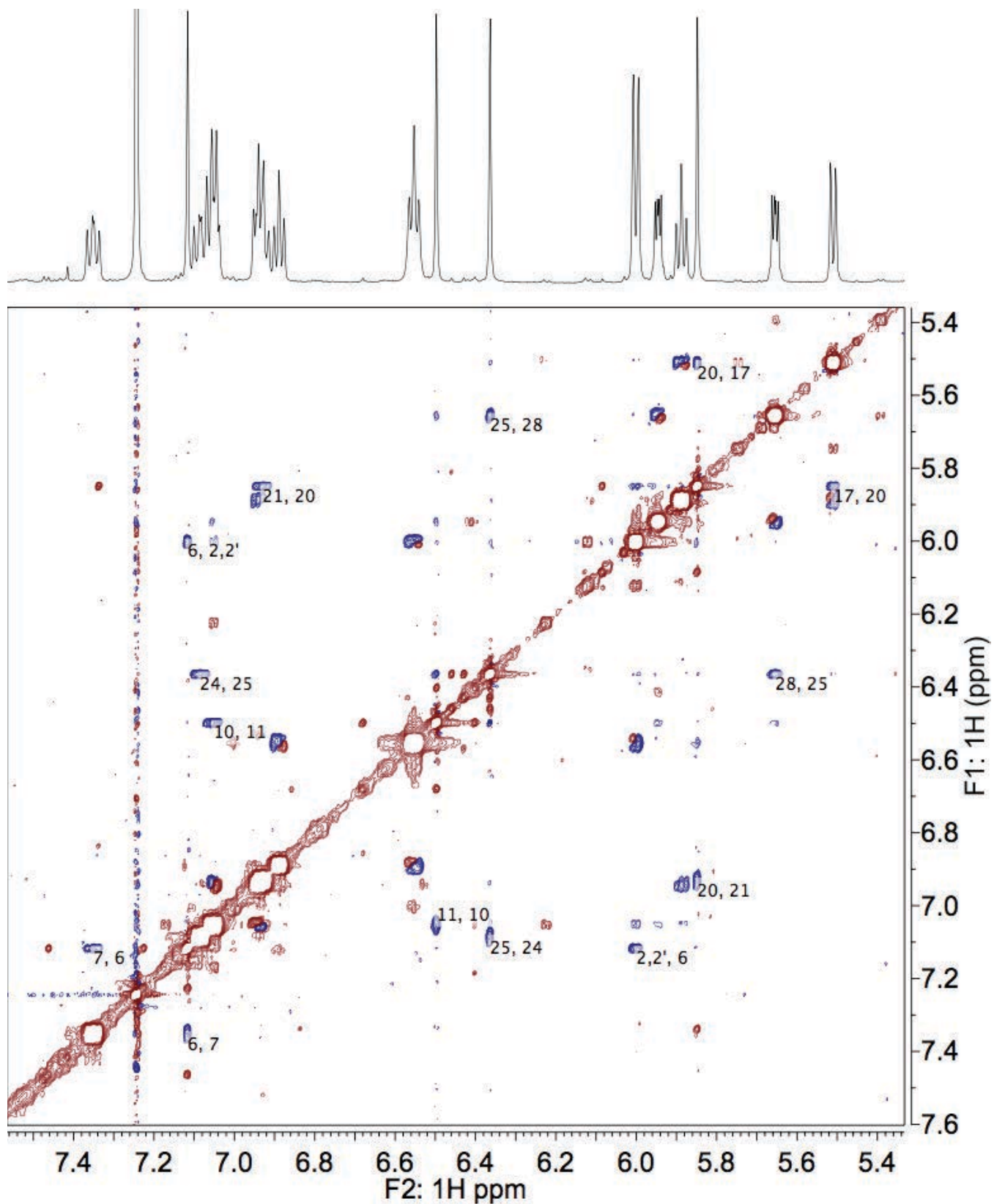


Figure S133. NOESY NMR (600 MHz) spectrum of F-Ar-4 in CDCl₃ at 0 °C.

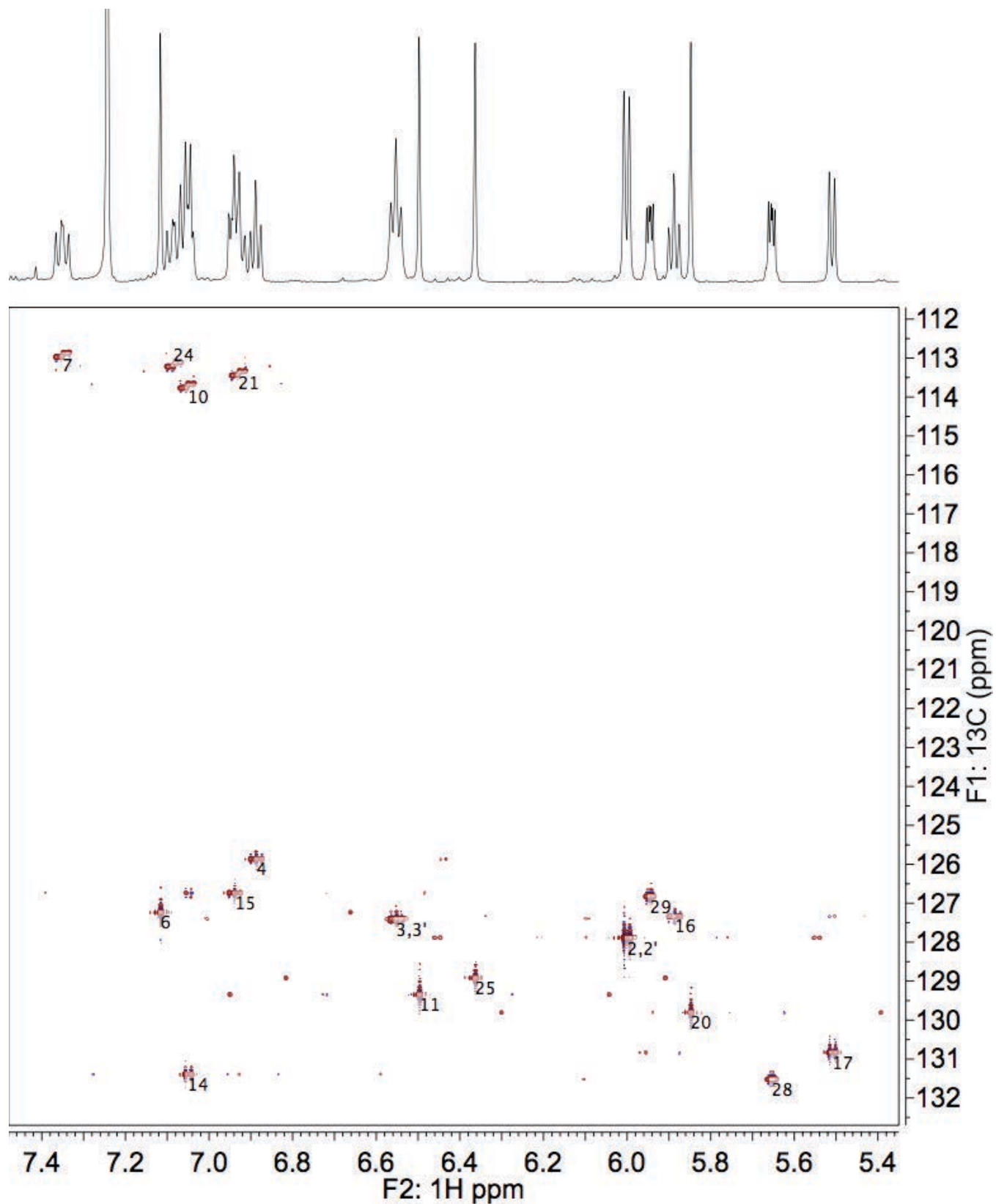


Figure S134. HMOC NMR (800 MHz) spectrum of **F-Ar-4** in CDCl_3 at 0 °C. The numbers in black correspond to the atom numbers of the major conformers, as defined in Figure S69.

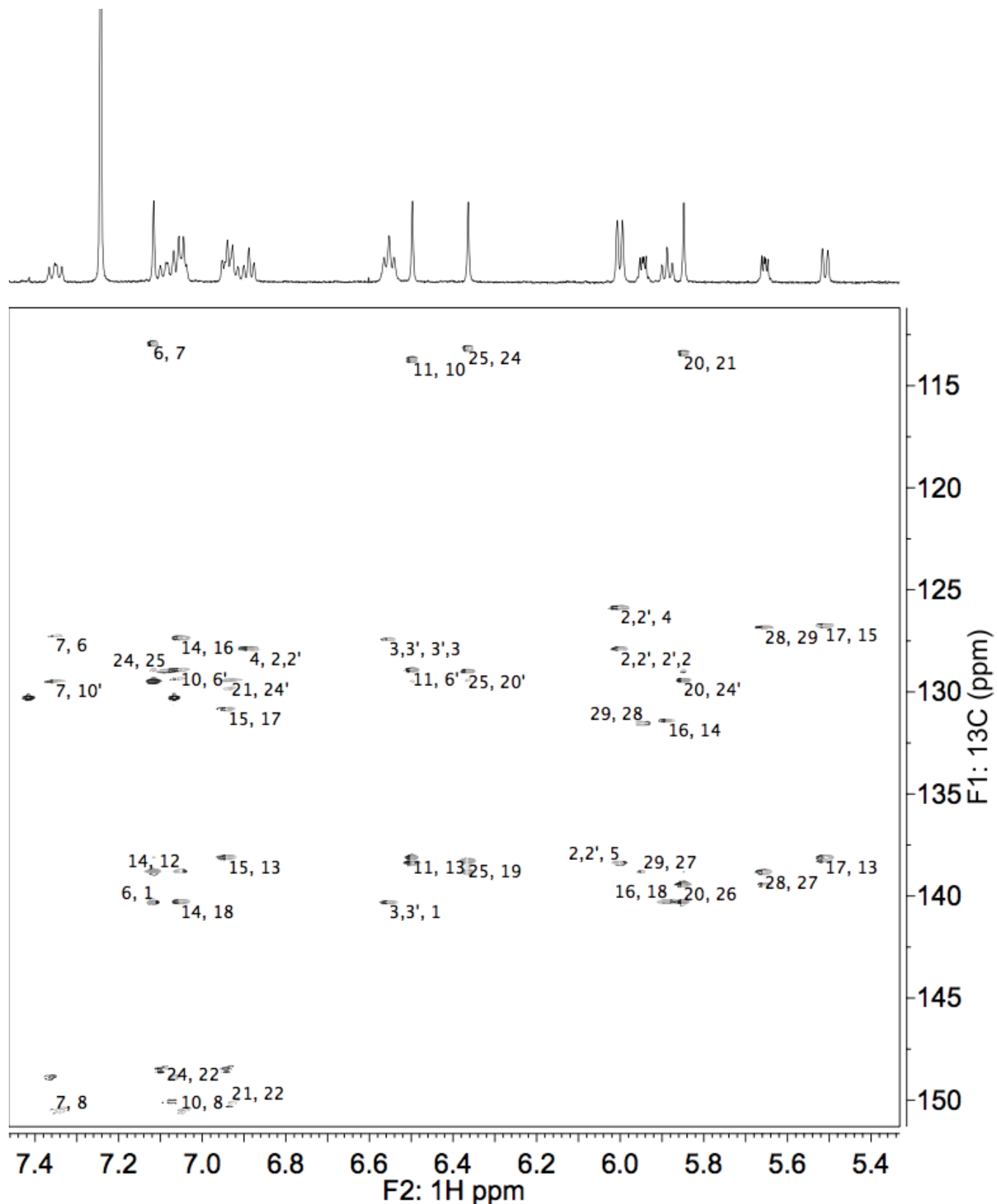


Figure S135. HMBC NMR (800 MHz) spectrum of **F-Ar-4** in CDCl_3 at 0 °C. The numbers in black correspond to the atom numbers of the major conformers, as defined in Figure S69.

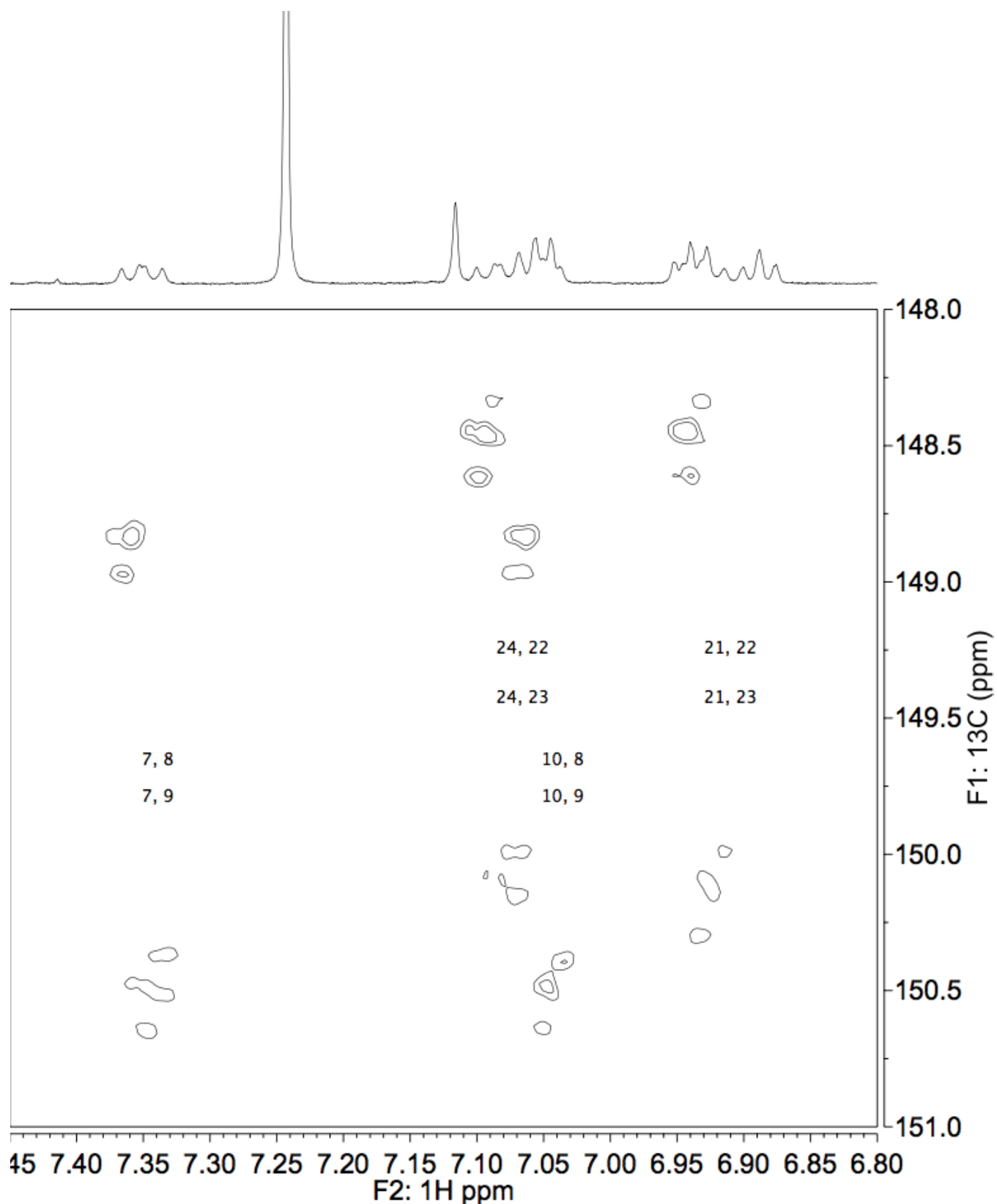


Figure S136. HMBC NMR (800 MHz) spectrum of **F-Ar-4** in CDCl₃ at 0 °C, F2: 7.45 to 6.80 ppm, F1: 151.0 to 148.0 ppm region. The numbers in black correspond to the atom numbers of the major conformers, as defined in Figure S69.

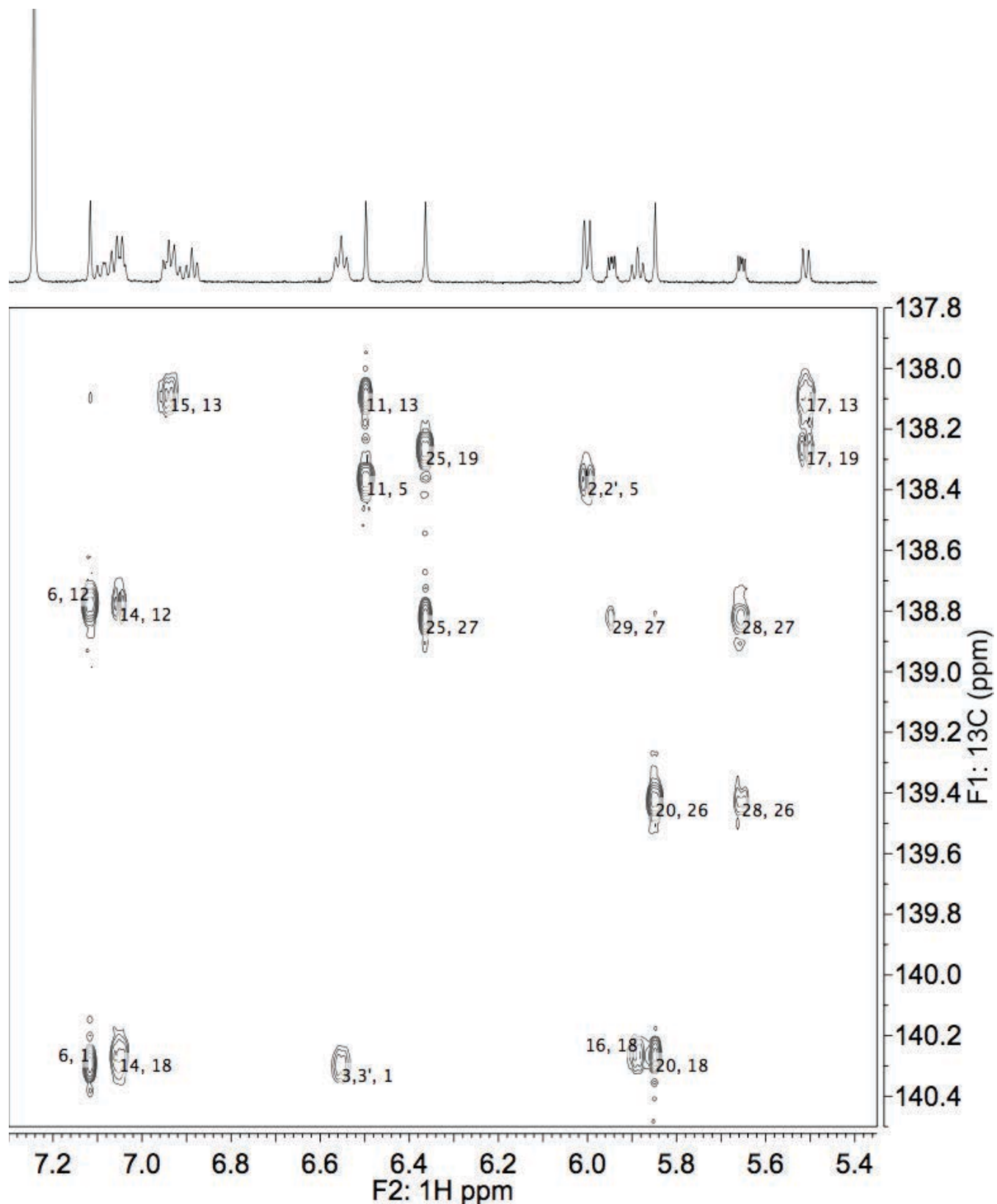


Figure S137. HMBC NMR (800 MHz) spectrum of **F-Ar-4** in CDCl_3 at 0 °C, F2: 7.30 to 5.35 ppm, F1: 140.5 to 137.8 ppm region. The numbers in black correspond to the atom numbers of the major conformers, as defined in Figure S69.

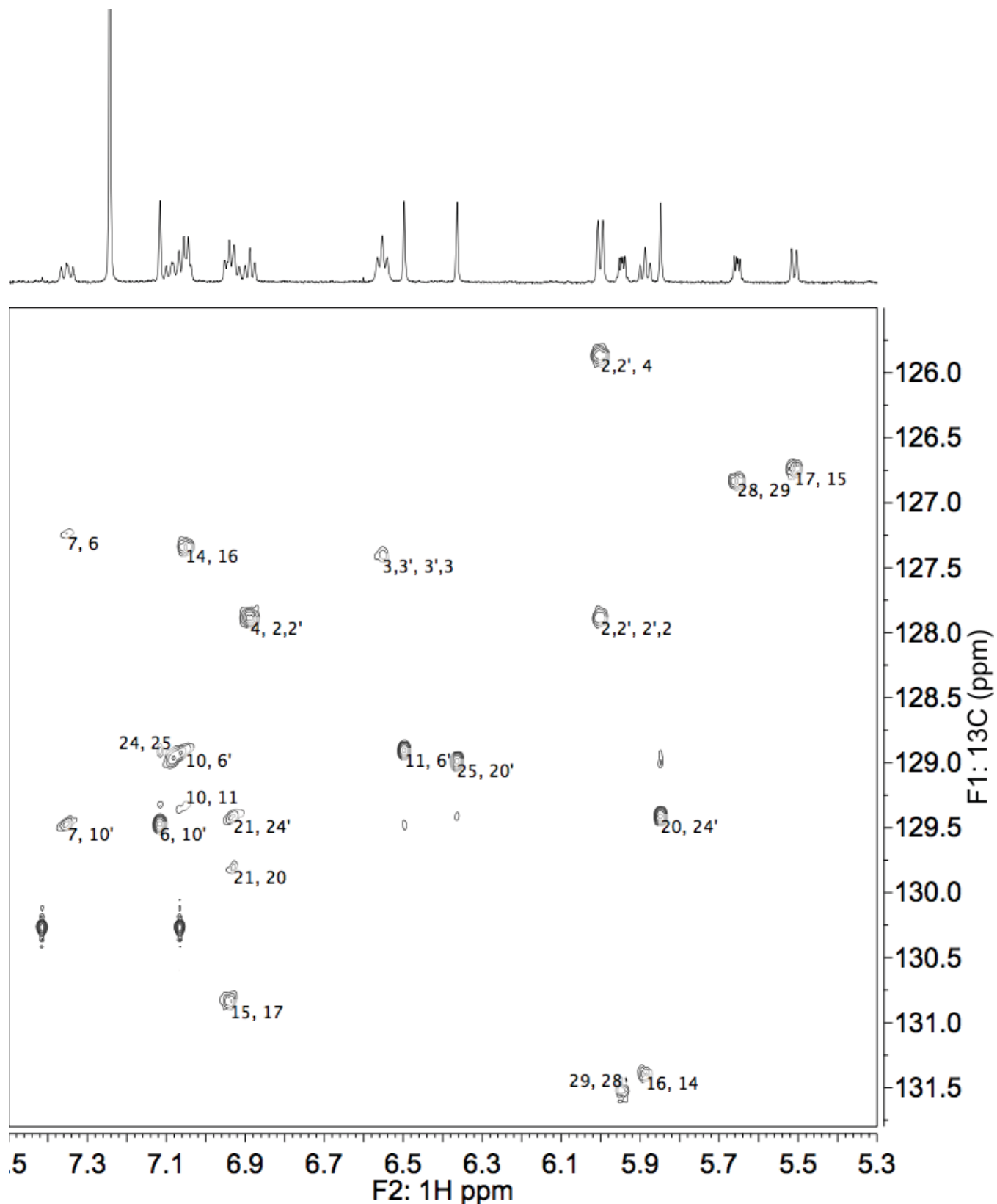


Figure S138. HMBC NMR (800 MHz) spectrum of **F-Ar-4** in CDCl_3 at 0 $^\circ\text{C}$, F2: 7.50 to 5.30 ppm, F1: 131.8 to 125.5 ppm region. The numbers in black correspond to the atom numbers of the major conformers, as defined in Figure S69.

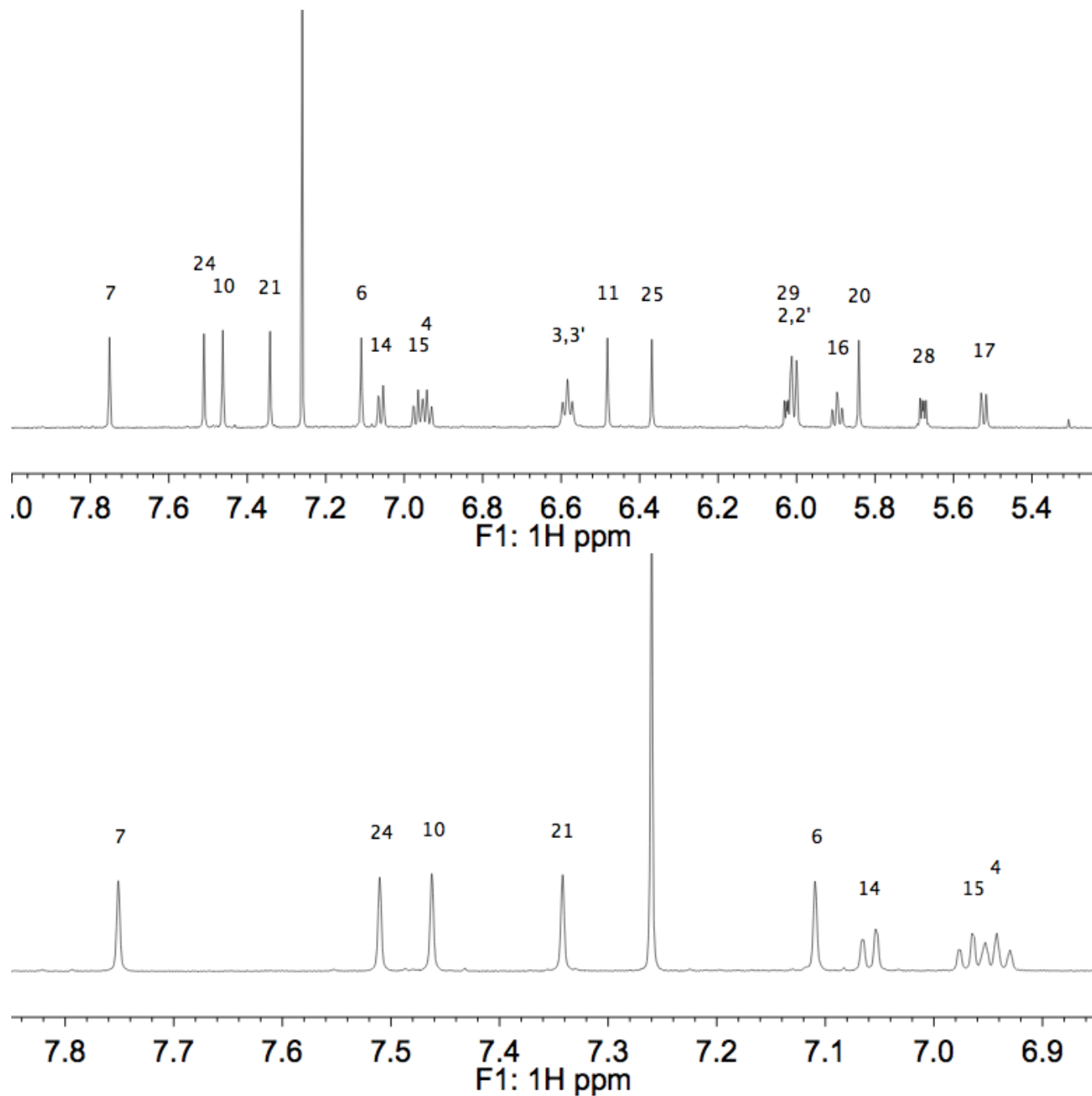


Figure S139. ¹H NMR (600 MHz) spectrum of Cl-Ar-4 in CDCl₃ at 0 °C: (top) full view, (bottom) 7.85 to 6.85 ppm region. The numbers in black numbers correspond to the atom numbers of the major conformer as defined in Figure S69.

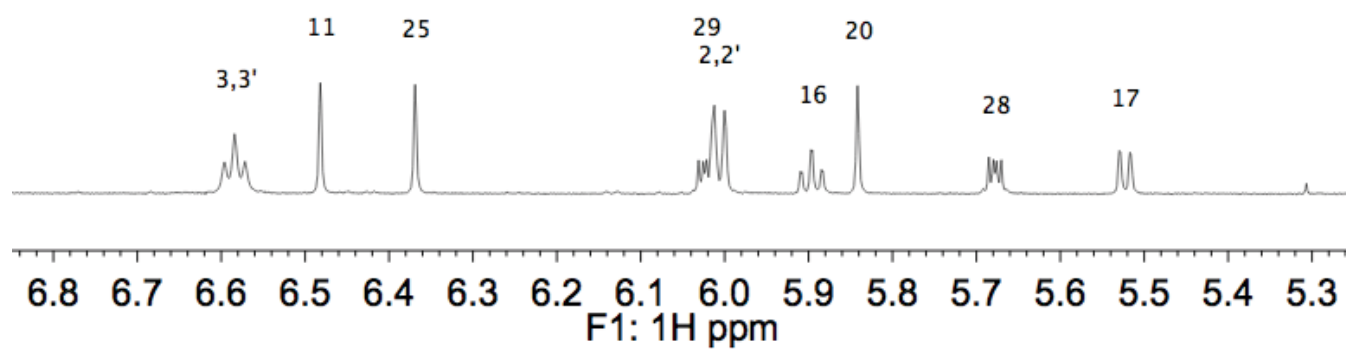


Figure S139 (continued). ¹H NMR (600 MHz) spectrum of **Cl-Ar-4** in CDCl₃ at 0 °C, 6.85 to 5.25 ppm region. The numbers in black correspond to the atom numbers of the major conformer as defined in Figure S69.

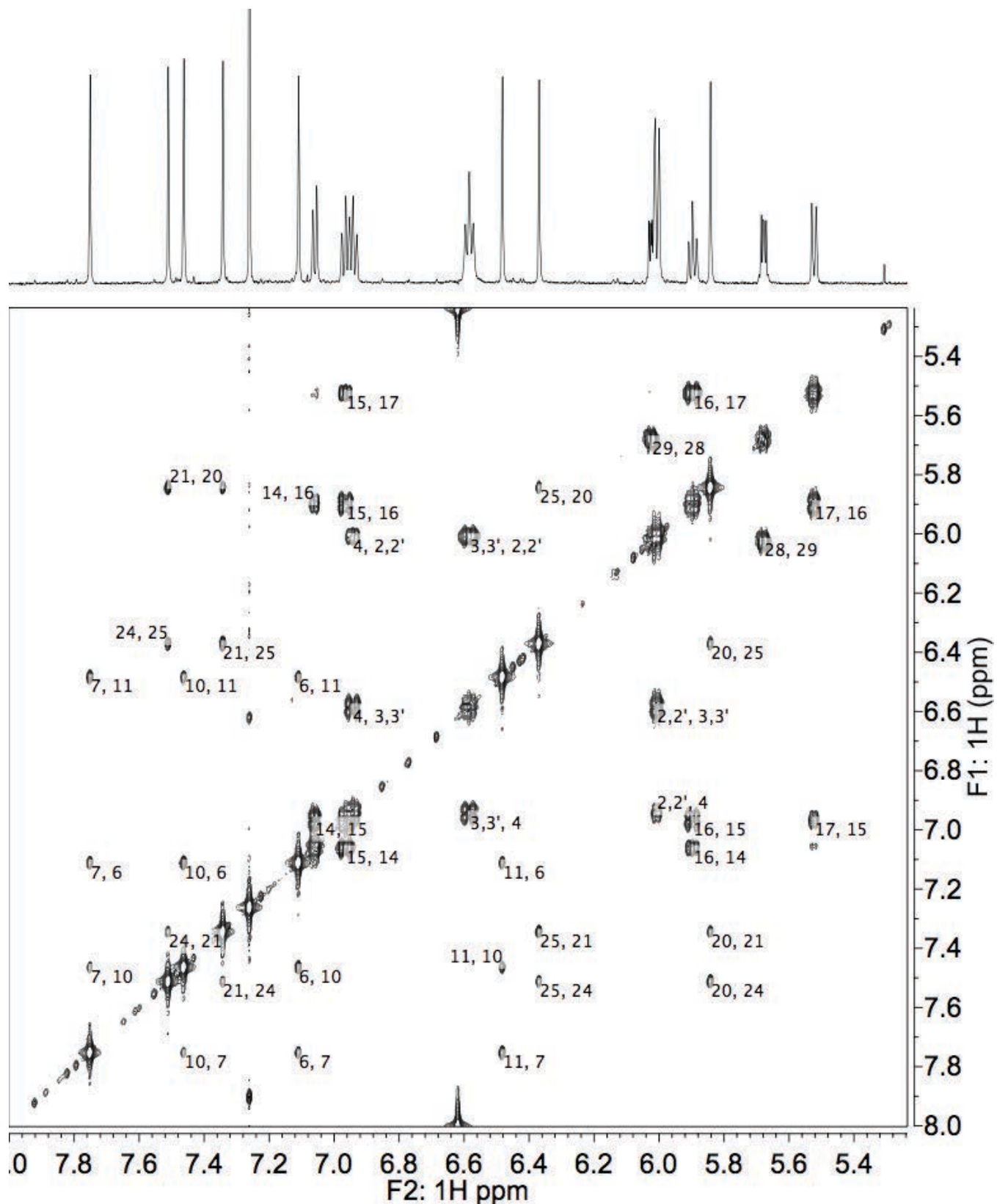


Figure S140. COSY NMR (600 MHz) spectrum of **Cl-Ar-4** in CDCl_3 at 0 °C, full view. The numbers in black correspond to the atom numbers of the major conformer as defined in Figure S69.

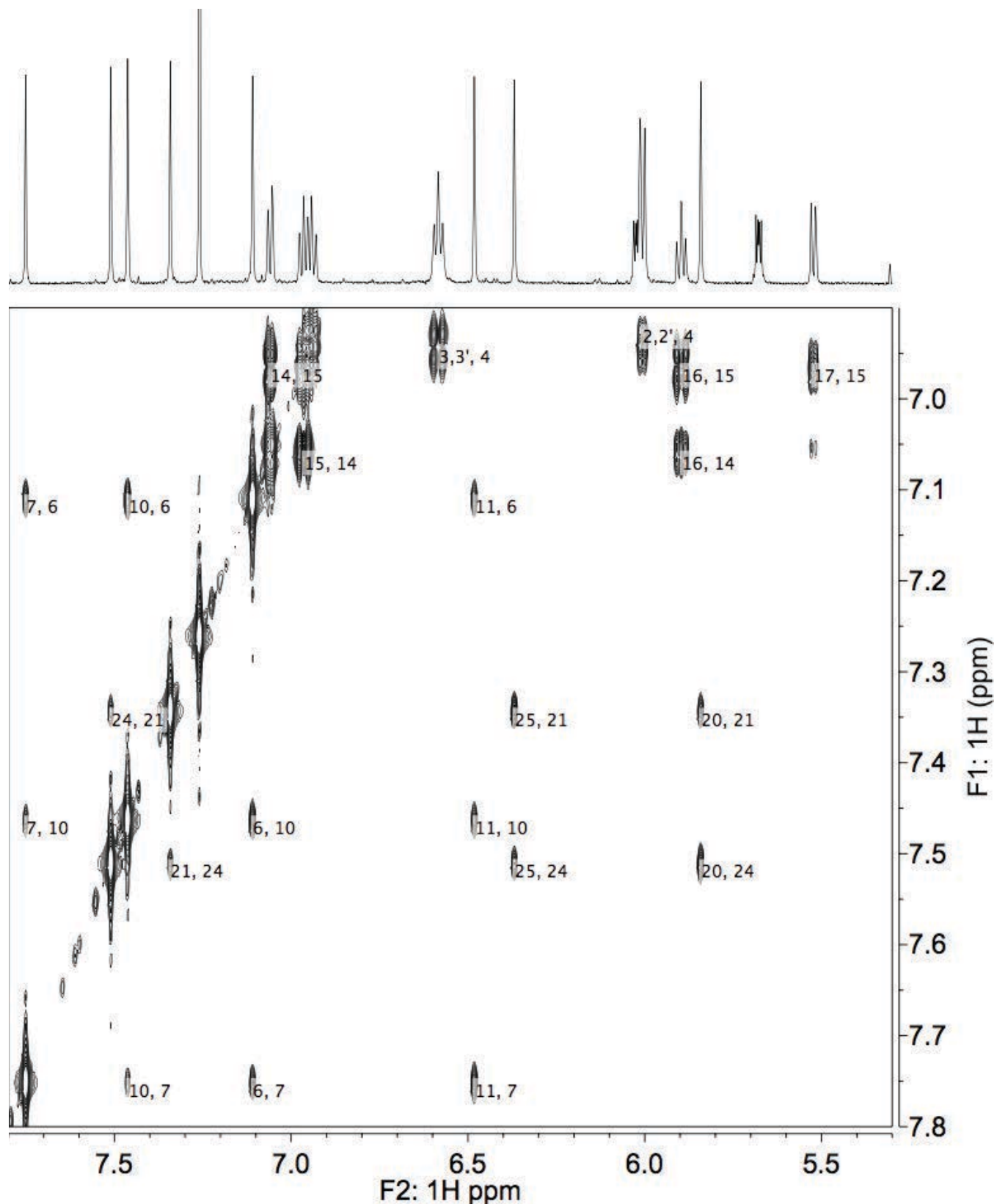


Figure S141. COSY NMR (600 MHz) spectrum of **Cl-Ar-4** in CDCl₃ at 0 °C, F2: 7.80 to 5.30 ppm, F1: 7.80 to 6.90 ppm region. The numbers in black correspond to the atom numbers of the major conformer as defined in Figure S69.

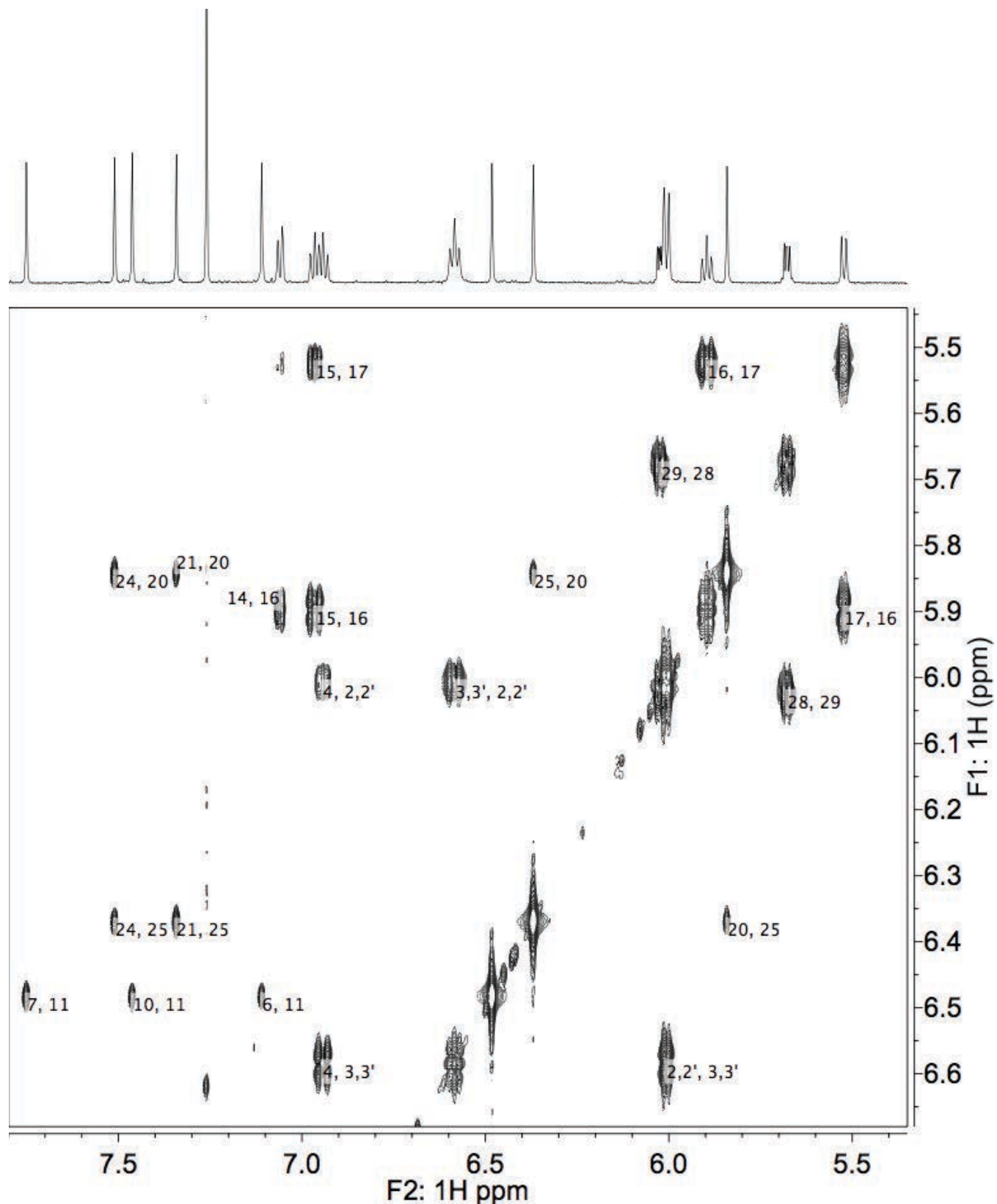


Figure S142. COSY NMR (600 MHz) spectrum of **Cl-Ar-4** in CDCl_3 at 0 °C, F2: 7.80 to 5.35 ppm, F1: 6.68 to 5.44 ppm region. The numbers in black correspond to the atom numbers of the major conformer as defined in Figure S69.

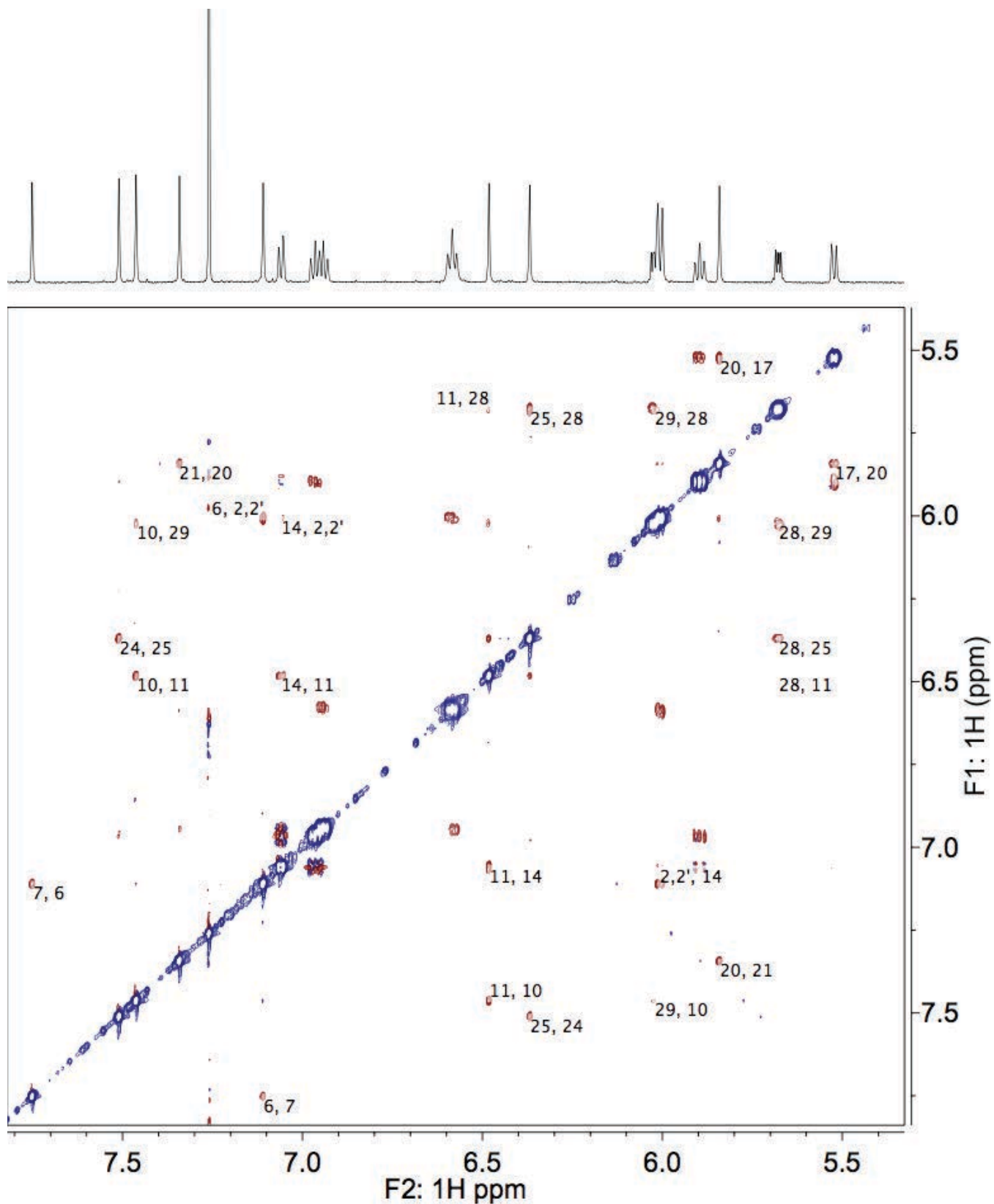


Figure S143. ROESY NMR (600 MHz) spectrum of Cl-Ar-4 in CDCl₃ at 0 °C.

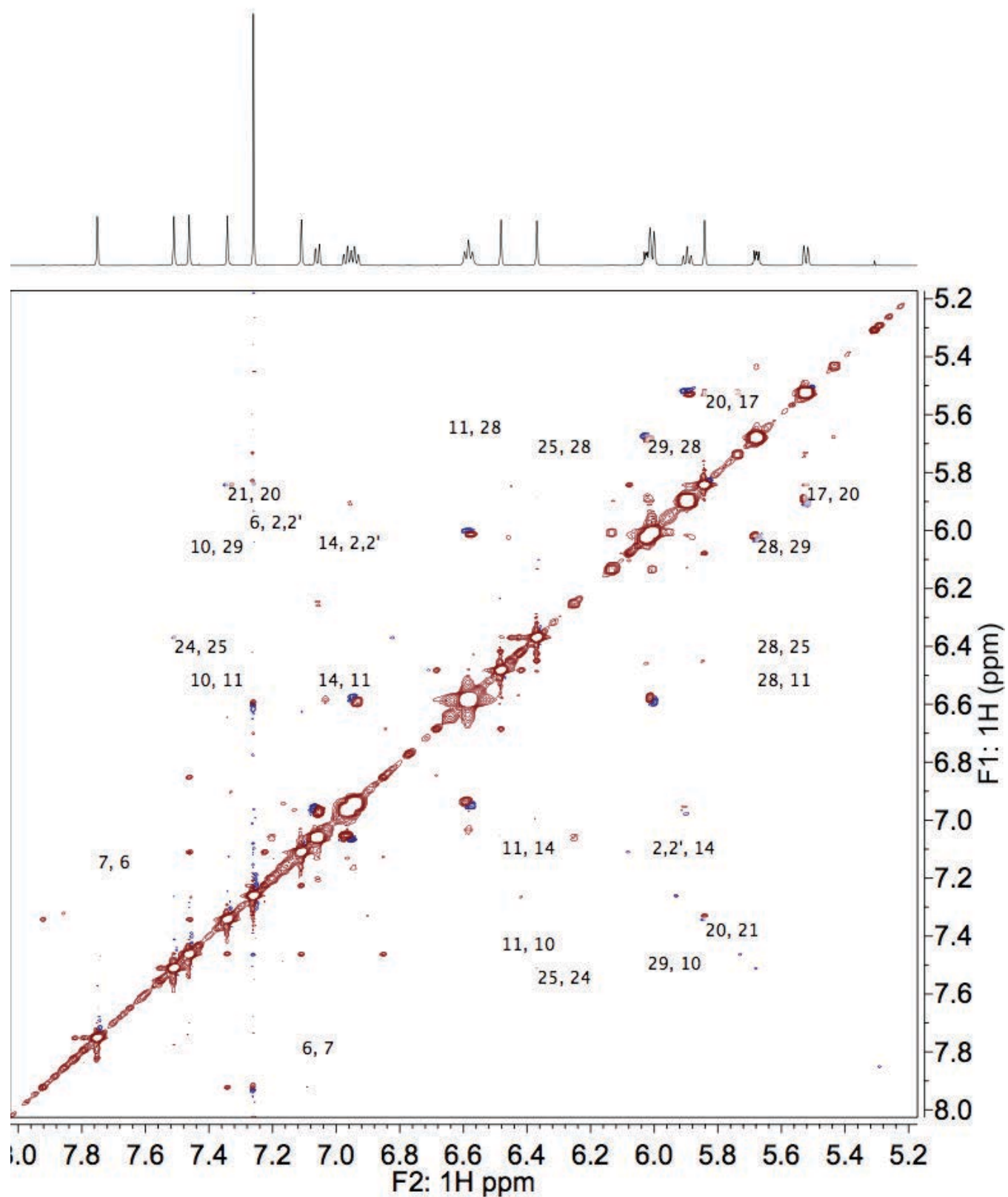


Figure S144. NOESY NMR (600 MHz) spectrum of Cl-Ar-4 in CDCl_3 at 0 °C.

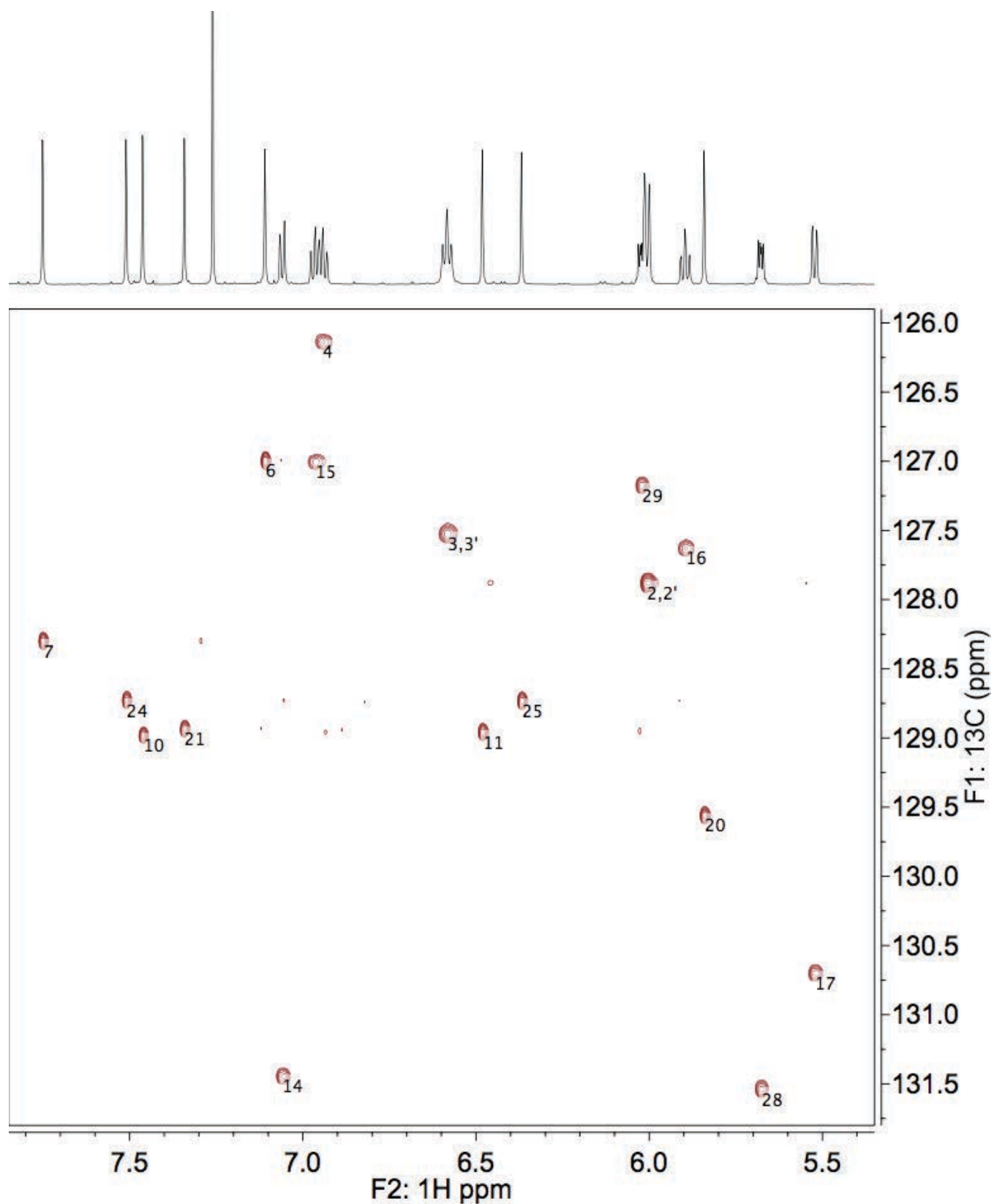


Figure S145. HSQC NMR (800 MHz) spectrum of **Cl-Ar-4** in CDCl₃ at 0 °C, F2: 7.85 to 5.35 ppm, F1: 131.8 to 125.9 ppm region. The numbers in black correspond to the atom numbers of the major conformers, as defined in Figure S69.

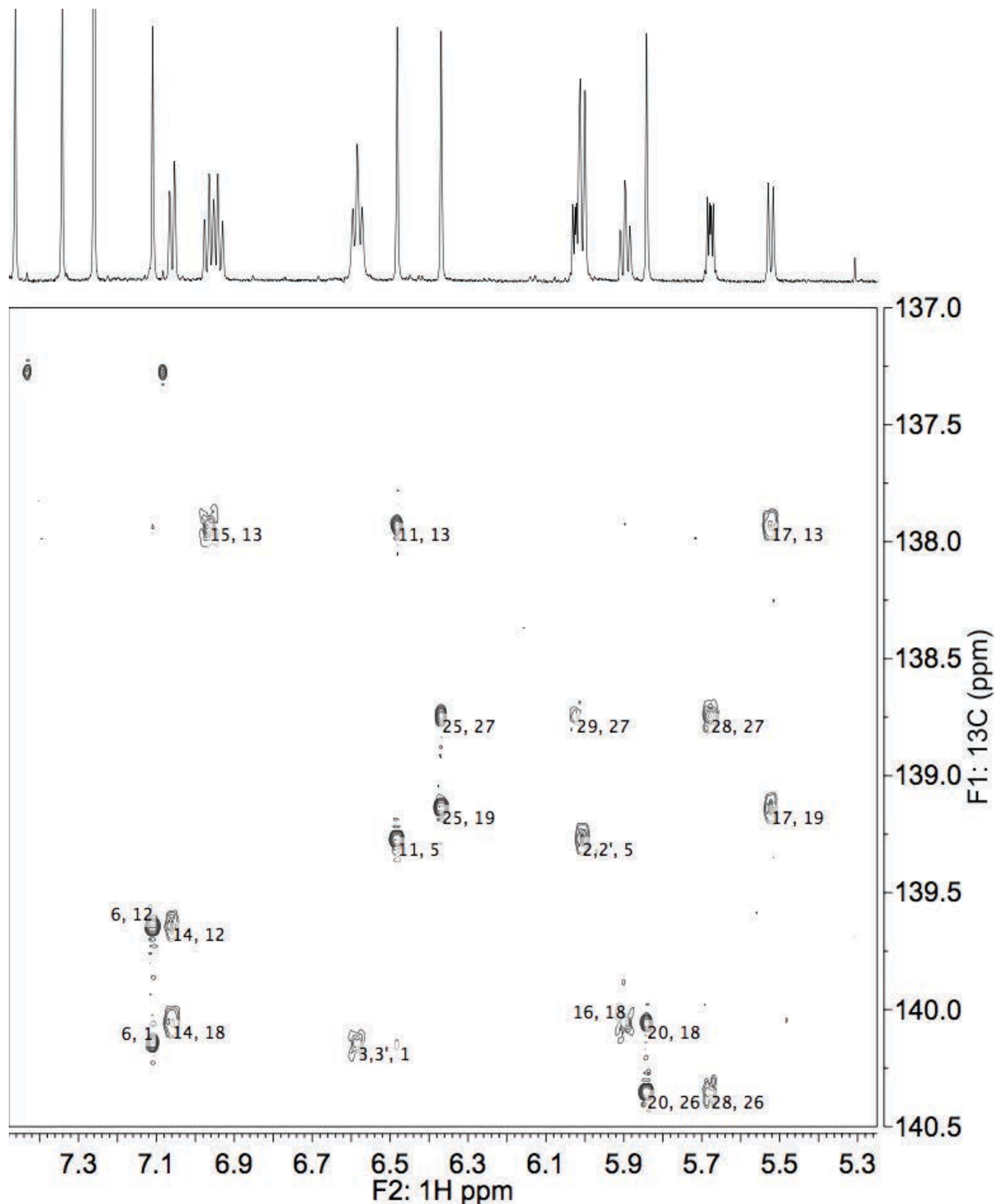


Figure S146. HMBC NMR (800 MHz) spectrum of Cl-Ar-4 in CDCl₃ at 0 °C, F2: 7.48 to 5.25 ppm, F1: 140.5 to 137.0 ppm region. The numbers in black correspond to the atom numbers of the major conformers, as defined in Figure S69.

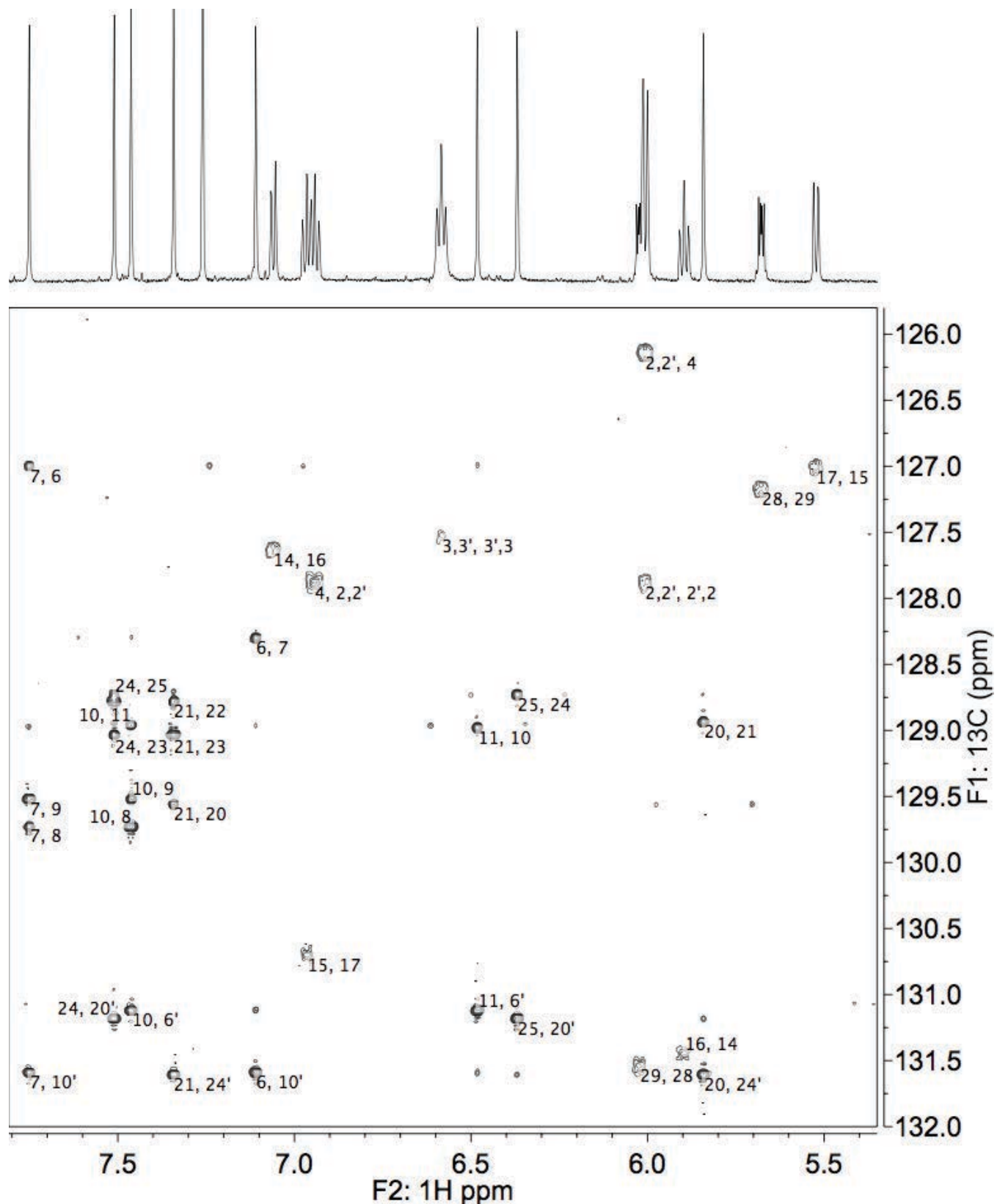


Figure S147. HMBC NMR (800 MHz) spectrum of **Cl-Ar-4** in CDCl₃ at 0 °C, F2: 7.81 to 5.35 ppm, F1: 132.0 to 125.8 ppm region. The numbers in black correspond to the atom numbers of the major conformers, as defined in Figure S69.

9.9 1-D and 2-D NMR Spectra of F-Ar-5 and F-Ar-6

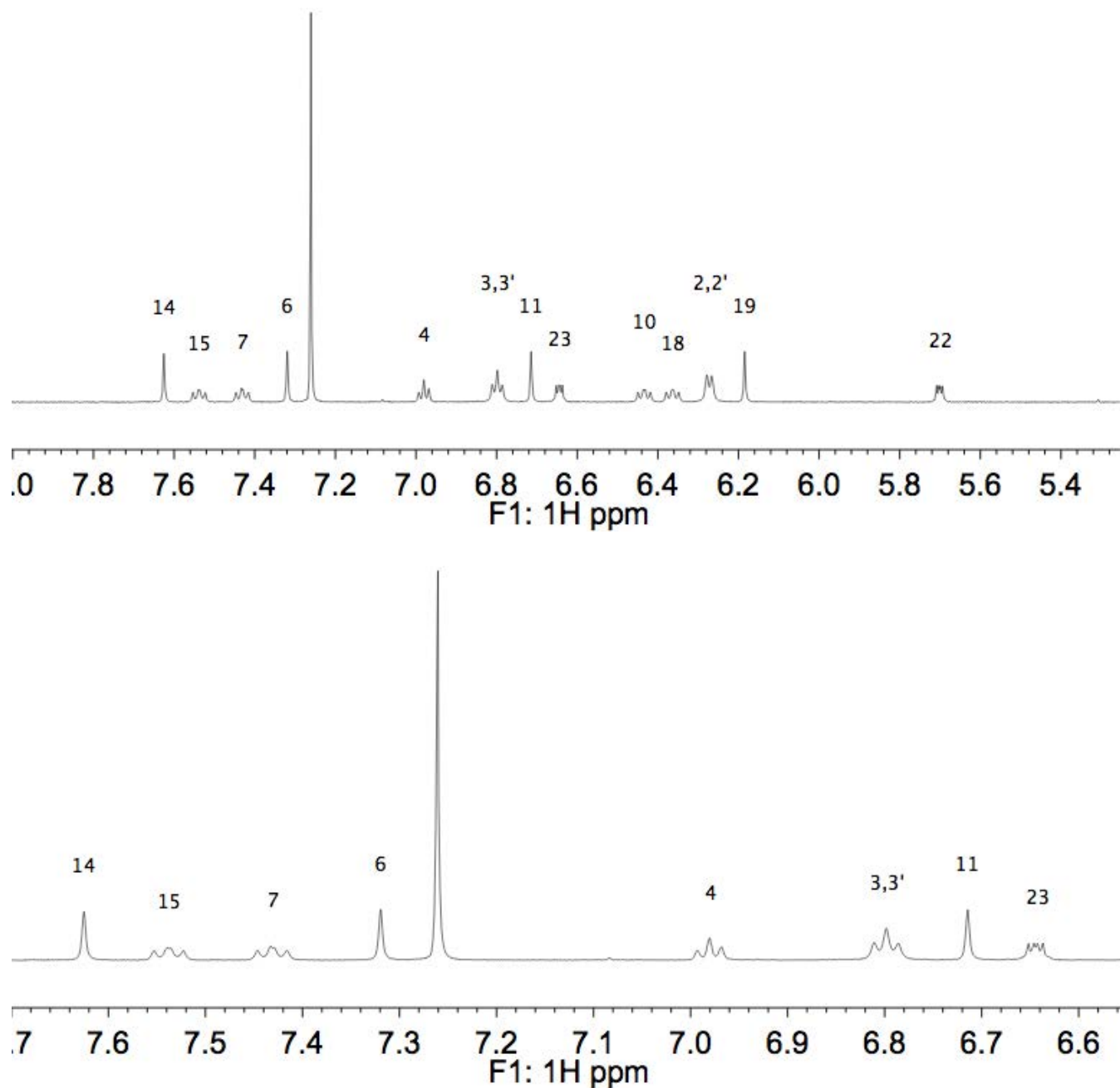


Figure S148. ¹H NMR (600 MHz) spectrum of F-Ar-5 in CDCl₃ at 0 °C: (top) full view, (bottom) 7.70 to 6.55 ppm region. The numbers in black numbers correspond to the atom numbers of the major conformer as defined in Figure S70.

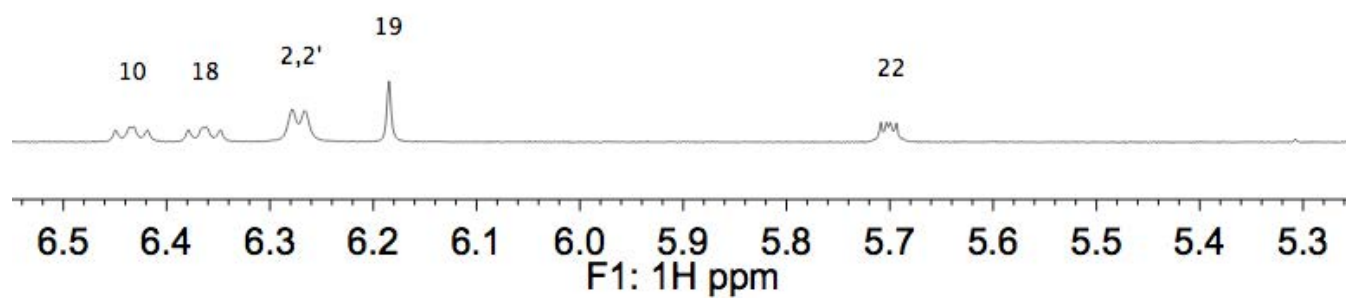


Figure S148 (continued). ¹H NMR (600 MHz) spectrum of **F-Ar-5** in CDCl₃ at 0 °C, 6.55 to 5.25 ppm region. The numbers in black correspond to the atom numbers of the major conformer as defined in Figure S70.

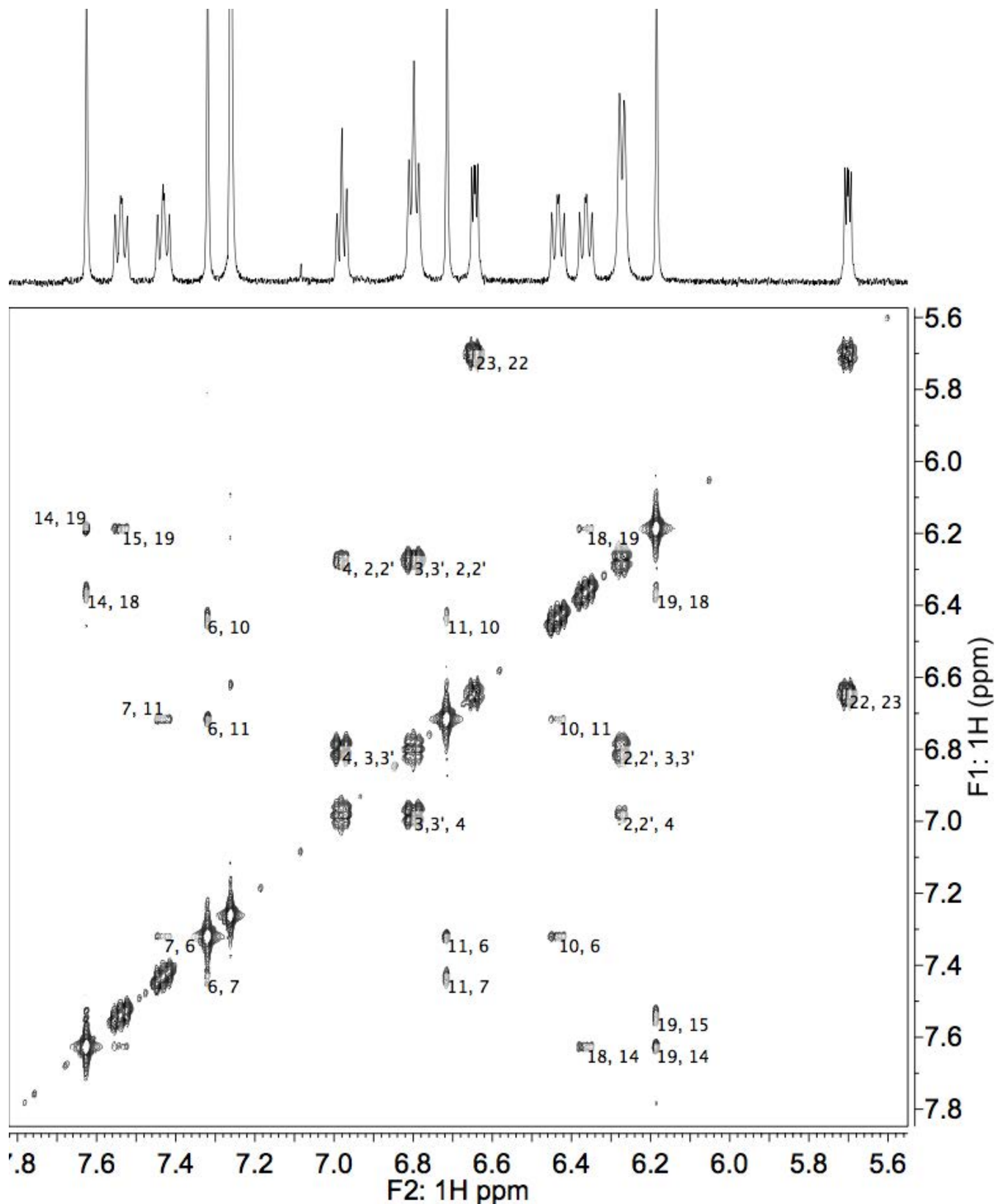


Figure S149. COSY NMR (600 MHz) spectrum of F-Ar-5 in CDCl₃ at 0 °C, full view. The numbers in black correspond to the atom numbers of the major conformer as defined in Figure S70.

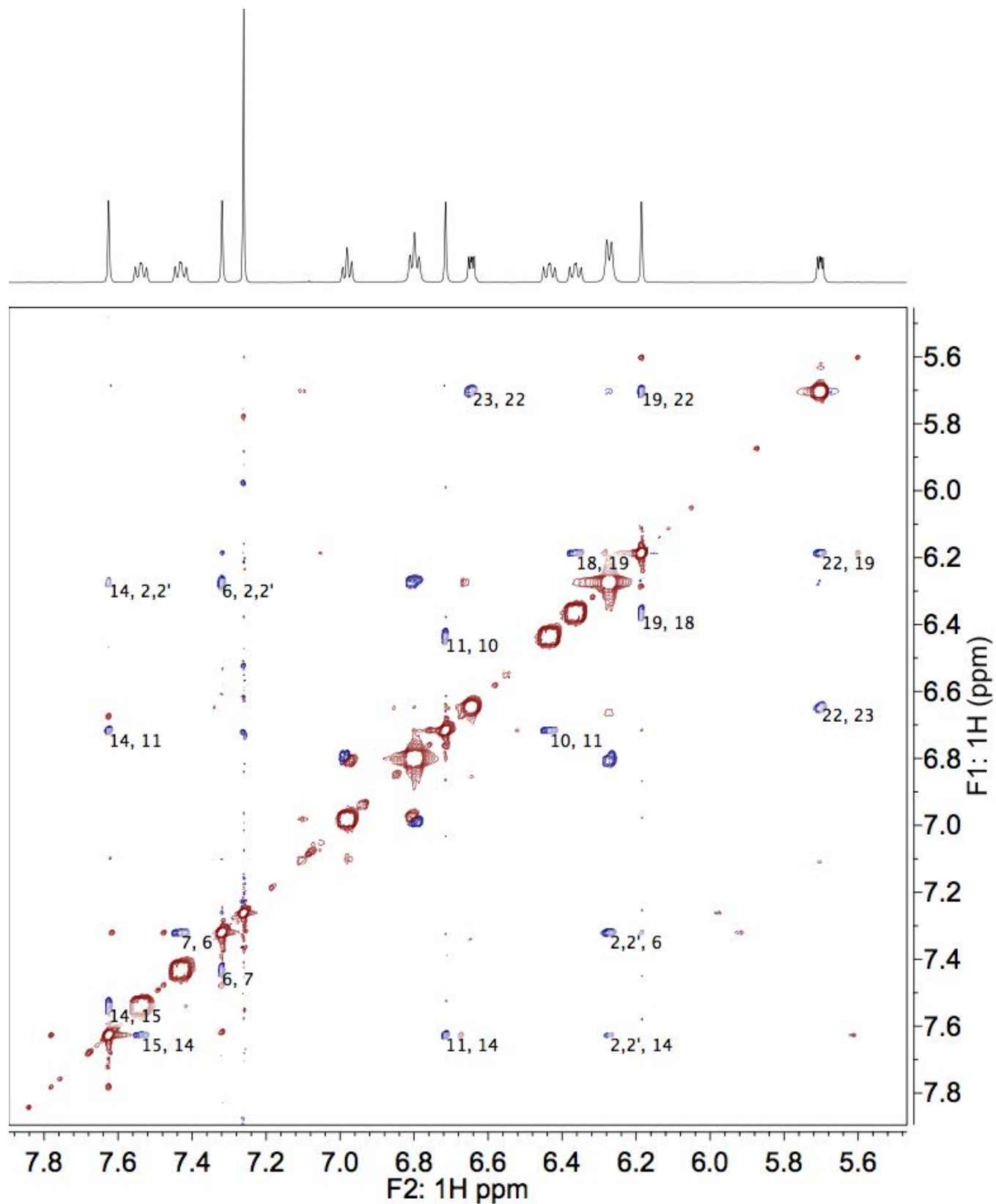


Figure S150. NOESY NMR (600 MHz) spectrum of F-Ar-5 in CDCl₃ at 0 °C.

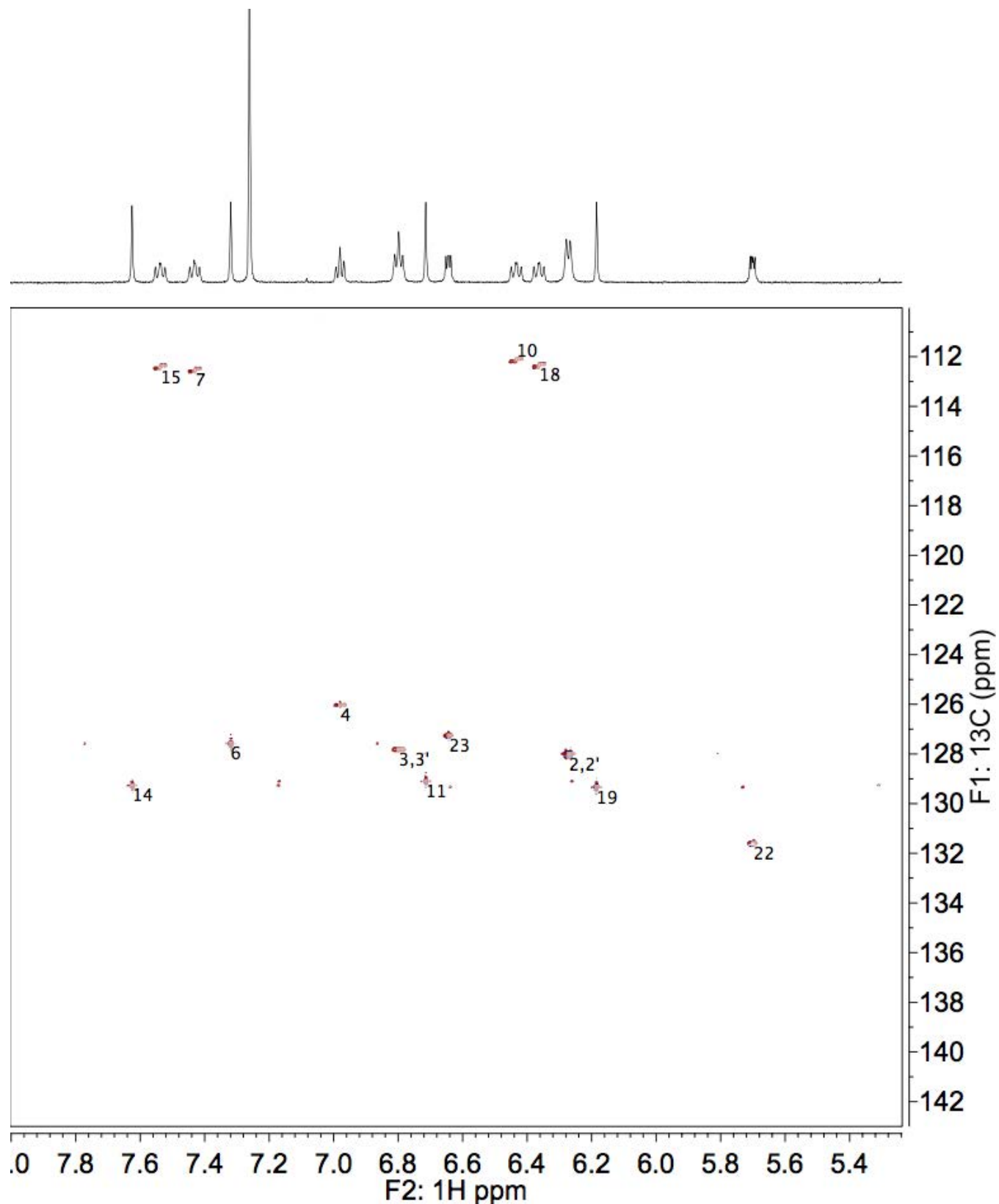


Figure S151. HSQC NMR (800 MHz) spectrum of **F-Ar-5** in CDCl_3 at 0 °C. The numbers in black correspond to the atom numbers of the major conformers, as defined in Figure S70.

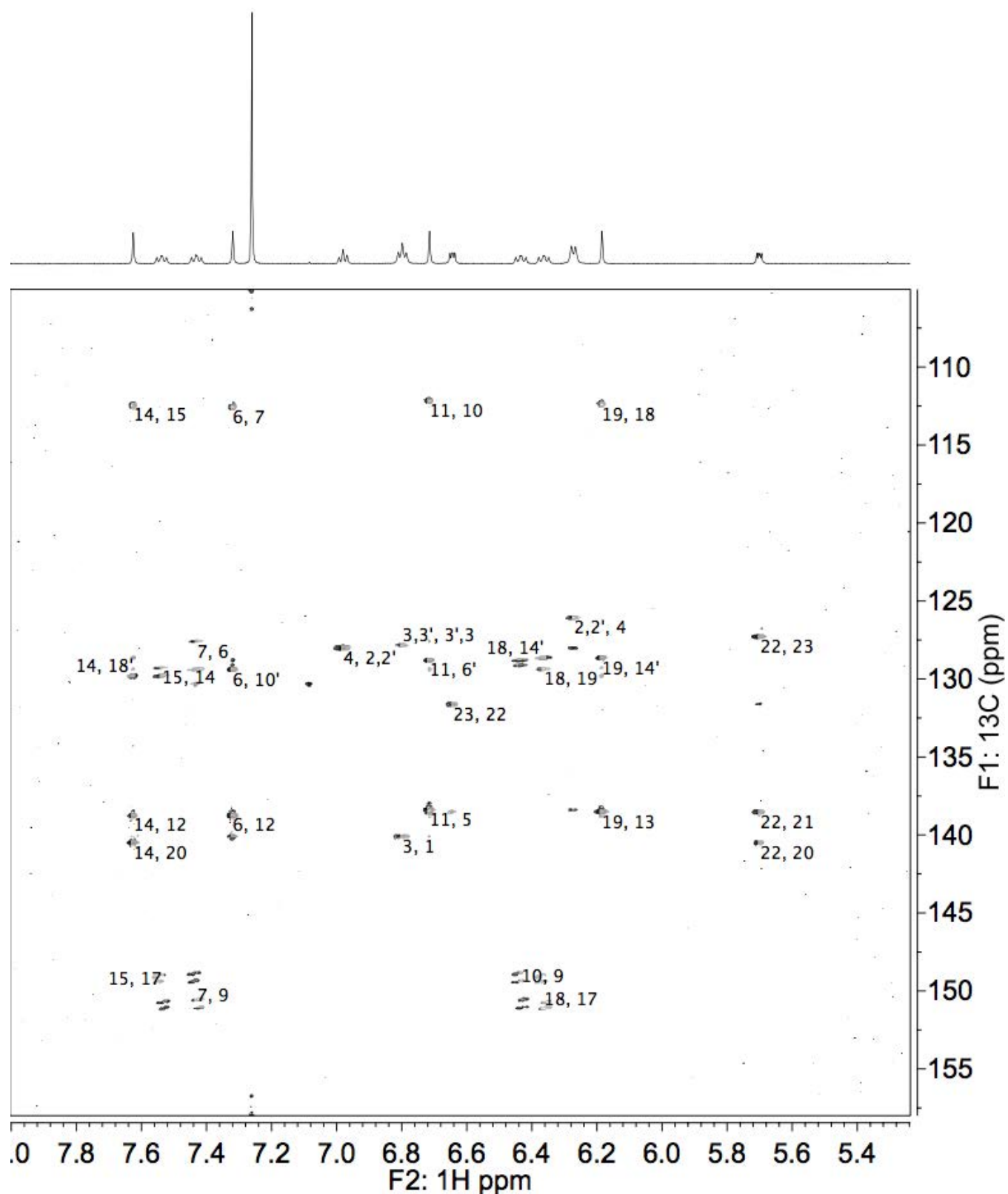


Figure S152. HMBC NMR (800 MHz) spectrum of **F-Ar-5** in CDCl_3 at 0 °C, full view.

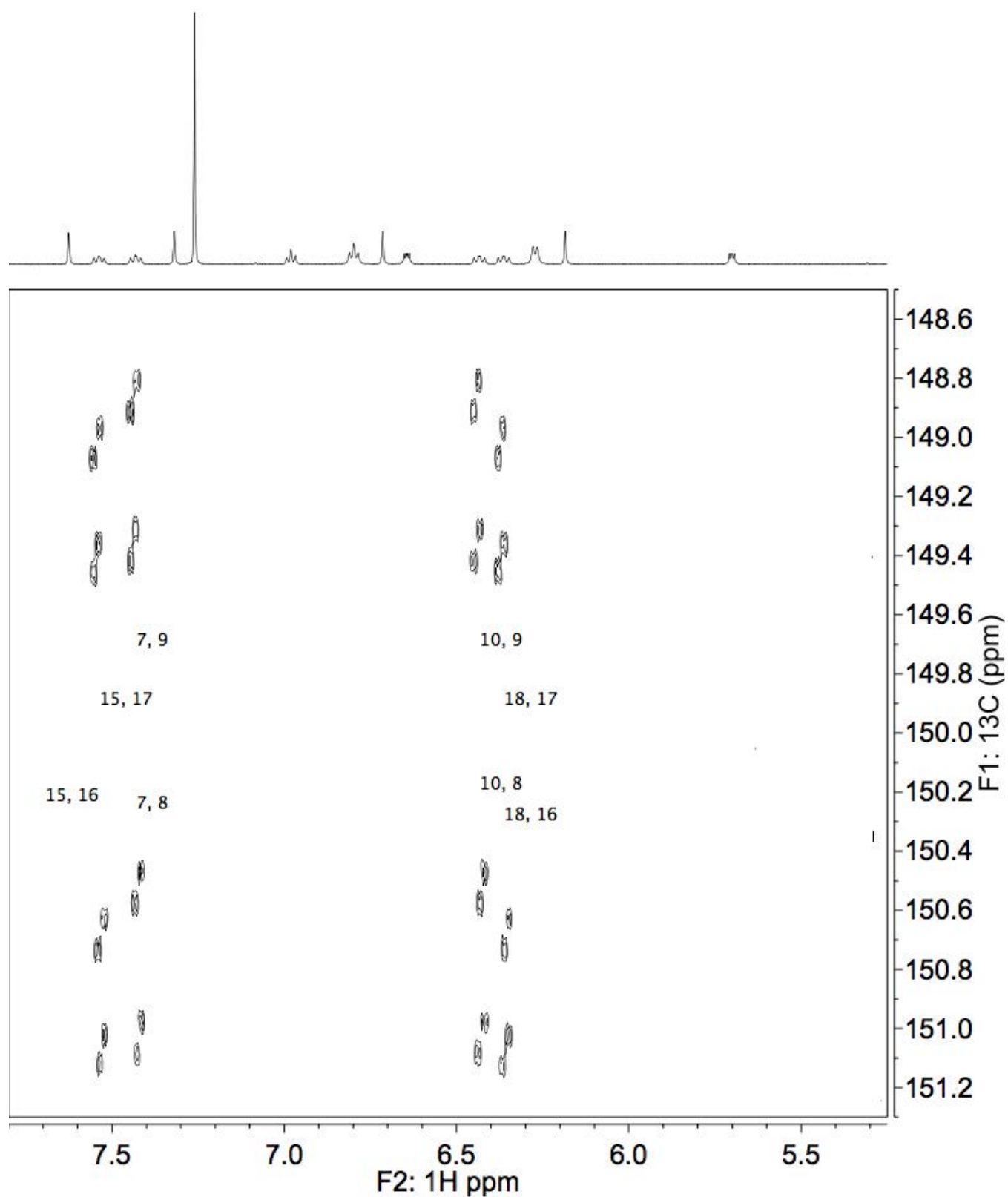


Figure S153. HMBC NMR (800 MHz) spectrum of **F-Ar-5** in CDCl_3 at 0 °C, δ_{H} 7.80 to 5.25 ppm and δ_{C} 151.3 to 148.5 ppm region. The numbers in black correspond to the atom numbers of the major conformer as defined in Figure S70.

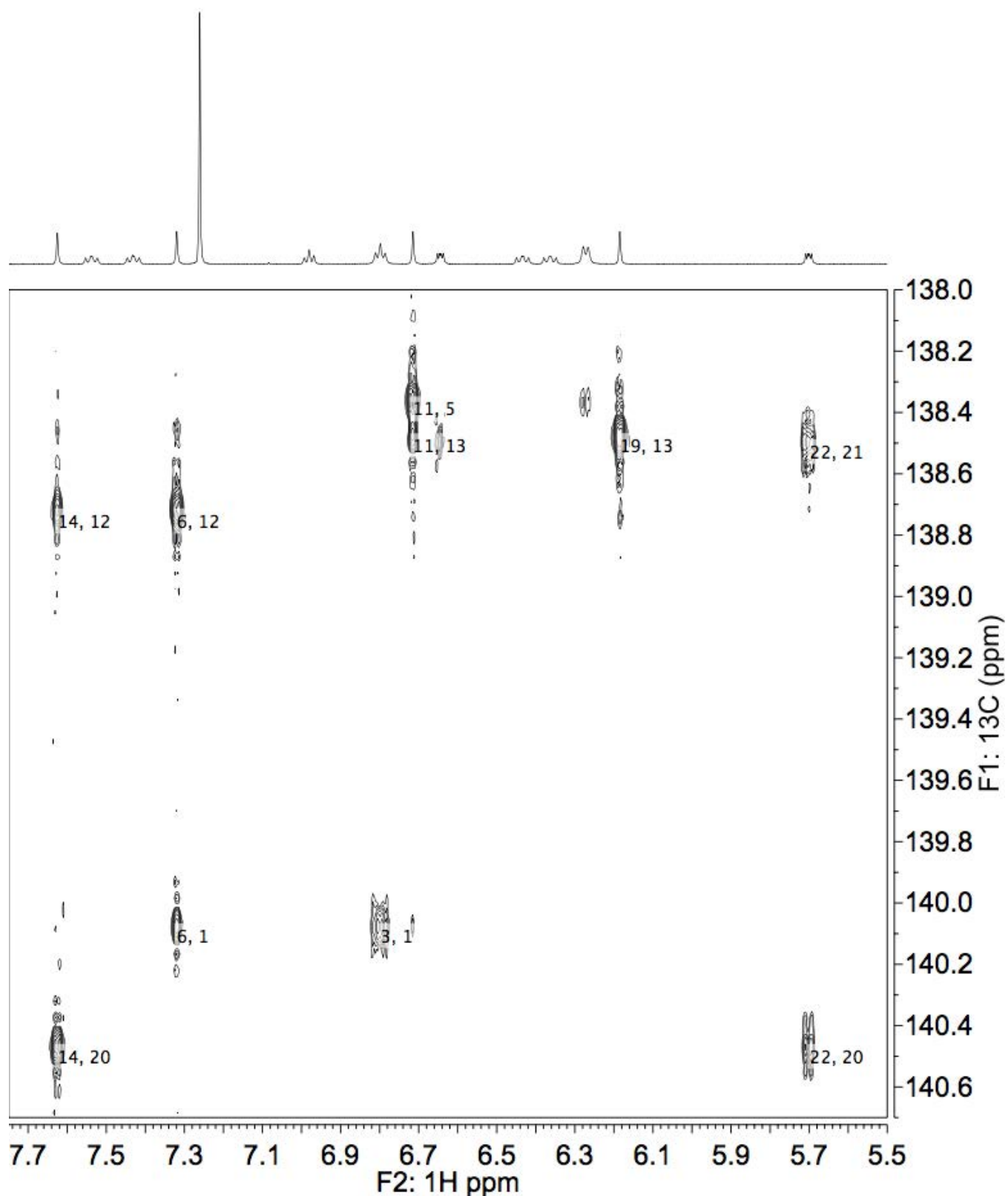


Figure S154. HMBC NMR (800 MHz) spectrum of **F-Ar-5** in CDCl_3 at 0 °C, δ_{H} 7.75 to 5.50 ppm and δ_{C} 140.7 to 138.0 ppm region. The numbers in black correspond to the atom numbers of the major conformer as defined in Figure S70.

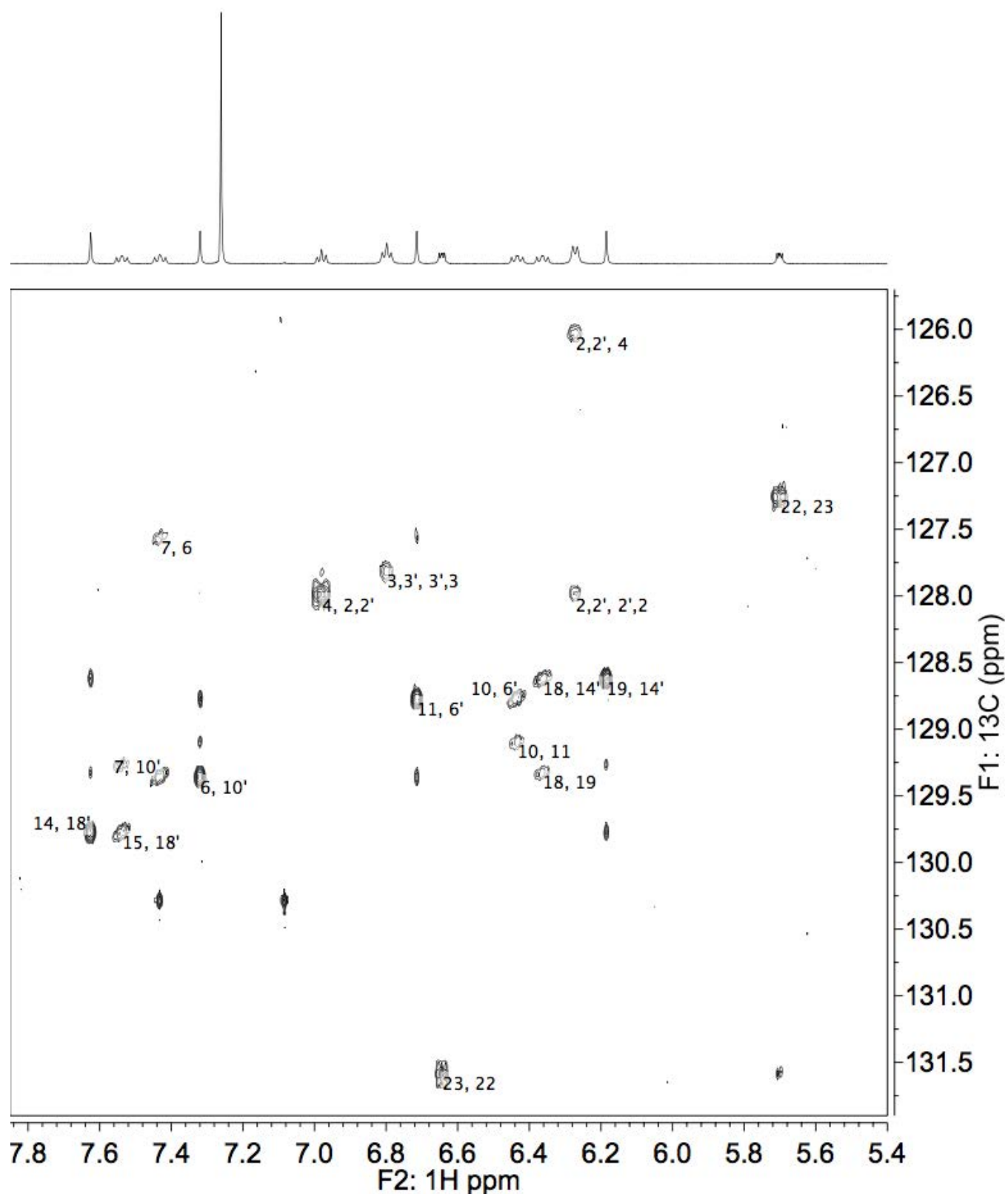


Figure S155. HMBC NMR (800 MHz) spectrum of **F-Ar-5** in CDCl_3 at 0 °C, δ_{H} 7.85 to 5.40 ppm and δ_{C} 131.9 to 125.7 ppm region. The numbers in black correspond to the atom numbers of the major conformer as defined in Figure S70.

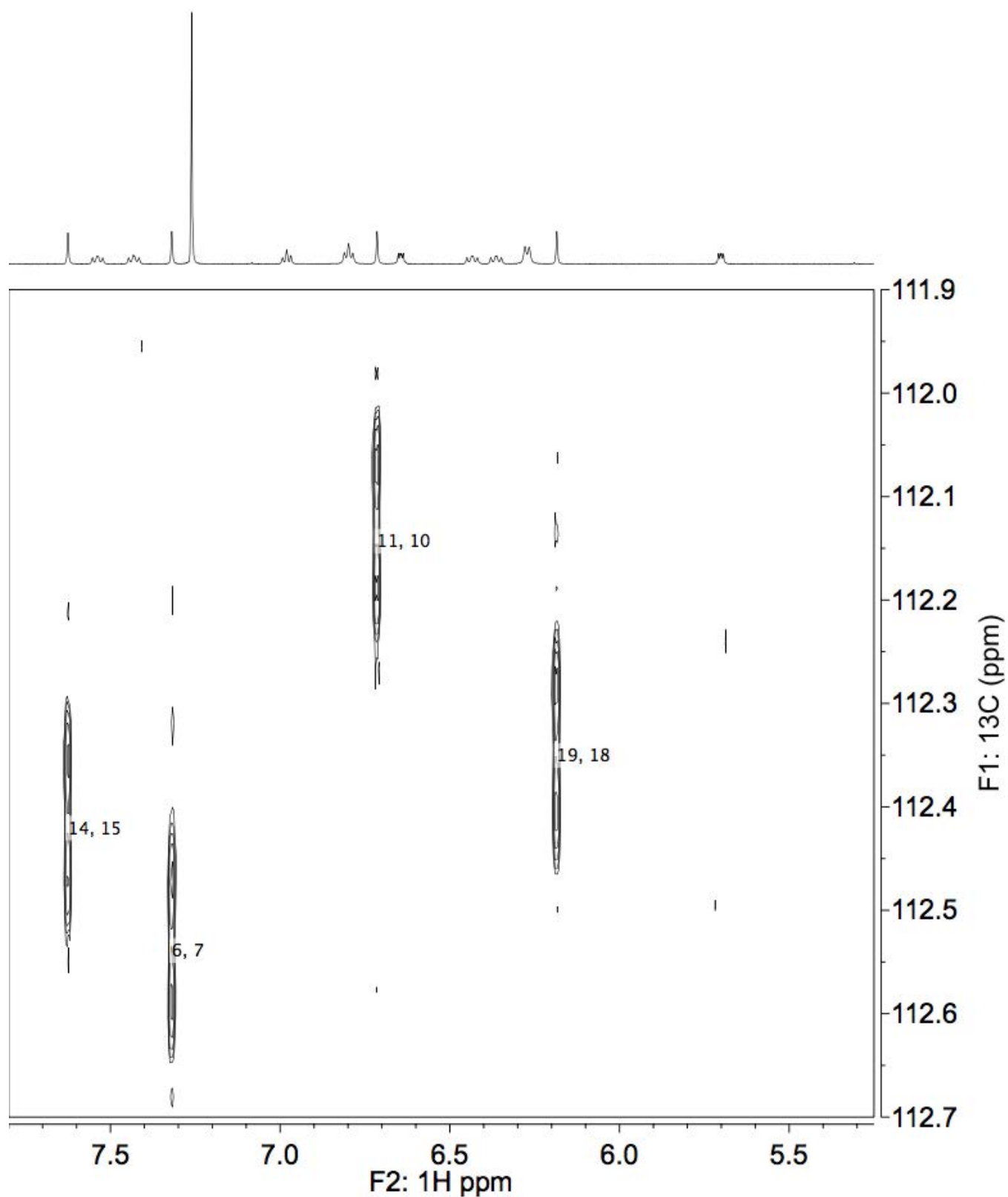


Figure S156. HMBC NMR (800 MHz) spectrum of **F-Ar-5** in CDCl_3 at 0 °C, δ_{H} 7.80 to 5.25 ppm and δ_{C} 112.7 to 111.9 ppm region. The numbers in black correspond to the atom numbers of the major conformer as defined in Figure S70.

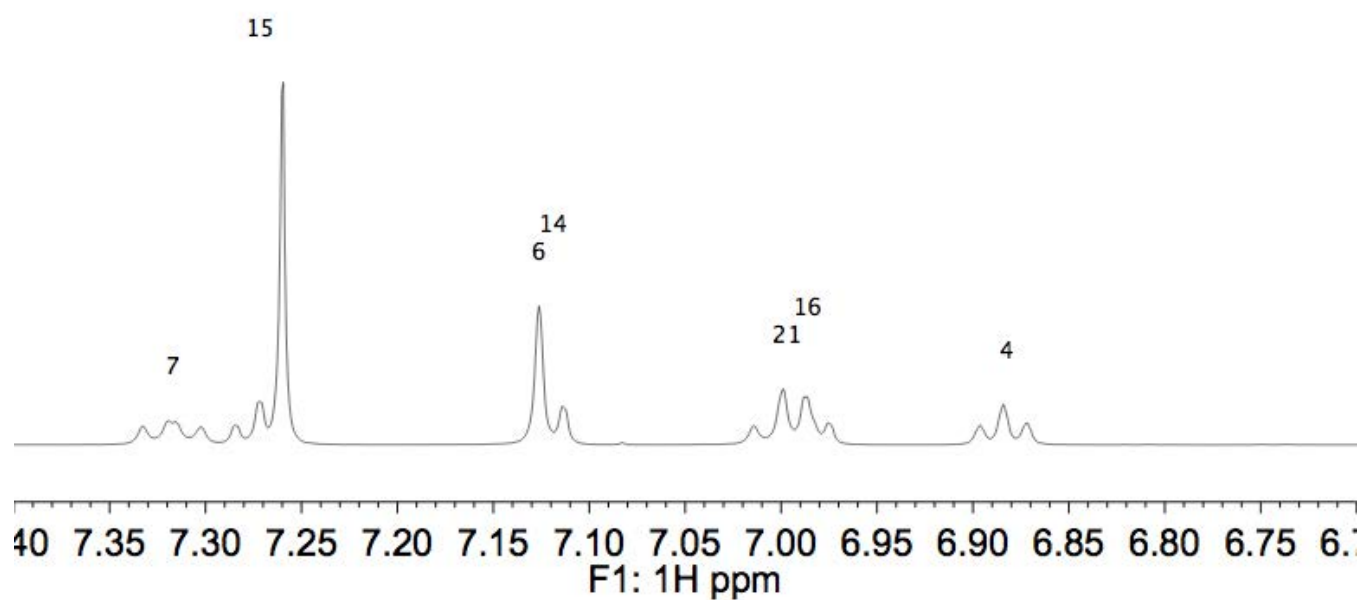
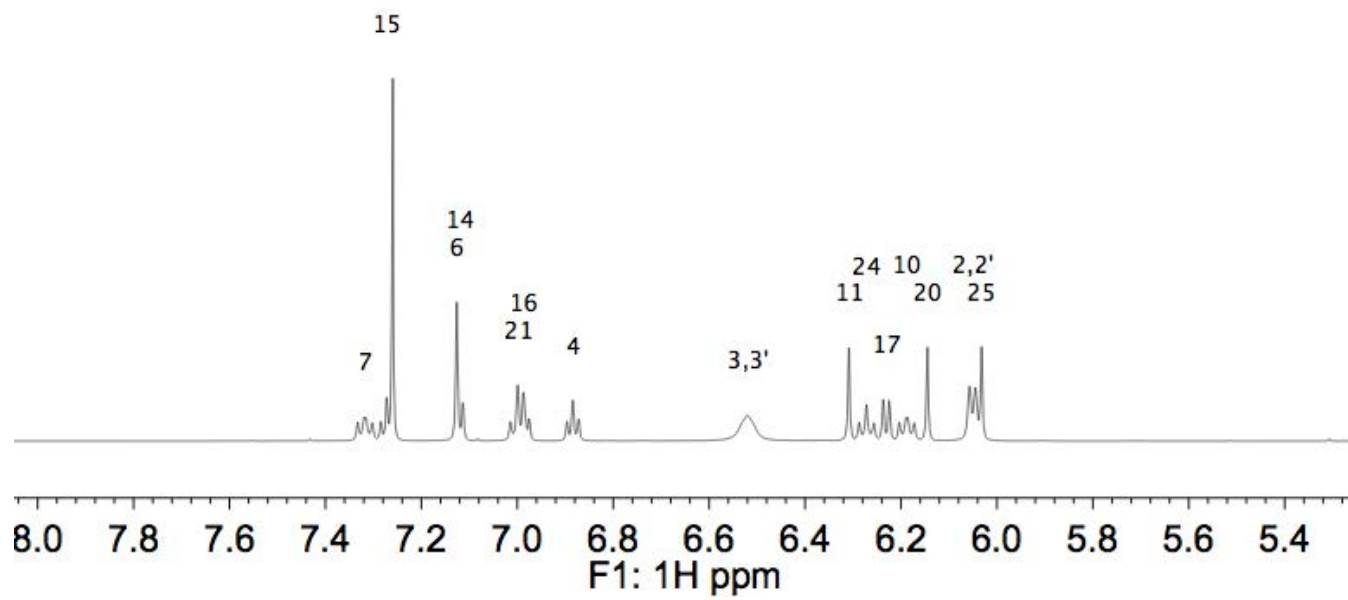


Figure S157. ^1H NMR (600 MHz) spectrum of **F-Ar-6** in CDCl_3 at $0\text{ }^\circ\text{C}$: (top) full view, (bottom) 7.40 to 6.70 ppm region. The numbers in black numbers correspond to the atom numbers of the major conformer as defined in Figure S70.

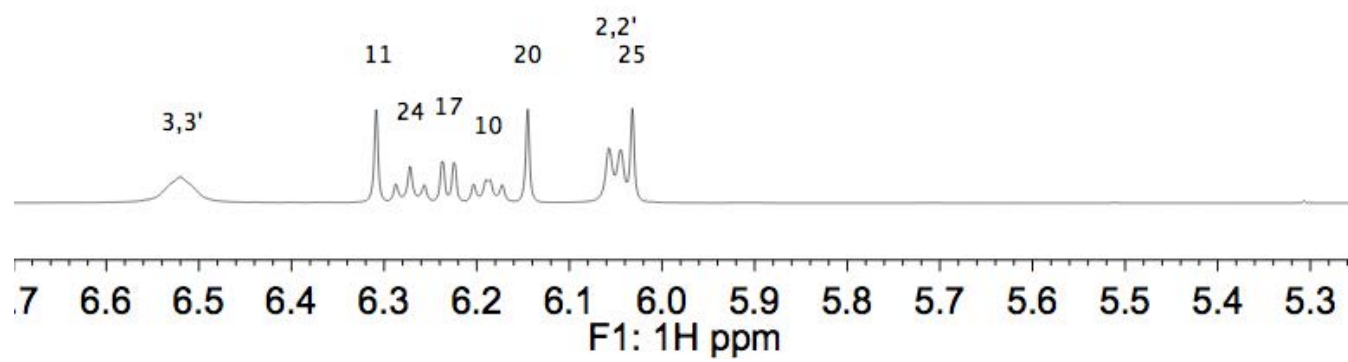


Figure S157 (continued). ¹H NMR (600 MHz) spectrum of **F-Ar-6** in CDCl₃ at 0 °C, 6.70 to 5.25 ppm region. The numbers in black correspond to the atom numbers of the major conformer as defined in Figure S70.

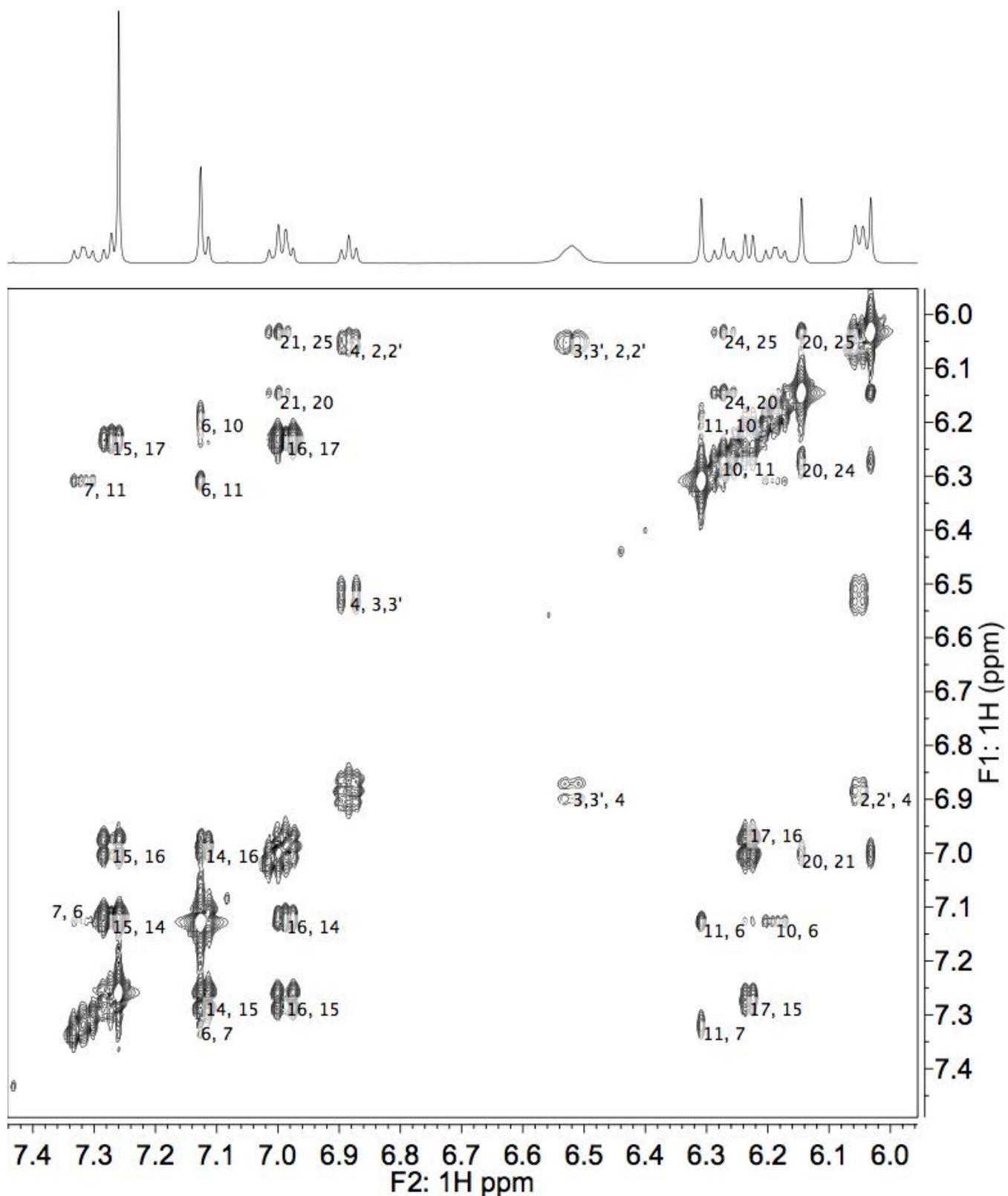


Figure S158. COSY NMR (600 MHz) spectrum of F-Ar-6 in CDCl₃ at 0 °C, full view. The numbers in black correspond to the atom numbers of the major conformer as defined in Figure S70.

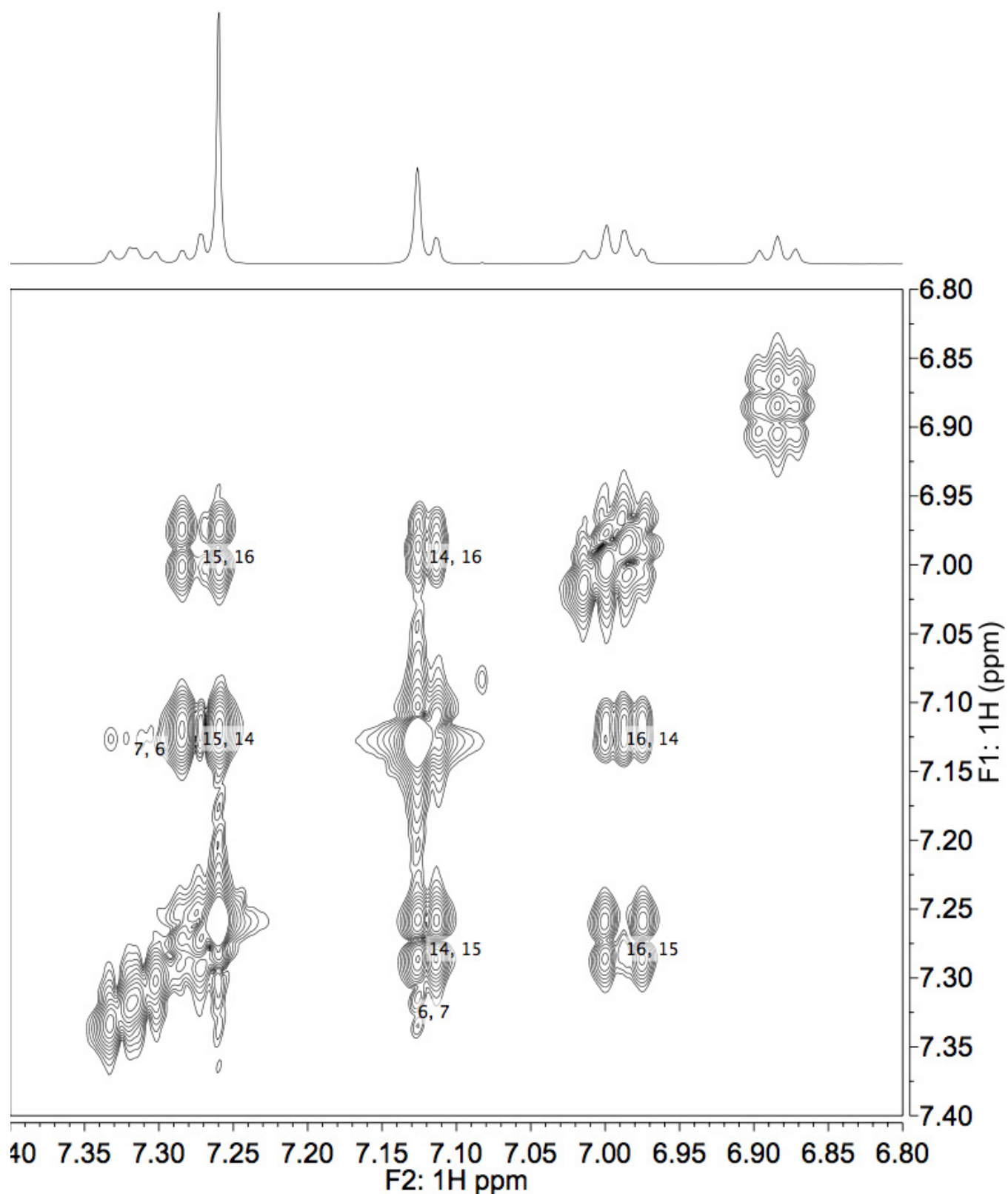


Figure S159. COSY NMR (600 MHz) spectrum of **F-Ar-6** in CDCl_3 at 0 °C, 7.40 to 6.80 ppm region. The numbers in black correspond to the atom numbers of the major conformer as defined in Figure S70.

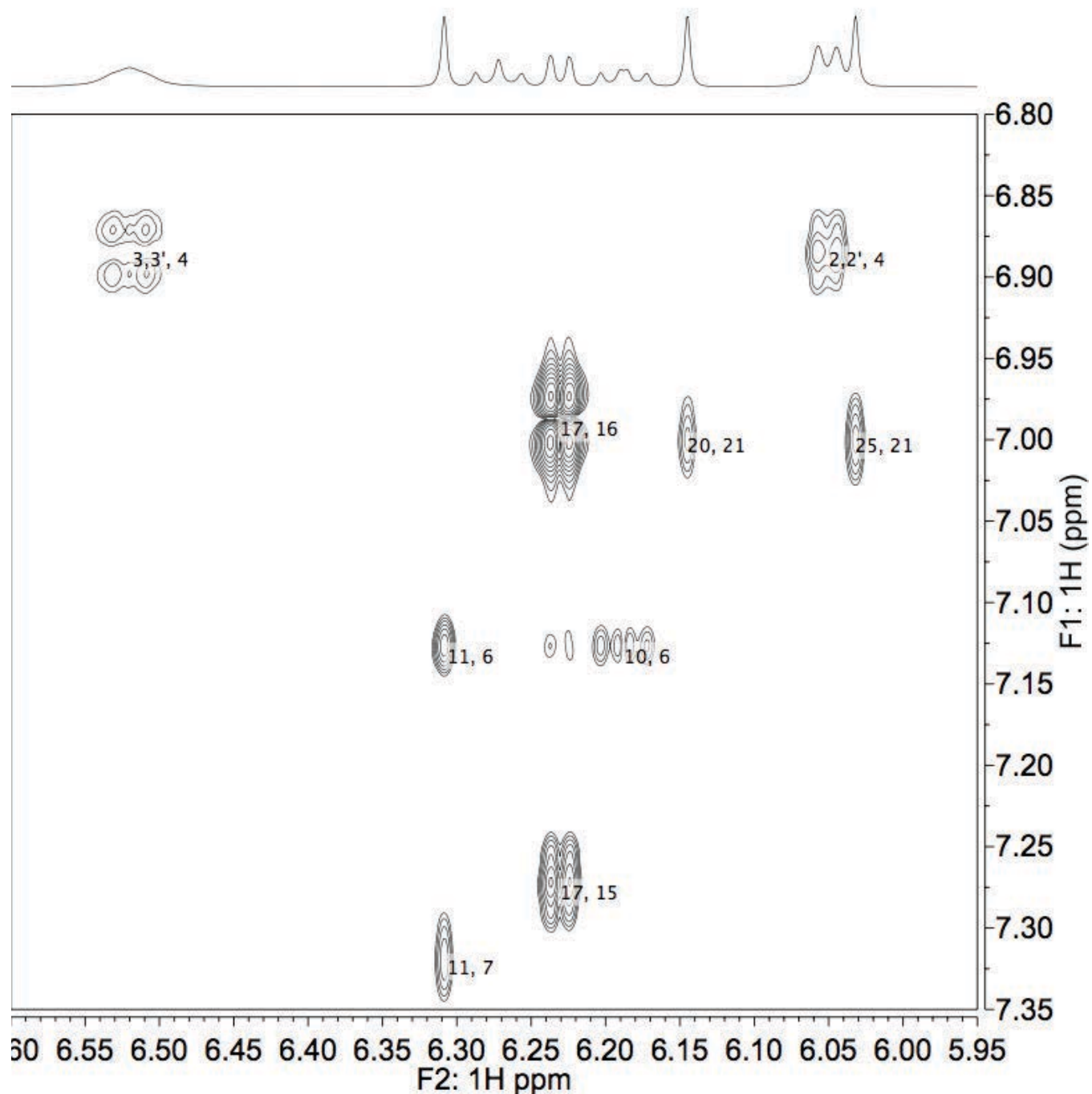


Figure S160. COSY NMR (600 MHz) spectrum of **F-Ar-6** in CDCl₃ at 0 °C, F2: 6.60 to 5.95 ppm, F1: 7.35 to 6.80 ppm region. The numbers in black correspond to the atom numbers of the major conformer as defined in Figure S70.

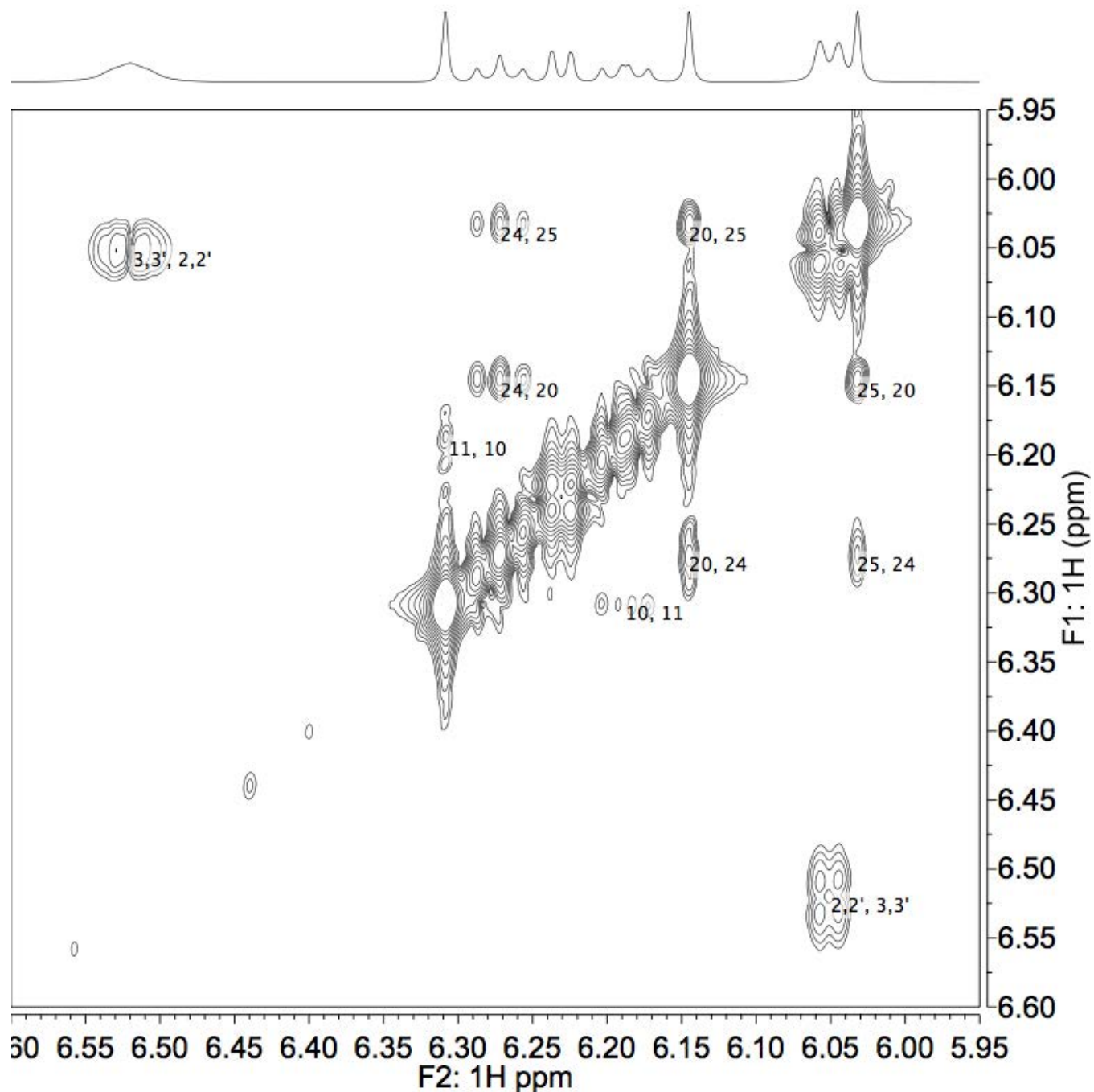


Figure S161. COSY NMR (600 MHz) spectrum of **F-Ar-6** in CDCl_3 at 0 °C, F2: 6.60 to 5.95 ppm, F1: 6.60 to 5.95 ppm region. The numbers in black correspond to the atom numbers of the major conformer as defined in Figure S70.

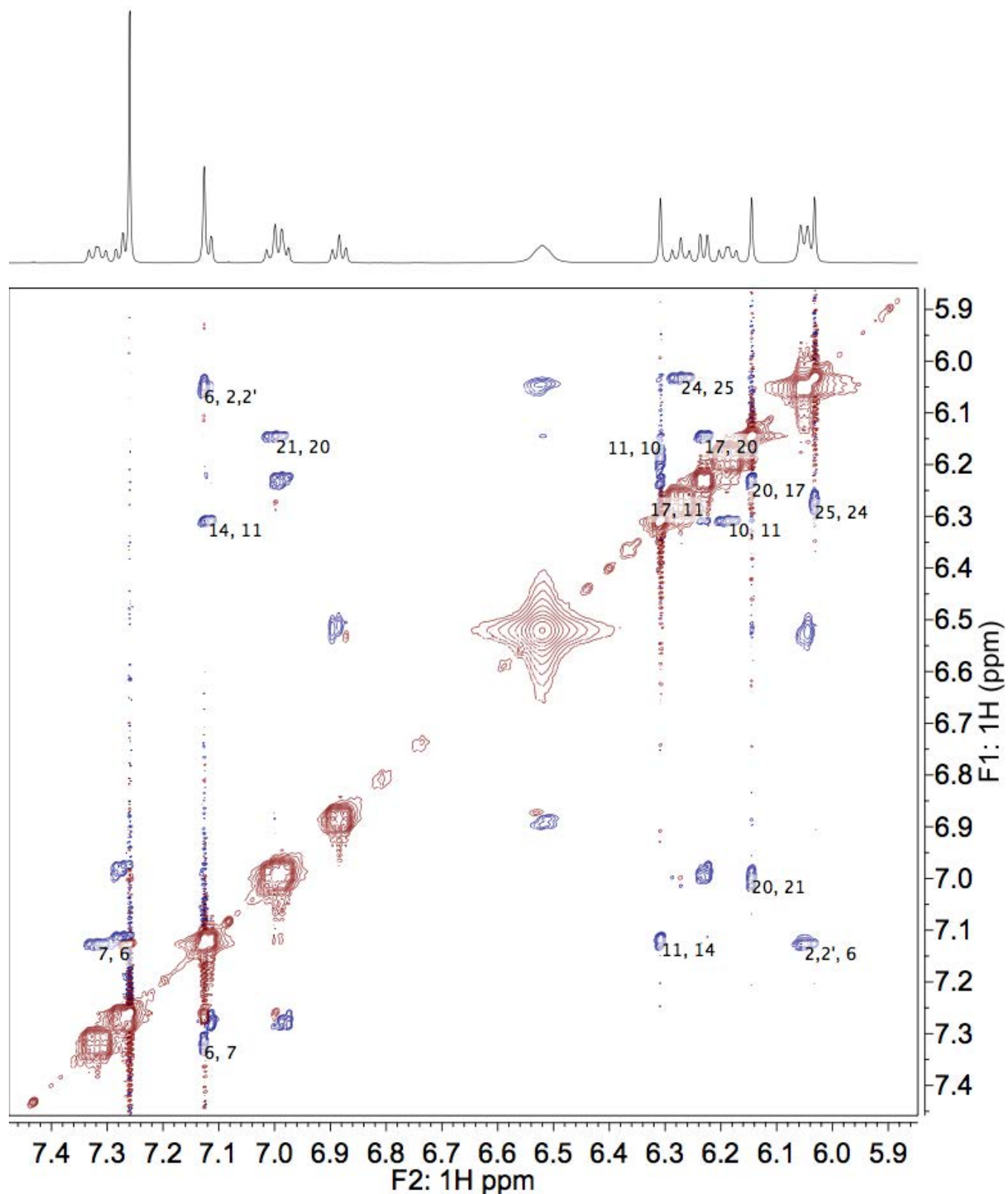


Figure S162. NOESY NMR (600 MHz) spectrum of F-Ar-6 in CDCl₃ at 0 °C.

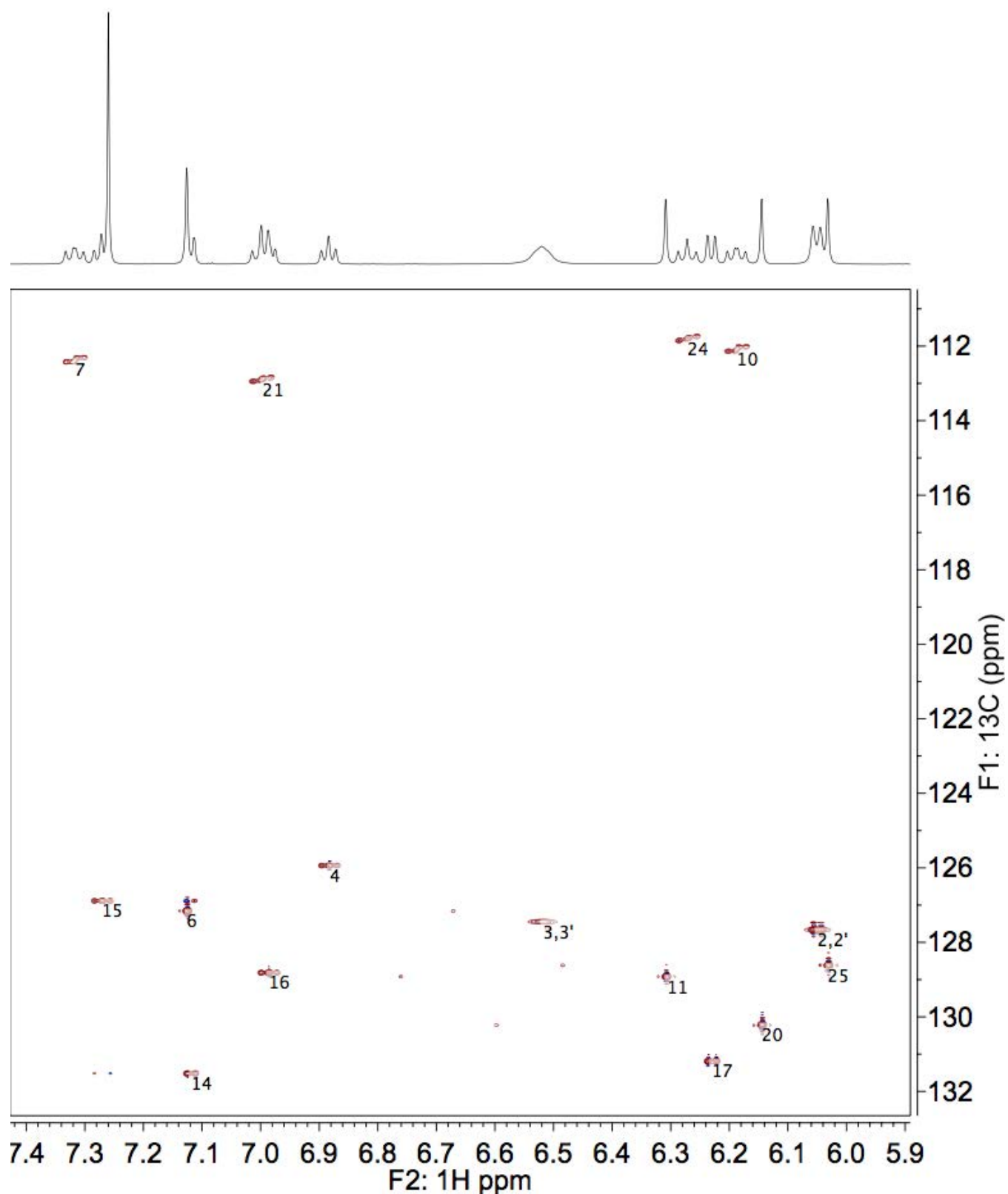


Figure S163. HSQC NMR (800 MHz) spectrum of **F-Ar-6** in CDCl_3 at 0 °C. The numbers in black correspond to the atom numbers of the major conformers, as defined in Figure S70.

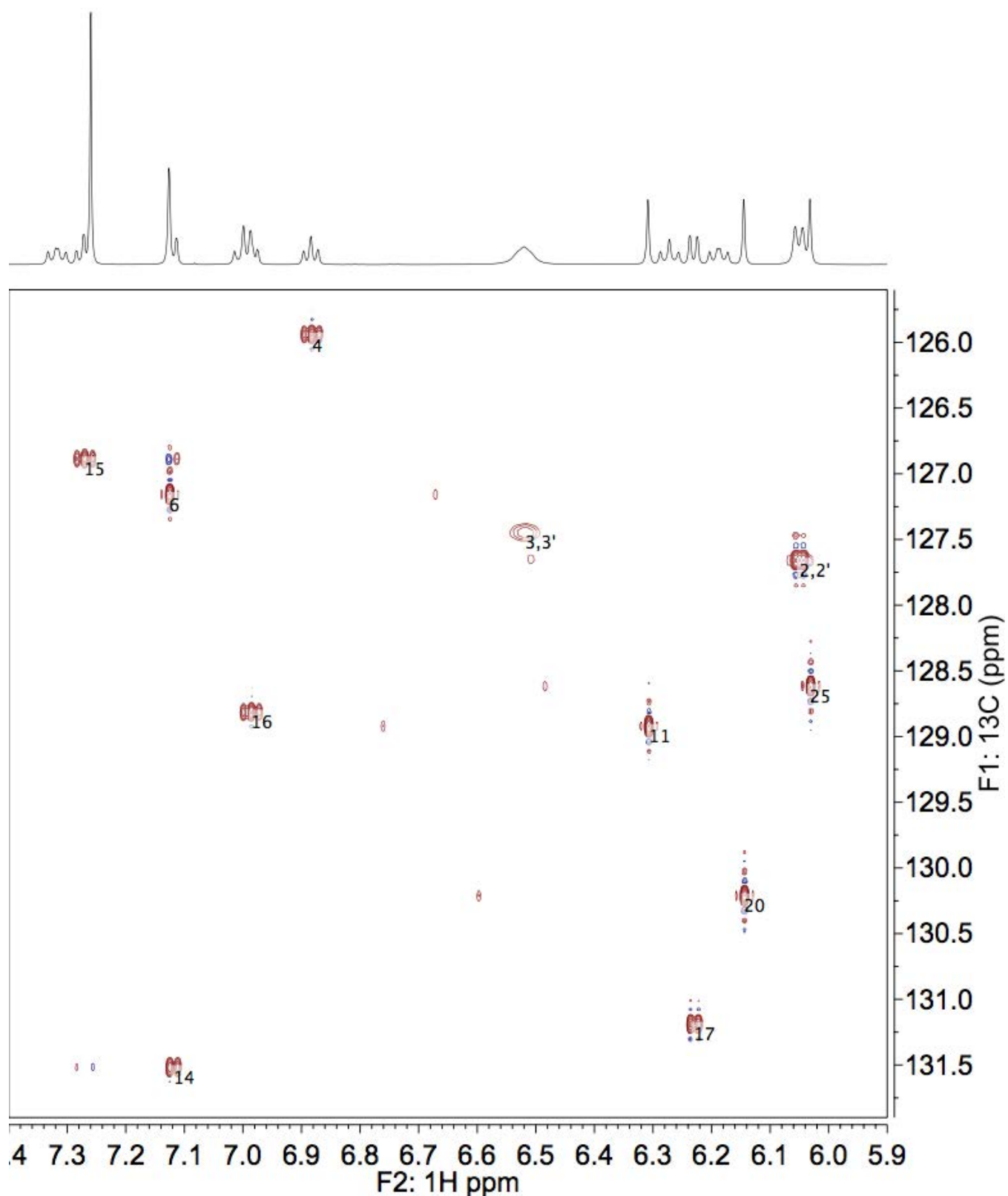


Figure S164. HSQC NMR (800 MHz) spectrum of **F-Ar-6** in CDCl_3 at 0°C , F2: 7.40 to 5.90 ppm, F1: 131.9 to 125.6 ppm region. The numbers in black correspond to the atom numbers of the major conformers, as defined in Figure S70.

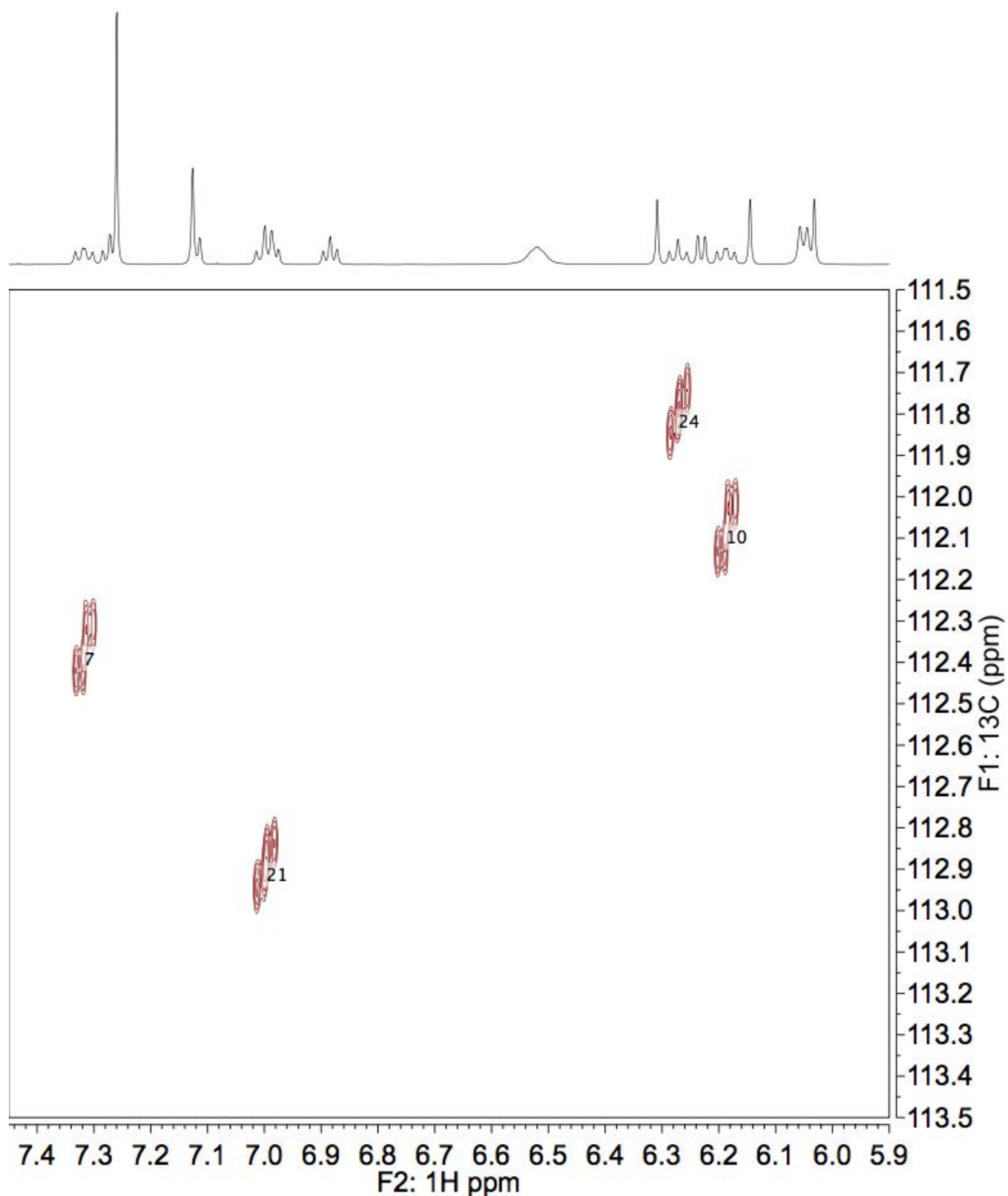


Figure S165. HSQC NMR (800 MHz) spectrum of **F-Ar-6** in CDCl_3 at 0 °C, F2: 7.45 to 5.90 ppm, F1: 113.5 to 111.5 ppm region. The numbers in black correspond to the atom numbers of the major conformers, as defined in Figure S70.

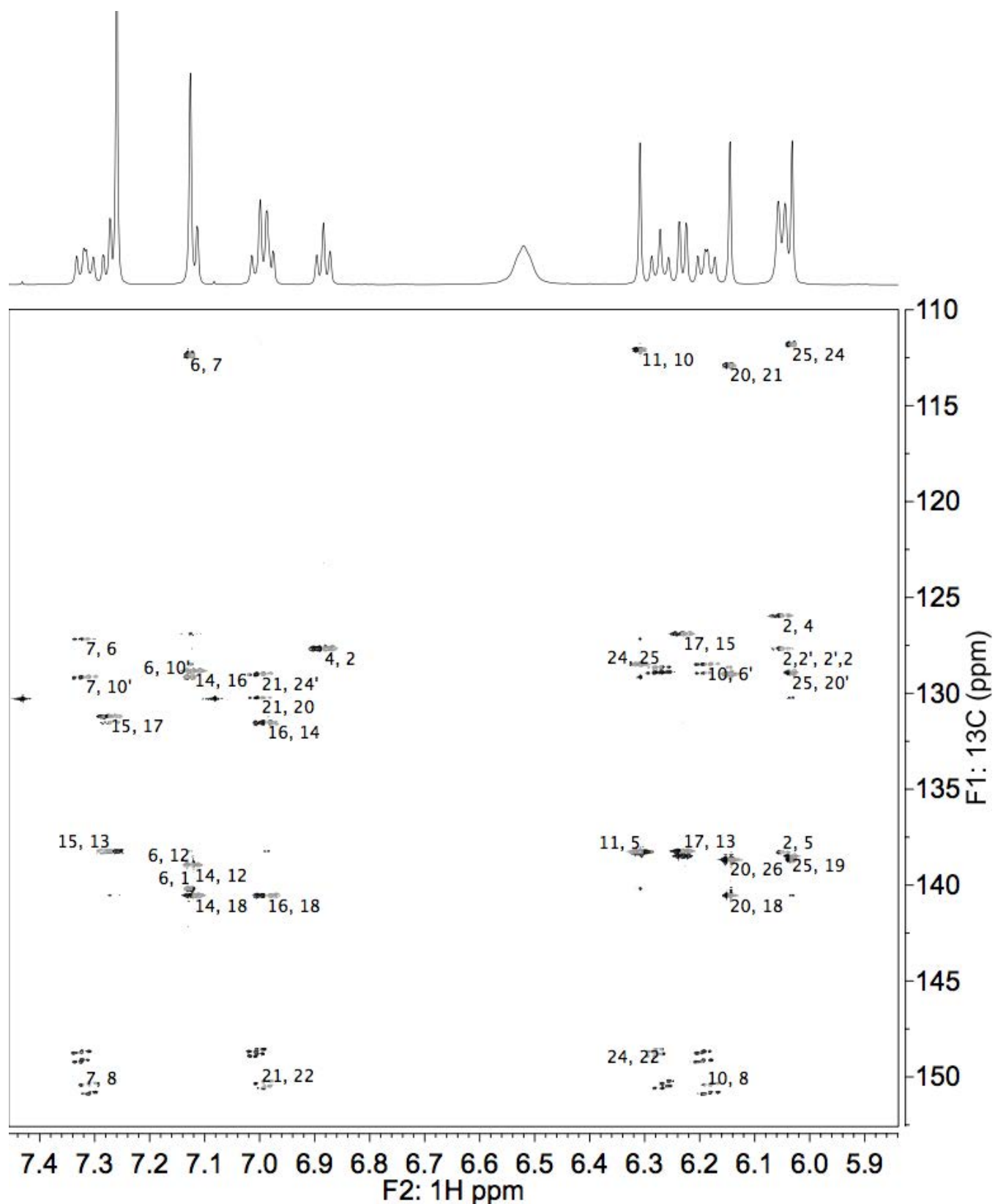


Figure S166. HMBC NMR (800 MHz) spectrum of **F-Ar-6** in CDCl_3 at 0°C , full view.

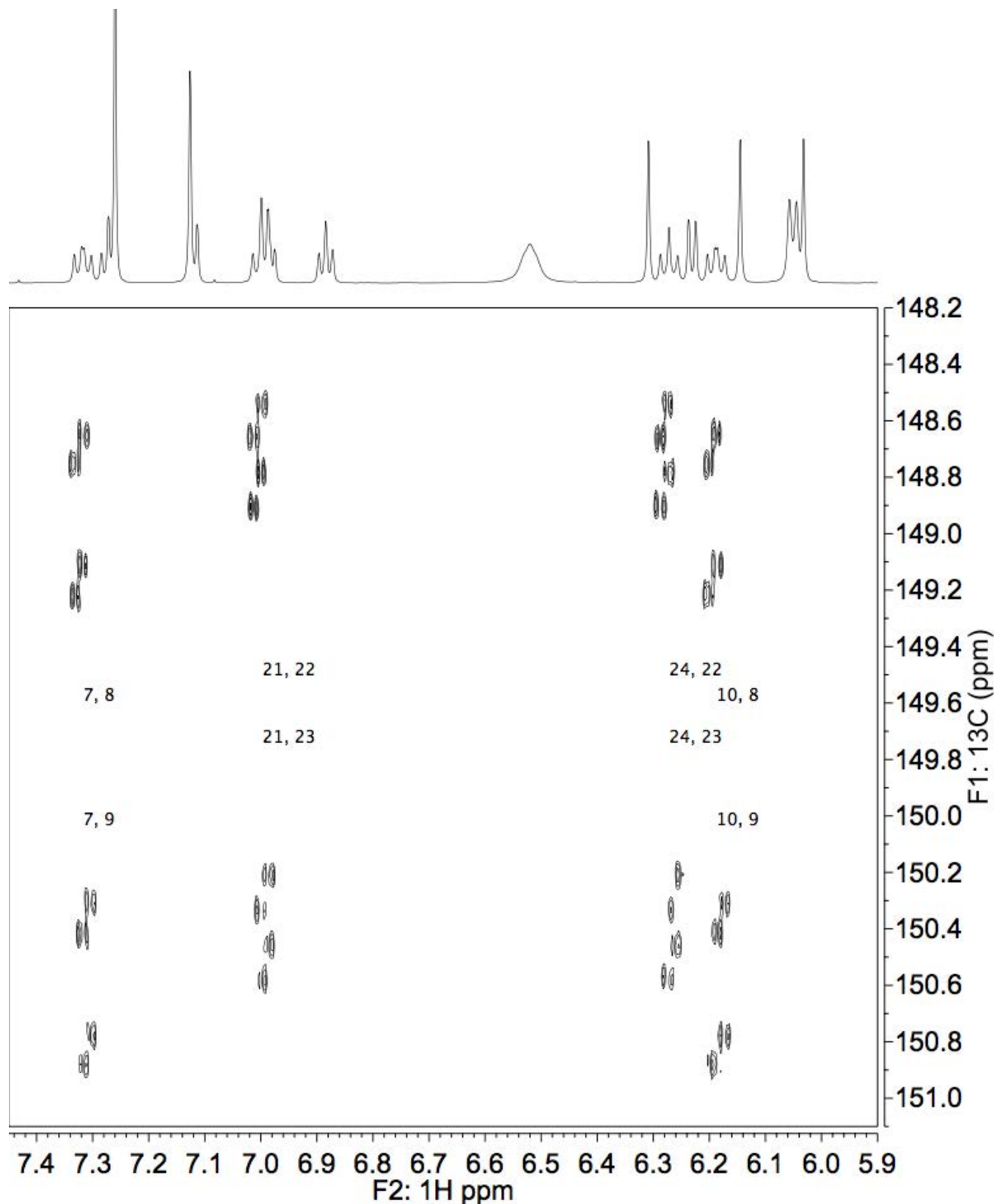


Figure S167. HMBC NMR (800 MHz) spectrum of **F-Ar-6** in CDCl_3 at 0 $^\circ\text{C}$, δ_{H} 7.45 to 5.90 ppm and δ_{C} 151.1 to 148.2 ppm region. The numbers in black correspond to the atom numbers of the major conformer as defined in Figure S70.

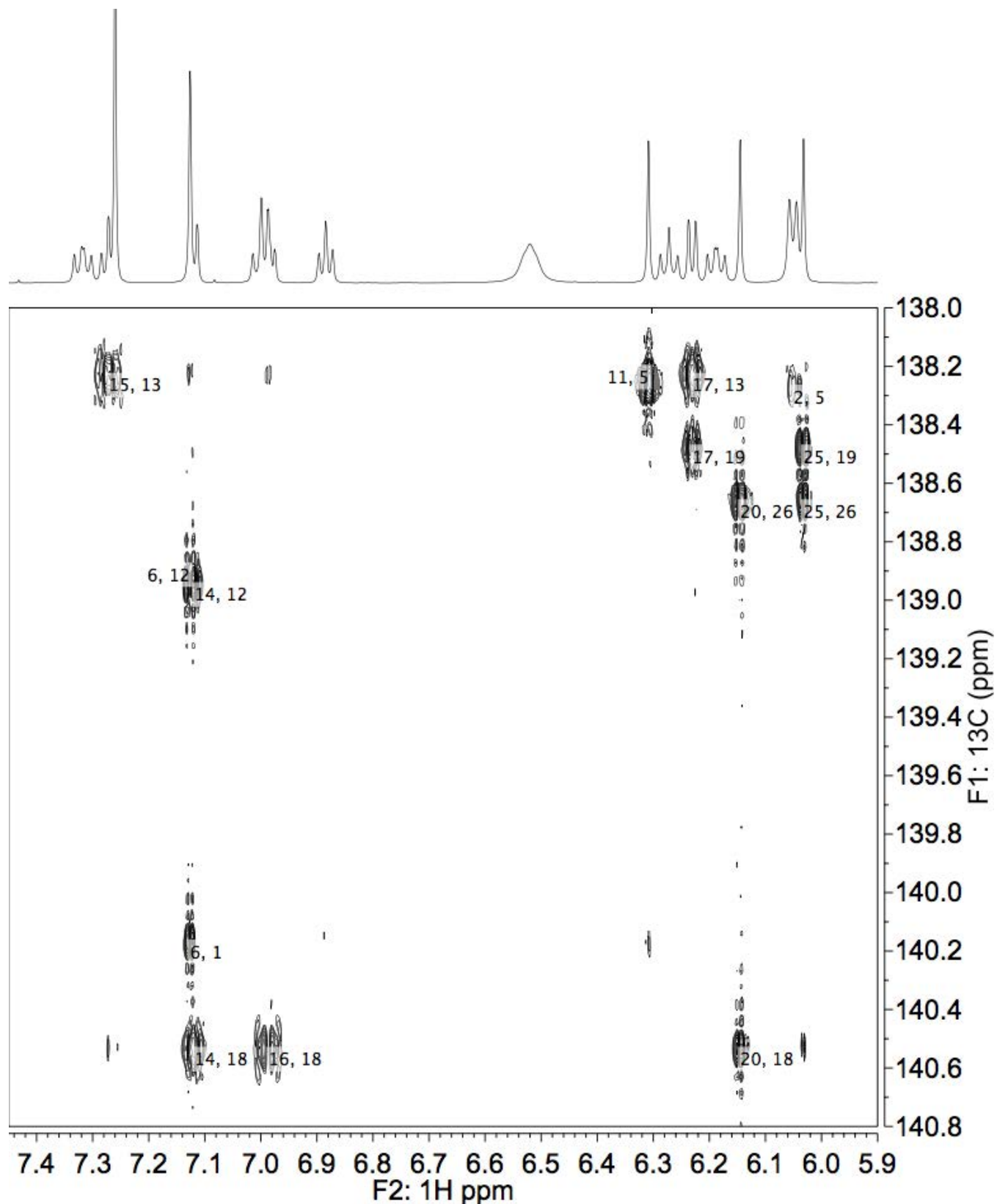


Figure S168. HMBC NMR (800 MHz) spectrum of **F-Ar-6** in CDCl_3 at 0 $^\circ\text{C}$, δ_{H} 7.45 to 5.90 ppm and δ_{C} 140.8 to 138.0 ppm region. The numbers in black correspond to the atom numbers of the major conformer as defined in Figure S70.

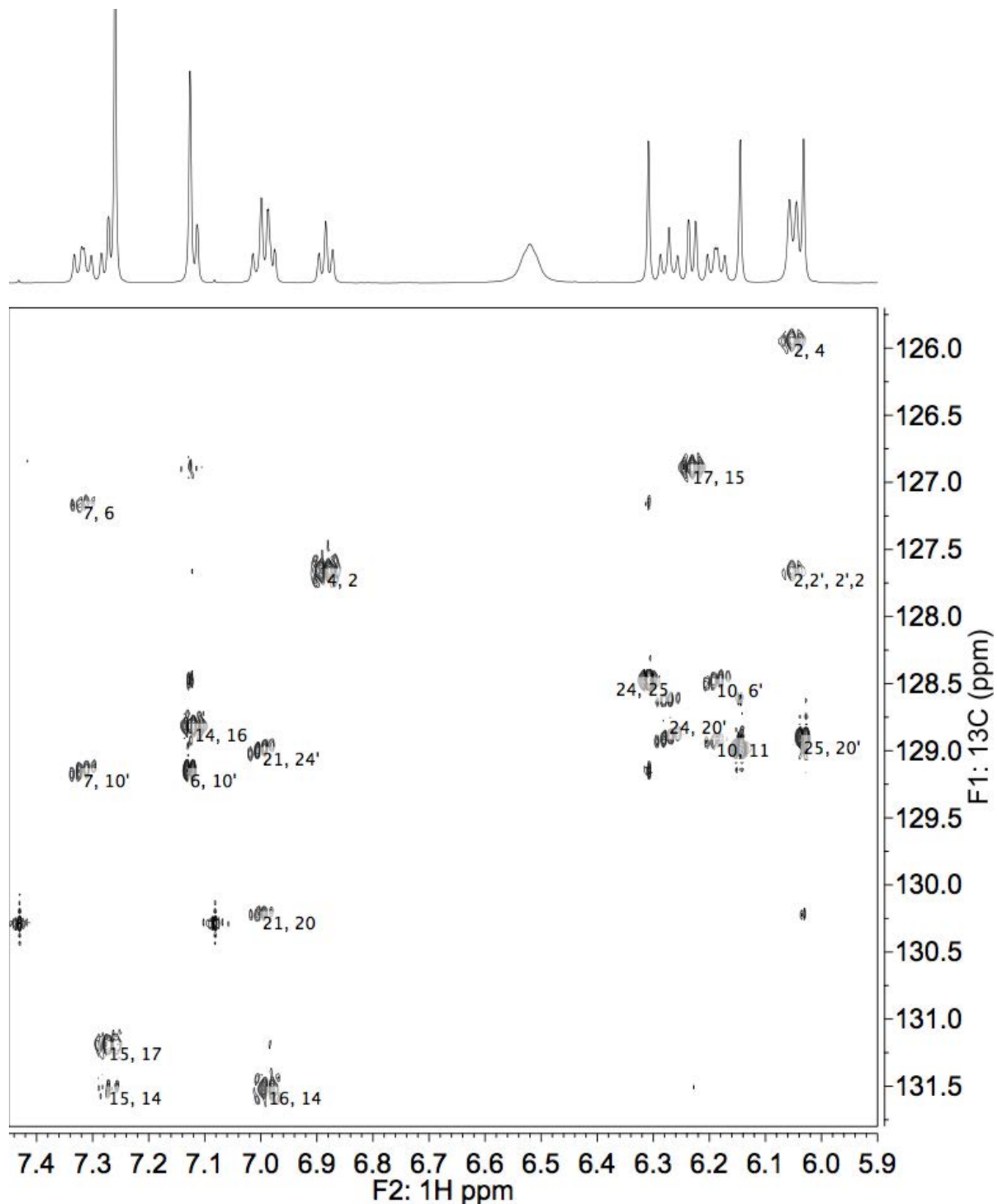


Figure S169. HMBC NMR (800 MHz) spectrum of **F-Ar-6** in CDCl_3 at 0 $^\circ\text{C}$, δ_{H} 7.45 to 5.90 ppm and δ_{C} 131.8 to 125.7 ppm region. The numbers in black correspond to the atom numbers of the major conformer as defined in Figure S70.

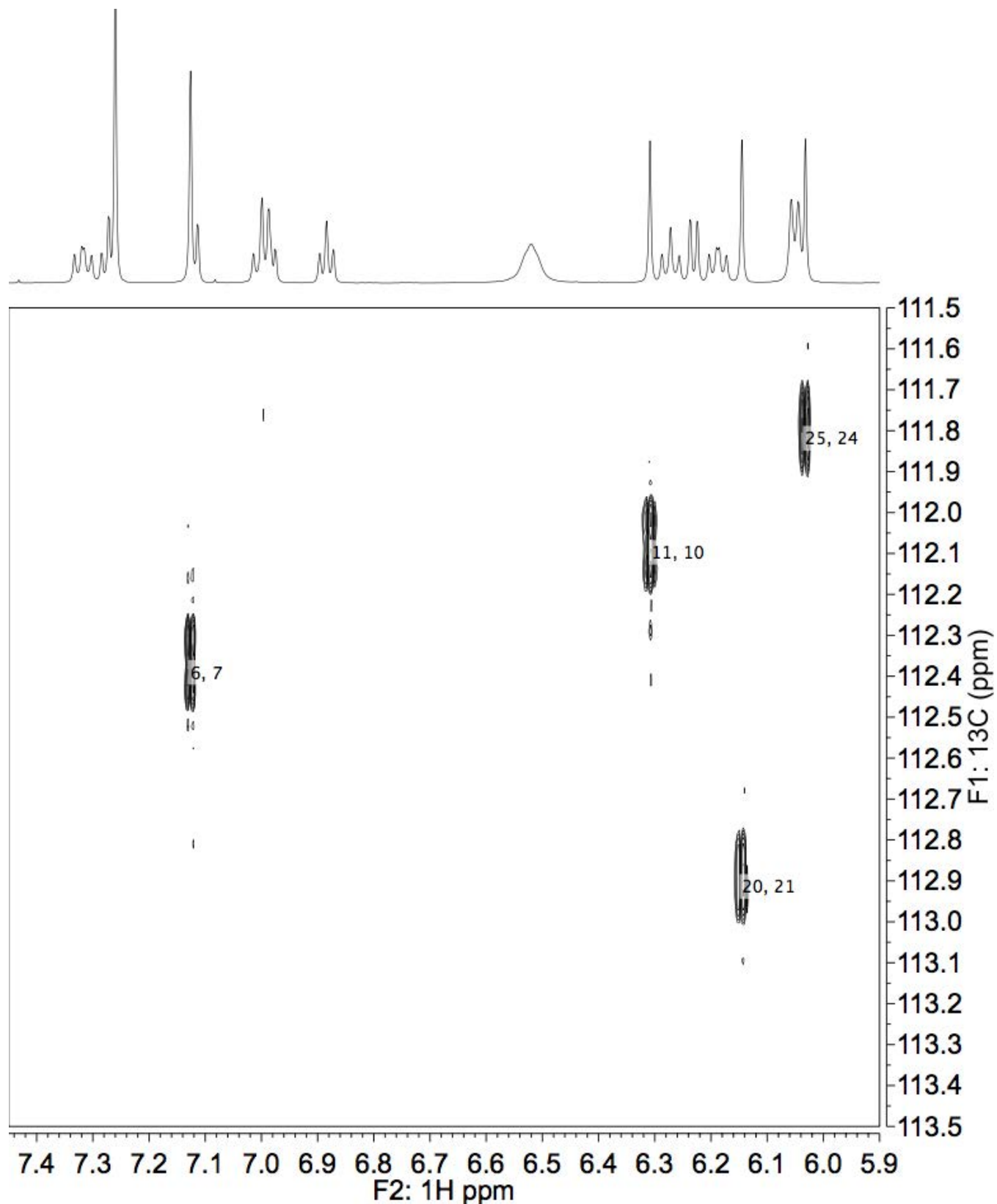


Figure S170. HMBC NMR (800 MHz) spectrum of **F-Ar-6** in CDCl₃ at 0 °C, δ_{H} 7.45 to 5.90 ppm and δ_{C} 113.5 to 111.5 ppm region. The numbers in black correspond to the atom numbers of the major conformer as defined in Figure S70.